

University of Szeged

Faculty of Pharmacy

Institute of Pharmaceutical Technology and Regulatory Affairs

Head: Prof. Dr. Ildikó Csóka Ph.D.

**QUALITY BY DESIGN BASED DEVELOPMENT AND
INVESTIGATION OF NASAL POLYMERIC MICELLES LOADED
WITH MELOXICAM**

Ph.D. Thesis

Dr. Bence Sipos

Pharmacist

Supervisor:

Dr. Gábor Katona, Ph.D.

2023

PUBLICATIONS RELATED TO THE THESIS

- I. **Sipos, B.**, Szabó – Révész, P., Csóka, I., Pallagi, E., Dobó, D. G., Bélteky, P., Kónya, Z., Deák, Á., Janovák, L., Katona, G. (2020). Quality by Design based formulation study of meloxicam-loaded polymeric micelles for intranasal administration. *Pharmaceutics*, 12(8), 697. **(Q1, IF: 6.321, Citation: 30)**
- II. **Sipos, B.**, Katona, G., Csóka, I. (2021). A systematic, knowledge space-based proposal on quality by design-driven polymeric micelle development. *Pharmaceutics*, 13(5), 702. **(Q1, IF: 6.525, Citation: 8)**
- III. **Sipos, B.**, Katona, G. (2022). Innovatív polimer alapú nanohordozók a központi idegrendszer betegségeinek kezelésére. *Gyógyszerészet*, 66, 182 – 188.
- IV. **Sipos, B.**, Bella, Z., Gróf, I., Veszélka, S., Deli, A.M., Szűcs, F.K., Sztojkov – Ivanov, A., Ducza, E., Gáspár, R., Kecskeméti, G., Janáky, T., Volk, B., Budai – Szűcs, M., Ambrus, R., Szabó-Révész, P., Csóka, I., Katona, G. (2023). Soluplus® promotes efficient transport of meloxicam to the central nervous system via nasal administration. *International Journal of Pharmaceutics*, 632, 122594 **(D1, IF: 6.510, Citation: -)**

OTHER PUBLICATIONS

- I. Katona, G., **Sipos, B.**, Budai – Szűcs, M., Balogh, G.T., Veszélka, S., Gróf, I., Deli, M.A., Volk, B., Szabó – Révész, P., Csóka, I. (2021). Development of in situ gelling meloxicam – human serum albumin nanoparticle formulation for nose – to – brain application. *Pharmaceutics*, 13(5), 646. **(Q1, IF: 6.525, Citation: 10)**
- II. Sabir, F., Katona, G., Ismail R., **Sipos, B.**, Ambrus, R., Csóka, I. (2021). Development and characterization of N-propyl gallate encapsulated solid lipid nanoparticles – loaded hydrogel for intranasal delivery. *Pharmaceutics*, 14(7), 696. **(Q1, IF: 5.215, Citation: 7)**
- III. **Sipos, B.**, Csóka, I., Budai – Szűcs, M., Kozma, G., Berkesi, D., Kónya, Z., Balogh, G.T., Katona, G. (2021). Development of dexamethasone – loaded mixed polymeric micelles for nasal delivery. *European Journal of Pharmaceutical Sciences*, 166, 105960. **(Q1, IF: 5.112, Citation: 7)**
- IV. Katona, G., **Sipos, B.**, Ambrus, R., Csóka, I., Szabó – Révész, P. (2022). Characterizing the drug – release enhancement effect of surfactants on megestrol-acetate – loaded granules. *Pharmaceutics*, 15(2), 113. **(Q1, IF: 5.215, Citation: 2)**

- V. Dobó, D.G., Németh, Z., **Sipos, B.**, Cseh, M., Pallagi, E., Berkesi, D., Kozma, G., Kónya, Z., Csóka, I. (2022). Pharmaceutical development and design of thermosensitive liposomes based on the QbD approach. *Molecules*, 27(5), 1536. **(Q1, IF: 4.927, Citation: 1)**
- VI. Katona, G., Sabir, F., **Sipos, B.**, Naveed, M., Schelz, Z., Zupkó, I., Csóka, I. (2022). Development of lomustine and n-propyl gallate co-encapsulated liposomes for targeting glioblastoma multiforme via intranasal administration. *Pharmaceutics*, 14(3), 631. **(Q1, IF: 6.525, Citation: 3)**
- VII. **Sipos, B.**, Csóka, I., Ambrus, R., Schelz, Z., Zupkó, I., Balogh, G.T., Katona, G. (2022). Spray-dried indomethacin – loaded polymeric micelles for the improvement of intestinal drug release and permeability. *European Journal of Pharmaceutical Sciences*, 174, 106200. **(Q1, IF: 5.112, Citation: 3)**
- VIII. **Sipos, B.**, Csóka, I., Szivacs, N., Budai – Szűcs, M., Schelz, Z., Zupkó, I., Szabó – Révész, P., Volk, B., Katona, G. (2022). Mucoadhesive meloxicam – loaded nanoemulsions: development, characterization and nasal applicability studies. *European Journal of Pharmaceutical Sciences*, 106229. **(Q1, IF: 5.112, Citation: 4)**
- IX. Németh, Z., Csóka, I., Semnani Jazani, R., **Sipos, B.**, Haspel, H., Kozma, G., Kónya, Z., Dobó, D.G. (2022). Quality by Design – driven zeta potential optimisation study of liposomes with charge imparting membrane additives. *Pharmaceutics*, 14(9), 1798. **(Q1, IF: 6.525, Citation: 1)**
- X. Katona, G., **Sipos, B.**, Csóka, I. (2022). Risk assessment – based optimization favours the development of albumin nanoparticles with proper characteristics prior to drug loading. *Pharmaceutics*, 14(10), 2036. **(Q1, IF: 6.525, Citation: 1)**
- XI. **Sipos, B.**, Budai – Szűcs, M., Kókai, D., Orosz, L., Burián, K., Csorba, A., Nagy, Z.Z., Balogh, G.T., Csóka, I., Katona, G. (2022). Erythromycin – loaded polymeric micelles: in situ gel development, in vitro and ex vivo ocular investigations. *European Journal of Pharmaceutics and Biopharmaceutics*, 180, 81 – 90. **(Q1, IF:5.589, Citation: 2)**
- XII. Mardikasari, S.A., **Sipos, B.**, Csóka, I., Katona, G. (2022). Nasal route for antibiotics delivery: advances, challenges and future opportunities applying the quality by design concepts. *Journal of Drug Delivery Science and Technology*, 103887. **(Q1, IF: 5.062, Citation: -)**
- XIII. **Sipos, B.**, Katona, G. (2022). Lipid- és fehérjealapú nanomedicinális készítmények a daganatterápiában *Gyógyszerészet*, 66, 633-637

PRESENTATIONS RELATED TO THE SUBJECT OF THE THESIS

A) Oral presentations

- I. **Sipos, B.**, Katona, G. (2019). NSAID tartalmú polimer micellák formulációja és vizsgálata, *XXII. Tavaszi Szél Konferencia*
- II. **Sipos B.**, Ambrus, R., Csóka, I., Szabó-Révész, P., Katona, G. (2019). Meloxicám tartalmú polimer micellák formulációja és vizsgálata, *XLII. Kémiai Előadói Napok*
- III. **Sipos, B.**, Csóka, I., Katona, G. (2020). Formulation and investigation of amphiphilic graft co-polymer based polymeric micelles, *Medical Conference for PhD Students and Experts of Clinical Sciences*
- IV. **Sipos, B.**, Katona, G., Csóka, I. (2021). Nose-to-brain applicability of Meloxicam-loaded Soluplus polymeric micelles, *III. Symposium of Young Researchers on Pharmaceutical Technology, Biotechnology and Regulatory Science*
- V. **Sipos, B.**, Katona, G., Csóka, I. (2022). Reflection on the regulatory status quo of polymeric micelles as innovative nanocarriers, *Figon & EUFEPS European Medicines Day*

B) Poster presentations

- I. **Sipos, B.**, Szabó-Révész, P., Katona, G. (2018). Formulation and investigation of amphiphilic graft co-polymer based polymeric micelles, *12th Central European Symposium on Pharmaceutical Technology and Regulatory Affairs*
- II. Katona, G., **Sipos, B.**, Ambrus, R., Csóka, I., Szabó-Révész, P. (2019). Formulation and characterization of Soluplus[®] based polymeric micelles, *3rd European Conference on Pharmaceutics*
- III. **Sipos, B.**, Ambrus, R., Pallagi, E., Szabó-Révész, P., Csóka, I., Katona, G. (2020). Quality by Design: a novel regulatory approach used in the development of nasal polymeric micelles, *Medical Conference for PhD Students and Experts of Clinical Sciences 2020*

ABBREVIATIONS

AD	Alzheimer's Disease
ANOVA	Analysis of variance
API	Active pharmaceutical ingredient
AUC	Area under the curve
BBB	Blood-brain barrier
CCD	Charge-coupled device
Cl	Clearance
CMA	Critical Material Attribute
CMC	Critical micellar concentration
CNS	Central nervous system
COX	Cyclooxygenase enzyme
CPP	Critical Process Parameter
CQA	Critical Quality Attribute
ΔG_s^0	Standard free energy of solubilization
D_H	Average hydrodynamic diameter
DLS	Dynamic light scattering
D-Tre	D-trehalose hydrate
EDTA	Ethylenediaminetetraacetic acid
EE	Encapsulation efficiency
EMA	European Medicines Agency
FBS	Fetal bovine serum
FITC	Fluorescein isothiocyanate
GC	Gas chromatography
HESI	Heated electrospray ionization
HPLC	High performance liquid chromatography
ICH	The International Council for Harmonization of Technical Requirements for Pharmaceuticals for Human Use
IN	intranasal
IV	intravenous
J	Flux
K_e	Elimination rate constant

K_p	Permeability coefficient
χ	Molar solubilization capacity
LC-MS/MS	Liquid chromatography with tandem mass spectrometry
LOD	Limit of detection
LOQ	Limit of quantification
MCC	Mucociliary clearance
MHLW	Ministry of Health, Labour and Welfare of Japan
MRT	Mean residence time
MWCO	Molecular weight cut-off
MX	Meloxicam
NaOH	Sodium hydroxide
ND	Neurodegenerative disease
P	Micelle-water partition coefficient
P_{app}	Apparent permeability
PBS	Phosphate-buffered saline
PdI	Polydispersity index
PEG	Poly(ethylene glycol)
PES	Polyether sulfone
P_M	Molar micelle-water partition coefficient
PRM	Parallel reaction monitoring
QbD	Quality by Design
QTPP	Quality Target Product Profile
SD	Standard deviation
SNES	Simulated Nasal Electrolyte Solution
SP	Soluplus [®]
$t_{1/2}$	Half-time
TEER	Transepithelial electrical resistance
T_g	Glass transition temperature
T_m	Melting temperature / Melting point
ζ	Zeta potential

TABLE OF CONTENTS

1. INTRODUCTION	1
2. AIMS	2
3. THEORETICAL BACKGROUND	3
3.1. Drug delivery to the central nervous system.....	3
3.1.1. Transport through the blood-brain barrier	3
3.1.2. Nanoparticles for drug delivery to the brain.....	3
3.2. Nasal drug delivery	4
3.2.1. Indirect (nose-to-blood) drug delivery pathway	5
3.2.2. Direct (nose-to-brain) drug delivery pathway	6
3.3. Polymeric micelles.....	6
3.3.1. Polymeric micelles in general.....	6
3.3.2. Recent results with polymeric micelles for drug delivery to the brain.....	8
3.4. Quality by Design	9
4. MATERIALS AND METHODS	11
4.1. Materials	11
4.2. Quality by Design – based risk assessment for meloxicam – loaded polymeric micelles	11
4.3. Formulation and optimization of meloxicam – loaded polymeric micelles	12
4.4. Quantification of meloxicam via High Performance Liquid Chromatography	13
4.5. Quantification of residual organic solvent via gas chromatography	13
4.6. Micelle characterization.....	14
4.6.1. Characterization of the optimized ex tempore dispersed nasal formulation .	14
4.6.2. Determination of thermodynamic solubility.....	14
4.6.3. Determination of encapsulation efficiency.....	15
4.6.4. Wetting properties and polarity calculation.....	15
4.6.5. X – ray powder diffraction study.....	16
4.6.6. Raman spectroscopic measurement.....	16
4.7. Long – term stability study	16
4.8. Nasal applicability studies	16
4.8.1. <i>In vitro</i> drug release study	16
4.8.2. <i>In vitro</i> mucoadhesion study	17
4.8.3. Cell cultures.....	17
4.8.4. Cell viability assay	18

4.8.5.	Permeability study on the cell culture model	18
4.8.6.	Immunohistochemistry	19
4.8.7.	<i>Ex vivo</i> permeability study across human nasal mucosa	20
4.8.8.	<i>In vivo</i> animal studies	20
4.8.9.	Quantification of MX in the <i>in vivo</i> samples.....	21
4.8.10.	Pharmacokinetic studies	22
5.	RESULTS AND DISCUSSION	23
5.1.	Risk assessment of meloxicam-loaded polymeric micelles.....	23
5.2.	Optimization via Box-Behnken factorial design.....	25
5.3.	Residual organic solvent content	28
5.4.	Micelle characterization.....	29
5.4.1.	Characterization of the optimized ex tempore dispersed nasal formulation .	29
5.4.2.	Determination of thermodynamic solubility and encapsulation efficiency...	30
5.4.3.	Wetting properties and polarity calculation.....	30
5.4.4.	X – ray powder diffraction study.....	31
5.4.5.	Raman spectroscopic measurement.....	32
5.5.	Long – term stability study	33
5.6.	Nasal applicability studies	34
5.6.1.	<i>In vitro</i> drug release study	34
5.6.2.	<i>In vitro</i> mucoadhesion study	35
5.6.3.	Cell viability assay	36
5.6.4.	MX permeability across the culture model of the nasal mucosa barrier	37
5.6.5.	Immunohistochemistry	37
5.6.6.	<i>Ex vivo</i> permeability measurement across nasal mucosa	37
5.6.7.	<i>In vivo</i> pharmacokinetic study.....	38
6.	CONCLUSION.....	41
7.	NOVELTY AND PRACTICAL ASPECTS.....	43
8.	REFERENCES	44
9.	ACKNOWLEDGEMENTS.....	51

1. INTRODUCTION

Advanced drug delivery systems are of increased interest based on the requirements of current patient expectations, the poor physicochemical properties of even the commonly applied active substances and the effective implementation of processability via industrial techniques [1,2]. This is especially true in case of nano drug delivery systems, such as polymeric micelles and the pharmaceutical engineering techniques aiming to reach hardly accessible areas and target points in the human body like the central nervous system [3].

Regulatory expectations of the marketing authorization process of medicinal products defines the main quality, safety and efficacy criteria of a given formulation in general and in the case of nanocarriers. In the early development stages, a proper knowledge space must be set up, presenting nanocarrier criteria and requirements. Besides this, a structured and well-designed formulation study must be conducted based on risk assessment [4-6]. In order to achieve the desired quality, safety and efficacy of the target product, the Quality by Design (QbD)-driven risk assessment can be a beneficial tool [7]. Since polymeric micelles are one of the non-biological complex drugs, the structural complexity and the reproducibility must be taken into consideration.

Challenges regarding the intranasal, as an alternative drug delivery pathway can be tackled with the utilization of polymeric micelles [8,9]. Since they can exert a solubilization effect up to an immense degree sided with permeability enhancement, rapid and burst-like drug release can be achieved. Compared to other carriers, polymeric micelles are also characterized with higher stability, especially the ones with poly(ethylene glycol) side chains [10]. With proper stability and the advantageous effects, the active substance can be transported to the site of action such as the central nervous system.

Polymeric micelles can be a solution as therapeutic carrier vehicles for numerous unmet clinical needs. A lot of potentially beneficial active substance also fail the clinical trials due to the incapability of administration to the target site [11]. Thus, specific administration in many cases can be only solved with invasive techniques which does not necessary fulfil the required pharmacological effect. That is why the demand is stated based on current clinical and industrial feedbacks, which is the quality-controlled development of advanced drug delivery systems administered through the correct and therapeutically most efficient delivery route [12].

2. AIMS

This Ph.D. work aimed to prepare a novel, innovative meloxicam-loaded polymeric micellar formulation for intranasal administration under a quality-driven basis which can deliver the model drug to the central nervous system more efficiently compared to currently commercialized formulations. The fulfillment of the expected advanced pharmacokinetic profile lies in the proper colloidal and particle characteristics and the increased water solubility induced drug release and permeability enhancement. Thus, the research work was conducted accordingly to the following steps:

- I. Based on our previous work, to establish a knowledge space and perform an initial risk assessment specified for the named active substance, applied micelle-forming co-polymer, the excipients, the formulation method and the desired drug delivery route. This was performed under the extended Quality by Design risk assessment procedure for the early stages of research and development process in a preclinical setting.
- II. To optimize the formulation strategy and composition via factorial design to achieve nano particle sized, monodisperse polymeric micelles with adequate colloidal stability based on their zeta potential value. To determine the fulfillment of the intranasal administration: osmolality and viscosity.
- III. To describe and evaluate the quantities and qualities related to the increase in water solubility. Also, to investigate the physical stability of the formulation in a long-term study accordingly to the International Council for Harmonization (ICH) Q1A guideline and to determine its physicochemical background.
- IV. To describe the nasal applicability of the formulation based on the route of the carrier system. At first, *in vitro* drug release study was performed, followed by *in vitro* mucoadhesion study at nasal conditions. Followed by *in vitro* cytotoxicity and permeability studies on human RPMI 2650 nasal epithelial cell line, we aimed to describe the cellular effects and transport across the nasal mucosa. *Ex vivo* human, nasal mucosal permeability study was also performed. The polymeric micellar system meets the requirements if increased permeability values are achieved.
- V. Lastly, we aimed to investigate the *in vivo* pharmacokinetic behavior of the formulation after nasal administration and to calculate and describe the related kinetic profile. To evaluate at this preclinical state the aimed burst-like and rapid drug transport to the central nervous system and whether our *in vitro* and *ex vivo* studies are validated.

3. THEORETICAL BACKGROUND

3.1. *Drug delivery to the central nervous system*

Drug delivery to the central nervous system (CNS) is of paramount importance which is hindered by the physiological barriers of the CNS. These barriers are essential interfaces which separate the CNS and the periphery regions. The most selective one is the blood-brain barrier (BBB) composed of endothelial cells connected by tight junctions and adherent junctions [13]. In current pharmaceutical approaches, bypassing the BBB is a challenging area of pharmaceutical technology but it comes with great rewards. In some pathological conditions the BBB is altered and becomes more permeable allowing the entry of molecules that can induce inflammatory responses alongside the neuronal damage [14]. Besides these facts, an increasing prevalence of Alzheimer's Disease (AD) have a huge impact on society and the economy and finally, on the patient's Quality of Life. Current therapeutic strategies are proved to be insufficient due to the inability to overcome the BBB in the appropriate degree [15-16].

3.1.1. *Transport through the blood-brain barrier*

One of the most important roles of the BBB is to separate the CNS from external substances unnecessary for the brain's physiological functions such as various molecules, proteins, viruses, bacteria, fungi, parasites and active pharmaceutical ingredients (API). The cerebral endothelium has such unique properties that allow to maintain BBB integrity, transendothelial transport of cells and angiogenic capability to allow revascularization when needed. The cohesiveness of the barrier lies in the success of expression of specific proteins, namely the tight- and adherent junctions. Tight junctions include *claudins*, *occludin*, *zonula occludens*, junction adhesion molecules and accessory proteins, mainly responsible for the selective permeability across the BBB [17,18]. The main transport route is the paracellular transport utilized for ions and solutes depending on the gradient concentration. The other main transport route is the transcellular and the balance of these two types will determine the degree of permeability in a healthy BBB. The transcellular pathway is defined mostly by passive diffusion in case of lipophilic molecules. Hydrophilic molecules however require specific transporters such as the glucose transporter-1 (GLUT-1) to successfully uptake the necessary amount of glucose [18,19].

3.1.2. *Nanoparticles for drug delivery to the brain*

The development of novel strategies to treat brain diseases is one of the most challenging and expensive market niches for pharmaceutical companies. Despite this fact, only a minor number of

products have reached the market (3 -5 %) since most of them failed the *in vivo* trials [20]. To overcome this failure, nanoparticles can be utilized. Nanoparticles are colloidal carriers composed of either a natural or synthetic origin and their size is in the nano-size range: 1 to 1000 nm. Synthetic nanoparticles may be prepared from polymeric materials such as poly(ethylenimine), poly(ϵ -caprolactone), poly(lactic-co-glycolic-acid), poly(ethylene glycol) (PEG) etc. or even inorganic materials such as silver, silica or gold [21-23]. By binding the drug to their proper site, they can reach the hardly accessible areas in the human body. The manner of it is mainly affected by the administration route and the carrier properties. Several studies have already demonstrated correlations between the decreased particle size and the increased BBB permeation [24-26]. However, proper control of these nanoparticles must be established which is affected by various factors as seen in Figure 1.

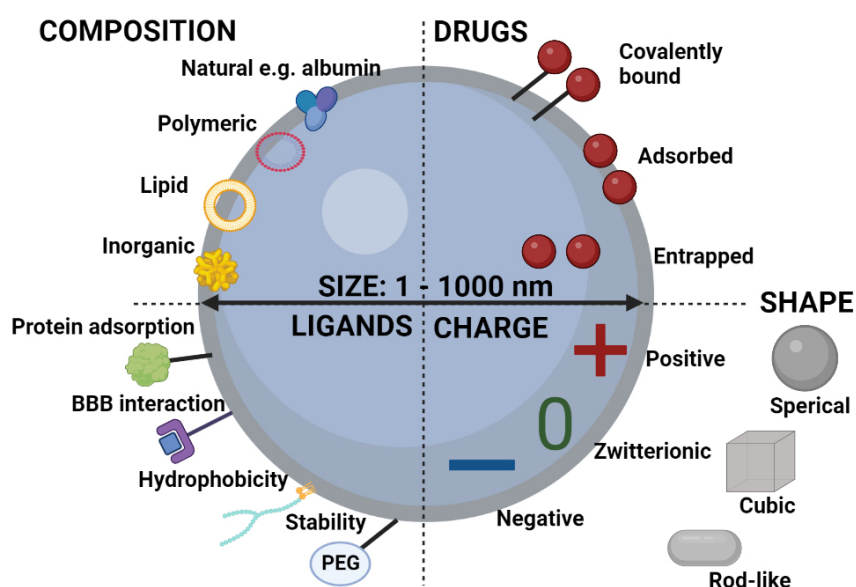


Figure 1. Nanoparticle features influencing systemic delivery and BBB passage. The main groups affecting the successful delivery are the drug’s physicochemical property and site in the carrier, the particle size, the surface charge, the shape, the ligands associated on the surface and the composition.

3.2. Nasal drug delivery

The nasal drug delivery route offers various possibilities when the aim is to enhance the bioavailability of poorly water soluble or permeable APIs. The nasal cavity can be divided into three regions: the nasal vestibule, the respiratory region and the olfactory region. The latter two regions would be responsible for delivering drugs to the central nervous system. The main advantage of this delivery route lies in the high surface area (approx. 160 cm²) of the highly

vascularized nasal mucosa, allowing rapid drug transport into the systemic circulation as well [27-29]. The other advantageous property is that we can bypass the hepatic first-pass effect which is a common problem and bioavailability limiting factor during conventional, peroral administration. However, there are formulation challenges which must be met [30]. Due to the mucociliary clearance (MCC), a rapid elimination process takes place in the nasal cavity leading to an average residence time of 15 to 20 min for the drug to be effectively released and absorbed through the mucosa. Two main strategies can be implemented to overcome this: (i) to formulate a drug delivery system which has a rapid, burst-like release and permeation profile; (ii) the utilization of mucoadhesive excipients, such as hyaluronic acid, chitosan or *in situ* gel forming polymers. The other challenge is the low administration dose per unit (50 – 150 μ l), which sets the demand for compact, concentrated dosage forms. As most of the current market's APIs have low water solubility, the solubilization techniques are of paramount importance to this problem to make up the most effective concentration at such low volumes [31,32]. The schematics of the nasal delivery route can be found in Figure 2.

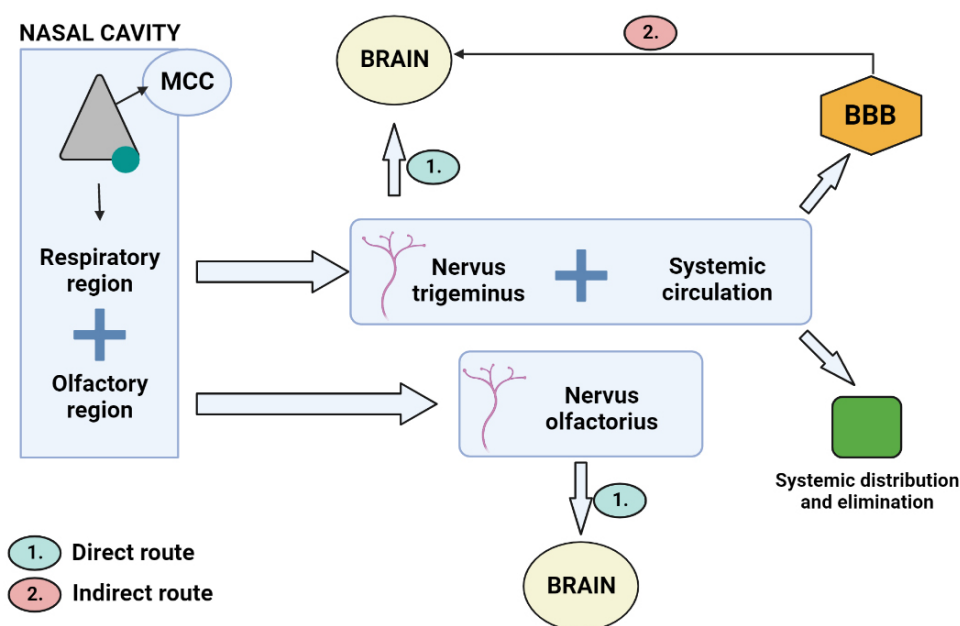


Figure 2. Schematics of the nasal drug delivery route describing the indirect and direct pathways in brief.

3.2.1. Indirect (nose-to-blood) drug delivery pathway

The nose-to-blood drug delivery can be achieved via a matrix system with rapid permeability profile alongside with the penetration enhancement effect of various polymers or lipids. The nanoparticles would be absorbed through the nasal mucosa based on the factors listed in Figure 1.

The most important however is the stability of the nanoparticle in the conditions of the circulation (e.g., pH, osmolality, presence of protein binding) which is mainly affected by the outer shell of the particle and the functional ligands on the surface on it. If we would make an order in the commonly applied polymers for stabilization, the ones with the PEG side chains would be the most suitable as they would provide up to 48 – 72 h of transit time without degradation and protect the API from enzymatic and chemical harms. As the drug-loaded carrier would travel to the BBB, it would be also important to determine which type of mechanism would take place: carrier-intact drug penetration or the carrier would be chemically/physically linked with the specific sites of the BBB and let the free, nano-sized, solubilized API through. Compared to the direct drug delivery pathway, we would always have to count on a lag time for the carrier to reach the BBB [34-36].

3.2.2. *Direct (nose-to-brain) drug delivery pathway*

The nose-to-brain drug delivery is achieved via axonal transport through the olfactory and trigeminal nerves which two innervate the nasal mucosa. The immense innervation can also hold therapeutical benefits. Studies have demonstrated before that the neural degradation associated with AD starts in the olfactory region, therefore the administration of drugs through that specific site would make a possible solution to at least delay the harmful process. The mechanism of this direct transport route is not yet fully described and discovered however it is certain that travel across nerve fibers and travel via a perivascular pathway are both accomplishable based on the nanoparticle behavior. Rapid drug delivery can be expected from this route as previous studies have demonstrated that nanoparticles would appear in less than 5 min in the olfactory bulb [37-40].

3.3. *Polymeric micelles*

3.3.1. *Polymeric micelles in general*

Polymeric micelles are novel nano drug delivery systems composed of amphiphilic (graft) co-polymers. Just like classical micelle-forming surfactants, they self-assemble into colloidal structures above the critical micellar concentration (CMC) and temperature. The building blocks may vary on the desired administration route and the potential of surface modification [41-43]. Most commonly applied co-polymers are derivatives of poly(ethylene glycol), poly(lactic acid), poly(acrylic acid) to name a few. Their main advantage is that they can encapsulate drugs with poor water solubility into their micellar core with stabilizing effect of the hydrophobic moiety whilst the hydrophilic outer shell would be responsible for the solubilization [44-46]. The schematics of the drug loading into polymeric micelles can be seen in Figure 3.

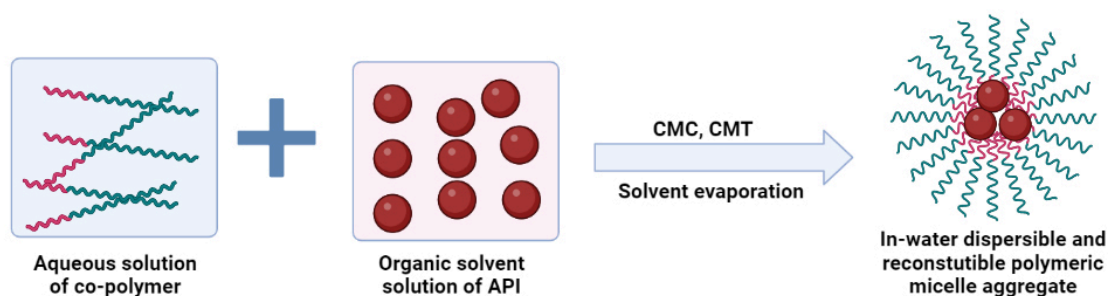


Figure 3. Schematic visualization of the self-assembly of drug-loaded polymeric micelles

Their aggregation number is in the order of several hundreds, while the average particle size is between 10 and 200 nm. This range is influenced by various factors, such as the molecular weight of the polymer, the aggregation number of amphiphilic parts, the relative ratio of hydrophilic and hydrophobic chains and the manufacturing process itself. During the synthesis of the amphiphilic co-polymers used for the preparation of polymeric micelles, a polymeric chain with a specific structure can be obtained which can be controlled with the help of the variable total molecular weight, chemical structure and morphological changes [10]. Micelles with a surface-active shell tend to disintegrate upon dilution which can lead to the lysis of cell membranes, however polymeric micelles are less prone to deliver this unwanted effect. The hydrophilic shell and the size in the nano size range prevent mechanical clearance by the filtration or the spleen. Otherwise, macrophages and antibodies in body fluids would ingest the API without its protective coating [47,48]. This significantly extends the residence time of the active substance in the blood circulation. The shell stabilizes the polymeric micelles and forms connections with plasma proteins and cell membranes, which also promote retention. The nano size reduces the chance of embolization occurring in the microcapillaries, on the contrary, compared to micron-sized drug carrier systems [49,50].

By optimizing the properties of the shell, it is not necessary to chemically modify the API itself. Substituted and linked with sugars and peptides, it could take on new biological and pharmacokinetic characteristics, which can also be used for receptor-mediated drug and gene targeting. Immunomicelles, which are endowed with monoclonal antibodies linked to the polymeric micelle's shell, resulting in high affinity, specificity and targetability to receptors and biological targets. With the further development of polymeric micelles, we would be able to create intelligent carrier systems in the future, which can change their structure sensitively to the environmental stimuli (temperature, pH, osmolality) in order to create a more stable system corresponding to the target site of the mechanism of action [51-55].

Polymeric micelles can also be characterized with various data and measurements. Chief among these is the definition of CMC. This is a key parameter of the production process. Polymeric micelles are formed above it, while below it they are continuously formed in quasi-equilibrium, but also fall apart, in which case we cannot speak of true micelle formation. Based on the Hardy-Harkins principle, the amphiphilic molecules will spread on the surface of the solvent in accordance with the appropriate polarity directions, forming a film. Many factors affect the CMC value, such as the salt concentration of the solvent, pH, temperature, hydrophilic-hydrophobic ratio. Other necessary characteristics include the definition of the nanoparticle in the colloidal range such as particle size, particle size distribution and the zeta potential. As high increase in water solubility is experienced, the description of it is also a must [56-58].

3.3.2. Recent results with polymeric micelles for drug delivery to the brain

Clonazepam-loaded polymeric micelles were formulated by Nour et al. which is a commonly applied drug in the treatment of *status epilepticus*. However, its therapeutic efficiency is hindered by its poor water solubility and bioavailability. Based on the pharmacodynamic radio isotopic mapping tests, it has been proven that the polymeric micelle formulation showed a much higher concentration in the brain. Also as demonstrated in their study, 99.3 % of the drug in the brain was achieved via the nose-to-brain pathway. As a result of the work, it can be claimed that it was a successful formulation that can be used in epilepsy with prolong residence time and effect of action [59].

Many newly synthesized APIs are directly formulated into nanocarriers prior to the conventional dosage forms regarding their potential for commercialization and clinical efficacy. Porkharkar et al. developed a lurasidone-loaded binary polymeric micelle in a hydrogel formulation, which is a novel drug applied for bipolar depression and schizophrenia. The same problem can be found, which is that its low water solubility sets an obstacle for it to reach the CNS. However, via the utilization of the binary polymeric micelle system, a prolonged and efficient concentration of the API could be found in the brain as shown in the *in vivo* studies [60].

Rotigotine is applied for the treatment of Parkinson's Disease, which API was encapsulated into a polymeric micelle formulation by Wang et al. The polymeric micelle formulation was embedded into a thermosensitive *in situ* gelling system. The response of the matrix system by temperature and the particle size reduction induced increase in the water solubility of rotigotine leading to a higher selectivity and concentration in various parts of the brain: cerebrum – 170.5 %, cerebellum – 166.5 % and striatum – 184.4% compared to the intravenous reference [61].

3.4. *Quality by Design*

Research and development has changed enormously in recent decades and leaders of pharma companies are in the midst of unprecedented change. With the increased prevalence of chronic diseases, vascular and neurological diseases, the aging population pyramid and finally, the occurrence of pandemics such as Covid-19 or Ebola accelerate pharmaceutical manufacturing and research processes that must be adhered to strict quality conditions. A newly manufactured and market-placed medicine must face obstacles for the industry players [62,63]. Changes in consumer attitude, cybersecurity threats, rapid advances in technology, non-adequate return on innovation and competition from companies in emerging economies are several of them. In the 21st century, a novel quality assurance approach, the Quality by Design (QbD) appeared, oriented towards quality of the product and the improved patient applicability during therapeutic use. Quality, safety and efficacy are the three cornerstones of the QbD approach, which is built around starting from preformulation studies all the way to the patient's own use [64-66].

The International Council for the Harmonization of Technical Requirements for Pharmaceuticals for Human Use has adapted the QbD approach and stated in the European Medicines Agency (EMA) directives. Namely the following contains the necessary information and requirements regarding QbD: ICH Q8 (Pharmaceutical Development), ICH Q9 (Quality Risk Management) and ICH Q10 (Pharmaceutical Quality System) [67-69]. Briefly, the QbD methodology includes the following steps:

1. Definition of Quality Target Product Profile (QTPP): It is a prospective summary of the desired quality characteristics of the drug-loaded product that ideally would be achieved to ensure the desired quality, safety and efficacy. General elements include e.g., the route of administration, absorption profile etc.
2. Identification of the critical elements, such as the critical quality attributes (CQAs), the critical material attributes (CMAs) and the critical process parameters (CPPs). According to the ICH guidelines, a CQA is a physical, chemical, biological or microbiological property that should be investigated and set within the appropriate limit. CMA parameters refer to the qualities and quantities of the applied drug, excipients, solvents etc., whilst CPPs are specific to the production method itself.
3. Risk assessment: can be performed by classic quality assurance techniques, such as the SWOT analysis, FMEA analysis [70]. In this study, the interdependence rating was applied, which includes the definition of the relations between the CQA – QTPP elements followed by the same definition for the CQA – CMA/CPP elements. Followed by this, to quantify

the effect and severity of each factor, a probability-based rating must be evaluated which calculates with the occurrence and treatability of the associated risk factors

4. Design space development: most commonly factorial or neural designs are applied.
5. Definition of control strategy.
6. Life cycle management.

QbD is a systemized, structured, knowledge- and risk assessment-focused approach, and the potentials of its extension to the early development stages have previously been shown by Csóka et al. [7]. Also in our previous study, we developed a general knowledge space based on literature data about polymeric micelle development and evaluated a risk assessment of the collected feasible factors [66].

4. MATERIALS AND METHODS

4.1. *Materials*

Meloxicam (MX) (4-hydroxy-2-methyl-N-(5-methyl-2-thiazolyl)-2H-1,2-benzothiazine-3-carboxamide-1,1-dioxide) was applied as model drug and acquired from EGIS Pharmaceuticals Plc. (Budapest, Hungary). Soluplus[®] (SP) (BASF GmbH, Hanover, Germany) was used as micelle-forming agent. 96 %v/v ethanol (Merck, Ltd., Budapest, Hungary) was used as organic solvent during our experiments. Microcrystalline sodium hydroxide (NaOH) as formulation excipient, chemicals for Simulated Nasal Electrolyte Solution (SNES) which is combined of 8.77 g sodium chloride (NaCl), 2.98 g potassium chloride (KCl), 0.59 g and anhydrous calcium chloride (CaCl₂) in 1000 ml of deionized water at pH 5.6 as well as disodium hydrogen phosphate (Na₂HPO₄), potassium dihydrogen phosphate (KH₂PO₄) for pH 7.4 Phosphate-buffered saline (PBS) dissolution medium and the cryoprotectant D-trehalose dihydrate (D-Tre) were acquired from Sigma-Aldrich Co., Ltd. (Budapest, Hungary). The composition for SNES were based on the work of Castile et al. [71]. Purified water for the experiments was filtered using the Millipore Milli-Q[®] (Merck, Ltd., Budapest, Hungary) Gradient Water Purification System. All other chemicals were also obtained from Sigma-Aldrich Co., Ltd. if otherwise not indicated.

4.2. *Quality by Design – based risk assessment for meloxicam – loaded polymeric micelles*

As QbD is a knowledge- and risk assessment-focused approach, qualitative and quantitative risk factors, expressed as severity scores, must be presented. LeanQbD[®] Software (QbD Works LLC, Fremont, CA, USA) was used for the risk assessment procedure. At first, an interdependence rating amongst the QTPPs and the CQAs and amongst the CQAs and the CMAs/CPs was performed. A three-level scale was used to describe the relation between these parameters: each relation was assigned with a “high” (H), “medium” (M) or “low” (L) attributive. The decision of assignment was performed based on numerous aspects including occurrence of the risk factor during formulation and/or final product development phase; controllability of the factor; whether the factor can be eliminated or can it be fixed at a certain value without affecting quality; detectability. The description of relations had the fundamental basis of how closely the factors are related and data from the collected literature, in addition to the regulatory aspects of a joint MHLW/EMA reflection paper on the development of block copolymer micelle medicinal products. Using the software, these qualitative relations were the basis of calculating the severity scores. The severity scores were transferred as percentages of the overall, cumulative severity scores and were depicted at the end of the interdependence tables [7,72-74].

4.3. Formulation and optimization of meloxicam – loaded polymeric micelles

First, a fixed value of 15 mg of MX was dissolved in the factorial design determined volume of alkaline ethanol under continuous stirring (750 rpm, 25 °C). The next step was to dissolve the required amount of SP in the solution of MX based on the factorial design. After 1 h of incubation, a Büchi R-210 (Büchi, Flawil, Switzerland) rotation vacuum evaporator was used to extract the solvent and a thin layer of matrix film was formed in the round-bottom flask. The temperature was set at 50 °C, with gradually decreasing pressure from 1000 to 100 mbar with a rate of 50 mbar/min, followed by 10 to 15 min of drying at 100 mbar. After hydration of the polymeric film with 6 ml of purified water, the pH was adjusted between 5.6 to 7.4 using diluted hydrochloride acid and 5 % w/v D-Tre was dissolved with the formulation. Thereafter, 1 ml aliquots of formulations were freeze-dried at – 40 °C for 12 h under a 0.013 mbar pressure with additional 3 h of secondary drying at 25 °C using a ScanVac CoolSafe 100-9 (LaboGene, ApS, Lyngø, Denmark) laboratory apparatus. After the freeze-drying process, samples were reconstituted in 1 ml of purified water with a nominal MX concentration of 2.5 mg/ml.

The hydrated formulation was applied for the Box-Behnken factorial design, which aimed to optimize the MX-loaded polymeric micelles prior to the stabilizing freeze-drying process. A 3-factor, 3-level design was set up. The independent variables were namely the following: the concentration of SP (mg/ml), the volume of ethanol (ml) and the volume of the 1 M NaOH solution (ml) as three critical parameters in the formulation. The range values of the independent factors can be seen in Table 1.

Table 1. Composition of the 3-factor, 3-level Box-Behnken factorial design in order to optimize the MX-loaded polymeric micelles

Independent factors	Level		
	-1	0	+1
SP (mg/ml)	6	9	12
Ethanol (ml)	5	7.5	10
1 M NaOH solution (ml)	3	4.5	6

The effect on Z-average and polydispersity index values was investigated prior to freeze-drying to investigate the effect of the composition without cryoprotectant whilst analyzing the quadratic response surface and to construct a second-order polynomial model using TIBCO Statistica® 13.4 software (Statsoft Hungary, Budapest, Hungary).

The relationship of the variables on the response could be described with the following second-order equation:

$$Y = \beta_0 + \beta_1x_1 + \beta_2x_2 + \beta_3x_3 + \beta_{12}x_1x_2 + \beta_{13}x_1x_3 + \beta_{23}x_2x_3 + \beta_{11}x_1^2 + \beta_{22}x_2^2 + \beta_{33}x_3^2 \quad (1)$$

where Y is the response variable, β_0 is a constant, β_1 , β_2 and β_3 are linear coefficients, β_{12} , β_{13} and β_{23} are linear interaction coefficients between the three factors, β_{11} , β_{22} and β_{33} are quadratic coefficients. The analysis of variance (ANOVA) statistical analysis was carried out and the results were evaluated in harmony with their *p*-value when we considered a variable significant if *p* was less than 0.05 at 95% confidence level. Response surface plots for average hydrodynamic diameter (D_H) and polydispersity index (PDI) in the form of contour plots were plotted according to the regression model by keeping one variable at the center level.

4.4. Quantification of meloxicam via High Performance Liquid Chromatography

To determine the concentration of MX during the experiments, high performance liquid chromatography (HPLC) measurements were performed using an Agilent 1260 (Agilent Technologies, Santa Clara, CA, USA) device. The stationary phase was a Kinetex[®] EVO C18 column (5 μ m, 150 mm x 4.6 mm (Phenomenex, Torrance, CA, USA)). The injection volume was 10 μ l. The temperature was set to 30 °C. As mobile phases, a 0.065 M KH₂PO₄ solution adjusted to pH 2.8 with *ortho*-phosphoric acid (A) and methanol (B) were used. A two-step gradient elution was used for the separation. The starting proportion of 50 % A eluent was reduced to 25 % in 14 min, and then raised again to 50 % in 20 min. The eluent flow rate was 1 ml/min, and the detection of the chromatograms was carried out at 355 \pm 4 nm using UV-Vis diode array detector. Data were evaluated using a ChemStation B.04.03 software (Agilent Technologies, Santa Clara, CA, USA). The retention time of MX was detected at 14.34 min. The determined limit of detection (LOD) and quantification (LOQ) were 16 ppm and 49 ppm, respectively.

4.5. Quantification of residual organic solvent via gas chromatography

Ethanol is a Class 3 solvent; thus, its residual concentration should be less than 5000 ppm in the daily dose of the final product according to ICH Q3C (R5) guideline for residual solvents [75]. The in-water dispersed formulation was analyzed by a Shimadzu GC – 14B gas chromatograph (Shimadzu Europa GmbH, Duisburg, Germany) equipped with a thermal conductivity and flame ionization detector. The calibration curve was previously determined in the range of 0 – 0.35 mM of ethanol. Each measurement was carried out in triplicate with individual batches.

4.6. *Micelle characterization*

4.6.1. *Characterization of the optimized ex tempore dispersed nasal formulation*

The average hydrodynamic diameter (D_H) and the polydispersity index (PDI) were measured by the means of dynamic light scattering (DLS) using a Malvern Zetasizer Nano ZS (Malvern Instruments, Worcestershire, UK). The zeta potential (ζ) of the formulations was also measured via this equipment. The formulations were dissolved in purified water, then measured at 25 °C in folded capillary cells with the refractive index of 1.720. Each measurement was carried out in triplicate with individual batches.

The reconstitution time of powder ampoules containing 2.5 mg/ml of MX was measured after adding 1.0 ml of purified water until a clean solution was formed under a constant stirring on a magnetic stirrer (100 rpm, 25 °C). After reconstitution, the pH of the colloidal solution was measured with WTW® inoLab® pH 7110 laboratory pH tester (Thermo Fisher Scientific, Budapest, Hungary). The osmolality of the in-water dispersed polymeric micelles was measured by means of an automatic osmometer (Knauer Semi-micro Osmometer, Berlin, Germany). Viscosity measurements were performed at 35 °C with a RheoStress 1 HAAKE instrument (Karlruhe, Germany) conducted with cone – plate geometry (radius: 49.9 mm, angle: 1°, gap: 0.052 mm). The apparent viscosity of the samples was measured over a shear rate sweep of 0.01 – 100 s⁻¹. Each measurement was carried out in triplicate with individual batches.

4.6.2. *Determination of thermodynamic solubility*

The thermodynamic solubility of MX and the SP – MX formulation was determined in purified water (pH = 6.4) at 25 °C, in SNES (pH = 5.6) at 35 °C and PBS (pH 7.4) at 37 °C to present the pH and temperature conditions of the nasal mucosa and the blood vessels. 1 – 1 ml of the liquids were measured, and the products were dissolved until visible saturation. A 72-h incubation time followed the process at the predetermined temperatures with a set stirring speed of 100 rpm. After incubation, they were filtered through a 0.22 µm pore sized polyether sulfone (PES) membrane filter and the content of the dissolved drug was determined via HPLC. Each measurement was carried out in triplicate with individual batches. Using the obtained solubility data, the following parameters were calculated (Eq. 2 – 4) [76]:

Molar solubilization capacity (χ) or moles of drug that can be solubilized per mol of co-polymer forming micelles:

$$\chi = \frac{S_{\text{tot}} - S_w}{C_{\text{copol}} - \text{CMC}} \quad (2)$$

Micelle – water partition coefficient (P), which is the ratio of the drug concentration in the micelle to the drug concentration in water:

$$P = \frac{S_{\text{tot}} - S_w}{S_w} \quad (3)$$

Standard free energy of solubilization (ΔG_s^0) estimated from the molar micelle – water partition coefficient (P_M):

$$\Delta G_s^0 = -RT \cdot \ln \frac{\chi \cdot (1 - \text{CMC})}{S_w} = -RT \cdot \ln (P_M) \quad (4)$$

In the equations S_{tot} means the total solubility of MX in the micellar solution, S_w is the solubility of MX in the dissolving media, CMC is the critical micelle concentration, C_{copol} is the copolymer concentration in each micellar solution and R is the universal constant of gases.

4.6.3. Determination of encapsulation efficiency

To determine the encapsulation efficiency (EE) of the optimized formulation, the indirect method was applied. The MX – containing polymeric micelles were separated from the aqueous medium via centrifugation using a Hermle Z323 K high performance refrigerated centrifuge (Hermle AG, Gosheim, Germany) at 17,500 rpm at 4 °C for 45 min. The clear supernatant was diluted 10 – fold with purified water. Quantitative measurements of MX were performed via HPLC. Each measurement was carried out in triplicate with individual batches. The EE was calculated via the following the equation [33, 72]:

$$EE(\%) = \frac{MX_{\text{initial}} (\text{mg}) - MX_{\text{measured}} (\text{mg})}{MX_{\text{initial}} (\text{mg})} \cdot 100 \quad (5)$$

4.6.4. Wetting properties and polarity calculation

OCA Contact Angle System (DataPhysics OCA 20, DataPhysics Inc., GmbH, Filderstadt, Germany) was used for studying the wettability of the optimized formulation in freeze – dried state. For the measurements, 0.10 g of powder was compressed under a pressure of 1 t by a Specac[®] hydraulic press (Specac Inc., Fort Washington, PA, USA). The liquid media used for the contact angle measurements included bidistilled water (interfacial tension of polar component (γ_i^p) = 50.2 mN/m, interfacial tension of disperse component (γ_i^d) = 22.6 mN/m) and diiodomethane (γ_i^p = 1.8 mN/m, γ_i^d = 49 mN/m). The contact angles of pressings were determined applying the method of Wu. The solid surface free energy is the sum of the polar (γ_i^p) and nonpolar (γ_i^d) components and was calculated according to the Wu equation (Eq. 6.) [77]:

$$(1 + \cos\Theta)\gamma_l = \frac{4(\gamma_s^d\gamma_l^d)}{\gamma_s^d\gamma_l^d} + \frac{4(\gamma_s^p\gamma_l^p)}{\gamma_s^p\gamma_l^p} \quad (6)$$

where Θ is the contact angle, γ_s is the solid surface free energy and γ_l is the liquid surface tension. The percentage polarity can be calculated from the γ^p and γ values (Eq. 7):

$$\text{Percentage polarity (\%)} = \frac{\gamma^p}{\gamma} \cdot 100 \quad (7)$$

4.6.5. X-ray powder diffraction study

The crystallinity of the formulations and the initial materials was measured with a Bruker D8 Advance X-ray powder diffractometer (Bruker AXS GmbH, Karlsruhe, Germany) with Cu K λ I radiation ($\lambda = 1.5406 \text{ \AA}$) and a VANTEC-1 detector. The samples were scanned at 40 kV voltage and 40 mA amperage. The angular rate was 3° to 40° 2θ , at a step time of 0.1 s and a step size of 0.007° . All manipulations and evaluations were carried out using DIFFRAC Plus EVA Software.

4.6.6. Raman spectroscopic measurement

For the Raman spectroscopic measurement of polymeric micelles, a Thermo Fisher DXR Dispersive Raman Instrument (Thermo Fisher Scientific, Inc., Waltham, MA, USA) equipped with a charge-coupled device (CCD) camera and a diode laser operating at 780 nm was used. Raman measurements were carried out with a laser power of 12 mW at 25 μm slit aperture size. The set exposure time was 2 s and the acquisition time was 6 s, for a total of 32 scans per spectrum in the spectral range of $3500 - 200 \text{ cm}^{-1}$ with cosmic ray and fluorescence corrections. The Raman spectra were normalized in order to eliminate the intensity deviation between the measured areas.

4.7. Long-term stability study

To determine the physical stability after freeze-drying the product in solid state, a long-term stability study was conducted in accordance with the ICH Q1A guideline in a refrigerator for 12 months at $5 \pm 3 \text{ }^\circ\text{C}$ [78]. Each month a portion was dissolved in purified water and then D_H and PdI were measured via the described DLS method. Each measurement was carried out in triplicate with individual batches.

4.8. Nasal applicability studies

4.8.1. In vitro drug release study

The modified paddle method (Hanson SR8 Plus, Teledyne Hanson Research, Chatsworth, CA, USA) was used to examine the rate of drug release of the SP-MX formulation compared to initial MX (suspended via 0.1% w/v hyaluronic acid solution). 1 – 1 ml of the dissolved SP-MX

formulation and the MX suspension were placed in dialysis bags (Spectra/Por[®] Dialysis Membrane with a MWCO value of 12-14 kDa (Spectrum Laboratories Inc., Rancho Dominguez, CA, USA)). 100 ml of SNES was applied as a dissolution medium at 35 °C. Each measurement was carried out in triplicate with individual batches.

4.8.2. *In vitro* mucoadhesion study

To investigate the mucoadhesive properties of the SP-MX formulation via tensile test, a TA-XT Plus (Texture Analyser (Metron Ltd., Budapest) instrument equipped with a 5 kg load cell and a 1 cm-in-diameter cylinder probe was used. The SP-MX formulation and blank SP solution were placed in contact with a wetted filter paper. For wetting, 50 µl of an 8 % w/w mucin dispersion as simulated mucosal membrane was used, where the mucin dispersion was prepared with a pH 5.6 SNES. Five parallel measurements were performed. 20 mg of the samples was attached to the probe and placed in contact with the mucin wetted filter paper. A 2500 mN preload was used for a duration of 3 min and the cylinder probe was moved upwards separating the sample from the substrate with a prefixed speed of 2.5 mm/min. The adhesive force as the maximum detachment force and the work of adhesion were measured. The work of adhesion was calculated as the area under the force versus distance curve (AUC). The formulations were thermostated at 35 °C for 30 min before the measurement and the experiment was carried out at this temperature. As references, SP and the SP-MX formulation were measured without the presence of mucin as negative controls, and as positive controls, 0.5 % w/v hyaluronic acid solution was applied due to its well-known mucoadhesive properties [79,80].

4.8.3. *Cell cultures*

Human nasal epithelial cells (RPMI 2650; ATCC cat. no. CCL 30) were grown in Dulbecco's Modified Eagle's Medium (DMEM, Gibco, Life Technologies, USA) supplemented with 10% fetal bovine serum (FBS, Pan-Biotech GmbH, Germany) in a humidified 37 °C incubator in presence of 5% carbon dioxide and 50 µg/ml gentamicin in order to prevent infection of the cells. The surfaces of the culture dishes were coated with 0.05% rat tail collagen dissolved in sterile distilled water before cell seeding and the medium was changed every 2 days. When RPMI 2650 cells reached approximately 80 – 90% confluency in the dish, they were trypsinized with 0.05% trypsin and 0.02% EDTA solution. One day before the experiment, retinoic acid (10 µM) and hydrocortisone (500 nM) were added to the cells to form a tighter barrier [81]. For the permeability measurements, epithelial cells were co-cultured with human vascular endothelial cells to create a more physiological barrier representing both the nasal epithelium and the submucosal vascular

endothelium [82,83]. The human vascular endothelial cells were differentiated from CD34⁺ stem cells isolated from human umbilical cord blood as described earlier [83]. Frozen batches of human vascular endothelial cells were received from the Laboratoire de la Barrière Hémato-Encéphalique, University of Artois, Lens, France. The endothelial cells were grown in endothelial culture medium (ECM-NG, Sciencell, USA) supplemented with 5% FBS, 1% endothelial growth supplement (ECGS, Sciencell, USA) and 0.5% gentamicin on 0.2% gelatin-coated culture dishes (10 cm diameter). For the permeability experiment, cells were used at passage 8.

4.8.4. Cell viability assay

To follow cell damage and/or protection in living barrier forming cells and to quantify the viability of adherent cells, real-time cell electronic sensing technique was used. To register the impedance of cell layers, a RTCA-SP instrument (ACEA Biosciences, USA) was used. The registration took place every 10 min, and the cell index was defined at each time point. The cell index was defined as $(R_n - R_b)/15$, where R_n is the cell-electrode impedance of the wall when it contains cells and R_b is the background impedance. E-plates with 96-well and built-in gold electrodes were coated in 0.2% gelatin and placed for 20 min in the incubator. After the incubation, the gelatin was removed and 50 μ l of the culture medium was added to each well. The dispensed RPMI 2650 cell suspension had a density of 2×10^4 cells/well. When cells reached a steady growth phase, they were treated with SP-MX and the building components. For the cell viability measurements 10 \times , 30 \times and 100 \times dilutions from SP-MX formulation as well as 2.5 mg/ml MX suspension, 83.3 mg/ml D-Tre, 16.7 mg/ml SP solutions, corresponding to the concentration of components in the SP-MX formulation were prepared in cell culture medium.

4.8.5. Permeability study on the cell culture model

Transepithelial electrical resistance (TEER) was measured to check the barrier integrity by an EVOM voltohmmeter (World Precision Instruments, USA) combined with STX-2 electrodes, and was expressed relative to the surface area of the monolayers as $\Omega \times \text{cm}^2$. TEER of cell-free inserts was subtracted from the measured data. After the cell layer reached steady TEER values, the cells were treated. RPMI 2650 cells were cultured on inserts (Transwell, polycarbonate membrane, 3 μ m pore size, 1.12 cm^2 , Corning Costar Co., MA, USA) placed in 12-well plates in the presence of endothelial cells for 5 days. To prepare the co-culture model, endothelial cells were passaged (1×10^5 cells/ cm^2) to the bottom side of tissue culture inserts coated with low growth factor containing Matrigel (BD Biosciences, NJ, USA) and nasal epithelial cells were seeded (2×10^5 cells/ cm^2) to the upper side of the membranes which were coated with rat tail collagen. For the permeability

experiments the inserts were transferred to 12-well plates containing 1.5 ml Ringer-HEPES buffer in the acceptor compartments. In the donor compartments 0.5 ml buffer was pipetted containing MX or the SP-MX polymeric micelle formulation. The plates were kept on a horizontal shaker (120 rpm) during the assay which lasted for 60 min. Samples from both compartments were collected and the MX concentration was measured by HPLC. To determine the tightness of the nasal epithelial co-culture model two passive permeability marker molecules were tested after the permeability experiment. In the donor compartments 0.5 ml buffer containing fluorescein isothiocyanate (FITC)-labeled dextran (FD10, 10 µg/ml; MW: 10 kDa) and Evans blue labeled albumin (167.5 µg/ml Evans blue dye and 10 mg/ml bovine serum albumin; MW: 67.5 kDa) was added. The inserts were kept in 12-well plates on a horizontal shaker (120 rpm) for 30 min. The concentrations of the marker molecules in the samples from the compartments were determined by a fluorescence multiwell plate reader (Fluostar Optima, BMG Labtechnologies, Germany; FITC: excitation wavelength: 485 nm, emission wavelength: 520 nm; Evans-blue labeled albumin: excitation wavelength: 584 nm, emission wavelength: 680 nm). The apparent permeability coefficients (P_{app}) were calculated as described previously [81]. Briefly, cleared volume was calculated from the concentration difference of the tracer in the acceptor compartment ($\Delta[C]_A$) after 30 min and in donor compartments at 0 h ($[C]_D$), the volume of the acceptor compartment (V_A ; 1.5 ml) and the surface area available for permeability (A ; 1.1 cm²) using Eq. 8.:

$$P_{app} \left(\frac{\text{cm}}{\text{s}} \right) = \frac{\Delta[C]_A \times V_A}{A \times [C]_D \times \Delta t} \quad (8)$$

For the permeability measurement, 2.5 mg/ml MX and 10× dilution of SP-MX were prepared in Ringer-Hepes buffer and added to the donor compartments.

4.8.6. Immunohistochemistry

To evaluate morphological changes in RPMI 2650 cells caused by the MX-loaded polymeric micelle formulation, immunostaining for junctional proteins *zonula occludens protein-1* (ZO-1) and *β-catenin* was made. After the permeability experiments, cells on culture inserts were washed with PBS and fixed with ice cold methanol-acetone (1:1) solution for 2 min then washed with PBS. The nonspecific binding sites were blocked with 3% bovine serum albumin in PBS. Primary antibodies rabbit *anti-ZO-1* (AB_138452, 1:400; Life Technologies, USA) and rabbit *anti-β-catenin* (AB_476831, 1:400) were applied as overnight treatment at 4 °C. Incubation with secondary antibodies anti-rabbit IgG Cy3 conjugated (AB_258792, 1:400) lasted for 1 h and Hoechst dye 33342 was used to stain cell nuclei. After mounting the samples (Fluoromount-G; Southern Biotech,

USA) staining was visualized by Leica TCS SP5 confocal laser scanning microscope (Leica Microsystems GmbH, Germany).

4.8.7. *Ex vivo permeability study across human nasal mucosa*

Ex vivo permeability tests were performed on human nasal mucosa (mucoperiosteum). The pieces of the nasal mucosa for primary study were collected during daily clinical routine nasal and sinus surgeries (septoplasty) under general or local anesthesia. The surgical field was infiltrated with 1 % w/v Lidocain-Tonogen local injection, and the mucosa was lifted from its base with a raspotirum or Cottle elevator. Transport from the operating room to the laboratory is performed in physiological saline solution. All experiments were performed freshly after the removal of the tissue. The experiments have been carried out under approval of University of Szeged's institutional ethics committee (ETT-TUKEB: IV/3880-1/2021/EKU).

To investigate *ex vivo* the transmucosal passive diffusion, a modified Side-Bi-Side[®] type horizontal diffusion apparatus was applied. The diffusion of MX suspension (2.5 mg/ml) and SP-MX formulation was tested across the excised human nasal mucosa. The nasal mucosa was mounted between the donor and the acceptor compartments with a diffusion surface area of 0.785 cm². The donor was prepared by mixing 1 ml of the formulations with 8 ml of SNES while the acceptor phase contained 9 ml of pH 7.4 PBS to simulate nasal conditions. The temperature of the chambers was controlled at 35 ± 0.5 °C using a heating circulator (ThermoHaake C 10-P5, Sigma-Aldrich Co., Ltd., Budapest, Hungary). The compartments were continuously stirred at 100 rpm using magnetic stirrers. 100 µl aliquots from the acceptor phase were taken at predetermined time points and immediately replaced with fresh medium. The concentration of MX was determined by HPLC. The flux (J (µg/cm²/h)) was calculated from the permeated drug quantity through the nasal mucosa (m_t), divided by the surface of the membrane insert (A) and the duration of the investigation (t) (Eq. 9). The permeability coefficient (K_p (cm/h)) was determined by dividing the flux (J) with the drug concentration in the donor phase (C_d (µg/cm³)) as seen in Eq. 10. [85].

$$J = \frac{m_t}{A \times t} \quad (9)$$

$$K_p = \frac{J}{C_d} \quad (10)$$

4.8.8. *In vivo animal studies*

All the experiments involving animal subjects were carried out with the approval of the National Scientific Ethical Committee on Animal Experimentation (permission number: IV/1247/2017). The animals were treated in accordance with the European Communities Council

Directives (2010/63/EU) and the Hungarian Act for the Protection of Animals in Research (Article 32 of Act XXVIII). A 60- μ g dose of MX from the 2.5 mg/ml SP-MX formulation was administered into the right nostril of 160 – 180 g male Sprague Dawley rats ($n=24$) via a pipette. At predetermined time points (5, 15, 30, 60, 120 and 240 min), the blood of the rats (under isoflurane anesthesia) was collected into heparinized tubes via cardiac puncture. Then, the animals were sacrificed by decapitation and brain tissues were removed, rinsed in ice-cold PBS, weighed and stored at $-80\text{ }^{\circ}\text{C}$ until assayed.

Plasma samples were centrifuged at $1500 \times g$ for 10 min at $5\text{ }^{\circ}\text{C}$. To 100 μ l of plasma sample, 10 μ l of 0.1 % w/v aqueous formic acid and 330 μ l acetonitrile containing 110 ng piroxicam (internal standard) were added and the mixture was spun for 60 s. The mixture was allowed to rest for 30 min at $-20\text{ }^{\circ}\text{C}$ to support protein precipitation. The supernatant was obtained via the centrifugation of the mixture for 10 min at $10,000 \times g$ at $4\text{ }^{\circ}\text{C}$. 20 μ l of clear supernatant was diluted using 380 μ l 0.1 % w/v aqueous formic acid and stirred for 30 s. 5 μ l was injected into the LC-MS/MS system for analysis. The rat plasma calibration standards of MX were prepared by moving the working standard solutions (in concentration range between 234 to 5000 ng/ml) into a pool of drug-free rat plasma. The sample preparation procedure described above was followed. The sample preparation procedure described above was followed.

Whole brain (1.6 to 2.0 g) of rats were homogenized in 1 % v/v aqueous acetic acid (1 g tissue/4 mL) using an UCD-500 ultrasonic cell disrupter (Biobase Biodustry, Shandong, China) in an ice bath for 2 min, interrupted by cooling. To 200 μ l of brain homogenate, 10 μ L of 0.1 % w/v aqueous formic acid and 630 μ l ice cold acetonitrile containing 1.6 ng piroxicam (internal standard) and 40 μ L 0.1 M perchloric acid were added. The mixture was vortex-mixed for 60 s and allowed to rest for 30 min $-20\text{ }^{\circ}\text{C}$. After centrifugation for 10 min at $10,000 \times g$ at $4\text{ }^{\circ}\text{C}$, 100 μ l supernatant was diluted with 100 μ l of 0.1 % w/v aqueous formic acid, vortexed and 20 μ l was analyzed by LC-MS/MS. Rat brain calibration standards of MX were prepared by moving the working standard solutions (in concentration range between 2.35 to 50 ng/ml) into a pool of drug-free rat brain homogenate. The sample preparation procedure described above was followed.

4.8.9. Quantification of MX in the *in vivo* samples

The quantitative analysis of MX for the *in vivo* studies was performed by using a Waters Acquity I-Class UPLCTM system (Waters, Manchester, UK), connected to a Q ExactiveTM Plus Orbitrap mass spectrometer (Thermo Fisher Scientific, San Jose, CA, USA) equipped with a heated ESI ion source (HESI). As internal standard piroxicam was used. Gradient chromatographic separation was performed at room temperature on a Acquity BEH C18 column (50 mm \times 2.1 mm,

particle size 1,7 μm) protected by a C18 guard column (2×2 mm, Phenomenex, Torrance, CA, USA) by using 0.1% aqueous formic acid as Solvent A and acetonitrile with 0.1% formic acid as Solvent B. The gradient applied for the analysis can be seen in Table 2.

Table 2. Gradient applied for the analysis of MX using LC-MS/MS analysis for the *in vivo* studies.

Time (min)	Eluent A (%)	Eluent B (%)	Flow rate ($\mu\text{g}/\text{min}$)
0	65	35	300
2	45	55	300
2.1	0	100	600
2.6	0	100	600
2.7	65	35	600
3.7	65	35	600
3.8	65	35	300
4.5	65	35	300

The mass spectrometer was used in a positive mode with the following parameters of the HESI source: spray voltage at 3.5 kV, capillary temperature at 256 $^{\circ}\text{C}$, aux gas heater temperature at 406 $^{\circ}\text{C}$, sheath gas flow rate at 47.5 l/h, aux gas flow rate at 11.25 l/h, sweep gas flow rate at 2.25 l/h, and S-lens radio frequency level at 50.0 (source auto-defaults). Parallel-reaction-monitoring (PRM) mode was used for quantifying by monitoring the following transitions: m/z 352 \rightarrow 115 for MX and m/z 332 \rightarrow 95 for piroxicam. The normalized collision energies for specific quantification were optimized to maximize the sensitivity. The NCEs were 24 for MX and 29 for piroxicam. A valve placed after the analytical column was programmed to switch the flow onto MS only when analytes of interest elute from the column (1.15–2.15 min) to prevent excessive contamination of the ion source and ion optics. Washing procedures of the autosampler before and after injecting samples were programmed in order to avoid the carry-over of analytes. Data acquisition and processing were carried out using Xcalibur and Quan Browser (version 4.5.474.0) software (Thermo Fisher Scientific, San Jose, CA, USA).

4.8.10. Pharmacokinetic studies

Pharmacokinetic parameters were analyzed via PK Solver 2.0 Software through non-compartmental analysis of the measured brain and plasma data. The area under the curve (AUC) of the time (min) – concentration curves of each animal were fitted with a linear trapezoidal method. All reported data are means \pm SD ($n=4$)

5. RESULTS AND DISCUSSION

5.1. Risk assessment of meloxicam-loaded polymeric micelles

As part of a QbD-based formulation study, a proper knowledge space is wished to be set up followed by the critical analysis of the collected variables by initial risk assessment and later by the evaluation of a factorial design. During our research work, previously we reported a general knowledge space development on polymeric micelles in general where numerous articles were analyzed to find all the variables affecting the safety, efficacy and quality of this specific nano drug delivery system [66]. Based on our findings, in addition to the EMA regulations, specific QTPPs, CQAs, CMAs and CPPs were identified [86]. At first, the specifications were listed as the QTPP elements of the proposed formulation (Table 3.)

Table 3. Quality Target Product Profile elements, the target and their justification regarding MX-loaded polymeric micelles for intranasal administration

QTPP element	Target	Justification
Indication	Inflammation	NDs, such as Alzheimer’s Disease and Multiple Sclerosis usually pairs with inflammation in the CNS resulting in decreasing quality of life.
Target patients	Adult (> 18 years)	The listed NDs usually concern adult, mostly elderly patients.
Administration route	Nasal	The API can directly reach the CNS bypassing the first-pass effect via “nose-to-brain” pathways.
Site of activity	CNS	COX enzymes play a large role locally in the CNS mediating neuroinflammation.
Absorption feature	Rapid uptake by the nasal mucosa	This QTPP is closely related to dissolution and permeability, which two main factors must be fitted to the requirements of the nasal administration route. With high absorption in a short period of time a rapid onset of action can be achieved which feature can be utilized as a reliever for neuroinflammation besides sustained therapy.
Drug release profile	Immediate	The duration of stay is around 15 to 20 min in the nasal cavity due to the mucociliary clearance.
Nanocarrier	Monodisperse polymeric micelles	The proper particle characteristics are a critical parameter in absorption from the nasal mucosa exploiting the “nose-to-brain” pathway. Furthermore, increase in specific surface area and decrease in size contributes to higher water solubility, leading to faster drug release and permeation.

Based on Table 3, our formulation QTPP can be characterized as a nano drug delivery system with a particle size between 10 to 200 nm in monodisperse distribution which contains MX encapsulated into a polymeric micelle formulation. If placed on market, adult patients should receive this preparation where the main indication would be inflammation in the central nervous system, as the site of action. It should be fit to the nasal administration criteria and should provide immediate drug release and would show a rapid uptake across the nasal mucosa. As these propositional statements were defined, the next step was to perform the risk assessment amongst the determined CQAs and QTPPs (Figure 4.)

QTPPs CQAs	Indication	Target patients	Administration route	Site of activity	Absorption feature	Drug release profile	Nanocarrier	Severity score (%)
Particle size	MEDIUM	LOW	HIGH	HIGH	HIGH	HIGH	HIGH	21.84
Excipients	LOW	LOW	MEDIUM	MEDIUM	HIGH	HIGH	HIGH	17.51
Solubility	MEDIUM	LOW	HIGH	MEDIUM	HIGH	HIGH	HIGH	11.49
Drug release time	LOW	LOW	HIGH	MEDIUM	MEDIUM	HIGH	HIGH	8.92
Permeability rate	HIGH	LOW	HIGH	HIGH	HIGH	MEDIUM	MEDIUM	8.49
Encapsulation efficiency	MEDIUM	LOW	MEDIUM	MEDIUM	HIGH	HIGH	MEDIUM	8.03
Wettability	MEDIUM	LOW	MEDIUM	MEDIUM	HIGH	HIGH	MEDIUM	6.26
Structure	LOW	LOW	MEDIUM	LOW	MEDIUM	MEDIUM	MEDIUM	5.75
Physical appearance	LOW	LOW	MEDIUM	HIGH	MEDIUM	MEDIUM	LOW	5.06
Stability	LOW	LOW	LOW	LOW	MEDIUM	LOW	LOW	3.77
Toxicity	LOW	LOW	MEDIUM	LOW	LOW	LOW	LOW	2.88

Figure 4. Interdependence rating amongst the CQA and QTPP elements. All connections are described with high/medium/low relations. The last column represents the severity score percentage of the CQA elements in decreasing order compared to the cumulative severity scores.

The first interdependence rating revealed that particle characteristics are much more risky factors compared to the nasal administration related factors. This theorem is highly supported as most factorial design-based optimization processes would consider these factors as the main dependent variables. Our quality criteria are that the particle size should be between 10 to 200 nm in monodisperse distribution. The excipients, such as the SP itself was predetermined, therefore even though the risk is high, it has a set qualitative aspect. However quantitatively it should be optimized. The following CQAs on the list of the first column were all later-on investigated factors.

The next step was to determine which CMA/ CPP factors can be characterized with high-risk ratios, therefore an interdependence rating amongst CQAs and CMAs/ CPPs was evaluated (Figure 5.)

CMA/CPPs CQAs	Composition	Mixing time	Rotation pressure	Rotation temperature	Rotation speed
Particle size	HIGH	HIGH	MEDIUM	MEDIUM	MEDIUM
Excipients	HIGH	MEDIUM	LOW	MEDIUM	LOW
Solubility	HIGH	HIGH	HIGH	MEDIUM	MEDIUM
Drug release time	HIGH	MEDIUM	LOW	LOW	MEDIUM
Permeability rate	HIGH	MEDIUM	MEDIUM	MEDIUM	MEDIUM
Encapsulation efficiency	HIGH	HIGH	MEDIUM	MEDIUM	LOW
Wettability	HIGH	MEDIUM	MEDIUM	MEDIUM	LOW
Structure	HIGH	LOW	LOW	MEDIUM	LOW
Physical appearance	MEDIUM	MEDIUM	LOW	LOW	MEDIUM
Stability	HIGH	LOW	LOW	LOW	LOW
Toxicity	MEDIUM	MEDIUM	LOW	LOW	LOW
Severity score (%)	47.78	21.88	15.39	7.82	7.13

Figure 5. Interdependence rating amongst the CQA and CMA/CPP elements. All connections are described with high/medium/low relations. The last row represents the severity score percentage of the CMA/CPP elements in decreasing order compared to the cumulative severity scores (%).

Based on the risk assessment specified on the thin-film hydration method aiming to formulate optimized polymeric micelles, it has been revealed that the composition of the formula has the highest risk factor besides time. Therefore, later the composition of each excipient was chosen as part of the factorial design. MX concentration was set with the goal of 2.5 mg/ml in the final product. The mixing time was not set prior the optimization process as volumes would vary prior to solvent extraction. The criterion was that it should be visibly dry after appropriate extraction.

5.2. Optimization via Box-Behnken factorial design

Based on the 3-level, 3-factor Box-Behnken factorial design, a 15-run experimental optimization was performed. The D_H and the PdI values were measured in triplicate from 3 individual batches. The results of the factorial design can be seen in Table 4. where the variability of the results proves the impact of the selected factors on the formulation.

Table 4. Results of the 3-level, 3 -factor Box-Behnken factorial design. Experiments were run in triplicate and data are presented as means \pm SD ($n = 3$). The average hydrodynamic diameter and the polydispersity index were measured via dynamic light scattering.

Run No.	Independent variables			D_H (nm)	PDI
	Soluplus [®] (mg/ml)	Ethanol (ml)	1M NaOH (ml)		
1	6.0	5.0	4.5	194.5 \pm 1.8	0.411 \pm 0.02
2	12.0	5.0	4.5	188.0 \pm 3.9	0.299 \pm 0.01
3	6.0	10.0	4.5	94.87 \pm 1.1	0.155 \pm 0.02
4	12.0	10.0	4.5	270.1 \pm 2.0	0.513 \pm 0.02
5	6.0	7.5	3.0	105.6 \pm 0.9	0.164 \pm 0.01
6	12.0	7.5	3.0	170.4 \pm 5.6	0.477 \pm 0.01
7	6.0	7.5	6.0	116.2 \pm 1.5	0.140 \pm 0.03
8	12.0	7.5	6.0	200.1 \pm 7.3	0.344 \pm 0.05
9	9.0	5.0	3.0	195.0 \pm 2.3	0.377 \pm 0.05
10	9.0	10.0	3.0	111.6 \pm 3.0	0.114 \pm 0.06
11	9.0	5.0	6.0	65.42 \pm 1.6	0.401 \pm 0.02
12	9.0	10.0	6.0	99.53 \pm 1.7	0.444 \pm 0.03
13	9.0	7.5	4.5	99.86 \pm 0.5	0.134 \pm 0.04
14	9.0	7.5	4.5	100.1 \pm 0.7	0.155 \pm 0.01
15	9.0	7.5	4.5	107.7 \pm 3.1	0.163 \pm 0.05

Based on the results of the factorial design, polynomial equations were generated aiming to describe the main and interaction effects of the chosen independent variables based on their impact of the dependent factors. The effect on the average hydrodynamic diameter can be seen in Eq. 11.:

$$D_H = 150.94 + 40.52x_1 - 7.03x_2 - 5.09x_3 + 45.43x_1x_2 + 4.78x_1x_3 + 29.38x_2x_3 - 28.63x_1^2 - 13.53x_2^2 + 5.87x_3^2 \quad (11)$$

The regression coefficient of the surface plot was 0.999 (R^2) whilst the adjusted regression coefficient was 0.993 ($R^{2, \text{adj}}$) indicating good and proper correlation. The concentration of SP (x_1) and the interaction coefficient between the concentration of SP and volume of ethanol (x_1x_2) were significant ($p < 0.05$). The positive coefficients indicate an increase in the average hydrodynamic diameter, if the parameter value is increased, whilst the negative ones are beneficial as they steer the formulation direction towards particle size reduction. The effect on polydispersity index was also evaluated which can be seen in Eq. 12.:

$$PDI = 0.319 + 0.084x_1 - 0.025x_2 + 0.003x_3 + 0.118x_1x_2 - 0.027x_1x_3 + 0.077x_2x_3 + 0.084x_1^2 - 0.025x_2^2 - 0.030x_3^2 \quad (12)$$

The resulting R^2 and $R^{2, \text{adj}}$ was 0.999 and 0.993, respectively, also indicating good correlation. The concentration of SP (x_1) and the volume of ethanol (x_2) had significant ($p < 0.05$) effect on the PdI of the formulations prepared in the 15-run trial. The same tendency can be observed here, just like in case of the D_H equation: increasing the value of the independent factors after the positive coefficients are unbeneficial, as they tend to form polydisperse formulations, whilst the negative ones are beneficial leading to a monodisperse formulation.

Based on the results of the factorial design, 3D contour plots were plotted (Figure 6.) which plots serve as the design space aiming to reach the proper formulation with nano particle size in monodisperse distribution. Most of the contour plots show one minimum points indicating that an adequate design was evaluated in accordance with the resulting regression coefficients. Based on equations 11. and 12., taking into consideration the effect of each coefficient and interaction coefficient and the 3D surface plots, the formulation methodology is the following for the optimized formulation: 15 mg of MX was dissolved in 10 ml Ethanol and 3 ml 1 M NaOH solution, followed by the dissolution of 100 mg SP. The following steps were the previously described rotary evaporation, the hydration and pH setting step with 6 ml of purified water and finally, the freeze-drying. The final product was named SP-MX. Solid-state characterization was performed with the freeze-dried product, whilst the in-water dispersed formulation with 2.5 mg/ml concentration of MX was applied for the liquid-state characterization and nasal studies.

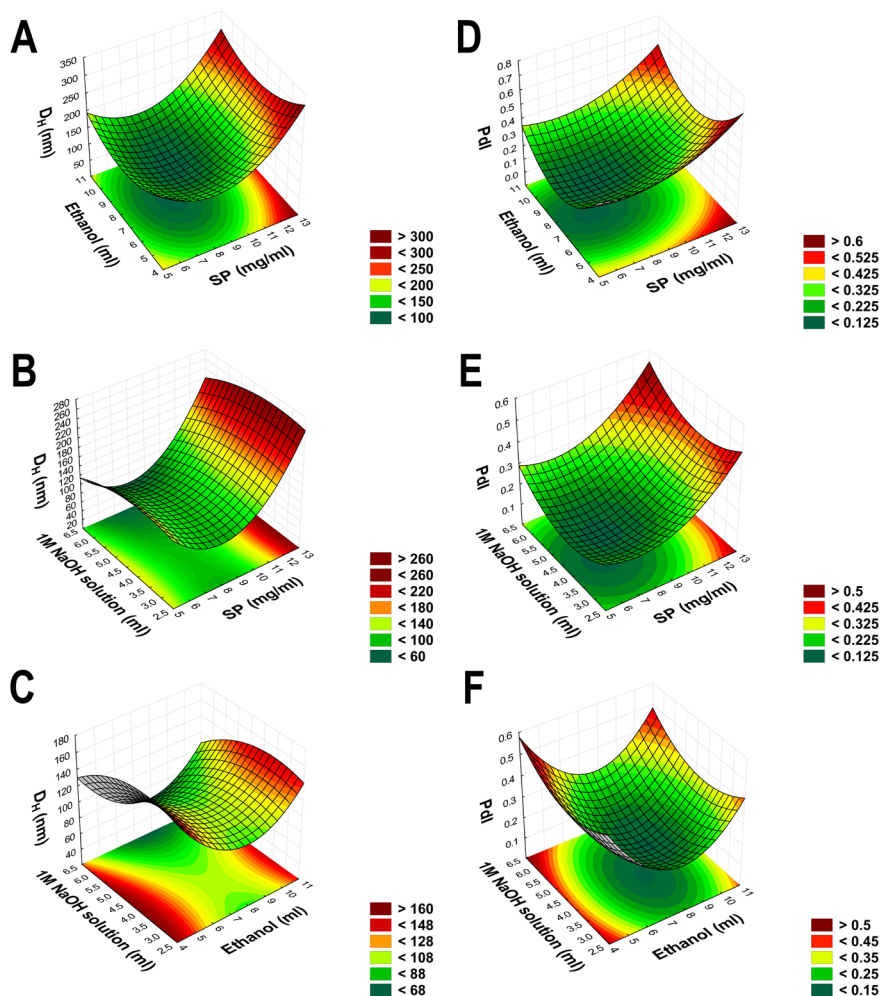


Figure 6. 3D surface plots based on the optimization process via the Box-Behnken factorial design. The effect of the independent factors on D_H (A-C) and on PDI (D-F).

5.3. Residual organic solvent content

According to the ICH Q3C (R5) guideline for residual solvents, all newly formulated pharmaceutical products must meet the criteria based on the solvent's classification [75]. Ethanol is in the class 3 solvent, meaning it has a low toxic potential. It is considered that the amount of ethanol should be below 5000 ppm per day. Based on the gas chromatographic investigation, the SP-MX formulation contains 0.1013 ± 0.0046 ppm Ethanol, which is significantly below the maximum residual level. Therefore, it would cause no harm due to the residual solvents even if it is administered whole in one day. This is due to the highly efficient thin-film hydration method, as one of the greenest and commonly applied technique for organic solvent extraction.

5.4. *Micelle characterization*

5.4.1. *Characterization of the optimized ex tempore dispersed nasal formulation*

After the optimization via Box-Behnken design, the characteristic of the in-water dispersed nasal formulation was the following. The measured average hydrodynamic diameter (D_H) value was 111.6 ± 3.0 nm, which is optimal and in the typical particle size range of polymeric micelles (10 to 200 nm). This particle size reduction can be categorized in the nanoencapsulation techniques, where the reduction is achieved via additional excipients, such as the co-polymer SP applied in our study. Not only it would hold the benefits of a nanoparticle with increased solubility and surface area, but the building co-polymer's beneficial properties would also come to surface. As SP micelles have PEG as its hydrophilic corona, it would also increase the stability in the circulation and during biodistribution. It would also increase the residence time in the blood without degradation and prolong the efficient time during therapy. Besides micelle size, its distribution is of paramount importance as well. PdI refers to the micelle size distribution, which in the case of the SP-MX formulation was 0.114 ± 0.06 . PdI values below 0.3 are considered monodisperse, therefore our formulation met this criterion. Not only does it affect the colloidal structure and properties of the nanocarrier, but it would also affect the drug release and permeation profile. Uniform drug release and permeation would only be possible if the formulation is monodisperse, as highly variable and polydisperse formulation would cause fluctuations in these kinetic profiles. Zeta potential refers to the surface charge properties of the colloidal system in liquid state. In case of SP-MX formulation, the measured zeta potential was -25.2 ± 0.4 mV. It is a relatively high absolute value, which prevents the aggregation of the dispersed nanoparticles due to the repulsion forces amongst them. Polymeric micelles with negative surface charge or without charge can also be described as mucopenetrating micelles, where the mucus layer allows the micellar carrier to be absorbed via transcytosis or paracellular transport [87].

The reconstitution time of the freeze-dried SP-MX formulation was 2 s, which far exceeds the requirements of the European Pharmacopoeia (Ph. Eur. 10), stating that a freeze-dried product should be constituted to a solution using an appropriate diluent prior to patient administration in less than 3 min. The physiological pH in the nose is between 5.6 to 7.4 which allows normal ciliary function. Also in this slightly acidic environment, lysozyme, which is a natural antimicrobial agent in the nasal cavity, can exert its beneficial effects, therefore it is advised not to change this. Besides this, irritation could occur if major deviations would take place. The SP-MX formulation had a pH of 6.49 which fits this criterion. Nasal preparations in general are normally isotonic (about 290 mOsmol/l), however deviation from isotonicity can also be beneficial. Hypertonic solutions can cause a shrinkage in the epithelial cell layer and can inhibit the normal ciliary activity. In our case,

a hypotonic solution (240 ± 12 mOsmol/l) was obtained, which can increase drug absorption. The viscosity of the formulation was 32.5 ± 0.28 mPas which is sufficiently low enough that can be administered via a nasal spray device. Also, it helps with the faster drug release, as the matrix area for diffusion is not concise to the extent where it would prolong the drug liberation from the carrier [88].

5.4.2. Determination of thermodynamic solubility and encapsulation efficiency

The thermodynamic solubility of the SP-MX formulation compared to initial MX was measured via the saturation method at 3 different pH and temperature conditions representing the nasal, storage and the blood conditions. At 5.6 pH and 35 °C represents the nasal conditions, the 6.4 pH at 25 °C the storage conditions after *ex tempore* dispersion and the 7.4 pH at 37 °C the blood conditions. The calculated solubility – related factors can also be found in Table 4. besides the measured encapsulation efficiency by the indirect method.

Table 4. Solubility, encapsulation efficiency and the calculated solubility-related parameters of the SP-MX formulation (S_{tot}) compared to raw MX (S_w). Data are presented as means \pm SD from 3 individual batches.

pH	S_w (mg/l)	S_{tot} (mg/l)	χ	P	P_M	ΔG_s^0 (kJ/mol)	EE (%)
5.6	6.92 ± 0.19	5419.7 ± 1.284	0.54	782.20	77.68	- 10.983	89.4 ± 2.7
6.4	6.99 ± 0.45	5527.0 ± 1.197	0.55	789.70	78.34	- 10.813	92.1 ± 1.5
7.4	7.09 ± 0.33	5775.9 ± 0.789	0.57	825.45	81.98	- 11.363	89.9 ± 3.6

The solubility of the SP-MX formulation is significantly higher in all cases which can be contributed with the nano particle size in monodisperse distribution and the high (approx. 90%) encapsulation efficiency. The micelle-water partition coefficient (P) is significantly higher than 1.00, so does the molar micelle-water partition coefficient (P_M). It means that more MX molecules are localized inside the micellar hydrophobic core compared to the whole system itself. The free energies of solubilization (ΔG_s^0) are also high values with negative sign meaning that the polymeric micelle formation is favorable compared to the dissociation of these colloidal structures.

5.4.3. Wetting properties and polarity calculation

Wetting properties are of paramount importance if the aim is to develop a product with rapid reconstitution in water. The contact angle of MX against water is high showing high hydrophobicity, whilst the SP polymeric micelle-forming co-polymer and the SP-MX formulation had relatively low contact angles (Table 5.). The calculated polarity values also prove that an increase of polarity is experienced after the solubilization of MX with the nanocarrier. The polarity

increase can be due to the high volume and mass ratio of the polar D-Tre in the formulation and the high polarity of SP itself. The high polarity alongside the high encapsulation efficiency can explain the short reconstitution time of approx. 2 s and the increased thermodynamic water solubility as measured before.

Table 5. Contact angles against water and diiodomethane, the calculated surface free energies and the polarity values of the SP-MX formulation (in freeze-dried state) compared to the initial MX and SP co-polymer. Data of contact angles are presented as means \pm SD ($n = 3$)

Samples	Θ_{water} [°]	$\Theta_{\text{diiodomethane}}$ [°]	γ^d [mN m ⁻¹]	γ^p [mN m ⁻¹]	γ [mN m ⁻¹]	Polarity (%)
MX	75.3 \pm 5.2	16.2 \pm 3.3	44.7	9.3	54.0	17.1
SP	33.4 \pm 0.3	16.4 \pm 0.0	44.02	29.20	73.22	39.6
SP-MX	11.3 \pm 0.5	23.4 \pm 0.1	42.08	37.13	79.21	47.0

5.4.4. X-ray powder diffraction study

On the diffractograms of initial MX, sharp and well-structured crystalline structure can be found, whilst in case of the micelle-forming SP, an amorphous diffractogram is visible. In the final product, also an amorphous structure is found, which can be due to the amorphous SP itself and D-Tre is also known for full amorphization after freeze- or spray drying. Since MX has a poor glass forming property ($T_g/T_m = 0.63$), it was proved before that it does not go through amorphization, so this theorem can be omitted. Most likely, which corresponds to the high encapsulation efficiency, MX become molecularly dispersed in the core of polymeric micelles and the amorphous sign of SP as micelle forming excipient suppressed the characteristic peaks of MX (Figure 7.). The amorphous nature also contributed to the rapid dispersion time.

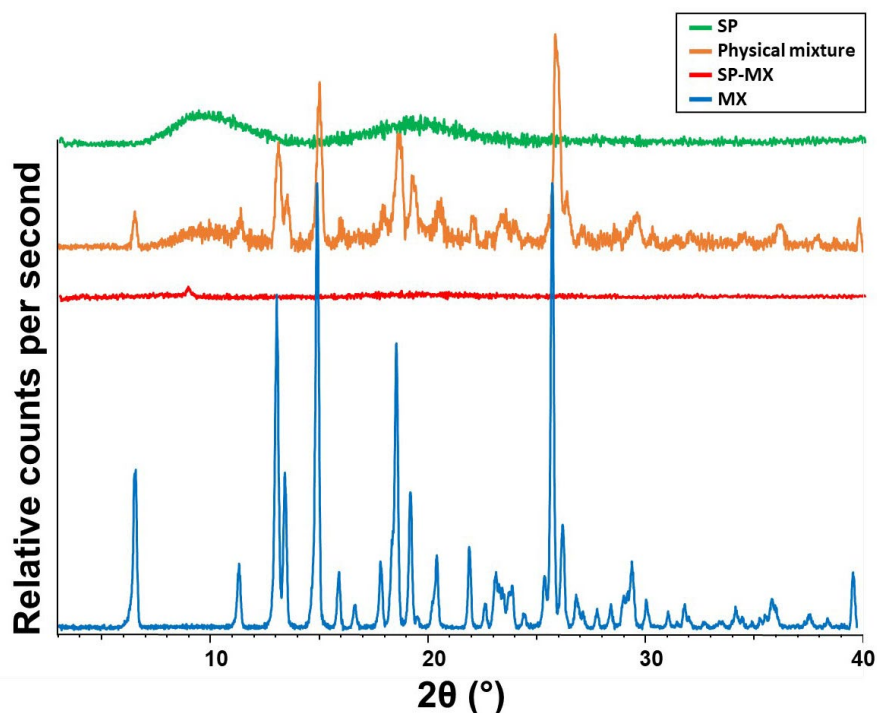


Figure 7. X-ray powder diffractograms of the initial MX, SP and the SP-MX formulation between 3 – 40° 2θ angles.

5.4.5. Raman spectroscopic measurement

Raman spectra of initial MX, SP, the physical mixture and the SP-MX formulation is shown in Figure 8. Aromatic ring vibration of benzothiazine at 1598 cm^{-1} can be found in the spectrum of MX, which derives from the bending vibration of CH_2 and the stretching vibration of $\text{C}=\text{C}$ or $\text{C}=\text{N}$ groups. A sharp peak can be also found at 1532 cm^{-1} which indicates a stretching vibration of $\text{C}=\text{N}$ in the thiazole ring of the molecule. Some other characteristics can be found at the following peaks: 1305 cm^{-1} (ν_{OH}), 1267 cm^{-1} ($\nu_{\text{C-N-C}}$) and 1164 cm^{-1} ($\nu_{\text{C-S}}$). A shift can be found in the SP-MX formulation as the band located at 1305 cm^{-1} in case of raw MX has shifted to higher energy at 1394 cm^{-1} as a result of deprotonation. The appearance of a new peak due to the deprotonation of phenolic OH changed the vibrational motion of $\text{C}=\text{C}$ and $\text{C}=\text{N}$ bonds. The magnitude of 89 cm^{-1} reflects the OH group attached to the 6-membered heteroatom ring attends in the hydrogen bond formation with SP.

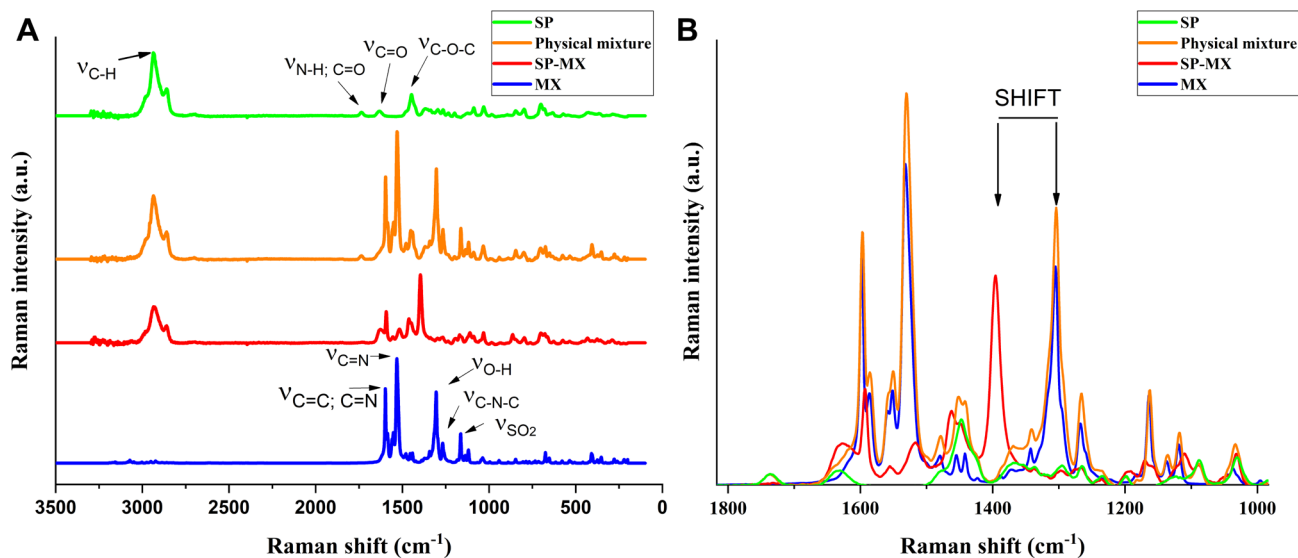


Figure 8. (A) Raman spectra of MX, SP, the physical mixture and the SP-MX formulation and (B) the enlarged region of the structural change.

5.5. Long – term stability study

In order to investigate the physical stability in solid state, a long-term stability study was conducted for 12 months. As the main goal was to formulate an *ex tempore* dispersible nasal product, each month a portion of the freeze-dried powder was dissolved in purified water followed by DLS measurements. The D_H and the PdI values were measured as main critical parameters. To calculate the absolute change, data value of the measurement of the freshly prepared formulation was subtracted from the final, 12th month measurement point. The D_H increased by 3.31 nm and the PdI by 0.016 after 12 months of storage (Table 6.). The results also prove that 5 % w/w D-Tre was a suitable choice as a cryoprotectant.

Table 6. Results of the 12-month physical stability examination. D_H and PdI values are means \pm SD ($n = 3$).

Sampling (month)	D_H (nm)	PdI
0	100.47 \pm 0.87	0.149 \pm 0.01
1	100.79 \pm 0.51	0.151 \pm 0.04
2	100.88 \pm 0.82	0.152 \pm 0.02
3	100.86 \pm 1.03	0.152 \pm 0.03
4	101.05 \pm 0.41	0.153 \pm 0.05
5	101.11 \pm 0.93	0.155 \pm 0.01
6	101.19 \pm 0.48	0.154 \pm 0.04
7	101.22 \pm 0.21	0.154 \pm 0.06
8	101.79 \pm 0.81	0.156 \pm 0.07
9	101.76 \pm 1.15	0.160 \pm 0.04
10	101.94 \pm 0.77	0.161 \pm 0.03
11	102.56 \pm 0.42	0.163 \pm 0.08
12	103.78 \pm 0.36	0.165 \pm 0.04
Absolute change	+ 3.31	+ 0.016

5.6. Nasal applicability studies

5.6.1. *In vitro* drug release study

In vitro drug release study was performed under simulated nasal conditions. Since no Pharmacopoeia directive states the drug release and dissolution studies of nasal liquid preparations, the dialysis bag method was applied which is commonly utilized in nanoparticle release behavior characterization. Dialysis bags with 12 – 14 kDa MWCO value have proved successful utilization before, especially designed for nanoparticulate systems for ocular, vaginal and nasal drug delivery routes. The higher drug release of the SP-MX formulation can be derived to the increased solubilized concentration which equals to the thermodynamic water solubility of MX in the formulation compared to raw MX alongside with the high polarity and nano particle size range. In the first 15 to 20 min, a burst effect can be experienced which is typical for drug delivery systems with rapid drug release (Figure 9.). It is critical in nasal administration, as the average residence time is approximately less than 20 min. Therefore, the SP-MX formulation met this criterion.

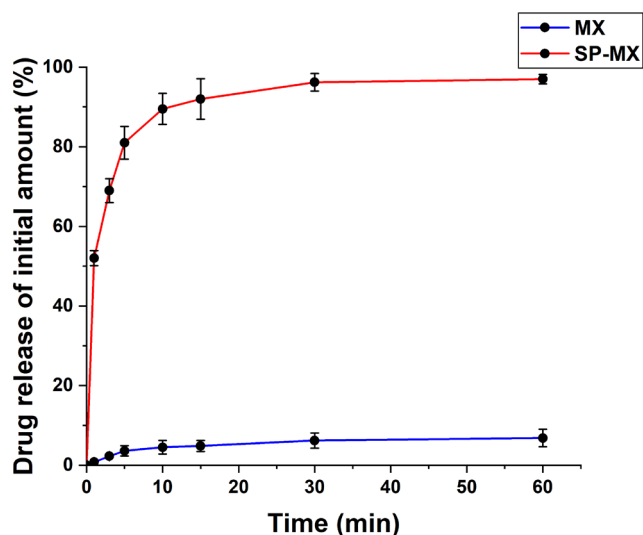


Figure 9. *In vitro* drug release curve of the SP-MX nanoformulation compared to initial MX suspension, measured via the dialysis bag method. Data are presented as means \pm SD ($n = 3$).

5.6.2. *In vitro* mucoadhesion study

The *in vitro* mucoadhesion study revealed that mucoadhesion between the mucin and the SP co-polymer and the SP-MX formulation has moderate values compared to strong mucoadhesive agents such as hyaluronic acid. This is represented by the measured mucoadhesive force and the calculated mucoadhesive work (Figure 10.). In our case, not too strong mucoadhesion, as the degree of physical and chemical bond formation between the outer PEG 6000 chain and the mucin, is beneficial as it would not hinder the rapid drug release and permeation through the nasal mucosa. As the QTPPs stated, a rapid liberation and absorption profile is expected. Despite this, a slight mucoadhesion can be observed which would help the carrier to reside in the nasal cavity for the desired 15 to 20 min period and work against the mucociliary clearance without suppressing the normal ciliary function. Without mucin, negligible adhesion properties could be experienced which also indicates that the main forces occur between the formulation and the mucin itself. Thus, as the value of mucoadhesive force and work regarding the formulation and the co-polymer SP solution lies in between these values, a moderately high mucoadhesion can characterize the product.

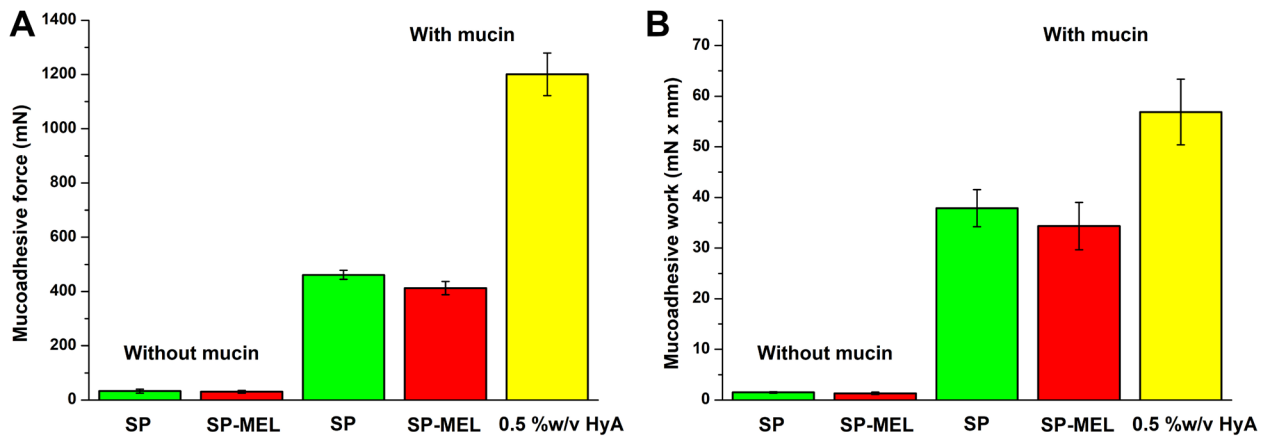


Figure 10. *In vitro* mucoadhesion study on SP solution and the SP-MX formulation at nasal conditions. Data are presented as means \pm SD ($n = 5$).

5.6.3. Cell viability assay

The cell viability assay proved that all components of the SP-MX formulation and SP-MX itself is non-toxic for the nasal cell line. This is corroborated with the high safety profile of SP, as clinical trials stated that 114 mg/kg of SP can be considered safe. Figure 11. shows the normalized cell ratio compared to the positive control physiological saline solution and the negative control Triton-X 100 detergent. This also proves the superiority of polymeric micelle forming co-polymers compared to classic surfactants, as they are less likely to cause nasal irritation and toxicity. Similar findings on other nasal cell lines (HT29-MTX) were found by Alopaeus et al., where even a high, 10 % w/w SP solution did not show any cytotoxic effect [89].

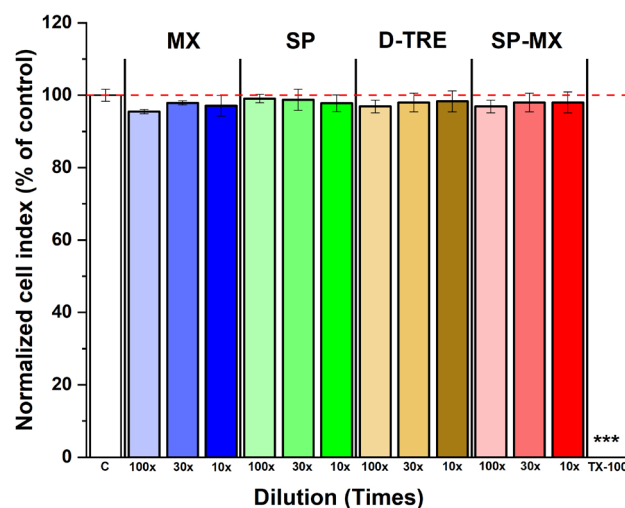


Figure 11. Cell viability of RPMI 2650 nasal epithelial cells after the treatment of SP-MX and its components measured by impedance. The values are presented as a percentage of the control group and as means \pm SD ($n = 6-12$). Statistical analysis: ANOVA followed by Dunett's test. *** $p < 0.01$.

5.6.4. MX permeability across the culture model of the nasal mucosa barrier

MX permeability across the nasal co-culture model showed a 5-fold increase compared to raw MX after the 1-hour treatment. The P_{app} value for MX was 8.265×10^{-6} cm/s and for the SP-MX formulation, it was 5.1116×10^{-5} cm/s. This significantly higher (***, $p < 0.001$) apparent permeability values can be validated by the nano particle size and the permeability enhancing effect of SP besides the increase in water solubility. TEER values were found good as reported before indicating that cell integrity and barrier property did not change during the measurement as they remained at the level of the control group validating the permeability model and the study.

5.6.5. Immunohistochemistry

We found no change in the staining pattern compared to the control group neither in case of MX nor the SP-MX formulation after the 1-hour treatment (Figure 12.). The cells remained cobblestone shaped with the visible junctional proteins (*ZO-1* and β -catenin) in a belt-like manner at the cell borders. The microscopic imaging also confirmed safe administration of MX and SP-MX intranasally corroborating the results from the impedance-based toxicity investigation.

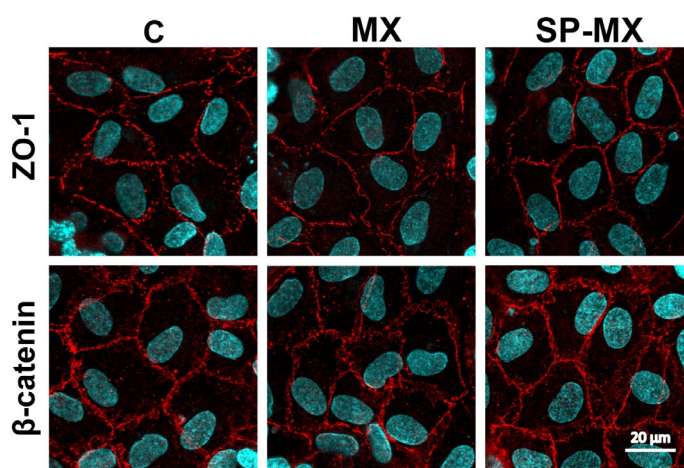


Figure 12. Immunostained junctional linker proteins on the human RPMI 2650 nasal epithelial cell layers after 1-hour of treatment with MX and SP-MX formulation. The control (C) group only received cell medium. Red color shows the stained junctional proteins and cell nuclei are blue.

5.6.6. Ex vivo permeability measurement across nasal mucosa

Ex vivo permeability measurements were carried out in order to describe the passive diffusion tendency of the SP-MX formulation compared to the initial MX. After quantification of the aliquots via HPLC, the cumulative permeability was calculated and was depicted as a function of time as it can be seen in Figure 13.

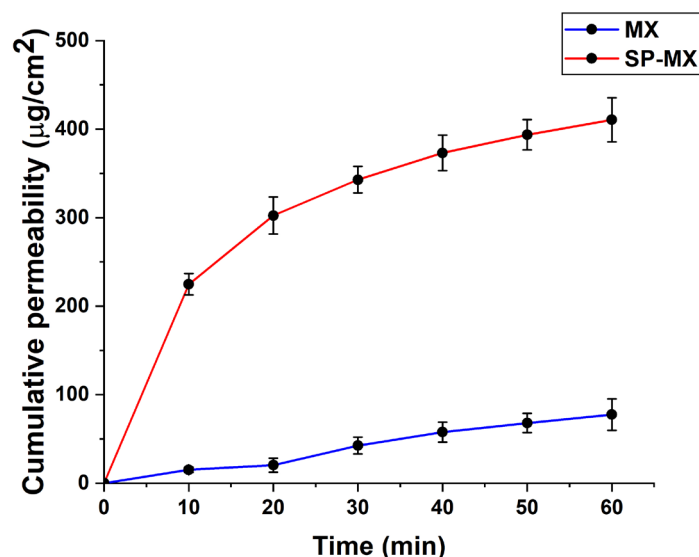


Figure 13. Result of the *ex vivo* quantitative permeability measurement across human nasal mucosa performed in a horizontal Side-bi-Side[®]-type diffusion cell. The cumulative permeability of SP-MX compared to MX is shown as a function time. All measurement were carried out in triplicate and data are presented as means \pm SD ($n = 3$).

The higher cumulative permeability values are contributed to the rapid and high-degree drug release of the formulation compared to raw MX. The nano size range also favors drug penetration across mucosal barriers. A burst-like drug permeation can be found in the first 15 to 20 min of the measurement similarly to the drug release study. This also proves that the moderate mucoadhesion would not affect this desired aim. Since the burst-like drug release and permeation are both presented in the same amount of time, no lag time could be expected resulting in immediate absorption. The calculated permeability coefficient is 0.493 cm/h and the calculated flux at the final time point is 410.54 $\mu\text{g}/\text{cm}^2$ regarding the SP-MX formulation. These values are significantly higher compared to the reference initial MX, where they were 0.068 cm/h and 77.491 $\mu\text{g}/\text{cm}^2$, respectively (** $p < 0.001$ in both cases).

5.6.7. *In vivo* pharmacokinetic study

During the *in vivo* pharmacokinetic study with the intranasally administered SP-MX formulation, plasma and brain concentration levels were determined via the described LC-MS/MS analytical method. The plasma and brain concentrations can be found on Figure 14.

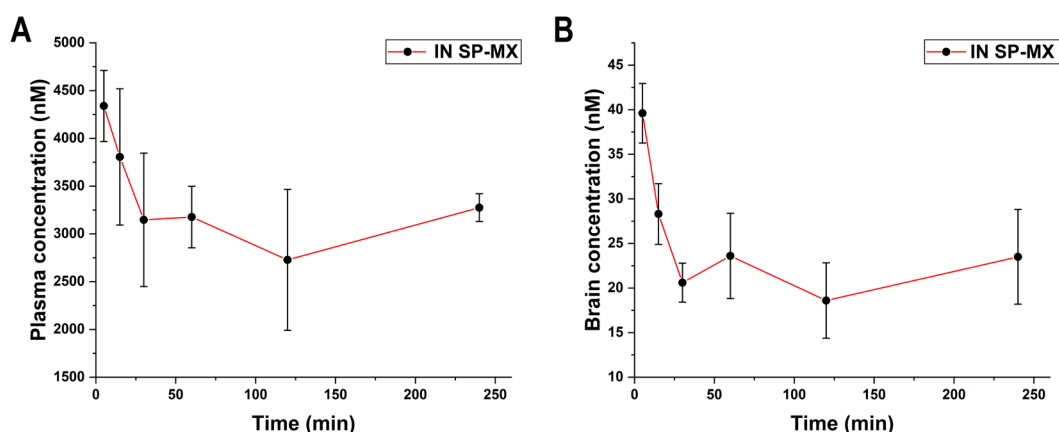


Figure 14. Results of the *in vivo* measurements in Sprague Dawley rats after the intranasal administration of the SP-MX formulation. (A) Plasma concentration levels and (B) Brain concentration levels of MX. Data are presented as means \pm SD ($n=4$).

As a reference data, our research group's intranasal and intravenous (IV) reference data were used in this discussion section [90]. Plasma levels did not reach the level of the IV data, which is reasonable as it is a natural law that the entire API enters the bloodstream immediately after IV administration. However, the brain concentrations exceed our previous findings. Bartos et al. investigated the effect of size reduction techniques such as spray drying on MX and its brain targetability after intranasal (IN) administration. In their case, the achieved MX concentration was less than 1 nM in all cases: IN and IV administration. Compared to our results, approx. 35 to 40-times higher concentration were achieved regarding the brain levels. The higher area under the curve (AUC) values also indicate that higher effective MX concentration was achieved in the central nervous system. See: approx. 35 nM \times min in case of the spray-dried formulation vs. approx. 5000 nM \times min in case of the SP-MX formulation. The superiority of nanocarriers over classic, only physical particle size reduction techniques have been proven. As mentioned earlier, *in vitro* and *ex vivo* studies corroborated that a burst-like drug release and absorption could be expected after IN administration. The highest concentration in the brain appeared after 5 min, which fact corroborates this theorem. A second new peak can be observed at lower concentrations at the 60-min time interval, which indicates that a slight portion of MX reached the brain after the delay. The rapid onset of action predicts the nose-to-brain rapid and direct transport, whilst the later one describes a typical nose-to-blood carrier system prior to BBB penetration. A slight increase can be observed at the final time point, meaning that prolonged effect and CNS targeting could be also achieved. The supporting pharmacokinetic parameters can be found in Table 7. calculated from the plasma and brain concentration vs. time curves.

Table 7. Calculated pharmacokinetic parameters of the IN administered SP-MX formulation. All data are presented as means \pm SD ($n=4$). Abbreviations: K_e – elimination rate constant; $t_{1/2}$ – half-time; AUC_{0-t} – area under curve value between 0 and the measurement time (t); $AUC_{0-\infty}$ -area under curve value between 0 and infinity; Cl – Clearance; MRT – mean residence time.

Pharmacokinetic parameter	Plasma	Brain
K_e (min^{-1})	$0.00091 \pm 2.2 \cdot 10^{-4}$	$0.00132 \pm 3.6 \cdot 10^{-5}$
$t_{1/2}$ (h)	804.143 ± 22.362	525.174 ± 14.378
AUC_{0-t} ($\mu\text{mol/ml} \times \text{min}$)	811.228 ± 12.281	5.263 ± 0.051
$AUC_{0-\infty}$ ($\mu\text{mol/ml} \times \text{min}$)	5115.035 ± 124.78	22.991 ± 0.674
Cl ($\mu\text{g/kg}/(\text{nmol/ml})/\text{min}$)	$7.6 \cdot 10^{-5} \pm 1.6 \cdot 10^{-5}$	$0.0163 \pm 4.8 \cdot 10^{-4}$
MRT (min)	1197.25 ± 315.44	796.337 ± 23.17

Based on the calculations, the AUC values of the brain are significantly higher to the previously mentioned spray-dried formulations where only physical particle size-reduced MX was presented in the system. The clearance and MRT values of the formulation indicates a slow elimination progress. This can be explained the residence time prolonging effect of PEG 6000, which is the outer shell of the polymeric micelle formulation. As the plasma curves entered to the natural elimination pathway, the early high concentration of MX in the brain can be further supported by the possibility of nose-to-brain transport. As mentioned earlier, regarding the zeta potential measurement, the SP-MX formulation has a negative surface charge which indicates a mucopenetrating effect across the nasal mucosa allowing carrier-intact direct axonal transport and rapid absorption to the blood. This is supported by the *in vitro* cell line and *ex vivo* permeability studies as well, since tremendously higher concentration of MX was achieved.

6. CONCLUSION

Polymeric micelles as smart nanocarrier systems are proved to be useful in case of improving the poor physicochemical properties of the model drug meloxicam which led to an increased brain concentration after nasal administration. In accordance with the defined QTPPs, a novel MX-loaded polymeric micelle formulation was designed meeting the criteria of a nanocarrier system. The applied system was applicable through the nasal drug delivery route as the potentially most efficient pathway to reach the central nervous system. The main conclusions can be summarized in the following points:

- I. During the work, successful determination of the critical factors affecting the product's applicability through nasal administration was performed. The implementation of knowledge space into a risk assessment process provided in-depth analysis regarding this non-biological complex drug delivery system aimed to deliver drugs to the central nervous system. With the establishment of product quality criteria in the form of the definition of the QTPP elements, the methodology and the transition from colloidal to in vivo studies was set up.
- II. A 3-factor, 3-level Box-Behnken factorial design provided the optimization platform to achieve polymeric micelles with particle size of 111.6 nm in monodisperse size distribution and proper colloidal stability with a zeta potential value of -25.2 mV. The SP-MX formulated fitted the criteria of ex tempore dispersible freeze-dried powders for the preparation of nasal liquids with a reconstitution time of 2 s. The pH was adjusted to fit the nasal pH range. The viscosity of the formulation makes it applicable through a nasal spray nozzle and the hypotonic nature of the formulation allows rapid drug absorption. Regarding these results, the nanoparticle characteristics were in accordance with the defined QTPP criteria.
- III. As main quality defining criterion, the water solubility and the related parameters were investigated. A high encapsulation efficiency of approx. 90 % was achieved which contributed to the immense increase in water solubility compared to raw MX. Besides this, the amorphous nature and proper wettability with increased polarity value also contributes to the performance of the formulation as a rapid dispersible formulation. The physical stability of the formulation is satisfying due to the formation of hydrogen bonds between MX and the micelle-forming co-polymer, SP. Thus, the structural properties

also led to meet the criteria of the defined QTPPs and prospected in advance the nasal behavior and applicability of the micellar carrier system.

- IV. *In vitro* drug release study proved that a rapid, burst-like effect can be achieved with the SP-MX formulation. The *in vitro* mucoadhesion study showed that moderate mucoadhesion between the nasal mucosa and the SP-MX formulation can be experienced, which does not hinder the mentioned rapid drug release. *In vitro* cell line studies showed safe administration of the formulation through nasal administration alongside with higher permeation across the cells. The later was also corroborated with *ex vivo* nasal mucosal permeation study where the increased flux value refers to the permeability enhancement.
- V. As tested at *in vivo* conditions, the main goal was achieved as MX has reached higher brain concentration via nasal administration compared to the particle size reduced MX formulations measured by our research group before. The burst-like rapid drug release and permeation profiles are also reflected in the brain concentration – time curves, meaning that the quality criteria were also fulfilled, and the product can be applied in acute distresses. The clearance and mean residence time values also showed that the formulation carry the benefits of a PEGylated system with increased residence time in the body.

7. NOVELTY AND PRACTICAL ASPECTS

The main new findings and practical aspects of the work can be summarized by the following:

1. The Ph.D. thesis aimed to construct, follow and evaluate a quality-driven methodology for nasal administration in case of a specific group of small molecular weight drug-loaded non-biological complex drugs: polymeric micelles. The methodology was constructed via the Quality by Design approach and in-depth analysis was performed regarding the criteria setup of MX-loaded Soluplus[®] polymeric micelles.
2. A novel approach has been proposed with this technique allowing further formulation opportunities in liquid dosage forms containing poorly water-soluble drugs. Meeting the criteria of both the nanoparticulate systems and the nasal administration route, this formulation can be utilized industrially in accordance with regulatory guidelines.
3. A novel biocompatible colloiddally stable system was achieved via the correct and most efficient co-polymer selection, namely the selection of Soluplus[®] as it was further proven that not only solid dispersions, but nanocarriers can be prepared via this novel excipient.
4. Successfully promoted the transport of MX to the central nervous system, which could solve the problem in the lack of clinical trials, as no investigable and therapeutically potential concentration was achieved in the brain prior to this work.
5. The results support that Soluplus[®] by alone can enhance the brain targeting efficacy without surface modification on the nanoparticulate system.

8. REFERENCES

1. Sindhvani, S., Chan, W. C. (2021). Nanotechnology for modern medicine: next step towards clinical translation. *Journal of Internal Medicine*, 290(3), 486-498. <https://doi.org/10.1111/joim.13254>
2. Contera, S. (2019). Nano comes to life: How nanotechnology is transforming medicine and the future of biology. *Princeton University Press*.
3. Hwang, D., Ramsey, J. D., Kabanov, A. V. (2020). Polymeric micelles for the delivery of poorly soluble drugs: From nanoformulation to clinical approval. *Advanced drug delivery reviews*, 156, 80-118. <https://doi.org/10.1016/j.addr.2020.09.009>
4. Paradise, J. (2019). Regulating nanomedicine at the food and drug administration. *AMA Journal of Ethics*, 21(4), 347-355. <https://doi.org/10.1001/amajethics.2019.347>.
5. Halamoda-Kenzaoui, B., Holzwarth, U., Roebben, G., Bogni, A., Bremer-Hoffmann, S. (2019). Mapping of the available standards against the regulatory needs for nanomedicines. *Wiley Interdisciplinary Reviews: Nanomedicine and Nanobiotechnology*, 11(1), e1531. <https://doi.org/10.1002/wnan.1531>
6. Zingg, R., Fischer, M. (2019). The consolidation of nanomedicine. *Wiley Interdisciplinary Reviews: Nanomedicine and Nanobiotechnology*, 11(6), e1569. <https://doi.org/10.1002/wnan.1569>
7. Csóka, I., Pallagi, E., Paál, T. L. (2018). Extension of quality-by-design concept to the early development phase of pharmaceutical R&D processes. *Drug Discovery Today*, 23(7), 1340-1343. <https://doi.org/10.1016/j.drudis.2018.03.012>
8. Suzuki, K., Yoshizaki, Y., Horii, K., Murase, N., Kuzuya, A., Ohya, Y. (2022). Preparation of hyaluronic acid-coated polymeric micelles for nasal vaccine delivery. *Biomaterials Science*, 10(8), 1920-1928. <https://doi.org/10.1039/D1BM01985F>
9. Abo El-Enin, H. A., Ahmed, M. F., Naguib, I. A., El-Far, S. W., Ghoneim, M. M., Alsalahat, I., Abdel-Bar, H. M. (2022). Utilization of Polymeric Micelles as a Lucrative Platform for Efficient Brain Deposition of Olanzapine as an Antischizophrenic Drug via Intranasal Delivery. *Pharmaceuticals*, 15(2), 249. <https://doi.org/10.3390/ph15020249>
10. Owen, S. C., Chan, D. P., Shoichet, M. S. (2012). Polymeric micelle stability. *Nano today*, 7(1), 53-65. <https://doi.org/10.1016/j.nantod.2012.01.002>
11. Belzung, C. (2014). Innovative drugs to treat depression: did animal models fail to be predictive or did clinical trials fail to detect effects?. *Neuropsychopharmacology*, 39(5), 1041-1051. <https://doi.org/10.1038/npp.2013.342>
12. Foulkes, R., Man, E., Thind, J., Yeung, S., Joy, A., Hoskins, C. (2020). The regulation of nanomaterials and nanomedicines for clinical application: Current and future perspectives. *Biomaterials science*, 8(17), 4653-4664. <https://doi.org/10.1039/D0BM00558D>
13. Obermeier, B., Verma, A., Ransohoff, R. M. (2016). The blood–brain barrier. *Handbook of clinical neurology*, 133, 39-59. <https://doi.org/10.1016/B978-0-444-63432-0.00003-7>
14. Huber, J. D., Witt, K. A., Hom, S., Egleton, R. D., Mark, K. S., Davis, T. P. (2001). Inflammatory pain alters blood-brain barrier permeability and tight junctional protein expression. *American Journal of Physiology-Heart and Circulatory Physiology*, 280(3), H1241-H1248. <https://doi.org/10.1152/ajpheart.2001.280.3.H1241>

15. Sharma, G., Sharma, A. R., Lee, S. S., Bhattacharya, M., Nam, J. S., Chakraborty, C. (2019). Advances in nanocarriers enabled brain targeted drug delivery across blood brain barrier. *International journal of pharmaceutics*, 559, 360-372. <https://doi.org/10.1016/j.ijpharm.2019.01.056>
16. Rabiee, N., Ahmadi, S., Afshari, R., Khalaji, S., Rabiee, M., Bagherzadeh, M., Fatahi, Y., Dinarvand, R., Webster, T. J. (2021). Polymeric nanoparticles for nasal drug delivery to the brain: relevance to Alzheimer's disease. *Advanced Therapeutics*, 4(3), 2000076. <https://doi.org/10.1002/adtp.202000076>
17. Wolburg, H., Lippoldt, A. (2002). Tight junctions of the blood–brain barrier: development, composition and regulation. *Vascular pharmacology*, 38(6), 323-337. [https://doi.org/10.1016/S1537-1891\(02\)00200-8](https://doi.org/10.1016/S1537-1891(02)00200-8)
18. Abbott, N. J., Patabendige, A. A., Dolman, D. E., Yusof, S. R., Begley, D. J. (2010). Structure and function of the blood–brain barrier. *Neurobiology of disease*, 37(1), 13-25. <https://doi.org/10.1016/j.nbd.2009.07.030>
19. Ponio, J. B. D., El-Ayoubi, F., Glacial, F., Ganeshamoorthy, K., Driancourt, C., Godet, M., Perrière, N., Guillevic, O., Couraud, P.O., Uzan, G. (2014). Instruction of circulating endothelial progenitors in vitro towards specialized blood-brain barrier and arterial phenotypes. *PloS one*, 9(1), e84179. <https://doi.org/10.1371/journal.pone.0084179>
20. Pardridge, W. M. (2007). Drug targeting to the brain. *Pharmaceutical research*, 24(9), 1733-1744. <https://doi.org/10.1007/s11095-007-9324-2>
21. Zhang, W., Mehta, A., Tong, Z., Esser, L., Voelcker, N. H. (2021). Development of polymeric nanoparticles for blood–brain barrier transfer—strategies and challenges. *Advanced Science*, 8(10), 2003937. <https://doi.org/10.1002/advs.202003937>
22. Raman, S., Mahmood, S., Hilles, A. R., Javed, M. N., Azmana, M., Al-Japairai, K. A. (2020). Polymeric nanoparticles for brain drug delivery-a review. *Current drug metabolism*, 21(9), 649-660. <https://doi.org/10.2174/1389200221666200508074348>
23. Persano, F., Batasheva, S., Fakhrullina, G., Gigli, G., Leporatti, S., Fakhrullin, R. (2021). Recent advances in the design of inorganic and nano-clay particles for the treatment of brain disorders. *Journal of Materials Chemistry B*, 9(12), 2756-2784. <https://doi.org/10.1039/D0TB02957B>
24. Ding, S., Khan, A. I., Cai, X., Song, Y., Lyu, Z., Du, D., Dutta, P., Lin, Y. (2020). Overcoming blood–brain barrier transport: Advances in nanoparticle-based drug delivery strategies. *Materials today*, 37, 112-125. <https://doi.org/10.1016/j.mattod.2020.02.001>
25. Ferraris, C., Cavalli, R., Panciani, P. P., Battaglia, L. (2020). Overcoming the Blood–Brain Barrier: Successes and Challenges in Developing Nanoparticle-Mediated Drug Delivery Systems for the Treatment of Brain Tumours. *International Journal of Nanomedicine*, 15, 2999. <https://doi.org/10.2147%2FIJN.S231479>
26. Gonzalez-Carter, D., Liu, X., Tockary, T. A., Dirisala, A., Toh, K., Anraku, Y., & Kataoka, K. (2020). Targeting nanoparticles to the brain by exploiting the blood–brain barrier impermeability to selectively label the brain endothelium. *Proceedings of the National Academy of Sciences*, 117(32), 19141-19150. <https://doi.org/10.1073/pnas.2002016117>
27. Laffleur, F., & Bauer, B. (2021). Progress in nasal drug delivery systems. *International Journal of Pharmaceutics*, 607, 120994. <https://doi.org/10.1016/j.ijpharm.2021.120994>

28. Forbes, B., Bommer, R., Goole, J., Hellfritsch, M., De Kruijf, W., Lambert, P., Caivano, G., Regard, A., Schiaretti, F., Trenkel, M., Vecellio, L., Williams, G., Sonvico, F., Scherließ, R. (2020). A consensus research agenda for optimising nasal drug delivery. *Expert opinion on drug delivery*, 17(2), 127-132. <https://doi.org/10.1080/17425247.2020.1714589>
29. Adnet, T., Groo, A. C., Picard, C., Davis, A., Corvaisier, S., Since, M., Bounoure, F., Rochais, C., Le Pluart, L., Dellamagne, P., Malzert-Fréon, A. (2020). Pharmacotechnical development of a nasal drug delivery composite nanosystem intended for Alzheimer's disease treatment. *Pharmaceutics*, 12(3), 251. <https://doi.org/10.3390/pharmaceutics12030251>
30. Kashyap, K., & Shukla, R. (2019). Drug delivery and targeting to the brain through nasal route: mechanisms, applications and challenges. *Current Drug Delivery*, 16(10), 887-901. <https://doi.org/10.2174/1567201816666191029122740>
31. Shim, S., & Yoo, H. S. (2020). The application of mucoadhesive chitosan nanoparticles in nasal drug delivery. *Marine drugs*, 18(12), 605. <https://doi.org/10.3390/md18120605>
32. Keller, L. A., Merkel, O., Popp, A. (2022). Intranasal drug delivery: Opportunities and toxicologic challenges during drug development. *Drug Delivery and Translational Research*, 12(4), 735-757. <https://doi.org/10.1007/s13346-020-00891-5>
33. Sipos, B., Csóka, I., Budai-Szűcs, M., Kozma, G., Berkesi, D., Kónya, Z., Balogh, G.T., Katona, G. (2021). Development of dexamethasone-loaded mixed polymeric micelles for nasal delivery. *European Journal of Pharmaceutical Sciences*, 166, 105960. <https://doi.org/10.1016/j.ejps.2021.105960>
34. Quintana, D. S., Guastella, A. J., Westlye, L. T., Andreassen, O. A. (2016). The promise and pitfalls of intranasally administering psychopharmacological agents for the treatment of psychiatric disorders. *Molecular Psychiatry*, 21(1), 29-38. <https://doi.org/10.1038/mp.2015.166>
35. Fatouh, A. M., Elshafeey, A. H., Abdelbary, A. (2017). Agomelatine-based in situ gels for brain targeting via the nasal route: statistical optimization, in vitro, and in vivo evaluation. *Drug Delivery*, 24(1), 1077-1085. <https://doi.org/10.1080/10717544.2017.1357148>
36. Fan, Y., Chen, M., Zhang, J., Maincent, P., Xia, X., Wu, W. (2018). Updated progress of nanocarrier-based intranasal drug delivery systems for treatment of brain diseases. *Critical Reviews™ in Therapeutic Drug Carrier Systems*, 35(5). <https://doi.org/10.1615/CritRevTherDrugCarrierSyst.2018024697>
37. Agrawal, M., Saraf, S., Saraf, S., Dubey, S. K., Puri, A., Gupta, U., Kesharwani, p., Ravichandiran, V., Kumar, P., Naidu, V.G.M., Murty, U.S., Ajazuddin, Alexander, A. (2020). Stimuli-responsive In situ gelling system for nose-to-brain drug delivery. *Journal of Controlled Release*, 327, 235-265. <https://doi.org/10.1016/j.jconrel.2020.07.044>
38. Martins, P. P., Smyth, H. D., Cui, Z. (2019). Strategies to facilitate or block nose-to-brain drug delivery. *International journal of pharmaceutics*, 570, 118635. <https://doi.org/10.1016/j.ijpharm.2019.118635>
39. Emad, N. A., Ahmed, B., Alhalmi, A., Alzobaidi, N., Al-Kubati, S. S. (2021). Recent progress in nanocarriers for direct nose to brain drug delivery. *Journal of Drug Delivery Science and Technology*, 64, 102642. <https://doi.org/10.1016/j.jddst.2021.102642>
40. Hong, S. S., Oh, K. T., Choi, H. G., Lim, S. J. (2019). Liposomal formulations for nose-to-brain delivery: recent advances and future perspectives. *Pharmaceutics*, 11(10), 540. <https://doi.org/10.3390/pharmaceutics11100540>

41. Ghezzi, M., Pescina, S., Padula, C., Santi, P., Del Favero, E., Cantù, L., Nicoli, S. (2021). Polymeric micelles in drug delivery: An insight of the techniques for their characterization and assessment in biorelevant conditions. *Journal of Controlled Release*, 332, 312-336. <https://doi.org/10.1016/j.jconrel.2021.02.031>
42. Sipos, B., Csóka, I., Ambrus, R., Schelz, Z., Zupkó, I., Balogh, G. T., Katona, G. (2022). Spray-dried indomethacin-loaded polymeric micelles for the improvement of intestinal drug release and permeability. *European Journal of Pharmaceutical Sciences*, 174, 106200. <https://doi.org/10.1016/j.ejps.2022.106200>
43. Junnuthula, V., Kolimi, P., Nyavanandi, D., Sampathi, S., Vora, L. K., Dyawanapelly, S. (2022). Polymeric Micelles for Breast Cancer Therapy: Recent Updates, Clinical Translation and Regulatory Considerations. *Pharmaceutics*, 14(9), 1860. <https://doi.org/10.3390/pharmaceutics14091860>
44. Chaudhuri, A., Ramesh, K., Kumar, D. N., Dehari, D., Singh, S., Kumar, D., Agrawal, A. K. (2022). Polymeric micelles: A novel drug delivery system for the treatment of breast cancer. *Journal of Drug Delivery Science and Technology*, 103886. <https://doi.org/10.1016/j.jddst.2022.103886>
45. Pham, D. T., Chokamonsirikun, A., Phattaravorakarn, V., Tiyaboonthai, W. (2021). Polymeric micelles for pulmonary drug delivery: a comprehensive review. *Journal of Materials Science*, 56(3), 2016-2036. <https://doi.org/10.1007/s10853-020-05361-4>
46. Lin, M., Dai, Y., Xia, F., Zhang, X. (2021). Advances in non-covalent crosslinked polymer micelles for biomedical applications. *Materials Science and Engineering: C*, 119, 111626. <https://doi.org/10.1016/j.msec.2020.111626>
47. Thotakura, N., Parashar, P., Raza, K. (2021). Assessing the pharmacokinetics and toxicology of polymeric micelle conjugated therapeutics. *Expert Opinion on Drug Metabolism & Toxicology*, 17(3), 323-332. <https://doi.org/10.1080/17425255.2021.1862085>
48. Shiraishi, K., Yokoyama, M. (2019). Toxicity and immunogenicity concerns related to PEGylated-micelle carrier systems: a review. *Science and technology of advanced materials*, 20(1), 324-336. <https://doi.org/10.1080/14686996.2019.1590126>
49. Cai, X., Jin, M., Yao, L., He, B., Ahmed, S., Safdar, W., Ahmad, I., Cheng, D-B., Lei, Z., Sun, T. (2022). Physicochemical properties, pharmacokinetics, toxicology and application of nanocarriers. *Journal of Materials Chemistry B*. <https://doi.org/10.1039/D2TB02001G>
50. Liao, Z., Wong, S. W., Yeo, H. L., Zhao, Y. (2020). Smart nanocarriers for cancer treatment: Clinical impact and safety. *NanoImpact*, 20, 100253. <https://doi.org/10.1016/j.impact.2020.100253>
51. Hsu, C. W., Hsieh, M. H., Xiao, M. C., Chou, Y. H., Wang, T. H., Chiang, W. H. (2020). pH-responsive polymeric micelles self-assembled from benzoic-imine-containing alkyl-modified PEGylated chitosan for delivery of amphiphilic drugs. *International Journal of Biological Macromolecules*, 163, 1106-1116. <https://doi.org/10.1016/j.ijbiomac.2020.07.110>
52. Subjakova, V., Oravczova, V., Hianik, T. (2021). Polymer nanoparticles and nanomotors modified by DNA/RNA aptamers and antibodies in targeted therapy of cancer. *Polymers*, 13(3), 341. <https://doi.org/10.3390/polym13030341>
53. Majumder, N., G Das, N., Das, S. K. (2020). Polymeric micelles for anticancer drug delivery. *Therapeutic delivery*, 11(10), 613-635. <https://doi.org/10.4155/tde-2020-0008>

54. Guo, Z., Zhao, K., Liu, R., Guo, X., He, B., Yan, J., Ren, J. (2019). pH-sensitive polymeric micelles assembled by stereocomplexation between PLLA-b-PLys and PDLA-b-mPEG for drug delivery. *Journal of Materials Chemistry B*, 7(2), 334-345. <https://doi.org/10.1039/C8TB02313A>
55. Guo, L. Y., Yan, S. Z., Tao, X., Yang, Q., Li, Q., Wang, T. S., Yu, S-Q., Chen, S. L. (2020). Evaluation of hypocrellin A-loaded lipase sensitive polymer micelles for intervening methicillin-resistant Staphylococcus Aureus antibiotic-resistant bacterial infection. *Materials Science and Engineering: C*, 106, 110230. <https://doi.org/10.1016/j.msec.2019.110230>
56. Perumal, S., Atchudan, R., Lee, W. (2022). A review of polymeric micelles and their applications. *Polymers*, 14(12), 2510. <https://doi.org/10.3390/polym14122510>
57. Xie, Y. J., Wang, Q. L., Adu-Frimpong, M., Liu, J., Zhang, K. Y., Xu, X. M., Yu, J. N. (2019). Preparation and evaluation of isoliquiritigenin-loaded F127/P123 polymeric micelles. *Drug Development and Industrial Pharmacy*. <https://doi.org/10.1080/03639045.2019.1574812>
58. Gao, M., Yang, Y., Bergfel, A., Huang, L., Zheng, L., Bowden, T. M. (2020). Self-assembly of cholesterol end-capped polymer micelles for controlled drug delivery. *Journal of nanobiotechnology*, 18(1), 1-10. <https://doi.org/10.1186/s12951-020-0575-y>
59. Nour, S. A., Abdelmalak, N. S., Naguib, M. J., Rashed, H. M., Ibrahim, A. B. (2016). Intranasal brain-targeted clonazepam polymeric micelles for immediate control of status epilepticus: in vitro optimization, ex vivo determination of cytotoxicity, in vivo biodistribution and pharmacodynamics studies. *Drug delivery*, 23(9), 3681-3695. <https://doi.org/10.1080/10717544.2016.1223216>
60. Pokharkar, V., Suryawanshi, S., Dhapte-Pawar, V. (2020). Exploring micellar-based polymeric systems for effective nose-to-brain drug delivery as potential neurotherapeutics. *Drug Delivery and Translational Research*, 10(4), 1019-1031. <https://doi.org/10.1007/s13346-019-00702-6>
61. Wang, F., Yang, Z., Liu, M., Tao, Y., Li, Z., Wu, Z., Gui, S. (2020). Facile nose-to-brain delivery of rotigotine-loaded polymer micelles thermosensitive hydrogels: In vitro characterization and in vivo behavior study. *International Journal of Pharmaceutics*, 577, 119046. <https://doi.org/10.1016/j.ijpharm.2020.119046>
62. Khanna, I. (2012). Drug discovery in pharmaceutical industry: productivity challenges and trends. *Drug discovery today*, 17(19-20), 1088-1102. <https://doi.org/10.1016/j.drudis.2012.05.007>
63. Schweizer, L.; Dingermann, T. (2020) Introduction: Trends and Developments in the Pharmaceutical and Life Sciences Industry. In *Advances in Pharma Business Management and Research: Volume 1*; Schweizer, L., Dingermann, T., Russe, O.Q., Jansen, C., Eds.; Springer International Publishing: Cham, Switzerland; pp. 1–5. ISBN 978-3-030-35918-8.
64. Patil, A. S., Pethe, A. M. (2013). Quality by Design (QbD): A new concept for development of quality pharmaceuticals. *International journal of pharmaceutical quality assurance*, 4(2), 13-19.
65. Yu, L. X., Amidon, G., Khan, M. A., Hoag, S. W., Polli, J., Raju, G. K., Woodcock, J. (2014). Understanding pharmaceutical quality by design. *The AAPS journal*, 16(4), 771-783. <https://doi.org/10.1208/s12248-014-9598-3>
66. Sipos, B., Katona, G., Csóka, I. (2021). A systematic, knowledge space-based proposal on quality by design-driven polymeric micelle development. *Pharmaceutics*, 13(5), 702. <https://doi.org/10.3390/pharmaceutics13050702>

67. ICH. Pharmaceutical Development Q8; ICH Harmonised Tripartite Guideline; ICH: Geneva, Switzerland, **2009**.
68. ICH. Quality Risk Management Q9; ICH Harmonised Tripartite Guideline; ICH: Geneva, Switzerland, **2005**
69. ICH. ICH Q10 Pharmaceutical Quality Systems; ICH: Geneva, Switzerland, **2008**.
70. Kalinin, E. V., Kalinina, L. L., Norkina, O. S. (2020). Modern concept analysis of failure modes and consequences for quality assurance of products and processes. In *IOP Conference Series: Materials Science and Engineering* (Vol. 966, No. 1, p. 012092). IOP Publishing. <https://doi.org/10.1088/1757-899X/966/1/012092>
71. Castile, J., Cheng, Y. H., Simmons, B., Perelman, M., Smith, A., Watts, P. (2013). Development of in vitro models to demonstrate the ability of PecSys®, an in situ nasal gelling technology, to reduce nasal run-off and drip. *Drug development and industrial pharmacy*, 39(5), 816-824. <https://doi.org/10.3109/03639045.2012.707210>
72. Falusi, F., Budai-Szűcs, M., Csányi, E., Berkó, S., Spaits, T., Csóka, I., Kovács, A. (2022). Investigation of the effect of polymers on dermal foam properties using the QbD approach. *European Journal of Pharmaceutical Sciences*, 173, 106160. <https://doi.org/10.1016/j.ejps.2022.106160>
73. Pallagi, E., Jójárt-Laczkovich, O., Németh, Z., Szabó-Révész, P., Csóka, I. (2019). Application of the QbD-based approach in the early development of liposomes for nasal administration. *International Journal of Pharmaceutics*, 562, 11-22. <https://doi.org/10.1016/j.ijpharm.2019.03.021>
74. Németh, Z., Pallagi, E., Dobó, D. G., Kozma, G., Kónya, Z., Csóka, I. (2021). An updated risk assessment as part of the QbD-based liposome design and development. *Pharmaceutics*, 13(7), 1071. <https://doi.org/10.3390/pharmaceutics13071071>
75. ICH. ICH Q3C (R6) on Impurities: Guideline for Residual Solvents; ICH: Geneva, Switzerland, **2016**.
76. Alvarez-Rivera, F., Fernández-Villanueva, D., Concheiro, A., Alvarez-Lorenzo, C. (2016). α -Lipoic acid in Soluplus® polymeric nanomicelles for ocular treatment of diabetes-associated corneal diseases. *Journal of pharmaceutical sciences*, 105(9), 2855-2863. <https://doi.org/10.1016/j.xphs.2016.03.006>
77. Wu, S. (1971) Calculation of interfacial tension in polymer systems. *Journal of Polymer Science* 34, 19–30. <https://doi.org/10.1002/polc.5070340105>
78. ICH. Stability testing of new drug substances and drug products Q1A (R2). In ICH Harmon Tripart Guidel; ICH: Geneva, Switzerland, **2003**; pp. 1–20.
79. Gieszinger, P., Csaba, N. S., Garcia-Fuentes, M., Prasanna, M., Gáspár, R., Sztojkov-Ivanov, A., Ducza, E., Márki, Á., Janáky, T., Kecskeméti, G., Katona, G., Szabó-Révész, P., Ambrus, R. (2020). Preparation and characterization of lamotrigine containing nanocapsules for nasal administration. *European Journal of Pharmaceutics and Biopharmaceutics*, 153, 177-186. <https://doi.org/10.1016/j.ejpb.2020.06.003>
80. Lim, S. T., Martin, G. P., Berry, D. J., Brown, M. B. (2000). Preparation and evaluation of the in vitro drug release properties and mucoadhesion of novel microspheres of hyaluronic acid and chitosan. *Journal of Controlled Release*, 66(2-3), 281-292. [https://doi.org/10.1016/S0168-3659\(99\)00285-0](https://doi.org/10.1016/S0168-3659(99)00285-0)

81. Kürti, L., Veszélka, S., Bocsik, A., Ozsvári, B., Puskás, L. G., Kittel, A., Szabó-Révész, P., Deli, M. A. (2013). Retinoic acid and hydrocortisone strengthen the barrier function of human RPMI 2650 cells, a model for nasal epithelial permeability. *Cytotechnology*, 65(3), 395-406. <https://doi.org/10.1007/s10616-012-9493-7>
82. Cecchelli, R., Aday, S., Sevin, E., Almeida, C., Culot, M., Dehouck, L., Coisne, C., Engelhardt, B., Dehouch, M-P., Ferreira, L. (2014). A stable and reproducible human blood-brain barrier model derived from hematopoietic stem cells. *PloS one*, 9(6), e99733. <https://doi.org/10.1371/journal.pone.0099733>
83. Pedroso, D. C., Tellechea, A., Moura, L., Fidalgo-Carvalho, I., Duarte, J., Carvalho, E., Ferreira, L. (2011). Improved survival, vascular differentiation and wound healing potential of stem cells co-cultured with endothelial cells. *PloS one*, 6(1), e16114. <https://doi.org/10.1371/journal.pone.0016114>
84. Bartos, C., Szabó-Révész, P., Horváth, T., Varga, P., Ambrus, R. (2021). Comparison of Modern In Vitro Permeability Methods with the Aim of Investigation Nasal Dosage Forms. *Pharmaceutics*, 13(6), 846. <https://doi.org/10.3390/pharmaceutics13060846>
85. Party, P., Bartos, C., Farkas, Á., Szabó-Révész, P., Ambrus, R. (2021). Formulation and in vitro and in silico characterization of “nano-in-micro” dry powder inhalers containing meloxicam. *Pharmaceutics*, 13(2), 211. <https://doi.org/10.3390/pharmaceutics13020211>
86. EMA. Joint MHLW/EMA Reflection Paper on the Development of Block Copolymer Micelle Medicinal Products; EMA: Amsterdam, The Netherlands, 2014.
87. Pepić, I., Lovrić, J., Filipović-Grčić, J. (2013). How do polymeric micelles cross epithelial barriers?. *European Journal of Pharmaceutical Sciences*, 50(1), 42-55. <https://doi.org/10.1016/j.ejps.2013.04.012>
88. Salade, L., Wauthoz, N., Goole, J., Amighi, K. (2019). How to characterize a nasal product. The state of the art of in vitro and ex vivo specific methods. *International journal of pharmaceutics*, 561, 47-65. <https://doi.org/10.1016/j.ijpharm.2019.02.026>
89. Alopaeus, J. F., Hagesæther, E., Tho, I. (2019). Micellisation mechanism and behaviour of Soluplus®-furosemide micelles: Preformulation studies of an oral nanocarrier-based system. *Pharmaceutics*, 12(1), 15. <https://doi.org/10.3390/ph12010015>
90. Bartos, C., Ambrus, R., Kovács, A., Gáspár, R., Sztojkov-Ivanov, A., Márki, Á., Janáky, T., Tömösi, F., Kecskeméti, G., Szabó-Révész, P. (2018). Investigation of absorption routes of meloxicam and its salt form from intranasal delivery systems. *Molecules*, 23(4), 784. <https://doi.org/10.3390/molecules23040784>

9. ACKNOWLEDGEMENTS

I would like to thank **Prof. Dr. Ildikó Csóka** for providing us with the quality conditions to work as a Ph.D. student at the Institute of Pharmaceutical Technology and Regulatory Affairs. I especially thank her for showing me how to think critically, ask the right scientific questions and how to search for innovative solutions during my daily work. I would also like to thank **Prof. Dr. Piroska Szabó-Révész** who provided insightful scientific mentoring and advises to my research work.

I am the most grateful to my supervisor, **Dr. Gábor Katona**, who embraced me when I was a graduate student and helped me always find the right path during my research. He showed me how to get things done and always inspired me. As years went by, not only he became the greatest supervisor I could ever hope for, but he also become my best friend. He also showed me that true friends aren't the ones who make your problems disappear, but they are the ones who won't disappear when you're facing them. He also showed me how to become the better me and cared for me during the deepest, most emotional parts of this journey and he cheered with me in my greatest joys. Thank you for standing by my side when times get hard and for making me laugh when I didn't even want to smile. **I dedicate this thesis to him showing my full support, friendship and respect towards him.**

I would like to thank **Dr. Rita Ambrus**, who took a great part in providing this research the financial and professional background. I am thankful to **Erika Boda** who helped me the most in the laboratory as a technical assistant during my years. My greatest laughs were with her during the research. I am also grateful for **Ágnes Balázs**, who as a member of the administration staff, always precisely helped with the project administration and made sure that everything was in order to conduct the research.

I would like to thank the people who helped me in cooperation with the establishment and delivery of this research work, especially **Dr. Mária Budai-Szűcs** from our Institution. I also thank **Dr. Dorina Gabriella Dobó**, and **Klára Kovács** for the help in certain measurements during my research works. I would like to thank all my cooperation partners who helped me to achieve my goals: **Dr. Ágota Deák and Dr. László Janovák** from the Department of Physical Chemistry and Materials Science; **Prof. Dr. Mária A. Deli, Dr. Szilvia Veszeka and Dr. Iona Gróf** from the Institute of Biophysics, Biological Research Centre, Szeged; **Dr. Róbert Gáspár and Dr. Kálmán F. Szűcs** from the Department of Pharmacology and Pharmacotherapy, Albert Szent-Györgyi Medical School, University of Szeged, **Dr. Eszter Ducza and Dr. Anita Sztojkov-Ivanov** from

the Department of Pharmacodynamics and Biopharmacy, Faculty of Pharmacy, University of Szeged, **Dr. Zsolt Bella** from the Department of Oto-Rhino-Laryngology and Head-Neck Surgery, University of Szeged; **Prof. Dr. Tamás Janáky** and **Dr. Gábor Kecskeméti** from the Department of Medical Chemistry, University of Szeged and last but not least, **Dr. Balázs Volk** from Egis Pharmaceuticals Plc.

I am thankful for my friends who helped and supported me during the Ph.D. work: **Dr. Szabina Csepregi**, **Dr. Fanni Falusi** and **Dr. Petra Party**. My most memorable moments are related to them, and they provided true and honest friendship towards me during all these years. I am forever grateful for **my parents and brother**, who helped me without hesitation during my studies and sacrificed so much of their own to let me finish my studies.




I acknowledge that the current thesis and other non-related projects were supported by the National Research, Development and Innovation Office, Hungary (GINOP-2.3.2–15-2016–00060), by the ÚNKP-19–2-SZTE-113; ÚNKP-21-3-SZTE-360 and ÚNKP-22-3-SZTE-160 New National Excellence Programs of the Ministry for Innovation and Technology and by Project no. TKP2021-EGA-32 implemented with the support provided by the Ministry of Innovation and Technology of Hungary from the National Research, Development and Innovation Fund, financed under the TKP2021-EGA funding scheme.

ANNEX

I.

Article

Quality by Design Based Formulation Study of Meloxicam-Loaded Polymeric Micelles for Intranasal Administration

Bence Sipos¹, Piroska Szabó-Révész¹ , Ildikó Csóka¹, Edina Pallagi¹, Dorina Gabriella Dobó¹, Péter Bélteky², Zoltán Kónya² , Ágota Deák³, László Janovák³ and Gábor Katona^{1,*} 

¹ Faculty of Pharmacy, Institute of Pharmaceutical Technology and Regulatory Affairs, University of Szeged, H-6720 Szeged, Hungary; sipos.bence96@gmail.com (B.S.); revesz@pharm.u-szeged.hu (P.S.-R.); csoka@pharm.u-szeged.hu (I.C.); edina.pallagi@pharm.u-szeged.hu (E.P.); dobo.dorina@pharm.u-szeged.hu (D.G.D.)

² Faculty of Science and Informatics, Department of Applied & Environmental Chemistry, H-6720 Szeged, Hungary; belteky@chem.u-szeged.hu (P.B.); konya@chem.u-szeged.hu (Z.K.)

³ Interdisciplinary Excellence Centre, Department of Physical Chemistry and Materials Science, H-6720 Szeged, Hungary; deak.agota@stud.u-szeged.hu (Á.D.); janovakl@chem.u-szeged.hu (L.J.)

* Correspondence: katona@pharm.u-szeged.hu; Tel.: +36-62-545-575

Received: 19 June 2020; Accepted: 23 July 2020; Published: 24 July 2020



Abstract: Our study aimed to develop an “ex tempore” reconstitutable, viscosity enhancer- and preservative-free meloxicam (MEL)-loaded polymeric micelle formulation, via Quality by Design (QbD) approach, exploiting the nose-to-brain pathway, as a suitable tool in the treatment of neuroinflammation. The anti-neuroinflammatory effect of nose-to-brain NSAID polymeric micelles was not studied previously, therefore its investigation is promising. Critical product parameters, encapsulation efficiency (89.4%), Z-average (101.22 ± 2.8 nm) and polydispersity index (0.149 ± 0.7) and zeta potential (-25.2 ± 0.4 mV) met the requirements of the intranasal drug delivery system (nanoDDS) and the targeted profile liquid formulation was transformed into a solid preservative-free product by freeze-drying. The viscosity (32.5 ± 0.28 mPas) and hypotonic osmolality (240 mOsmol/L) of the reconstituted formulation provides proper and enhanced absorption and probably guarantees the administration of the liquid dosage form (nasal drop and spray). The developed formulation resulted in more than 20 times faster MEL dissolution rate and five-fold higher nasal permeability compared to starting MEL. The prediction of IVIVC confirmed the great potential for in vivo brain distribution of MEL. The nose-to-brain delivery of NSAIDs such as MEL by means of nanoDDS as polymeric micelles offers an innovative opportunity to treat neuroinflammation more effectively.

Keywords: NSAID; nanoDDS; polymeric micelle; quality by design; preformulation study; freeze-drying; reconstituted nasal formulation; nose-to-brain delivery; solubility enhancement; prediction of IVIVC

1. Introduction

Among the leading mortality causes, neurodegenerative diseases are in the forefront. Their increasing prevalence poses a challenge to find the effective therapy worldwide. Alzheimer’s disease (AD) is one of the most common causes of dementia, accounting for approximately 60–70%. The estimated proportion of the general population aged 60 and over with dementia at a given time is between 5–8%. The total number of people with dementia is projected to reach 82 million in 2030 and 152 in 2050 because with the increasing life expectancy, a dramatic rise in the number of age-associated diseases can be predicted, therefore there is an increased demand for easy-to-apply medications which can improve patient adherence [1]. Strategies for facilitating medication adherence in patients with

dementia include applying as few medicines as possible, tailoring dose regimens to personal habits and minimizing the drug dosing intervals as much as possible [2], therefore smart drug delivery systems are required. Within symptomatic therapies, the treatment of cyclooxygenase (COX) enzymes mediated neuroinflammation plays a prominent role, which is primarily attributable to nonsteroidal anti-inflammatory drugs (NSAIDs). Inhibition of COX enzymes can reduce amyloid deposition and inhibit glia activity, which has been already demonstrated in a mouse model [3,4]. Subsequently, numerous studies have demonstrated their pharmacological activity in the central nervous system (CNS). Treating neuroinflammation by NSAIDs could be possibly based on protection by depolarizing the mitochondria and inhibiting the calcium uptake, due to the ionizable carboxylic group, having a similar effect to mild mitochondrial uncouplers [5,6]. However, the blood–brain barrier (BBB) is an obstacle to the therapy because it prevents the release of active substances that could be used by its protective function [7]. In addition to the appropriate technological formulation, the route of administration also plays a pivotal role [8].

The intranasal administration route can be exploited both in systemic and local therapy. Due to the high surface area and rich vascularization of nasal mucosa, drugs or drug-delivery systems can be easily absorbed from the nasal cavity. This direct way can also protect the API from the first-pass metabolism, thus preserving its pharmacological activity [9–11]. Studies have shown that AD starts in the entorhinal cortex, which is associated with olfactory nerves and begins to spread in a corresponding pattern [12], therefore the intranasal administration of the API can be advantageous. The potential for colloidal carriers to increase drug bioavailability is in the focus of research [13]. Nano drug delivery systems (nanoDDSs) are able to bypass the BBB through the trigeminal and olfactory nerves, resulting in higher brain concentration of the incorporated active pharmaceutical ingredient, moreover their application is required in the case of NSAID administration, because of their low solubility at the pH (5.3–5.6) of the nasal cavity and low residence time (10–15 min) due to mucociliary clearance [14].

Our research group has been working on nanoDDSs aiming to transfer APIs through or bypassing the blood–brain barrier exploiting the applicability of NSAIDs in a nasal formulation. Based on the previous results of the research group, a good *in vitro*–*in vivo* correlation (IVIVC) was achieved by focusing on the administered API's concentration in the brain. Different nanotechnological methods were applied in order to achieve this goal. As a disintegration method, the co-grinding process with different excipients was used, which resulted in nanonization of the drug, thereby offering higher permeability to biologic barriers and therefore transporting them across the nasal mucosa [15,16]. Besides the top–down methods, bottom–up techniques were also successfully applied, in order to incorporate the API into nanoDDS. Liposomes as lipid-based nanoDDS with reduced particle size and the bilayer lipid membrane provided high and fast transport of encapsulated lamotrigine through the nasal mucosa [17]. The *in vivo* studies of meloxicam (MEL)-containing human serum albumin nanoparticles corroborated the *in vitro* dissolution and permeability studies contributed to determine the criteria of trans-epithelial and axonal transport ensuring higher cerebral concentration of the API [18]. These results gave the background of the investigation of polymeric micelles, which may offer more favorable pharmacokinetics and higher protection to the API.

Polymeric micelles are composed of amphiphilic graft copolymers, consisting of a hydrophilic and a hydrophobic block moiety. They show concentration dependent variation in the physicochemical properties similar to classic surfactant molecules, such as spontaneously self-assembling above the critical micellar concentration (CMC) or forming association colloids into nanosized micelles above the critical micellar temperature. Among their benefits, they can incorporate drugs with poor water solubility and permeability into their hydrophobic core while the hydrophilic shell is responsible for solubilizing. This property predicts increased bioavailability and offers the possibility to administer the drug via alternative administration routes [19–21]. Two main ways of drug release are known from the micellar core: one is the dissociation of the micelle breaking down to monomers and the other is based on drug–polymer bond breakage in the micellar core allowing diffusion from there. Simple diffusion from the core can be controlled by different stimuli (e.g., pH) with appropriate engineering [22].

Along with the development of novel drug delivery conventional and novel synthetic or natural excipients provide opportunities to design dosage forms with the required features including their bioavailability [23]. In the composition design of polymeric micelles amphiphilic micelle forming graft copolymer Soluplus[®] was chosen, due to its advantageous properties: low CMC value in water, mucoadhesion, biodegradability. Soluplus[®] has low toxicity, according to the manufacturer data (BASF SE, Ludwigshafen, Germany), the oral and dermal median lethal dose values (lethal dose, 50%; LD50) were both >5 g/kg, therefore its nasal application is safe. Its amphiphilic nature is due to the following composition: 13% polyethylene glycol (PEG) 6000 as hydrophilic, 57% vinyl caprolactam and 30% vinyl acetate as the hydrophobic block. The PEG chain forms the strain on which the other two lipophilic monomer side chains are incorporated. Due to its bifunctional character, it can be used for preparing solid solutions as well as for solubilizing active substances with poor water solubility as many previous research studies have shown [24,25].

This study reports MEL as a model drug, which could be a promising active substance for the treatment of neuroinflammation with selective COX-2 inhibition. With this selectivity we can exclude the opportunity to harm the gastric mucosa. It has poor water solubility (BCS class II), especially in the pH range of the nasal cavity, which impedes liberation from the formulation, resulting in low absorption as well as bioavailability [26]. By encapsulating MEL in a polymeric micelle, the drug could be absorbed by the nasal epithelial cells, thereby delivering it directly through axonal transport pathway into the CNS [18,27].

Quality by design (QbD) is a systematic industrial approach to the formulation of pharmaceutical products, which begins with predefined objectives and emphasizes product and process understanding and process control, based on quality risk management [28,29]. In addition, submissions for marketing authorization must contain QbD elements according to the regulatory authorities' requirements. Based on ICH guidelines (Q8 R2, Q9, Q10, Q11) the establishment and the control of quality must be grounded on risk-based concepts and principles. The essential elements in a QbD approach are the following: determining the quality target product profile (QTPP), selecting the critical quality attributes (CQAs) and critical process parameters (CPPs), risk assessment (RA), design of experiments (DoE), developing a design space (DS) with a proper control strategy and eventually managing the product's lifecycle, including the aspects of continuous improvement. The CQAs are related to the quality, safety and efficacy profile of the product while the critical material attributes (CMAs) and the CPPs are related to the selected production method. With evaluating a risk estimation matrix, we can truly generate a risk-and-knowledge-based quality management method by ranking CQAs and CPPs regarding their degree of impact on the targeted product quality [30]. This classical QbD model was also favorable in terms of preformulation studies of nanoDDSs, as well as for nasal formulations [31–33].

Our study aimed to formulate "ex tempore" reconstitutable MEL-loaded Soluplus[®] polymeric micelles for intranasal application, exploiting the nose-to-brain pathway optimized via quality by design (QbD) approach. Preformulation studies were carried out to develop a stable nasal formulation that is preservative-free and does not contain added viscosity enhancer. The experimental design and in vitro characterization were focused on the IVIVC (in vitro-in vivo correlation) as guidance to reduce the number of animal studies [34–36] which was predicted using a mathematical model.

2. Materials and Methods

2.1. Materials

MEL (4-hydroxy-2-methyl-*n*-(5-methyl-2-thiazolyl)-2H-benzothiazine-3-carboxamide-1,1-dioxide) was applied as model drug and acquired from EGIS Plc. (Budapest, Hungary). Soluplus[®] (BASF GmbH, Hanover, Germany) was used as micelle-forming agent. Ethanol (Merck, Ltd., Budapest, Hungary) as organic solvent was used during our experiment. Microcrystalline sodium hydroxide (NaOH) as formulation excipient, chemicals for Simulated Nasal Electrolyte Solution (SNES) [16] which combined 8.77 g sodium chloride (NaCl), 2.98 g potassium chloride (KCl), 0.59 g and anhydrous

calcium chloride (CaCl₂) in 1000 mL of deionized water at pH 5.6 as well as disodium phosphate (Na₂HPO₄), monopotassium phosphate (KH₂PO₄) for pH 7.4 Phosphate-buffered saline (PBS) dissolution media and the cryoprotectant D-trehalose dihydrate were acquired from Sigma-Aldrich Co., Ltd. (Budapest, Hungary). Purified water for the experiments was filtered using the Millipore Milli-Q® (Merck, Ltd., Budapest, Hungary) 140 Gradient Water Purification System.

2.2. Initial Risk Assessment and Knowledge Space Development

The first step in QbD-based initial RA was the determination of the QTPP of the target product. The identification of CQAs and the CPPs of the formulation method was the second step. A primary knowledge space development was made as part of the QbD methodology and a cause and effect (Ishikawa) diagram was set up [37]. The LeanQbD® software (QbD Works LLC, Fremont, CA, USA, www.qbdworks.com) was used for the RA procedure. First, the interdependence rating among QTPPs and CQAs and CPPs and CQAs was evaluated. A three-level scale was used to describe the relation between the parameters: “high” (H), “medium” (M) or “low” (L). Then a probability rating step was made, where a 0–10 scale was used for occurrence estimation of the CPPs where the values were assigned to a similar H/M/L ranking structure. As the output of the RA evaluation, Pareto diagrams [38] were generated presenting the numeric data and the ranking of the CQAs and CPPs according to their potential impact on product quality. Table 1 shows the defined requirements expressed as the QTPPs of MEL-containing polymeric micelles.

Table 1. Elements of the quality target product profile (QTPP), their targets and justification.

QTPP Element	Target	Justification
Indication	Neuroinflammation	NDs, such as Alzheimer’s Disease and Multiple Sclerosis usually pairs with inflammation in the CNS resulting in decreasing quality of life (QoL)
Target patients	Adult (>18 years)	The listed NDs usually concern adult, mostly elderly patients.
Administration route	Nasal	The API can directly reach the CNS bypassing the first-pass effect via “nose-to-brain” route [8].
Site of activity	CNS	COX enzymes play a large role locally in the CNS mediating neuroinflammation [1].
Absorption feature	Rapid uptake by the nasal mucosa	This QTPP is closely related to dissolution and permeability, which two main factors must be fitted to the requirements of the nasal administration route. With high absorption in a short period of time a rapid onset of action can be achieved which feature can be utilized as a reliever for neuroinflammation besides sustaining therapy.
Dissolution profile	Immediate drug-release	The duration of stay is around 10–15 min due to mucociliary clearance therefore it is crucial to efficacy.
Nanocarrier	Polymeric micelles with particle size between 80 and 120 nm with monodisperse distribution	The proper particle characteristics are a critical parameter in absorption from the nasal mucosa exploiting the “nose-to-brain” pathway. Furthermore, increase in specific surface area and decrease in size contributes to higher water solubility, leading to faster dissolution.

2.3. Production of MEL–Soluplus® Polymeric Micelles via Box–Behnken Factorial Design Optimization

First, the appropriate amount of MEL was dissolved in ethanol under continuous stirring by dropwise addition of 1 M NaOH solution. The NaOH solution provided an alkaline medium, therefore the weak acidic character (pK_a = 4.08) of MEL could easily deprotonate and dissolve in the organic solvent. Because of the oxo-enolic tautomeric balance a bright yellow solution was acquired. The next step was the dissolution of Soluplus® in the solution of MEL under the constant stirring of the mixture

for an hour. Then a Büchi R-210 (Büchi, Flawil, Switzerland) rotation vacuum evaporator was used to extract the solvents and a thin layer of matrix film was formed in the round-bottom flask. For the investigations, samples were collected into petri dishes then dried under vacuum for 6 h at ambient temperature (25 ± 2 °C) in a vacuum dryer to provide further solvent removal. The rehydration process was carried out with 6 mL purified water by mechanical agitation using a magnetic stirrer at 500 rpm. MEL's concentration was designed to be constant (2.5 mg/mL) after the rehydration, which is a fraction of the active ingredient content of the currently marketed per os formulations (products contain 15 mg of MEL in their dosage form on the market). Then the rehydrated polymeric micelle formulation was freeze-dried into a stable product. Freeze-drying of solid products were carried out using ScanVac CoolSafe 100–9 (LaboGene, ApS, Lynge, Denmark) laboratory apparatus. Vials were filled with 1.5 mL of polymeric micelles solution and 5 w/w% of trehalose-dihydrate added as cryoprotectant, then freeze-dried at -40 °C and 0.013 mbar for 12 h. Secondary drying was carried out at 25 °C and 0.013 mbar for 3 h. The rehydrated formulation was applied for the Box–Behnken factorial design, micelle characterization and solid-state studies to focus on the effect of MEL and Soluplus®. Freeze-dried products were applied for all the investigations for stability studies, nasal product characterization and in vitro studies.

In order to optimize the formulation of MEL-containing polymeric micelles a 3-factor, 3-level Box–Behnken factorial experimental design was set up. The independent variables were, namely the following: the concentration of Soluplus® (mg/mL), the volume of ethanol (mL) and of 1-M NaOH solution (mL) as three critical parameters in the formulation. Based on the factorial design the ethanolic solution before vacuum evaporation contained the concentration of Soluplus® ranged from 6 to 12 mg/mL, the volume of ethanol from 5 to 10 mL and 1-M NaOH solution from 3 to 6 mL (Table 2). Formulation was prepared in triplicate for parallel measurements. The effect on polydispersity index (PDI) and Z-average values was investigated before freeze-drying to investigate the effect of composition without cryoprotectant analyzing the quadratic response surface and to construct a second-order polynomial model using TIBCO Statistica® 13.4 (Statsoft Hungary, Budapest, Hungary) the relationship of the variables on the response could be described with the following second-order equation:

$$Y = \beta_0 + \beta_1x_1 + \beta_2x_2 + \beta_3x_3 + \beta_{12}x_1x_2 + \beta_{13}x_1x_3 + \beta_{23}x_2x_3 + \beta_{11}x_1^2 + \beta_{22}x_2^2 + \beta_{33}x_3^2, \quad (1)$$

where Y is the response variable; β_0 is a constant, β_1 , β_2 , β_3 are linear coefficients, β_{12} , β_{13} , β_{23} are interaction coefficients between the three factors; and β_{11} , β_{22} , β_{33} are quadratic coefficients. The analysis of variance (ANOVA) statistical analysis was carried out and the results were evaluated in harmony with their *p*-value when we considered a variable significant if *p* was less than 0.05 at 95% confidence level. Response surface plots for PDI and Z-average in the form of contour plots were plotted according to the regression model by keeping one variable at the center level.

2.4. Micelle Characterization

2.4.1. Particle Size Analysis

The average hydrodynamic diameter (Z-average), PDI and zeta potential were measured via dynamic light scattering (DLS) using a Malvern Zetasizer Nano ZS (Malvern Instruments, Worcestershire, UK). The formulations were dissolved in purified water, then measured at 25 °C in folded capillary cells with the refractive index of 1.72. Each measurement was carried out in triplicate with independent formulations. Our criteria were that the particle size (which is closely related to Z-average in stable suspensions) should range from 80 to 120 nm, the PDI less than 0.2 defined by the QTPP with a proper negative zeta potential.

Table 2. Composition and responses of the Box–Behnken factorial design.

Standard Run.	Independent Variables			Z-Average * (nm)	PDI *
	Soluplus® (mg/mL)	Ethanol (mL)	1-M NaOH (mL)		
1	6.0	5.0	4.5	194.5 ± 1.8	0.411 ± 0.02
2	12.0	5.0	4.5	188.0 ± 3.9	0.299 ± 0.09
3	6.0	10.0	4.5	94.87 ± 1.1	0.155 ± 0.02
4	12.0	10.0	4.5	270.1 ± 2.0	0.513 ± 0.07
5	6.0	7.5	3.0	105.6 ± 0.9	0.164 ± 0.01
6	12.0	7.5	3.0	170.4 ± 5.6	0.477 ± 0.04
7	6.0	7.5	6.0	116.2 ± 1.5	0.140 ± 0.03
8	12.0	7.5	6.0	200.12 ± 7.3	0.344 ± 0.11
9	9.0	5.0	3.0	195.0 ± 2.3	0.377 ± 0.05
10	9.0	10.0	3.0	111.6 ± 3.0	0.114 ± 0.06
11	9.0	5.0	6.0	65.4 ± 1.6	0.401 ± 0.17
12	9.0	10.0	6.0	99.5 ± 1.7	0.444 ± 0.06
13	9.0	7.5	4.5	99.86 ± 0.5	0.134 ± 0.04
14	9.0	7.5	4.5	100.12 ± 0.7	0.155 ± 0.08
15	9.0	7.5	4.5	107.7 ± 3.1	0.163 ± 0.05

* Data are means ± SD ($n = 3$ independent formulations).

2.4.2. Morphology

The morphology of the freeze-dried (explained in 2.5.6.) MEL-containing polymeric micelles was characterized using transmission electron microscopy (TEM). The TEM records were captured with FEI Tecnai G2 X-Twin HRTEM (FEI, OR, USA) operating at 200 kV accelerating voltage. Suspensions were prepared from the formulations with ethanol then spread to a copper grid coated with a 3-mm-diameter carbon film. For particle size and distribution analysis, a public domain image analyzer software, ImageJ was used (<https://imagej.nih.gov/ij/index.html>). One hundred particles were measured via the software and the percentage distribution of the particle size was plotted against the particle size. The criterion for particle size distribution was that it is monodisperse when the percentage distribution of one particle size range is greater than 60%.

2.4.3. Thermodynamic Solubility

The thermodynamic solubility of MEL and MEL-containing polymeric micelles was determined in purified water (pH = 7.02; $\kappa = 0.05 \mu\text{S}/\text{cm}$) at 25 °C, in SNES buffer (pH = 5.6) at 30 °C and PBS buffer (pH = 7.4) at 35 °C to present the pH and temperature conditions of the nasal mucosa and blood vessels. One milliliter of liquids was measured, and products were dissolved until visible oversaturation. After the stirring of the mixtures with a magnetic stirrer for 24 h, they were filtrated through 0.22- μm PES membrane and the content of the dissolved drug was determined with HPLC.

Using the data received from the solubility test the following parameters were calculated [39]:

1. Molar solubilization capacity (χ) or moles of drug that can be solubilized per mol of copolymer forming micelles.

$$\chi = \frac{S_{\text{tot}} - S_w}{C_{\text{copol}} - \text{CMC}}, \quad (2)$$

2. Micelle–water partition coefficient (P), which is the ratio of the drug concentration in the micelle to the drug concentration in water.

$$P = \frac{S_{\text{tot}} - S_w}{S_w} \quad (3)$$

3. Standard free energy of solubilization (ΔG_s^0), estimated from the molar micelle–water partition coefficient (P_M).

$$\Delta G_s^0 = -RT \cdot \ln \frac{\chi \cdot (1 - \text{CMC})}{S_w} = -RT \cdot \ln(P_M), \quad (4)$$

In the equations S_{tot} means the total solubility of MEL in the micellar solution, S_w is the solubility of MEL in water, CMC is the critical micelle concentration, C_{copol} is the copolymer concentration in each micellar solution and R is the universal constant of gases.

2.4.4. Encapsulation Efficiency

To determine the encapsulation efficiency for the optimized formulation, we used the indirect method. The MEL-containing polymeric micelles were separated from the aqueous media via centrifugation using a Hermle Z323 K high performance refrigerated centrifuge (Hermle AG, Gosheim, Germany) at 22,500 rpm at 4 °C for 45 min. The clear supernatant was diluted 10-fold with purified water. Quantitative measurements of MEL were performed using HPLC. The encapsulation efficiency (EE%), as the actual MEL content in the optimized formulation, was calculated from this equation:

$$\text{EE\%} = \frac{\text{initial MEL (mg)} - \text{measured MEL (mg)}}{\text{initial MEL (mg)}} \cdot 100, \quad (5)$$

2.4.5. Quantitative Analysis of MEL Using HPLC

The determination of MEL concentration was performed with high performance liquid chromatography (HPLC) using an Agilent 1260 (Agilent Technologies, Santa Clara, CA, USA). As stationary phase a Kinetex[®] C18 column (5 μm , 150 mm \times 4.6 mm (Phenomenex, Torrance, CA, USA)) was used. Ten microliters of the samples was injected to determine the concentration of MEL. The temperature was set at 30 °C. The mobile phases used were 0.065-M KH_2PO_4 solution adjusted to pH = 2.8 with phosphoric acid (A) and methanol (B). The separation was performed in two steps by gradient elution. The proportion of starting 50% A eluent was reduced to 25% in 14 min and then raised again to 50% in 20 min. The eluent flow rate was set at 1-mL/min and the chromatograms were detected at 355 ± 4 nm using UV-Vis diode array detector. Data were evaluated using ChemStation B.04.03. Software (Agilent Technologies, Santa Clara, CA, USA). The retention time of MEL was at 14.34 min. The linear regression of the calibration line was 0.999. The determined limit of detection (LOD) and quantification (LOQ) in the case of MEL were 16 ppm and 49 ppm.

2.4.6. Surface Free Energy and Polarity Investigation

OCA Contact Angle System (DataPhysics OCA 20, DataPhysics, Inc., GmbH, Filderstadt, Germany) was used for studying the wettability of the polymeric micelles and its components. For the measurements 0.10 g of powder containing the components was compressed under a pressure of 1 t by a Specac[®] hydraulic press (Specac, Inc., Fort Washington, PA, USA). The liquid mediums used for our contact angle measurements included bidistilled water (interfacial tension of polar component (γ_i^{P}) = 50.2 mN/m, interfacial tension of disperse component (γ_i^{d}) = 22.6 mN/m) and diiodomethane (γ_i^{P} = 1.8 mN/m, γ_i^{d} = 49 mN/m). The contact angles of pressings were determined applying the method of Wu. The solid surface free energy is the sum of the polar (γ_i^{P}) and nonpolar (γ_i^{d}) components and was calculated according to the Wu equation [40]:

$$(1 + \cos \Theta) \gamma_1 = \frac{4(\gamma_s^{\text{d}} \gamma_1^{\text{d}})}{\gamma_s^{\text{d}} \gamma_1^{\text{d}}} + \frac{4(\gamma_s^{\text{P}} \gamma_1^{\text{P}})}{\gamma_s^{\text{P}} \gamma_1^{\text{P}}}, \quad (6)$$

where Θ is the contact angle, γ_s is the solid surface free energy and γ_l is the liquid surface tension. The percentage polarity can be calculated from the γ_p and γ values:

$$\text{Percentage polarity [\%]} = \frac{\gamma^p}{\gamma} \cdot 100, \quad (7)$$

2.5. Characterization of MEL–Soluplus[®] Interaction in Solid State

2.5.1. X-Ray Powder Diffraction (XRPD)

Using X-ray powder diffraction, the changes in the crystalline structure were investigated. The formulations were measured with a Bruker D8 Advance X-ray powder diffractometer (Bruker AXS GmbH, Karlsruhe, Germany) with Cu K α radiation ($\lambda = 1.5406 \text{ \AA}$) and a VANTEC-1 detector. The samples were scanned at 40 kV voltage and 40 mA amperage. The angular range was 3° to $40^\circ 2\theta$, at a step time of 0.1 s and a step size of 0.007° . All manipulations and evaluations were carried out using EVA software.

2.5.2. Differential Scanning Calorimetry (DSC)

DSC measurements were performed in order to investigate the encapsulation of MEL inside the polymeric micelle. Examinations were carried out using a METTLER-Toledo 821e DSC (Mettler-Toledo GmbH, Gießen, Germany) at the temperature interval of $0\text{--}300^\circ\text{C}$ with the heating rate of $10^\circ\text{C}/\text{min}$ under a constant argon flow of $150 \text{ mL}/\text{min}$. Every measurement was normalized to the sample size and was evaluated with STARe Software.

2.5.3. Thermogravimetry (TGA)

TGA measurements were carried out in order to investigate the thermal stability of polymeric micelles. Investigations were performed with a METTLER-Toledo TGA/DSC 1 (Mettler-Toledo GmbH, Gießen, Germany). Then, $5 \pm 0.2\text{-mg}$ was measured into aluminum pans, closed and inserted into the furnace. The furnace was heated up from 25°C to 275°C with $10^\circ\text{C}/\text{min}$ heating rate and we measured the thermic changes in the sample. The results were evaluated using STARe Software.

2.5.4. Fourier Transform Infrared (FT-IR) Spectroscopy

FT-IR spectroscopic study was performed using an Avatar 330 FT-IR spectrometer (Thermo Nicolet, Waltham, MA, USA) to investigate the interactions between MEL and Soluplus[®]. Pastilles from the samples and 0.15 g potassium bromide were formed using a Specac[®] hydraulic press (Specac, Inc., USA) by 10 t pressing force. The infrared spectra of the pastilles were collected in the range of $400\text{--}4000 \text{ 1}/\text{cm}$ with deuterated triglycine sulfate detector. The spectral resolution was set at $4 \text{ 1}/\text{cm}$ and 128 parallel scans were averaged.

2.5.5. Raman Spectroscopy

For the investigation of polymeric micelles, a Thermo Fisher DXR Dispersive Raman instrument (Thermo Fisher Scientific, Inc., Waltham, MA, USA) equipped with a CCD camera and a diode laser operating at a wavelength of 780 nm was used. Raman measurements were carried out with a laser power of 12 mW at $25\text{-}\mu\text{m}$ slit aperture size with an exposure time of 2 and acquisition time of 6 s, for a total of 32 scans per spectrum in the spectral range $3500\text{--}200 \text{ 1}/\text{cm}$ with cosmic ray and fluorescence corrections. The distribution of MEL was investigated by Raman chemical mapping in the formulation. A $90 \mu\text{m} \times 90\text{-}\mu\text{m}$ size surface were analyzed with step size of $10 \mu\text{m}$ with an exposure time of 2 s and acquisition time of 4 s, for a total of 4 scans per spectrum. The Raman spectra were normalized in order to eliminate the intensity deviation between the measured areas.

2.5.6. Physical-Stability via Freeze-Drying

Polymeric micelles are fragile dynamic systems; therefore, it is highly desirable to stabilize the nanoparticles by freeze-drying. In accordance with the ICH Q1A guideline we conducted a stability study in a refrigerator for 12 months at $5\text{ }^{\circ}\text{C} \pm 3\text{ }^{\circ}\text{C}$ [41]. Each month a portion was dissolved in purified water and then particle size and PDI were measured using the Section 2.4.1 method.

2.6. Residual Organic Solvent Determination

Ethanol belongs to Class 3 solvents; thus its residual concentration should be less than 5000 ppm in the daily dose of the final product according to the requirement of the International Council of Harmonization (ICH) Q3C (R5) guideline for residual solvents [42]. For safety and quality profiling the residual ethanol content of the dissolved polymeric micelles was analyzed by a Shimadzu GC-14B gas chromatograph (Shimadzu Europa GmbH, Duisburg, Germany) equipped with a thermal conductivity (TCD) and a flame ionization detector (FID). The calibration curve was previously determined in the range of 0–0.35 mM of ethanol. The concentration of ethanol (c_{ethanol}) is directly proportional to the area of the peak for ethanol (E_{ethanol}):

$$c_{\text{ethanol}} = \frac{A_{\text{ethanol}}}{36613992.1} \quad (8)$$

2.7. Characterization of Ex Tempore Redispersed Nasal Formulation

The main parameters of ex tempore redispersed lyophilized polymeric micelle formulation were characterized for intranasal applicability. The reconstitution time of powder ampoules containing 3.0 mg of MEL was measured after adding 1.0 mL of purified water (pH = 6.53). After reconstitution, the pH of the colloidal solution was measured with WTW[®] inoLab[®] pH 7110 laboratory pH tester (Thermo Fisher Scientific, Budapest, Hungary). Particle size, PDI and zeta potential were determined with dynamic light scattering as described above. The osmolality of the redispersed polymeric micelles was measured by means of an automatic osmometer (Knauer Semi-micro Osmometer, Berlin, Germany) in three parallels. The determination of osmolality is based on the measurement of the freezing point depression of the colloidal solution. Viscosity measurements were performed at 35 °C nasal temperature with a RheoStress 1 HAAKE instrument (Karlsruhe, Germany) conducted with cone–plate geometry (radius 49.9 mm, 1° angle and 0.052 mm gap). The apparent viscosity of the samples was measured over a shear rate sweep of 0.01–100 s^{−1}.

2.8. In Vitro Characteristics

2.8.1. In Vitro Dissolution Test

The modified paddle method (Hanson SR8 Plus (Teledyne Hanson Research, Chatsworth, CA, USA) was used to examine the rates of dissolution of the polymeric micelle formulations and determine the drug release profile from the samples. One hundred milliliters of SNES was used as a dissolution medium at 35 °C. The paddle was rotated at 100 rpm, and the sampling was performed up to 60 min. Three parallel measurements took place with the optimized formulations. Quantification of aliquots was performed by HPLC after filtration with the method described previously.

From the data acquired from the dissolution test, the following statistical analysis of MEL dissolution profile was evaluated [32]. The percentage dissolution efficiency (%DE) for MEL and each MEL-containing polymeric micelle formulation was calculated as the percentage ratio of the area under the dissolution curve up to time t to that of the area of the rectangle described by 100% dissolution at the same time as follows:

$$\%DE = \frac{\int_0^t y \cdot dt}{y_{100} \cdot t} \cdot 100\%, \quad (9)$$

The trapezoidal method was used to calculate the area under the curve (AUC_{0-t}) which is the sum of all the trapezia defined by:

$$AUC = \sum_{i=1}^{i=n} \frac{(t_i - t_{i-1})(y_{i-1} + y_i)}{2}, \quad (10)$$

where t_i is the time point and y_i is the percentage of product dissolved at time t_i .

The relative dissolution (RD) time at 15 min (RD_{15}) in the case of the formulations compared to crystalline MEL was calculated using the formula:

$$RD_{15 \text{ min}} = \frac{\%DE_{15 \text{ min}} \text{Pol_mic}}{\%DE_{15 \text{ min}} \text{MEL}}, \quad (11)$$

The mean dissolution time (MDT) was calculated using this expression:

$$MDT = \frac{\sum_{i=1}^n t_{\text{mid}} \Delta M}{\sum_{i=1}^n \Delta M}, \quad (12)$$

where i is the dissolution sample number, n is the number of dissolution times, t_{mid} is the time at the midpoint between times t_i and t_{i-1} and ΔM is the amount of MEL dissolved (mg) between times t_i and t_{i-1} .

2.8.2. In Vitro Nasal Diffusion

In vitro nasal diffusion study of MEL from the nasal cavity was performed in a modified Side-Bi-Side[®] horizontal diffusion cell. A cellulose membrane impregnated with isopropyl myristate having a surface of 0.785 cm², the cell volume was 9.0 mL and the diffusion was investigated at 35 °C. The donor phase consisted of pH 5.6 SNES solution simulating the nasal fluid and the acceptor phase was a pH 7.4 phosphate buffer simulating the plasma in the nasal vessels. Absorbance was inline measured in each 50 ms for 60 min on an AvaSpec 204 BB spectrophotometer (Avantes, Apeldoorn, The Netherlands) at 364 nm in the acceptor phase. Three parallel measurements took place with the optimized formulations (Pol_mic1–3). The flux (J) of the drug was calculated from the quantity of MEL which permeated through the membrane, divided by the surface of the membrane insert and the duration (μg/cm²/h) [43]. The permeability coefficient (K_p) was determined from J and the drug concentration in the donor phase (C_d (μg/cm³):

$$K_p \left[\frac{\text{cm}}{\text{h}} \right] = \frac{J}{C_d} \quad (13)$$

Relative permeability (RP) at 15 min (RP_{15}) in the case of the formulations compared to crystalline MEL was calculated using this formula:

$$RP_{15 \text{ min}} = \frac{\text{Diffused MEL}_{15 \text{ min}} \text{Pol_mic}}{\text{Diffused MEL}_{15 \text{ min}} \text{MEL}} \quad (14)$$

where the diffused MEL values were calculated from the slopes between 10 and 20 min.

2.8.3. In Vitro and In Vivo Correlation (IVIVC)

According to the FDA guidance [34–36], an IVIVC is defined as a predictive mathematical model describing the relationship between an in vitro property of a dosage form and an in vivo response. Thus, IVIVC can be used to predict the in vivo pharmacokinetics of the formulation from its in vitro dissolution and diffusion data. In contract, it can also help to design the optimal in vitro dissolution and diffusion profiles of the formulation for the desired in vivo pharmacokinetics. Therefore, once the predictability of IVIVC has been established, the in vitro dissolution and diffusion may provide a surrogate for in vivo experiments [36]. Among the different levels of IVIVC, a level-C IVIVC allows for

predicting the relationship between in vivo pharmacokinetic parameters (e.g., API brain distribution–AUC) and in vitro data (dissolution rate, diffusion rate) at a single point, but it does not substitute bioequivalence study. As IVIVC is generally described by a linear relationship between parameters derived from the in vitro and in vivo experiments, the Pearson correlation was applied to investigate that relationship. Previous in vitro and in vivo data of different MEL containing nasal formulations with equal drug content was used for IVIVC to predict the in vivo brain distribution of intranasal administration of MEL-containing polymeric micelles. Data were expressed as means \pm SD, and groups were compared by Student's t-test using TIBCO Statistica® 13.4 (Statsoft Hungary, Budapest, Hungary). Differences were considered statistically significant when $p < 0.05$.

3. Results

3.1. Initial Risk Assessment and Knowledge Space Development

QTPP was defined as Soluplus®-based polymeric micelles containing MEL, as a nonsteroidal anti-inflammatory drug, with proper particle size and distribution and optimal physicochemical profile. The formulations should ensure proper dissolution and permeability parameters, in order to reach the central nervous system via intranasal administration bypassing the first-pass effect, which can be applied by an adult population suffering from neurodegenerative diseases. Due to the fact, that polymeric micelles are one of the nanodrug delivery systems, a special regulatory aspect is needed to exclude potential nanotoxicity. This needs further information on safety, efficacy and the quality of the product in the submissions during the authorization process. By targeting the brain via this administration route, we must also consider avoiding systemic side effects. Risks can originate from the final product itself, e.g., physical-stability, dissolution and permeability issues, solubility and polarity as well as from the therapeutic use (irritation, damage of the nasal mucosa, effects on nasal function, e.g., smell). The patient could belong to a risk group during administration (lack of adherence, increased effect with side effects due to fast dissolution).

During the knowledge space development, which is the collection of the influencing factors, the potential factors which can influence the final product were grouped into four sections based on the classic 4-M Ishikawa (or cause and effect) diagram: material characteristics, production method, product characteristics and therapeutic expectations (Figure 1).

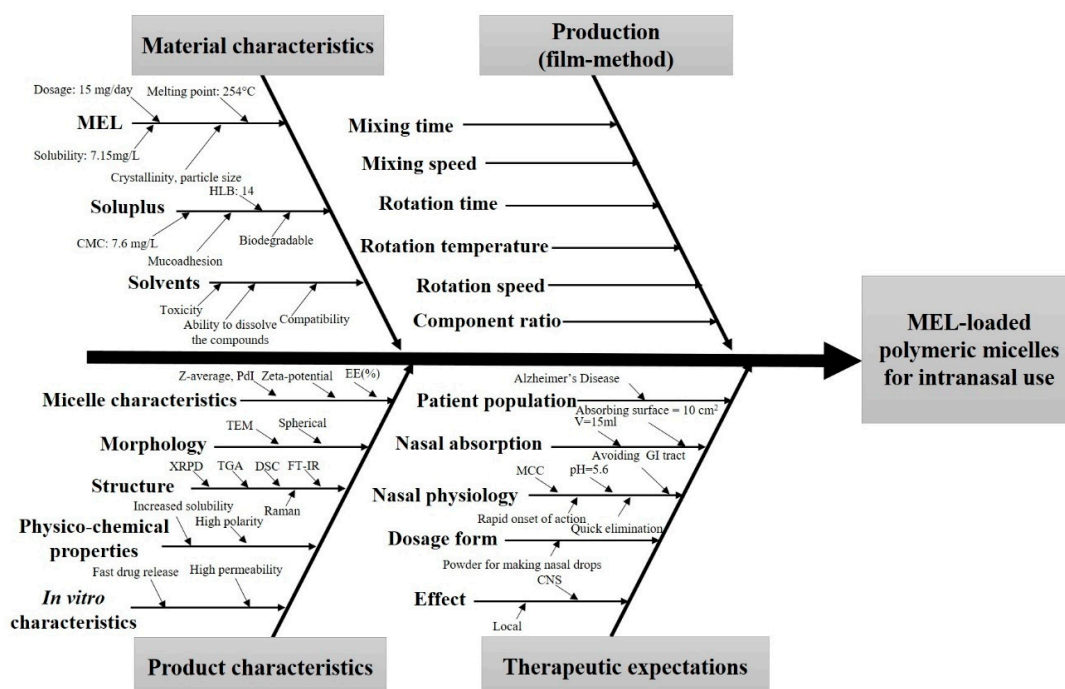


Figure 1. Ishikawa—or cause and effect diagram—of the influencing parameters of meloxicam (MEL)-containing polymeric micelles for intranasal use. Abbreviations not mentioned before: HLB—hydrophile–lipophile balance; GI—gastrointestinal; MCC—mucociliary clearance.

For CPPs the following were selected: composition, mixing time, rotation pressure, temperature and speed. These parameters were followed carefully during the formulation and became one of the bases for further factorial experimental design. CQAs were the following: particle size, excipients, encapsulation efficiency (EE%), dissolution time, solubility, permeability, wettability, structure, stability, physical appearance and toxicity/irritation, as these factors have critical effects on the QTPP. Among the QTPP elements, CQAs and CPPs an initial RA was performed (Figure 2).

A

QTPP \ CQA	Indication	Adult	Nasal	Site of activity: CNS	Monodisperse polymeric micelles	Immediate drug-release	Absorption feature	Severity score [%]
Particle size	M	L	H	H	H	H	H	21.84
Excipients	L	L	M	M	H	H	H	17.51
Solubility	M	L	H	M	H	H	H	11.49
Dissolution time	L	L	H	M	M	M	M	8.92
Permeability	H	L	H	H	M	M	H	8.49
Encapsulation efficiency	M	L	M	M	M	H	H	8.03
Wettability	M	L	M	M	M	H	H	6.26
Structure	L	L	M	L	M	M	M	5.75
Physical appearance	L	L	M	M	L	M	M	5.06
Stability	L	L	L	L	L	L	M	3.77
Toxicity/irritation	L	L	M	L	L	L	L	2.88

B

CQA \ CPP	Excipients	Particle size	Physical appearance	Dissolution time	Toxicity/irritation	Structure	Stability	Encapsulation efficiency	Wettability	Solubility	Permeability	Severity score [%]
Composition	H	H	M	H	M	H	H	H	H	H	H	47.78
Mixing time	M	H	M	M	M	L	L	H	M	H	M	21.88
Rotation pressure	L	M	L	L	L	L	L	M	M	H	M	15.39
Rotation temperature	M	M	L	L	L	M	L	M	M	M	M	7.82
Rotation speed	L	M	M	M	L	L	L	L	L	M	M	7.13

Figure 2. Risk assessment of the MEL-loaded polymeric micelles. (A,B) Interdependence ratings between (A) CQAs and QTPPs and CQAs and (B) CPPs with the calculated severity scores of CQAs and CPPs in decreasing order of risks. Abbreviations: QTPP—quality target product profile; CQA—critical quality attributes; CPP—critical process parameters; L—low; M—medium; H—high.

Tables of Figure 2 present the estimated relationships of the selected critical factors. Three levels were assigned for each interaction. The ones that have minimal effect on each other are marked green, the interactions with medium effect are marked yellow and the ones with the highest impact are marked red. Using the Lean QbD[®] Software, the severity score was determined, and the factors were ranked from highest to lowest based on their impact. It was found that, theoretically, particle size, excipients, dissolution time, EE%, solubility and permeability had the highest impacts among CQAs on the quality and efficacy of MEL-loaded polymeric micelles. The analogous diagram shows that among CPPs, the composition of the formulation was expected to have the highest influence. The other CPPs

can be easily adjusted and may have a minimal effect on the quality of the final product. The results of the RA gave the basis of the factorial experimental design which was built up based on variations of the composition. As for CQAs, particle size (expressed as Z-average) and particle size distribution (expressed as PDI) can be primarily optimized with the appropriate composition. They have a direct impact on EE%, solubility, dissolution and permeability, which were later investigated as well.

3.2. Production and Optimization of MEL–Soluplus® Polymeric Micelles via Box–Behnken Factorial Design

Using the experimental design, the ratio of Soluplus® and ethanol with the excipient 1-M NaOH solution was investigated. After rotary evaporation and vacuum drying, the films were rehydrated with 6 mL of purified water and Z-average and PDI were measured in triplicate with independent formulations. The results from the 15 formulations were analyzed by TIBCO Statistica 13.4 software and are shown in Table 2.

Polynomial equations were generated to describe the individual main effects and interaction effects of the independent variables on the dependent factors individually. According to the ANOVA and regression analysis of the data, the relationship of the variables on PDI (Y_1) could be described with the following equation:

$$Y_1 = 0.319 + 0.084x_1 - 0.025x_2 + 0.003x_3 + 0.118x_1x_2 - 0.027x_1x_3 + 0.077x_2x_3 + 0.084x_1^2 - 0.025x_2^2 - 0.030x_3^2. \quad (15)$$

The regression coefficient of the surface plot was 0.998 (R^2), the adjusted was 0.989 (R^2) which indicates good correlation. The concentration of Soluplus® (x_1) and the volume of ethanol (x_2) affected ($p < 0.05$) the PDI significantly. The positive coefficients before the independent variables (x_1 , x_3 , x_1x_2 , x_2x_3 , x_1^2) are unfavorable, because it means that by increasing the value of the variables, we increase the PDI while the negative coefficients (x_2 , x_1x_3 , x_2^2 , x_3^2) decrease it. The proper concentration of the polymeric micelle forming agent in the right volume of ethanol solvent resulted in favorable formulation. Our criteria were to reach PDI less than 0.2 with a Z-average ranging from 80 to 120 nm. Increasing the concentration was unfavorable for PDI because the higher the concentration, the more excess polymer dissolves, which results in unloaded, blank polymeric micelles. These have lower Z-average resulting in high PDI compared to the MEL-loaded ones with monodisperse distribution.

The effect of the independent factors on Z-average (Y_2) can be described using the following equation:

$$Y_2 = 150.94 + 40.52x_1 - 7.03x_2 - 5.09x_3 + 45.43x_1x_2 + 4.78x_1x_3 + 29.38x_2x_3 - 28.63x_1^2 - 13.53x_2^2 + 5.87x_3^2. \quad (16)$$

The regression coefficient of the surface plot was 0.999 (R^2), the adjusted was 0.993 (R^2), which also indicates good correlation. The concentration of Soluplus® (x_1) and the interaction between the concentration of Soluplus® and the volume of ethanol (x_1x_2) were significant ($p < 0.05$). The positive coefficients before the independent factors (x_1 , x_1x_2 , x_1x_3 , x_2x_3 , x_1^2) result in increased particle size which also clashes with our criteria that the particle size (expressed in Z-average, therefore in hydrodynamic diameter) should be in the range of 80 to 120 nm. The negative coefficients before the factors (x_2 , x_3 , x_2^2 , x_3^2) decrease the particle size. The contour plots in Figure 3 also indicate the proper amount of independent factors.

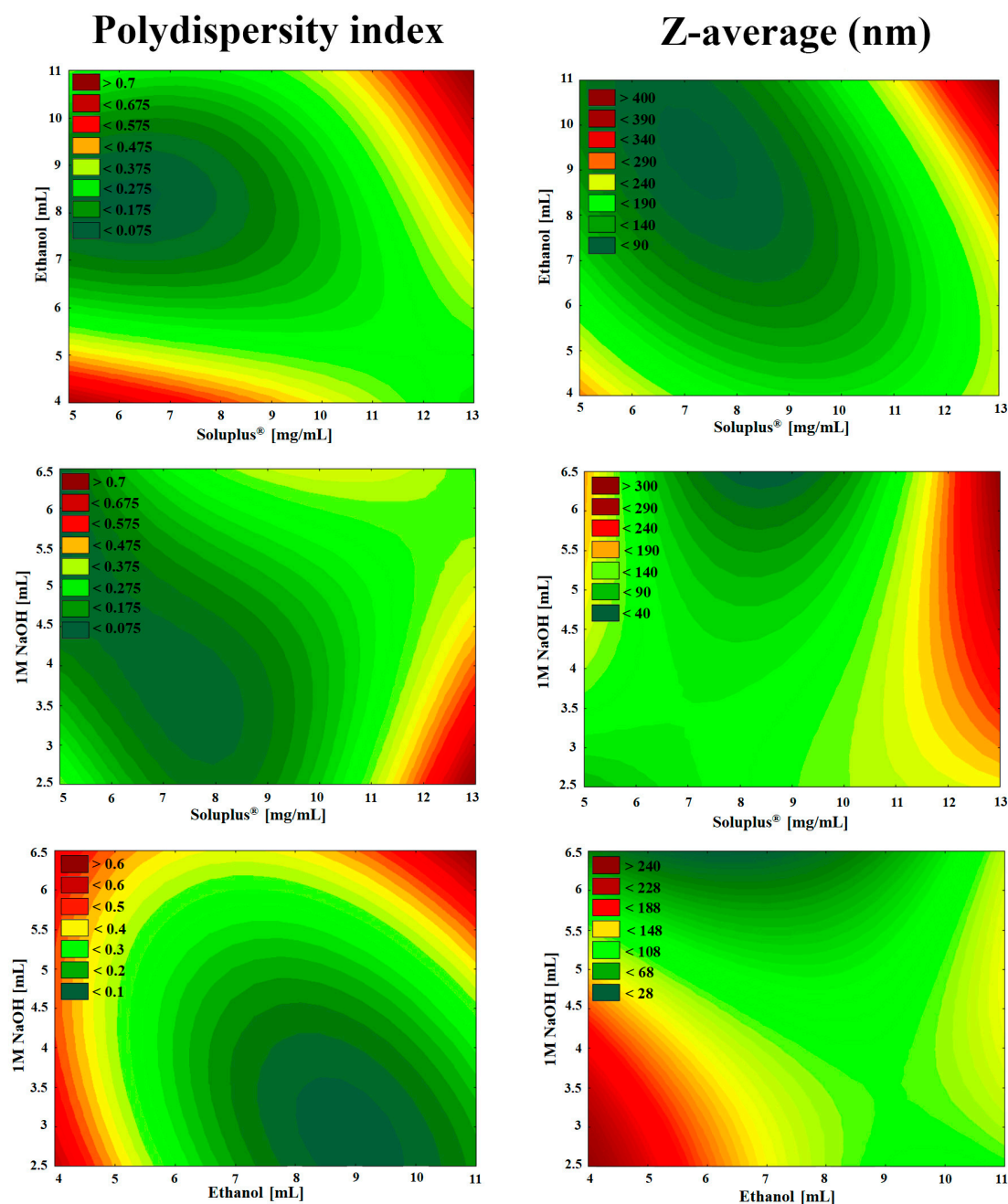


Figure 3. Two-dimensional surface plots of the effect of independent variables in the Box–Behnken factorial design.

As seen in the Box–Behnken factorial design, the volume of 1 M NaOH solution was not linearly significant either in the cases of PdI or Z-average. The high melting point of MEL (254 °C), thermal stability and the glass transition temperature of Soluplus® (70 °C) allowed a safe and controllable formulation. As a result, solid MEL-containing polymer micelles were obtained which dissolve rapidly in small volumes of purified water. The solution visibly showed a bluish opalescence (Tyndall effect) which is a characteristic of the colloidal, especially the nanoscale systems. Based on the design space (Figure 3 green area) the optimized composition of formulation contained 2.5-mg/mL MEL, 9-mg/mL Soluplus®, 10 mL Ethanol and 3 mL NaOH with suitable Z-average (111.6 ± 3.0), monodisperse size distribution (PdI of 0.114 ± 0.06) and the zeta potential value was -25.2 ± 0.4 mV. This surface charge prevents the aggregation of the nanoparticles, i.e., they are dispersed stably and meet the physicochemical criteria. This optimized formulation was applied for further characterization.

In case of formulations having large PDI there was a mixture of subpopulation of different sizes. These compositions showed heterogeneous size distribution, a mixture of subpopulation of different sizes with a peak at 80 nm corresponding to unloaded micelles and a peak with the maximum higher than 500 nm referred to aggregation of micelles may occur.

3.3. Micelle Characterization

3.3.1. Morphologic Characterization

TEM images and the particle size distribution of rehydrated polymeric micelles are shown in Figure 4. The polymeric micelles are spherical and have a smooth surface. They feature a quasi-monodispersed diameter distribution with particle size ranging from 85 to 135 nm which corresponds to our DLS measurements explained above. The previously set criterion was fulfilled, with particle distribution of 68% in the range of 100 to 105 nm. In the images suspended D-threitol dihydrate bigger in diameter can be detected as well, which was excluded from the particle size analysis.

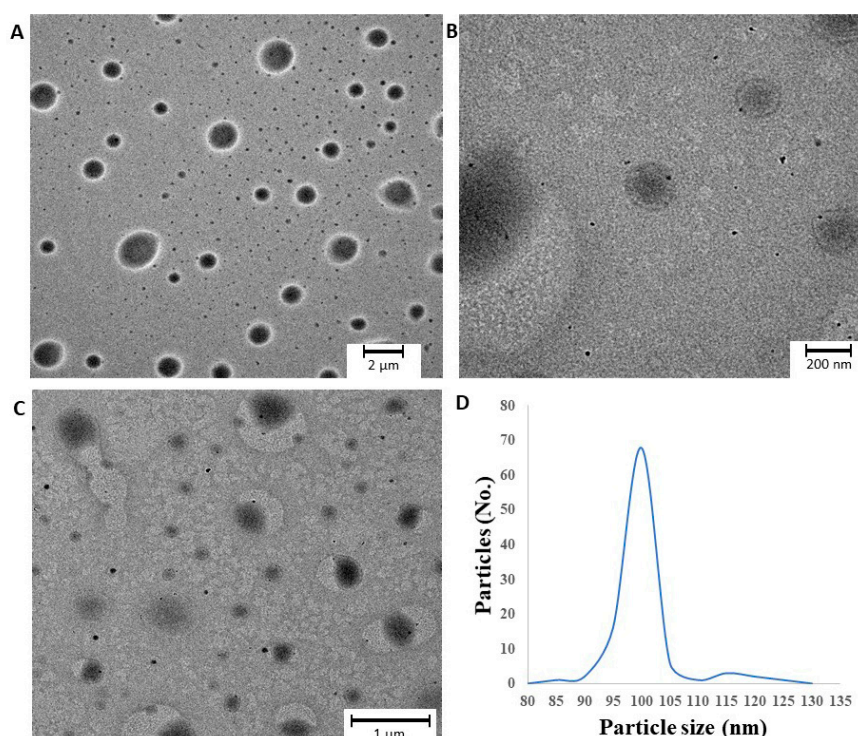


Figure 4. (A–C) TEM images of optimized freeze-dried MEL-loaded polymeric micelles and (D) particle size distribution.

3.3.2. Encapsulation Efficiency and Solubility Studies

Table 3 summarizes the parameters which were used to quantify the efficiency of solubilization. The solubility test showed that the solubility values of the MEL-containing polymeric micelles are much higher compared to the crystalline MEL in all three media. The solubility increases parallel with the pH, as MEL is a weak acid ($pK_a = 4.08$), therefore its solubility is higher in the weakly alkaline environment. The polymeric micelles follow the same tendency. The micelle–water partition coefficient recorded was highly above 1, ranging from 782.20 to 825.45, and the P_M value ranged from 77.68 to 81.98, which means that there are more MEL molecules localized in the core of the polymeric micelles than free (solubilized) ones. These results confirmed efficient incorporation supported by negative free energy of solubilization, which resulted in spontaneous association and was thermodynamically favored by the hydrophobicity of Soluplus[®] polymeric micelle cores. The results can be explained by the monodispersed, proper particle size decrease because of Soluplus[®] and the high encapsulation

efficiency. The amorphous state and the lack of lattice energy also support these results which could predict the faster dissolution rate and nasal diffusion of MEL-loaded polymeric micelles.

Table 3. Solubility, encapsulation efficiency and calculated parameters of drug-loaded polymeric micelles.

pH	S _w (mg/L)	S _{tot} (mg/L)	χ	P	P _M	ΔG _s ⁰ (kJ/mol)	EE (%)
5.6	6.92 ± 0.19	5419.7 ± 1.284	0.54	782.20	77.68	−10.983	89.4
7.03	6.99 ± 0.45	5527.0 ± 1.197	0.55	789.70	78.34	−10.813	92.1
7.4	7.09 ± 0.33	5775.9 ± 0.798	0.57	825.45	81.98	−11.363	89.9

3.3.3. Surface Free Energy and Polarity Investigation

The wettability study showed that the formulations had a more hydrophilic character as compared with crystalline MEL (Table 4). The contact angle of MEL (75.3°) was relatively high, showing its poor hydrophilicity, while the contact angle of formulations was lower (11.3°) predicting higher hydrophilic character. Soluplus[®] by itself has a good polarity as well. By encapsulating MEL in the polymeric micelle, the surface characteristics and polarity increased. These results corroborate the thermodynamic solubility mentioned earlier because higher polarity presumes higher solubility in water.

Table 4. Wetting properties of components and polymeric micelles.

Samples.	Θ _{water} (°)	Θ _{diiodomethane} (°)	γ ^d (mN m ^{−1})	γ ^p (mN m ^{−1})	γ (mN m ^{−1})	Polarity (%)
MEL	74.1 ± 5.2	15.9 ± 3.3	44.7	9.77	54.47	17.9
Soluplus [®]	33.4 ± 0.3	16.4 ± 0.0	44.02	29.20	73.22	39.6
Physical mixture	34.3 ± 1.7	19.2 ± 2.1	43.34	29.00	72.34	40.0
Polymeric micelle	11.3 ± 0.5	23.4 ± 0.1	42.08	37.13	79.21	47.0

3.4. Characterization of MEL–Soluplus[®] Interaction in Solid State

3.4.1. X-Ray Powder Diffraction (XRPD) Study

During our experiment, the diffractograms of crystalline MEL, Soluplus[®], their physical mixture and the polymeric micelles were recorded. The diffractograms in Figure 5, show that the characteristic peaks of crystalline MEL could not be detected in the polymeric micelles compared to the physical mixture components. Based on the results, we can conclude that a new system was formed between MEL and Soluplus[®] with the encapsulation process, only the amorphous structure of the micelle forming excipient can be observed in the diffractogram of polymeric micelles. MEL itself has a poor glass forming property ($T_g/T_m = 0.63$), which proves that MEL did not go through amorphization, it was molecularly dispersed into the core of polymeric micelles and the amorphous sign of Soluplus[®] as micelle shell forming agent suppressed its characteristic peaks [44].

3.4.2. Differential Scanning Calorimetry (DSC) Measurement

The DSC curves (Figure 6) support the results of the XRPD study, the endothermic peak corresponding to the melting point of MEL disappears in the formulation, suggesting the encapsulation inside the micelle, unlike in the physical mixture. A slight reduction in the melting point from 264 °C to 254 °C in the physical mixture can be observed, which could occur due to the formation of a solid dispersion.

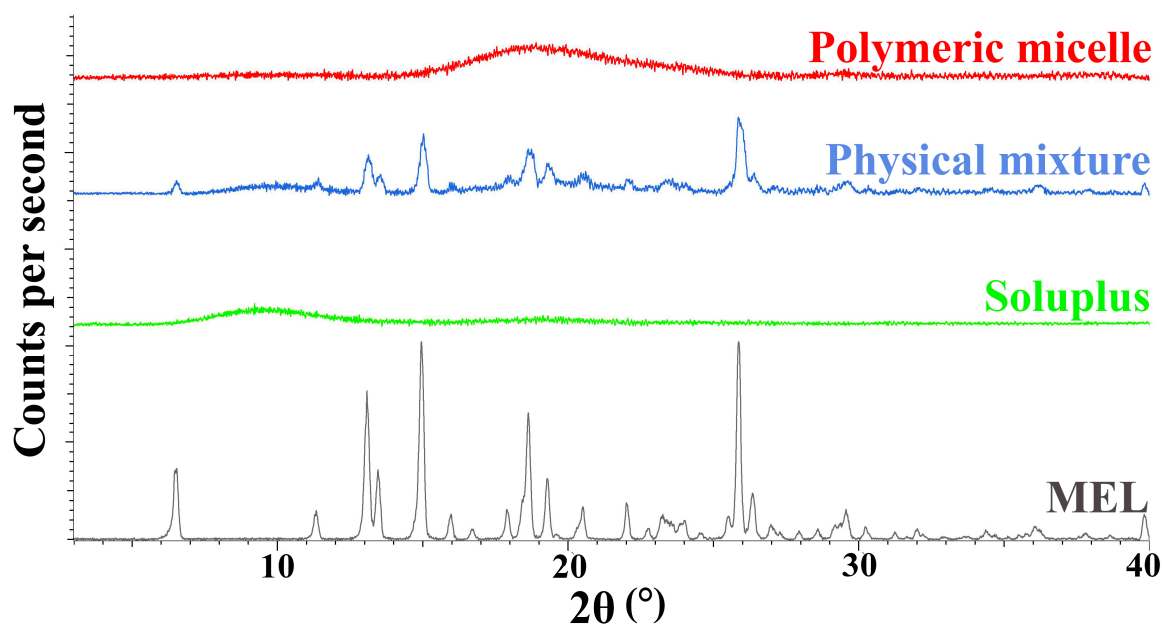


Figure 5. X-ray powder diffractograms of the components and the formulation.

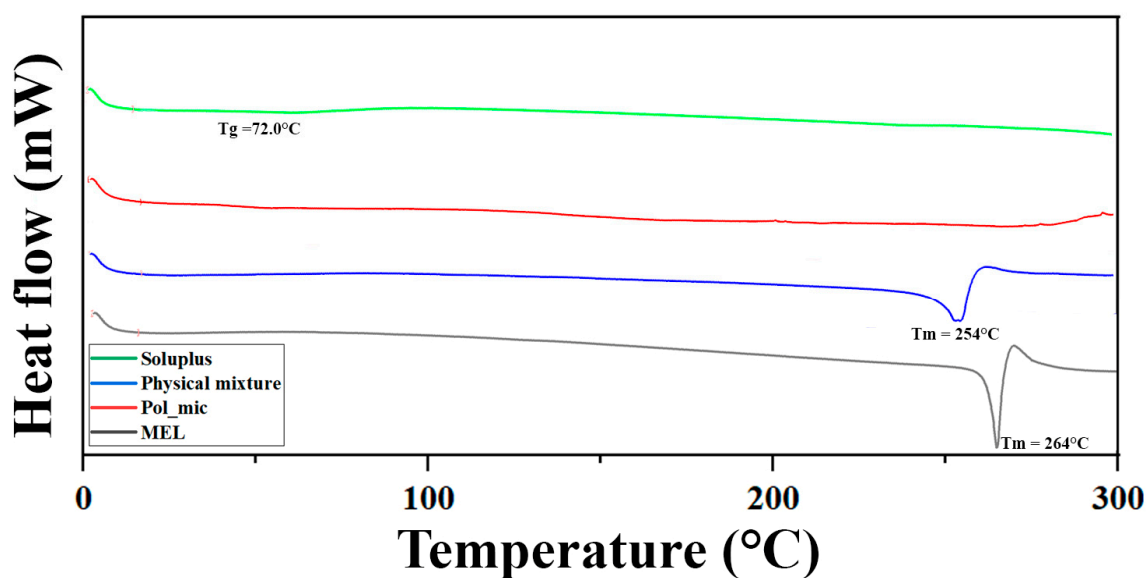


Figure 6. Differential scanning calorimetry (DSC) curves of the components and the formulation.

3.4.3. Thermogravimetric Analysis (TGA)

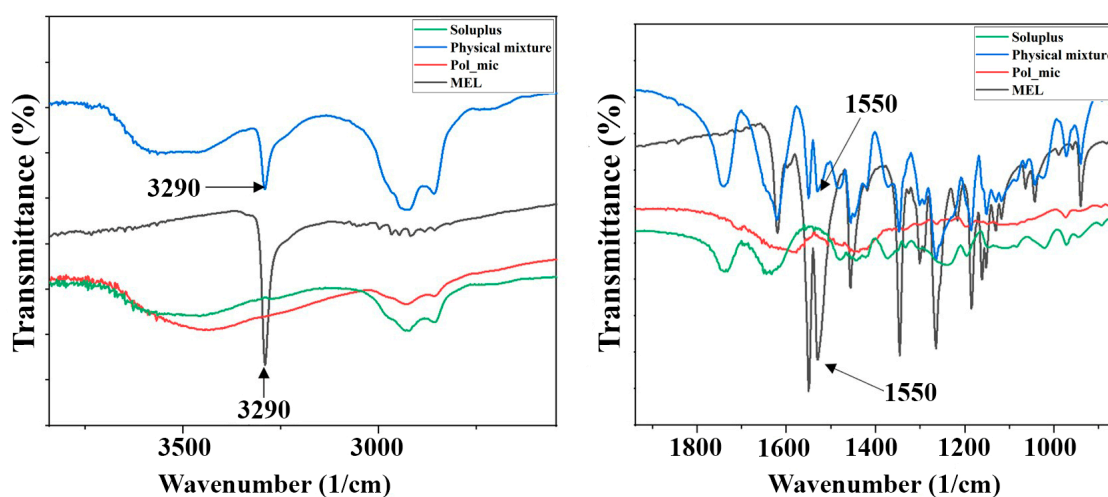
TGA measurements were carried out to investigate the thermal stability of the formulation. The degradation was examined in the temperature interval between 25 °C to 275 °C. The weight loss of each component was measured, which can be seen in Table 5, showing that the polymeric micelles are stable against temperature. For the polymeric micelles two data were collected, one at 103 °C where it lost almost 1% of its weight and one at 237 °C losing 5% of it. As these are already extreme conditions, both during the storage of the formulation and in the production of polymeric micelles, it is safe to say that the products are stable against temperature increase. The loss of weight corresponds with the reduction of hydroxyl groups of PEG 6000 portion in Soluplus[®] by condensation.

Table 5. Thermal behavior of components and the formulation.

Material	Starting Point of Weight Loss (°C)	Maximal Weight Loss at 275 °C (%)
Meloxicam	257	2.92
Soluplus®	241	5.33
Physical mixture	185	7.14
Polymeric micelle	103	4.98

3.4.4. Fourier-Transform Infrared (FT-IR) Spectroscopy

Hydrogen bonding among polymeric micelle forming components can enhance the intra-micelle interaction and micelle stability. Hydrogen bonding interactions are selective and noncovalent interactions, which only form between hydrogen bonding donors and acceptors. The participation of hydrogen bonding interactions directs the self-assembly of copolymers and stabilizes the micellar cores, which exhibit great potential as nanoDDSs. Vibrational spectroscopy is a suitable tool for the determination of H-bonding. The FT-IR spectra of polymeric micelles and components can be seen in Figure 7.

**Figure 7.** FT-IR spectra of the enlarged regions indicating the secondary interactions.

The spectral peak at 3290 cm^{-1} for the hydroxyl group attached to an aromatic ring of MEL, as well as the vibration of the carbonyl group at 1550 cm^{-1} are not visible in the spectrum of polymeric micelle. The disappearance of the characteristic peaks indicates the formation of a new composition that is, they cannot be described on either the polymer or the MEL. The investigation of the new entity was further characterized using Raman spectroscopy.

3.4.5. Raman Spectroscopy and Chemical Mapping

A Raman spectrum of MEL, Soluplus®, their physical mixture and MEL-loaded polymeric micelles is shown in Figure 8A. MEL shows bands of aromatic ring vibration of benzothiazine at 1598 cm^{-1} , which derives from the stretching vibration of C=C or C=N and the bending vibration of CH_2 . The sharp peak at 1532 cm^{-1} indicates the stretching vibration of C=N in thiazole ring. Other characteristic absorptions appeared at 1305 cm^{-1} (ν_{OH}), 1267 cm^{-1} ($\nu_{\text{C-N-C}}$) and 1164 cm^{-1} ($\nu_{\text{C-S}}$). The Raman spectrum of the polymeric micelle showed that the band located at 1305 cm^{-1} for starting meloxicam shifted to higher energy at 1394 cm^{-1} as a result of the deprotonation of the molecule. The appearance of a new peak due to the deprotonation of phenolic OH changed the vibrational motion of C=C and C-N bonds [45]. The magnitude of the shift in the spectrum was 89 cm^{-1} , which reflects the OH group attached to the six-membered heteroatom ring attends in the H-bond forming with Soluplus® (Figure 8B).

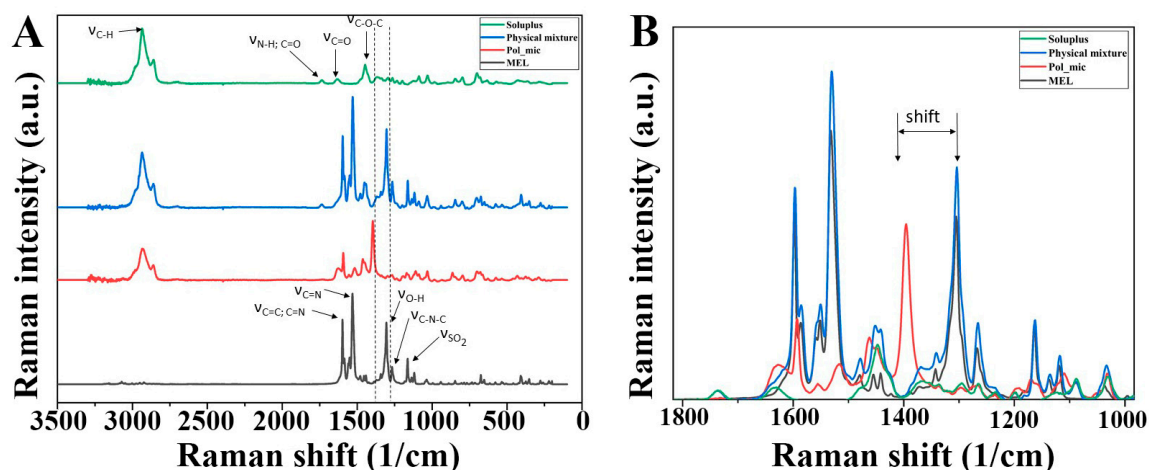


Figure 8. (A) Raman spectra of the materials and the (B) enlarged region of structural change.

In order to confirm the distribution of H-bonding in the polymeric micelle Raman mapping of the physical mixture and the polymeric micelle was carried out. The characteristic bands of phenolic OH shifting (1394→1305) as highlighted regions were used to visualize with chemical mapping (Figure 9). The chemical maps showed the Raman shift of phenolic OH can be observed on the whole surface of polymeric micelles in contrast to the physical mixture. This phenomenon confirms the existing H-bonding in the polymeric micelles.

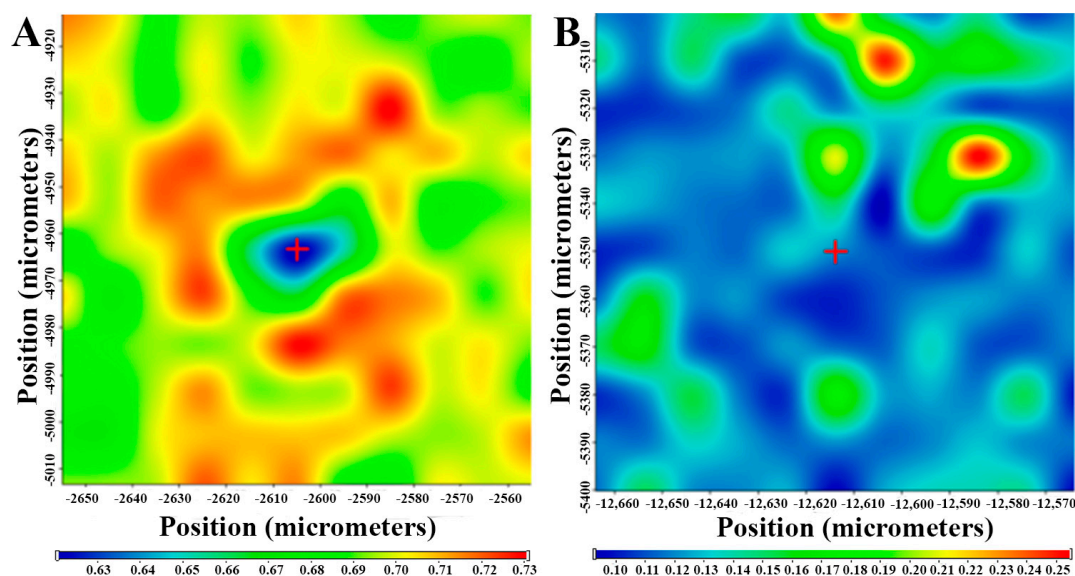


Figure 9. Intensity changes in Raman chemical maps indicating the (A) shifting at 1305 nm of physical mixture and (B) polymeric micelle; color intensity: blue—extinction of peak at 1305 nm, red—existence of peaks at 1305 nm.

3.4.6. Physical-Stability of Freeze-Dried Formulations

Freeze-dried samples were analyzed continuously at specific times during the stability test. The particle size and PDI of aliquots dissolved in purified water were determined as seen in Table 6. To calculate the absolute change, 0th month data were extracted from 12th month, since it has the largest difference from the starting point. The particle size increased by 3.31 nm, while PDI by 0.016 after 12 months of storage. The samples met the requirements previously set, i.e., having a particle size ranging from 80 to 120 nm and a PDI of less than 0.2. The 5 w/w% D-trehalose dihydrate was a suitable cryoprotectant for solid storage of freeze-dried MEL-containing polymeric micelles.

Table 6. Results of DLS measurements after 12 months of physical-stability examination.

Sampling (Month)	Z-Average * (nm)	PdI *
0	100.47 ± 0.87	0.149 ± 0.01
1	100.79 ± 0.51	0.151 ± 0.04
2	100.88 ± 0.82	0.152 ± 0.02
3	100.85 ± 1.03	0.152 ± 0.03
4	101.05 ± 0.41	0.153 ± 0.05
5	101.11 ± 0.93	0.155 ± 0.01
6	101.19 ± 0.48	0.154 ± 0.04
7	101.22 ± 0.21	0.154 ± 0.06
8	101.79 ± 0.81	0.156 ± 0.07
9	101.76 ± 1.15	0.160 ± 0.04
10	101.94 ± 0.77	0.161 ± 0.03
11	102.56 ± 0.42	0.163 ± 0.08
12	103.78 ± 0.36	0.165 ± 0.04
absolute change	+3.31	+0.016

* Data are means ± SD ($n = 3$ independent formulations).

3.5. Residual Organic Solvent Determination with Gas Chromatography

All new products that are planned to be placed on market must comply with very strict rules on impurities and residual formulation excipients based on The International Council of Harmonization (ICH) Q3C (R5)) guideline for residual solvents [46]. With the film-method we could achieve a formulation having a low concentration of ethanol. As the concentration of the polymer is at the CMC value, polymer chains associate to form micelles in a way that hydrophobic parts avoid contact with the aqueous media, therefore encapsulating some of the non-aqueous media, in our case: ethanol. At CMC we could detect the highest concentration in the micellar core with the largest particle size, but as the solvents evaporate, and the polymer concentration increases above CMC, the equilibrium favors micelle formation. The micelles will take their lowest energy state configuration and the remaining solvent will gradually release from the core. The decrease of particle size will follow this [47]. After evaporation, secondary drying in the vacuum chamber also contributed to the loss of ethanol without damaging or changing the micellar structure in solid form allowing to dissolve the formulations in water. The results can be seen in Table 7.

Table 7. Concentration of residual organic solvent in the optimized formulation.

Ethanol (mM)	Ethanol (ppm)	Maximum Residual Level * (ppm)
0.0022 ± 0.0001	0.101345 ± 0.0046	5000

* based on the ICH Q3C (R5).

3.6. Characterization of Ex Tempore Redispersed Nasal Formulations

The main parameters influencing nasal absorption were measured after the reconstitution of the lyophilized formulation (Table 8).

Table 8. Physicochemical parameters of the nasal formulation.

Parameter	Value
Reconstitution time (s)	2
pH	6.49
Z-average (nm)	100.47 ± 0.87
PdI	0.149 ± 0.01
Zeta potential (mV)	−26.7 ± 0.6
Osmolality (mOsmol/L)	240
Viscosity (35 °C) (mPas)	32.5 ± 0.28

The reconstitution time of lyophilized polymeric micelles was 2 s, which meets the requirements of European Pharmacopoeia (Ph. Eur. 10), according to which a lyophilized product reconstituted to a solution using an appropriate diluent prior to patient administration should be less than 3 min. The physiological pH in the nose is 6.4 on average and this allows normal ciliary function. In this slightly acidic environment, lysozyme, the natural antimicrobial agent in the nose, is effective in the prevention of growth of pathogenic bacteria in the nasal passage. A major deviation from this causes irritation of the nasal mucosa. To avoid that, formulation pH should be kept between 4.5 and 6.5 so our formulation satisfies that criterion [48]. The Z-average, PDI and zeta potential values meet the requirements of intranasally administered nanoparticles. The Z-average (100.47 ± 0.87 nm) of polymeric micelles is low enough for fast absorption. The PDI (0.149 ± 0.01) shows monodisperse size distribution, which ensures the homogeneity of polymeric micelles in the aqueous media. The zeta potential (-26.7 ± 0.6 mV) is high enough to avoid aggregation in liquid form through the repulsion among the nanoparticles. The osmolality of the polymeric micelle formulation was hypotonic (240 mOsmol/L). Nasal preparations are normally isotonic (about 290 mOsmol/L), which is also best tolerated, but sometimes a deviation from isotonicity may be an advantage. Hypertonic solutions shrink epithelial cells and inhibit ciliary activity. On the other side, hypotonic solutions can increase drug absorption, as we also expect from our formulation. The resulting viscosity of the preparation will directly affect the droplet size of the spray depending on rheological properties and spray characteristics of the spray plume. The viscosity of the formulation was 32.5 ± 0.28 mPas which is suitable to form intranasal liquid formulation, likely through mild mucoadhesive property [49]. On the other hand, more viscous formulations provide less efficient systemic nasal drug delivery due to slower diffusion [50].

3.7. In Vitro Characteristics

3.7.1. In Vitro Dissolution Study

The in vitro dissolution test was used to ascertain that the improved rate of dissolution of MEL is achieved as shown in Figure 10. The optimized formulation was examined in 3 parallel measurements. The rate of dissolution of crystalline MEL with particles in the micrometer size range was very slow, only 4.83% of the drug was dissolved in 15 min. Formulation of the MEL-containing polymeric micelles improved greatly the dissolution rate to 93.6% in average in 15 min. This improvement of dissolution can lead to a rapid onset of action. For nasal formulations it is a criterion that the drug must have an almost complete dissolution profile in 15 to 20 min, because of the quick elimination caused by mucociliary clearance (MCC). The increased surface area due to the formulation of nanosized MEL-contained polymeric micelles, the surface-active Soluplus[®] and the improved wettability and higher polarity may have contributed to the increase. As mentioned before in the introduction the polymeric micelles can release the drug in two ways: either diffusion or breaking into monomers. With the promising results it can be said that these mechanisms can be accomplished on the pH of the nasal cavity ending up in rapid release. As the TEM images showed above, the formulations have a spherical morphology, which is known that a sphere has the highest surface area of all equal volume spatial shapes which factor may also contributes to the increase.

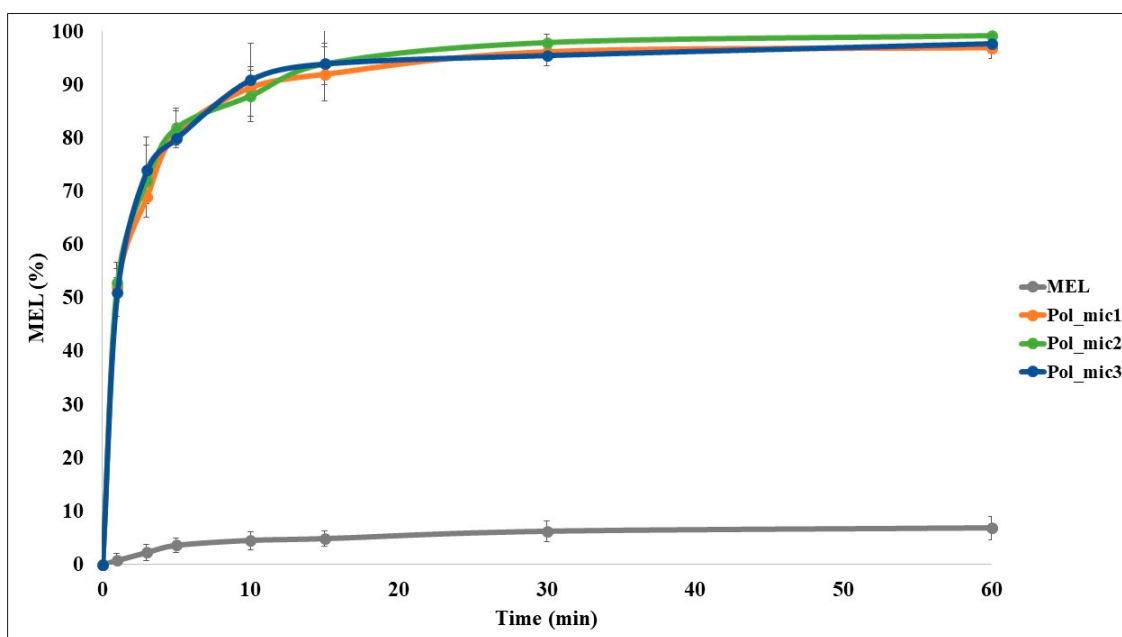


Figure 10. In vitro release study of crystalline MEL and the optimized formulation in triplicate; data are means \pm SD ($n = 3$ independent formulations)

It can be seen in Table 9 that the dissolution efficiency at 30 min was enhanced (from 4.52% to 87.01%) due to the formulation and the same increase could be observed in the case of RD values (from 1.00 to 19.23). The MDT values decreased from 11.50 to 3.59, which means that the dissolution became faster due to the earlier explained reasons.

Table 9. Statistical analysis of the in vitro dissolution test.

Samples	%DE _{10 min.}	%DE _{15 min.}	%DE _{30 min.}	%DE _{60 min.}	RD _{15 min.}	MDT
MEL	2.96	3.53	4.52	5.52	1.00	11.50
Pol_mic1	72.33	78.74	86.28	91.44	22.23	3.44
Pol_mic2	73.05	79.03	87.52	93.08	22.39	3.76
Pol_mic3	73.20	79.63	87.22	91.96	22.56	3.58
Average (formulations)	72.86	79.04	87.01	92.16	22.39	3.59
SD (formulations)	0.465	0.454	0.647	0.838	0.118	0.160

3.7.2. In Vitro Nasal Diffusion Study

The cumulative amount of MEL that diffused through the membrane from MEL-loaded polymeric micelles was measured against time on the modified Side-Bi-Side[®] horizontal diffusion cell (Figure 11). The measurements took place in real time where the absorbance was detected every 50 ms. Three parallel measurements took place from the same formulation. The diffusion from the formulation containing MEL nanoparticles was highly increased compared to crystalline MEL, due to the rapid dissolution of MEL. The diffused MEL ratio was ranging from 72.18% to 83.29% which is higher than crystalline MEL with a value of 25.08%. The results can be explained by the particle size reduction and high solubility and polarity values determined before. The flux (J), which shows the amount of MEL that permeates through the membrane within 1 h increased in case of the polymeric micelles. The permeability coefficient (K_p) showed the same tendency in all three parallel measurements as well (Table 10). The RP₁₅ value showed an approximately fivefold increase in the extent of degree of diffusion. These results are a must in the case of intranasal administration, and they are typical of fast diffusing systems.

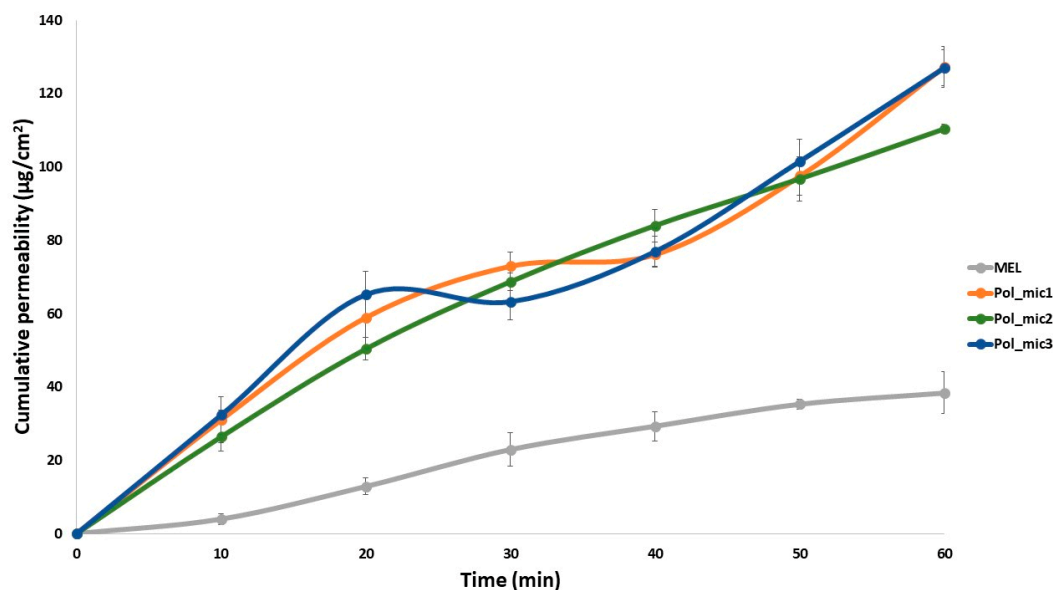


Figure 11. In vitro permeability study of MEL-loaded polymeric micelles in triplicate compared to crystalline MEL; data are means \pm SD ($n = 3$ independent formulations).

Table 10. Results of in vitro permeability study. Flux (J); permeability coefficient (K_p) and relative permeability at 15 min ($RP_{15 \text{ min}}$) values of MEL-loaded polymeric micelles compared to crystalline MEL.

Samples	J ($\mu\text{g}/\text{cm}^2/\text{h}$)	K_p (cm/h)	$RP_{15 \text{ min}}$
Crystalline MEL	7.67	0.005752	1.00
Pol_mic1	127.33	0.095550	5.35
Pol_mic2	110.32	0.082746	4.56
Pol_mic3	127.02	0.095277	5.80
Average (formulations)	121.56	0.091191	5.24
SD (formulations)	9.73	0.007315	0.63

3.7.3. In Vitro and In Vivo Correlation (IVIVC) of Polymeric Micelles

To estimate the statistical in vivo brain distribution of MEL-containing polymeric micelles IVIVC was performed applying in vitro and in vivo data of previous experiments, namely a MEL suspension, MEL-containing human serum albumin nanoparticles with Tween-20 (MEL-HAS-Tween) and without surfactant (MEL-HAS) [18] as well as a MEL-containing nanosuspension [27]. These formulations contained MEL in the same concentration. For investigating the relationship between in vitro and in vivo data, Pearson correlation was used. The Pearson correlation coefficients showed good fit both in the case of in vitro dissolution (0.9694) and diffusion (0.9957). Based on the regression curves, the possible in vivo brain distribution of MEL containing polymeric micelles was estimated to be approximately $15,017 \pm 5327 \text{ ng}\cdot\text{min}/\text{mL}$. The comparative studies according to $AUC_{0-60 \text{ min}}$ values of in vitro dissolution, in vitro diffusion and in vivo brain distribution have shown that a significant difference is expected between the measured in vitro and the estimated in vivo results of polymeric micelle formulation and the different MEL-containing intranasal formulations applied for comparison. The in vitro dissolution and diffusion of MEL from polymeric micelles was significantly higher than from the other drug delivery systems, but its expected $AUC_{0-60 \text{ min}}$ value of in vivo brain distribution, in comparison to MEL-HSA-Tween, showed no significant difference (Figure 12).

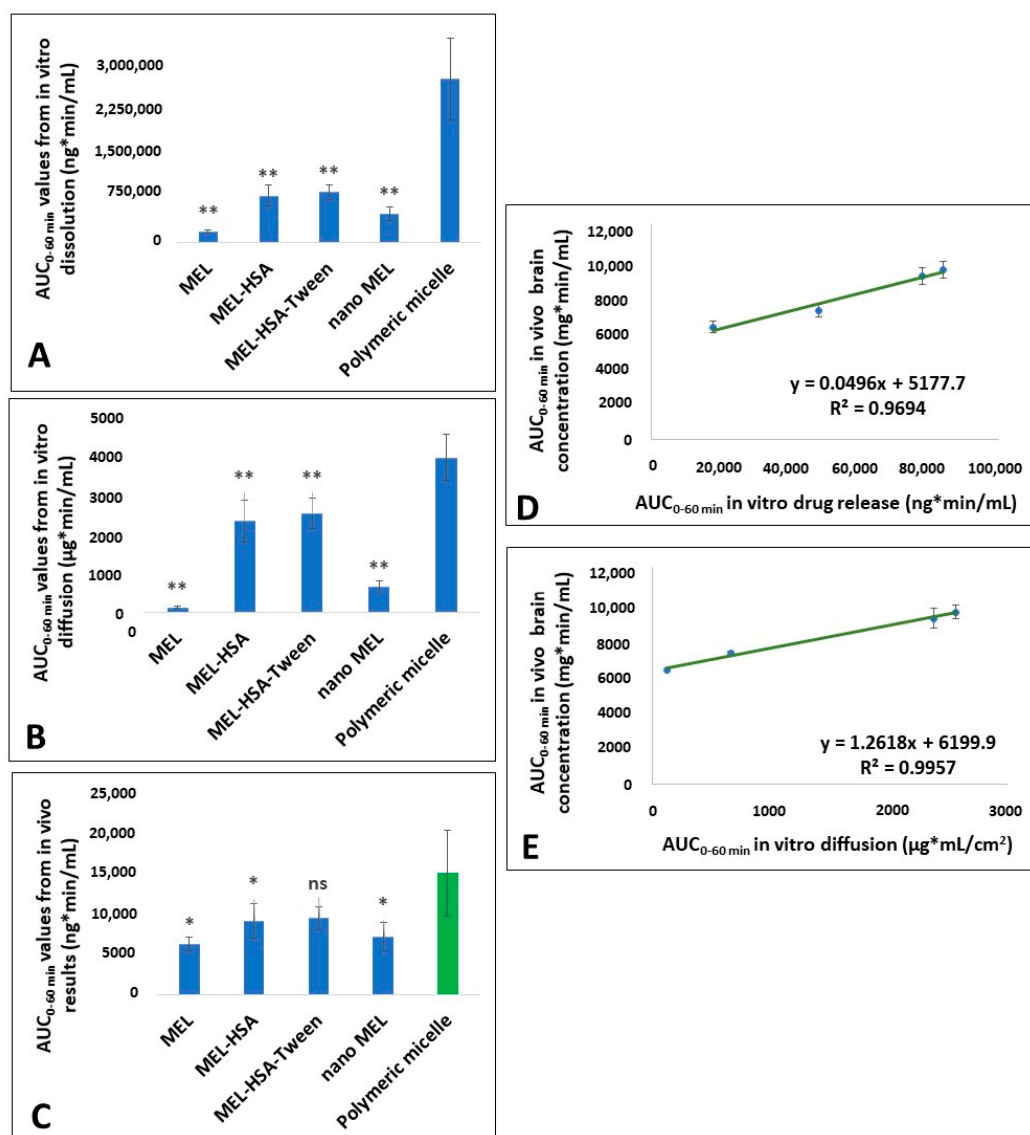


Figure 12. Figures of the IVIVC evaluation. (A) Calculated $AUC_{0-60 \text{ min}}$ values from the in vitro dissolution test; (B) Calculated $AUC_{0-60 \text{ min}}$ values from the in vitro diffusion test; (C) $AUC_{0-60 \text{ min}}$ values from the in vivo results with the predicted polymeric micelle value (marked as green); (D) Pearson correlation based on dissolution; (E) Pearson correlation based on diffusion. Statistics: * = $p < 0.05$; ** = $p < 0.01$; ns = not significant.

4. Discussion

The aim of this study was to formulate MEL-loaded Soluplus[®] polymeric micelles for intranasal application to target the brain using a variation of the film-method or otherwise known as the rotary-evaporation method. As neuroinflammation plays a pivotal role in the progression of neurodegenerative diseases, the nose-to-brain administration of NSAIDs in a smart nanoDDS can be advantageous. Previous studies described improved bioavailability of nose-to-brain administered polymeric micelles containing CNS targeted drugs such as sumatriptan [51] or clonazepam [52]. An improved anti-neuroinflammatory effect was experienced in case of monoterpenoids like geraniol charged polymeric micelles [53], but intranasal NSAID-containing polymeric micelle formulations were not investigated yet, therefore it is considered a novel way of application.

The formulation was developed using a QbD driven factorial experimental design. Polymeric micelles were prepared using the film method by the rotary evaporation of solution containing MEL and Soluplus[®] dissolved in ethanol and sodium hydroxide solution. The optimal MEL-Soluplus[®]

ratio was approximately 1:4. The polymeric micelles were formed after rehydration of the matrix film by addition of purified water. The main advantage of this method is that the organic solvent can be practically completely removed and may also result in a significant increase in drug loading [54]. The technology used is scalable, environmentally friendly and also meets the requirements of ICH in terms of residual solvent [46]. In the formulation study the average particle size, polydispersity index (PDI) and zeta potential had the highest impacts among critical quality attributes (CQAs) on the quality and efficacy of MEL-loaded polymeric micelles.

The critical product parameters of reconstituted polymeric micelles, such as Z-average (100.47 ± 0.87 nm) of polymeric micelles was low enough for fast absorption [55] and PDI (0.149 ± 0.01), shows monodisperse size distribution, ensuring to overcome recognition and removal by the reticuloendothelial system (RES) [56]; moreover, the zeta potential (-26.7 ± 0.6 mV) also met the requirements of nano DDSs ensuring monodispersity through the high charge–charge repulsion among the particles [57]. The Soluplus[®] as micelle-forming agent ensured a good wettability attribute and polarity (47.0%) leading to high solubility (5419.7 ± 1.284 mg/L) and high encapsulation efficiency (89.4%) at pH 5.6.

The developed MEL-containing liquid micellar delivery system was converted to a solid phase product by freeze-drying using D-trehalose dihydrate in five mass percent as a cryoprotectant agent to stabilize the system. After 12 months of storage the particle size remained decent: 103.78 ± 0.36 nm with a PDI of 0.165 ± 0.04 , the particle size increased only by 3.31 nm, while PDI by 0.016 based on the DLS and TEM results. The product met the requirements previously set, i.e., having a particle size ranging from 80 to 120 nm and a PDI of less than 0.2. The five mass percent D-trehalose dihydrate was a suitable cryoprotectant for solid storage of freeze-dried MEL-containing polymeric micelles. DSC and XRPD results confirmed the amorphous nature of polymeric micelles which also contributes to the solubilization of MEL. TGA measurements revealed the relatively high thermal stability of the nanoDDS, the formulation remained stable as the temperature increased up to 103 °C. FT-IR and Raman investigations showed interactions were formed between Soluplus[®] and MEL stabilizing the drug delivery system.

The reconstitution time of ex tempore reconstituted polymeric micelles was only two seconds, which met the requirements of Ph. Eur. 10 (<3 min). Other nasal formulation characterization studies were also carried out recommended by the EMA [58]. The pH of liquid formulation was 6.49, which allows normal ciliary function [59]. The Z-average, PDI and zeta potential values meet the requirements of intranasally administered nanoparticles. The osmolality of the polymeric micelle formulation was hypotonic (240 mOsmol/L), which can increase drug absorption [60], as we also expect from our formulation. The viscosity of the formulation was 32.5 ± 0.28 mPas which is suitable to form intranasal liquid formulation possibly through mild mucoadhesive property [49].

The in vitro dissolution and permeability experiments also fulfill the criteria of intranasal administration having high dissolution ($\%DE_{15 \text{ min}} = 79.04 \pm 0.454$) and permeability (121.56 ± 9.73 $\mu\text{g}/\text{cm}^2/\text{h}$) values at 15 min supported by the statistical analysis. Five-fold higher nasal permeability and more than 20-fold faster drug dissolution was reached by polymeric micelles in comparison to starting MEL.

The experimental design and the in vitro dissolution and permeability results were focused on the IVIVC to estimate the potential in vivo brain distribution of MEL. Based on the results, a good brain distribution for intranasal application of the developed formulation is expected to be approximately $15,017 \pm 5327$ ng·min/mL. In the early stage development IVIVC is also justified as regulatory guideline in order to minimize the number of further animal studies [61]. The IVIVC results of polymeric micelles suggest the great potential for in vivo brain distribution of MEL. The nose-to-brain delivery of NSAIDs such as MEL using nanoDDS as polymeric micelles may provide a new opportunity to treat neuroinflammation more effectively.

5. Conclusions

A QbD driven initial product design study of MEL-loaded Soluplus® polymeric micelles provides a new possibility of intranasal NSAID administration against neuroinflammation, which was not described previously. In this approach a “value-added” solid phase viscosity enhancer- and preservative-free nasal product can be successfully developed, which can be easily converted “ex tempore” to a liquid product and is ready-to-use as a nasal drop or spray and may substitute current therapeutics.

Author Contributions: Conceptualization, B.S., G.K., P.S.-R. and I.C.; methodology B.S., G.K., E.P., D.G.D., Á.D. and I.C.; software G.K., P.B., Á.D., D.G.D.; validation I.C., Z.K. and L.J.; formal analysis G.K., P.S.-R., E.P. and I.C.; investigation B.S., G.K., E.P., D.G.D., P.B. and Á.D.; resources, I.C., Z.K. and L.J.; data curation, G.K., D.G.D., Á.D. and B.S.; writing—original draft preparation, B.S.; writing—review and editing, P.S.-R., G.K., E.P. and I.C.; visualization B.S. and G.K.; supervision P.S.-R., G.K. and I.C.; project administration G.K.; funding acquisition P.S.-R., L.J. and I.C. All authors have read and agreed to the published version of the manuscript.

Funding: The publication was funded by The University of Szeged Open Access Fund (FundRef, Grant No. 4751).

Acknowledgments: The work was supported by the Nation Research, Development and Innovation Office, Hungary (GINOP-2.3.2-15-2016-00060), by the UNKP-19-2-SZTE-113 New National Excellence Program of the Ministry for Innovation and Technology. The authors also express their gratitude for financial support to the Ministry of Human Capacities, Hungary [grant 20391-3/2018/FEKUSTRAT], to the UNKP-20-5 New National Excellence Program of the Ministry For Innovation of Technology and to the János Bolyai Research Scholarship of the Hungarian Academy of Sciences.

Conflicts of Interest: The authors declare no conflict of interest.

References

- World Health Organization. 2019. Available online: <https://www.who.int/news-room/fact-sheets/detail/dementia> (accessed on 19 June 2020).
- Arlt, S.; Lindner, R.; Rösler, A.; von Renteln-Kruse, W. Adherence to medication in patients with dementia: Predictors and strategies for improvement. *Drugs Aging* **2008**, *25*, 1033–1047. [[CrossRef](#)] [[PubMed](#)]
- Heneka, M.T.; Carson, M.J.; El Khoury, J.; Landreth, G.E.; Brosseron, F.; Feinstein, D.L.; Jacobs, A.H.; Wyss-Coray, T.; Vitorica, J.; Ransohoff, R.M.; et al. Neuroinflammation in Alzheimer’s Disease. *Lancet Neurol.* **2015**, *14*, 388–405. [[CrossRef](#)]
- Choi, S.H.; Aid, S.; Caracciolo, L.; Sakura Minami, S.; Niikura, T.; Matsuoka, Y.; Turner, R.S.; Mattson, M.P.; Bosetti, F. Cyclooxygenase-1 inhibition reduces amyloid pathology and improves memory deficits in a mouse model of Alzheimer’s disease. *J. Neurochem.* **2013**, *124*, 59–68. [[CrossRef](#)] [[PubMed](#)]
- Calvo-Rodríguez, M.; Núñez, L.; Villalobos, C. Non-steroidal anti-inflammatory drugs (NSAIDs) and neuroprotection in the elderly: A view from the mitochondria. *Neural Regen. Res.* **2015**, *10*, 1371–1372. [[CrossRef](#)] [[PubMed](#)]
- Sanz-Blasco, S.; Calvo-Rodríguez, M.; Caballero, E.; Garcia-Durillo, M.; Nunez, L.; Villalobos, C. Is it All Said for NSAIDs in Alzheimer’s Disease? Role of Mitochondrial Calcium Uptake. *CAR* **2018**, *15*, 504–510. [[CrossRef](#)]
- Novakova, I.; Subileau, E.A.; Toegel, S.; Gruber, D.; Lachmann, B.; Urban, E.; Chesne, C.; Noe, C.R.; Neuhaus, W. Transport rankings of non-steroidal antiinflammatory drugs across blood-brain barrier in vitro models. *PLoS ONE* **2014**, *9*, e86806. [[CrossRef](#)]
- Merkus, F.W.; van den Berg, M.P. Can nasal drug delivery bypass the blood-brain barrier? *Drugs R D* **2007**, *8*, 133–144. [[CrossRef](#)]
- Mistry, A.; Stolnik, S.; Illum, L. Nanoparticles for direct nose-to-brain delivery of drugs. *Int. J. Pharm.* **2009**, *379*, 146–157. [[CrossRef](#)]
- Agrawal, M.; Saraf, S.; Antimisiaris, S.G.; Chougule, M.B.; Shoyele, S.A.; Alexander, A. Nose-to-brain drug delivery: An update on clinical challenges and progress towards approval of anti-Alzheimer drugs. *J. Control. Release* **2018**, *281*, 139–177. [[CrossRef](#)]
- Lalatsa, A.; Schatzlein, A.G.; Uchegbu, I.F. Strategies to deliver peptide drugs to the brain. *Mol. Pharm.* **2014**, *11*, 1081–1093. [[CrossRef](#)]

12. Van Hoesen, G.W.; Hyman, B.T.; Damasio, A.R. Entorhinal cortex pathology in Alzheimer's disease. *Hippocampus* **1991**, *1*, 1–8. [[CrossRef](#)] [[PubMed](#)]
13. Teskač, K.; Kristl, J. The evidence for solid lipid nanoparticles mediated cell uptake of resveratrol. *Int. J. Pharm.* **2010**, *390*, 61–69. [[CrossRef](#)] [[PubMed](#)]
14. Szabó-Révész, P. Modifying the physicochemical properties of NSAIDs for nasal and pulmonary administration. *Drug Discov. Today Technol.* **2018**, *27*, 87–93. [[CrossRef](#)]
15. Kürti, L.; Gáspár, R.; Márki, Á.; Kápolna, E.; Bocsik, A.; Veszélka, S.; Bartos, C.; Ambrus, R.; Vastag, M.; Deli, M.A.; et al. In vitro and in vivo characterization of meloxicam nanoparticles designed for nasal administration. *Eur. J. Pharm. Sci.* **2013**, *50*, 86–92. [[CrossRef](#)] [[PubMed](#)]
16. Kiss, T.; Alapi, T.; Varga, G.; Bartos, C.; Ambrus, R.; Szabó-Révész, P.; Katona, G. Interaction studies between levodopa and different excipients to develop coground binary mixtures for intranasal application. *J. Pharm. Sci.* **2019**, *108*, 2552–2560. [[CrossRef](#)] [[PubMed](#)]
17. Pallagi, E.; Jójárt-Laczkovich, O.; Németh, Z.; Szabó-Révész, P.; Csóka, I. Application of the QbD-based approach in the early development of liposomes for nasal administration. *Int. J. Pharm.* **2019**, *562*, 11–22. [[CrossRef](#)]
18. Katona, G.; Balogh, G.T.; Dargó, G.; Gáspár, R.; Márki, Á.; Ducza, E.; Sztojkov-Ivanov, A.; Tömösi, F.; Kecskeméti, G.; Janáky, T.; et al. Development of meloxicam-human serum albumin nanoparticles for nose-to-brain delivery via application of a quality by design approach. *Pharmaceutics* **2020**, *12*, 97. [[CrossRef](#)]
19. Croy, S.R.; Kwon, G.S. Polymeric micelles for drug delivery. *Curr. Pharm. Des.* **2006**, *12*, 4669–4684. [[CrossRef](#)]
20. Kanazawa, T.; Taki, H.; Tanaka, K.; Takashima, Y.; Okada, H. Cell-penetrating peptide-modified block copolymer micelles promote direct brain delivery via intranasal administration. *Pharm. Res.* **2011**, *28*, 2130–2139. [[CrossRef](#)]
21. Movassaghian, S.; Merkel, O.M.; Torchilin, V.P. Applications of polymer micelles for imaging and drug delivery. *Wiley Interdiscip. Rev. Nanomed. Nanobiotechnol.* **2015**, *7*, 691–707. [[CrossRef](#)]
22. Ahmad, Z.; Shah, A.; Siddiq, M.; Kraatz, H.B. Polymeric micelles as drug delivery vehicles. *RSC Adv.* **2014**, *4*, 17028–17038. [[CrossRef](#)]
23. Palcsó, B.; Zelkó, R. Different types, applications and limits of enabling excipients of pharmaceutical dosage forms. *Drug Discov. Today Technol.* **2018**, *27*, 21–39. [[CrossRef](#)]
24. Hansen, K.; Kim, G.; Desai, K.G.H.; Patel, H.; Olsen, K.F.; Curtis-Fisk, J.; Tocce, E.; Jordan, S.; Schwendeman, S.P. Feasibility investigation of cellulose polymers for mucoadhesive nasal drug delivery applications. *Mol. Pharm.* **2015**, *12*, 2732–2741. [[CrossRef](#)] [[PubMed](#)]
25. Jin, X.; Zhou, B.; Xue, L.; San, W. Soluplus[®] micelles as a potential drug delivery system for reversal of resistant tumor. *Biomed. Pharmacother.* **2015**, *69*, 388–395. [[CrossRef](#)]
26. Noble, S.; Balfour, J.A. Meloxicam. *Drugs* **1996**, *51*, 424–430. [[CrossRef](#)] [[PubMed](#)]
27. Bartos, C.; Ambrus, R.; Kovács, A.; Gáspár, R.; Sztojkov-Ivanov, A.; Márki, Á.; Janáky, T.; Tömösi, F.; Kecskeméti, G.; Szabó-Révész, P. Investigation of absorption routes of meloxicam and its salt form from intranasal delivery systems. *Molecules* **2018**, *23*, 784. [[CrossRef](#)]
28. Csóka, I.; Pallagi, E.; Paál, T.L. Extension of quality-by-design concept to the early development phase of pharmaceutical R&D processes. *Drug Discov. Today* **2018**, *23*, 1340–1343. [[CrossRef](#)]
29. Pallagi, E.; Ambrus, R.; Szabó-Révész, P.; Csóka, I. Adaptation of the quality by design concept in early pharmaceutical development of an intranasal nanosized formulation. *Int. J. Pharm.* **2015**, *491*, 384–392. [[CrossRef](#)]
30. ICH. Quality Risk Management Q9. In *ICH Harmon Tripart Guidel*; ICH: Geneva, Switzerland, 2005; pp. 1–23.
31. Bartos, C.; Pallagi, E.; Szabó-révész, P.; Ambrus, R.; Katona, G.; Kiss, T. Formulation of levodopa containing dry powder for nasal delivery applying the quality-by-design approach. *Eur. J. Pharm. Sci.* **2018**, *123*, 475–483. [[CrossRef](#)]
32. Gieszinger, P.; Csóka, I.; Pallagi, E.; Katona, G.; Jójárt-Laczkovich, O.; Szabó-Révész, P.; Ambrus, R. Preliminary study of nanonized lamotrigine containing products for nasal powder formulation. *Drug Des. Dev. Ther.* **2017**, *11*, 2453–2466. [[CrossRef](#)]
33. Pallagi, E.; Karimi, K.; Ambrus, R.; Szabó-Révész, P.; Csóka, I. New aspects of developing a dry powder inhalation formulation applying the quality-by-design approach. *Int. J. Pharm.* **2016**, *511*, 151–160. [[CrossRef](#)] [[PubMed](#)]

34. Emami, J. In vitro-in vivo correlation: From theory to applications. *J. Pharm. Pharm. Sci.* **2006**, *9*, 169–189. [PubMed]
35. Shen, J.; Burgess, D.J. In vitro–in vivo correlation for complex non-oral drug products: Where do we stand? *JCR* **2015**, *219*, 644–651. [CrossRef]
36. Kim, T.H.; Shin, S.; Jeong, S.W.; Lee, J.B.; Shin, B.S. Physiologically Relevant In Vitro-In Vivo Correlation (IVIVC) Approach for Sildenafil with Site-Dependent Dissolution. *Pharmaceutics* **2019**, *11*, 251. [CrossRef] [PubMed]
37. Ishikawa, K. What is total quality control? The Japanese way. *Qual. Toolbox* **1985**, 247–249. Available online: <http://asq.org/learn-about-quality/cause-analysis-tools/overview/fishbone.html> (accessed on 19 June 2020).
38. Powell, T.; Sammut-Bonnic, T. Pareto Analysis. In *Wiley Encyclopedia of Management*; Cooper, C.L., Ed.; John Wiley & Sons, Ltd.: Hoboken, NJ, USA, 2014. [CrossRef]
39. Alvarez-Rivera, F.; Fernández-Villanueva, D.; Concheiro, A.; Alvarez-Lorenzo, C. α -Lipoic acid in Soluplus[®] polymeric nanomicelles for ocular treatment of diabetes-associated corneal diseases. *J. Pharm. Sci.* **2016**, *105*, 2855–2863. [CrossRef]
40. Wu, S. Calculation of interfacial tension in polymer systems. *J. Polym. Sci.* **1971**, *34*, 19–30. [CrossRef]
41. ICH. Stability testing of new drug substances and drug products Q1A (R2). In *ICH Harmon Tripart Guidel*; ICH: Geneva, Switzerland, 2003; pp. 1–20.
42. ICH, I.G. Q3c (R6) on Impurities: Guideline for Residual Solvents. In *International Conference for Harmonisation of Technical Requirements for Registration of Pharmaceuticals for Human Use (ICH)*; ICH: Geneva, Switzerland, 2016.
43. Bartos, C.; Ambrus, R.; Sipos, P.; Budai-Szűcs, M.; Csányi, E.; Gáspár, R.; Márki, Á.; Seres, A.B.; Sztojkov-Ivanov, A.; Horváth, T.; et al. Study of sodium hyaluronate-based intranasal formulations containing micro-or nanosized meloxicam particles. *Int. J. Pharm.* **2015**, *491*, 198–207. [CrossRef]
44. Mártha, C.; Jójártné, L.O.; Szabóné, R.P. Amorphous form in pharmaceutical technological research. *Acta Pharm. Hung.* **2011**, *81*, 37–42.
45. Kytariolos, J.; Charkoftaki, G.; Smith, J.R.; Voyiatzis, G.; Chrissanthopoulos, A.; Yannopoulos, S.N.; Fatouros, D.G.; Macheras, P. Stability and physicochemical characterization of novel milk-based oral formulations. *Int. J. Pharm.* **2013**, *444*, 128–138. [CrossRef]
46. ICH. Guideline Q3C (R5) on Impurities: Guideline for Residual Solvents. Available online: <https://www.tga.gov.au/sites/default/files/ichq3cr5.pdf> (accessed on 19 June 2020).
47. Jones, M.C.; Leroux, J.C. Polymeric micelles—A new generation of colloidal drug carriers. *Eur. J. Pharm. Biopharm.* **1999**, *48*, 101–111. [CrossRef]
48. Salade, L.; Wauthoz, N.; Goole, J.; Amighi, K. How to characterize a nasal product. The state of the art of in-vitro and ex-vivo specific methods. *Int. J. Pharm.* **2019**, *561*, 47–65. [CrossRef] [PubMed]
49. Furubayashi, T.; Inoue, D.; Kamaguchi, A.; Higashi, Y.; Sakane, T. Influence of formulation viscosity on drug absorption following nasal application in rats. *Drug Metab. Pharmacokinet.* **2007**, *22*, 206–211. [CrossRef] [PubMed]
50. Scherließ, R. Nasal formulations for drug administration and characterization of nasal preparations in drug delivery. *Ther. Deliv.* **2020**, *11*, 183–191. [CrossRef] [PubMed]
51. Jain, R.; Nabar, S.; Dandekar, P.; Hassan, P.; Aswal, V.; Talmon, Y.; Shet, T.; Borde, L.; Ray, K.; Patravale, V. Formulation and evaluation of novel micellar nanocarrier for nasal delivery of sumatriptan. *Nanomedicine* **2018**, *5*, 575–587. [CrossRef]
52. Nour, S.A.; Abdelmalak, N.S.; Naguib, M.J.; Rashed, H.M.; Ibrahim, A.B. Intranasal brain-targeted clonazepam polymeric micelles for immediate control of status epilepticus: In vitro optimization, ex vivo determination of cytotoxicity, in vivo biodistribution and pharmacodynamics studies. *Drug Deliv.* **2016**, *23*, 3681–3695. [CrossRef] [PubMed]
53. M Soliman, S.; M Sheta, N.; MM Ibrahim, B.; M El-Shawwa, M.; M Abd El-Halim, S. Novel Intranasal Drug Delivery: Geraniol Charged Polymeric Mixed Micelles for Targeting Cerebral Insult as a Result of Ischaemia/Reperfusion. *Pharmaceutics* **2020**, *12*, 76. [CrossRef] [PubMed]
54. Pepic, I.; Lovric, J.; Filipovic-Grcic, J. Polymeric micelles in ocular drug delivery: Rationale, strategies and challenges. *Chem. Biochem. Eng. Q.* **2012**, *26*, 365–377.
55. Sonvico, F.; Clementino, A.; Buttini, F.; Colombo, G.; Pescina, S.; Stanisçuaski Guterres, S.; Pohlmann, A.R.; Nicoli, S. Surface-modified nanocarriers for nose-to-brain delivery: From bioadhesion to targeting. *Pharmaceutics* **2018**, *10*, 34. [CrossRef]

56. Hussein, Y.H.; Youssry, M. Polymeric micelles of biodegradable diblock copolymers: Enhanced encapsulation of hydrophobic drugs. *Materials* **2018**, *11*, 688. [[CrossRef](#)]
57. Sikora, A.; Bartczak, D.; Geißler, D.; Kestens, V.; Roebben, G.; Ramaye, Y.; Varga, Z.; Palmi, M.; Shard, A.G.; Goenaga-Infante, H.; et al. A systematic comparison of different techniques to determine the zeta potential of silica nanoparticles in biological medium. *Anal. Methods* **2015**, *7*, 9835–9843. [[CrossRef](#)]
58. Trows, S.; Wuchner, K.; Spycher, R.; Steckel, H. Analytical challenges and regulatory requirements for nasal drug products in Europe and the U.S. *Pharmaceutics* **2014**, *6*, 195–219. [[CrossRef](#)] [[PubMed](#)]
59. Washington, N.; Steele, R.J.C.; Jackson, S.J.; Bush, D.; Mason, J.; Gill, D.A.; Pitt, K.; Rawlins, D.A. Determination of baseline human nasal pH and the effect of intranasally administered buffers. *Int. J. Pharm.* **2000**, *198*, 139–146. [[CrossRef](#)]
60. Behl, C.R.; Pimplaskar, H.K.; Sileno, A.P.; deMeireles, J.; Romeo, V.D. Effects of physicochemical properties and other factors on systemic nasal drug delivery. *Adv. Drug Deliv. Rev.* **1998**, *29*, 89–116. [[CrossRef](#)]
61. Uppoor, V.R.S. Regulatory perspectives on in vitro (dissolution)/in vivo (bioavailability) correlations. *J. Control. Release* **2001**, *72*, 127–132. [[CrossRef](#)]



© 2020 by the authors. Licensee MDPI, Basel, Switzerland. This article is an open access article distributed under the terms and conditions of the Creative Commons Attribution (CC BY) license (<http://creativecommons.org/licenses/by/4.0/>).

II.



Article

A Systematic, Knowledge Space-Based Proposal on Quality by Design-Driven Polymeric Micelle Development

Bence Sipos , Gábor Katona and Ildikó Csóka *

Faculty of Pharmacy, Institute of Pharmaceutical Technology and Regulatory Affairs, University of Szeged, Eötvös Str. 6, H-6720 Szeged, Hungary; sipos.bence@szte.hu (B.S.); katona.gabor@szte.hu (G.K.)

* Correspondence: csoka.ildiko@szte.hu; Tel.: +36-62-546-116

Abstract: Nanoparticle research and development for pharmaceuticals is a challenging task in the era of personalized medicine. Specialized and increased patient expectations and requirements for proper therapy adherence, as well as sustainable environment safety and toxicology topics raise the necessity of well designed, advanced and smart drug delivery systems on the market. These stakeholder expectations and social responsibility of pharma sector open the space and call new methods on the floor for new strategic development tools, like Quality by Design (QbD) thinking. The extended model, namely the R&D QbD proved to be useful in case of complex and/or high risk/expectations containing or aiming developments. This is the case when we formulate polymeric micelles as promising nanotherapeutics; the risk assessment and knowledge-based quality targeted QbD approach provides a promising tool to support the development process. Based on risk assessment, many factors pose great risk in the manufacturing process and affect the quality, efficacy and safety profile. The quality-driven strategic development pathway, based on deep prior knowledge and an involving iterative risk estimation and management phases has proven to be an adequate tool, being able to handle their sensitive stability issues and make them efficient therapeutic aids in case of several diseases.

Keywords: Quality by Design; polymeric micelle; risk assessment; quality management; knowledge phase; preformulation space



Citation: Sipos, B.; Katona, G.; Csóka, I. A Systematic, Knowledge Space-Based Proposal on Quality by Design-Driven Polymeric Micelle Development. *Pharmaceutics* **2021**, *13*, 702. <https://doi.org/10.3390/pharmaceutics13050702>

Academic Editor: Bruno Sarmento

Received: 19 April 2021

Accepted: 10 May 2021

Published: 12 May 2021

Publisher's Note: MDPI stays neutral with regard to jurisdictional claims in published maps and institutional affiliations.



Copyright: © 2021 by the authors. Licensee MDPI, Basel, Switzerland. This article is an open access article distributed under the terms and conditions of the Creative Commons Attribution (CC BY) license (<https://creativecommons.org/licenses/by/4.0/>).

1. Introduction

Research and development (R&D) has changed enormously in recent decades and leaders of pharma companies are in the midst of unprecedented change. With the increased prevalence of chronic pulmonary diseases due to pollution, vascular and neurological diseases from obesity and the aging population pyramid and, last but not least, the occurrence of pandemics such as COVID-19 or Ebola accelerate pharmaceutical manufacturing and research processes that must be adhered to strict quality conditions. A newly manufactured and market-placed medicine has to face obstacles for the industry players. Changes in consumer attitudes, cybersecurity threats, rapid advances in technology, non-adequate return on innovation and competition from companies in emerging economies are several of them [1,2]. In the 21st century, a novel quality assurance approach, Quality by Design (QbD), appeared, oriented towards quality of the product and the improved patient applicability during therapeutic use. Quality, safety and efficacy are the three cornerstones of the QbD approach, which is built around starting from preformulation studies all the way to the patient's own use [3,4].

With the development of nano drug delivery systems (nanoDDS), the previous quality assurance systems were no longer sufficient, which also supports the QbD method based on quality, knowledge and risk assessment [5]. Lipid-, polymer-based or other nanoDDSs all require a specific regulatory environment [6,7]. On the one hand, the reason for this is to be found in the production process, as conventional production line equipment is

not necessarily suitable for the production of these products besides the need of special conditions and constant control. The opportunity is there in the hands of all developers to apply this method and in the course of our research group, the existence was proven on many occasions for nanoDDSs, such as liposomes [8], polymeric micelles [9] and human serum albumin nanoparticles [10]. On the other hand, safety must also be proven, as an increase in efficacy is expected due to the advanced properties of the systems, but in the case of improperly optimized preparations, it can lead to nanotoxicity and severe side effects [11,12].

Polymeric micelles are self-assembling association colloidal systems composed of amphiphilic copolymers capable of entrapping hydrophobic drugs [13]. They have a number of advantages, perhaps the most important of which is the increase in water solubility, along with a reduction in particle size. Together, these two factors contribute to a more favourable pharmacokinetic profile and to the incorporation of certain poorly soluble or penetrating active pharmaceutical ingredients (APIs) into a liquid dosage form [14]. The physical stability of the polymeric micelles proves to be adequate and they are able to maintain their particle size even during the circulation time in the bloodstream. In addition to administration by alternative administration routes, they show increased resistance to the body's metabolic effects, which is also important for maintaining the active, effective form of the API [15]. For safety and quality assured development, every developer must consider all possible outcomes before, in between and after the preparation of nanotherapeutics, which needs a holistic and systematic knowledge space-based development [16]. As mentioned, the leaders of pharma industry must create innovative dosage forms in order to stand a chance in the global market. To achieve this, polymeric micelles are an excellent solution. Compared to liquid formulations, these nanosized systems have the higher ground when talking about decrease of dosage strength; therefore, the occurrence of side effects, the ability to offer higher permeability and flux values across biological membranes and, last but not least, the pleasing carrier integrity through the circulation in the body.

The aim of this research article is to collect and evaluate the critical parameters affecting polymeric micelles as promising drug delivery systems as part of the extension of QbD to the early development phase of pharmaceutical R&D processes [17]. This article develops the formulation space through the adaptation of literature data into exact quality-influencing factors. Based on our previous experience from formulation studies in the field of nanotechnology and polymeric micelles supplemented by literature data, quantified risk severities based on this systematic summary was calculated in order to help and encourage professionals in the pharmaceutical field to apply QbD in the development processes. Later, described possible Quality Target Product Profile (QTPP) and Critical Quality Attributes (CQAs) were collected and an extensive risk assessment (RA) was performed on them. The Critical Process Parameters (CPPs) and Critical Material Attributes (CMAs) went through a RA also and because many formulation methods exist in the development of polymeric micelles, these methods were evaluated individually.

2. Materials and Methods

2.1. General Methodology of QbD

Based on specified guidelines of the International Council of Harmonisation of Technical Requirements for Pharmaceuticals for Human Use [18–20], the QbD procedure followed the following steps (Figure 1).

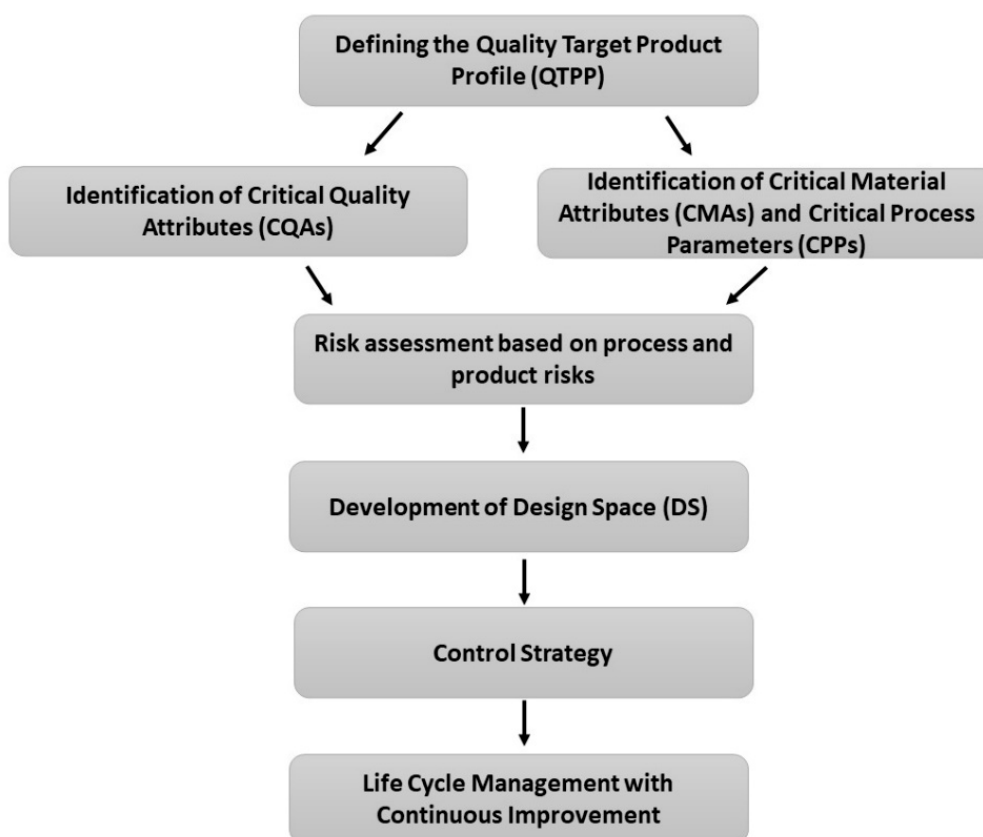


Figure 1. Schematics for the Quality by Design methodology.

At first, QTPPs were determined representing the desired quality characteristics of a finalized API-loaded polymeric micelle. The ICH guidelines state the mandatory QTPP elements such as indication, route of administration etc. and other safety and efficacy influencing factors were taken into account [18]. CQAs, CPPs and CMAs were selected in the next step. CQAs are physicochemical, biological or microbiological characteristics which should be controlled in an appropriate range to ensure product quality. CPPs and CMAs are related to the production of the product, which should be monitored [18–20]. Based on the collection process, a risk assessment was evaluated [20]. Data from the literature were collected using journal publishers’ search engines.

2.2. Risk Assessment Procedure

As QbD is a knowledge- and risk assessment-focused approach, qualitative and quantitative risk factors, expressed as severity scores, must be presented [17]. LeanQbD Software (QbD Works LLC, Fremont, CA, USA) was used for the RA procedure. At first, an interdependence rating amongst the QTPPs and the CQAs and the CQAs and the CPPs was performed. A three-level scale was used to describe the relation between these parameters: each relation was assigned with a “high” (H), “medium” (M) or “low” (L) attributive. The decision of assignment was performed based on numerous aspects including: occurrence of the risk factor during formulation and/or final product development phase; controllability of the factor; whether the factor can be eliminated or can it be fixed at a certain value without affecting quality; detectability. The description of relations had the fundamental basis of how closely the factors are related and data from the collected literature, in addition to the regulatory aspects of a joint MHLW/EMA reflection paper on the development of block copolymer micelle medicinal products [21]. Using the software, these qualitative relations were the basis of calculating the severity scores. As the output of the RA, Pareto diagrams were generated, presenting numeric data and ranking of the CQAs and the CPPs representing the potential impact on the final product [22].

3. Results

3.1. Collection of QTPPs for Polymeric Micelle Development

The definition of QTPPs is the first major step in the development of nanoDDS; in this case, polymeric micelles. In addition to the mandatory elements of the ICH guidelines, optional QTPPs can be defined, which mainly depends on the nature of the target product. Defining the indication is of paramount importance. This QTPP is most often due to the properties and previous application of the API. By forming a polymeric micelle formulation, the indications in the previous SPCs can be also supplemented [23]. Achieving this plays an important role mainly in immune and cancer therapy [24]. On the other hand, by innovating the mode of application, the API can be delivered to biological spaces which previous conventional formulations are not capable of. A particularly good example of this is the delivery of non-steroidal anti-inflammatory drugs to the central nervous system (CNS) for the treatment of neuroinflammation, in which case, conventional peroral formulations do not or only a small extent can enter [25].

The patient population as QTPP is also a mandatory clarifying factor that can be expanded beyond the age associated with the general drug. The development into a liquid dosage form is beneficial for the patient, as the product can be used even in case of swallowing difficulty. This is especially important in pediatric and geriatric medication, where patient experience is of paramount importance to improve therapy fidelity, the so-called adherence [26]. Polymeric micelle formulations designed for a conventional route of administration are aimed primarily to increase the bioavailability of products previously authorized for that route. However, new development trends prefer alternative routes of administration, of which the ophthalmic, topical and nasal delivery play the largest role [27–29]. A significant number of active substances are able to exert their effect only at certain point of action in the body, in the given indication. However, this does not mean that their potential is not greater and nanoformulations are able to deliver APIs to new sites. Of these, the intake of the drug into the CNS and cancer cells should be highlighted [30,31]. The dosage strength of the formulation depends on many things: indication, API features and the administration route. Manufacturers should clearly indicate the proposed dosage form of the formulation because they have different stability and product quality in colloidal solution, colloidal gelling system or freeze-dried form [14].

Physicochemical characteristics are common amongst QTPPs as well, depending on the indication and the administration route. Most commonly, viscosity, osmolality, pH and mucoadhesive properties are presented. The particle characteristics of polymeric micelles include the particle size (expressed as Z-average), particle size distribution (expressed as polydispersity index, PDI), zeta potential, encapsulation efficiency (EE%) and drug loading (DL%). These are the factors that facilitate the implementation of the other QTPP elements. They can also appear as CQAs, but in the scope of regulation of nanosystems, these factors must be defined in the initial plan, as part of the basis of technological innovation lies in their regulation [8,12].

The properties of the copolymers and the API determine the safety profile of the target product the most. The main criterion for polymers is that they are biocompatible with the human body and that, after their metabolism, the degradation products do not cause harmful side effects [32]. Where necessary, sterility is also required, as well as the product characteristics that allow the safe use of the dosage form and the administration route. The stability of polymeric micelles can be approached in several ways. Stability in aqueous solutions means a constant particle size after redispersion and a reduction in the tendency to aggregate. In addition to the liquid form, it is also worth checking these parameters during storage after freeze-drying [14]. Some copolymers are temperature and pH sensitive, so it is important to know whether a particular product can provide the expected effect under these factors. Changes in structure are expected after drug loading and which are also critical parameters of product characteristics. The classification of solubility among QTPPs is also a common case, as reducing redispersion time, improving solubility rate and increasing wetting properties are also the goal in the production of polymeric

micelles. This is closely related to drug release, such as QTPP, where different aims can be achieved. Most commonly, the aim is the rapid onset of action, but in other cases, sustained release with prolonged circulation time can be accomplished after modifying the polymeric micelle structure [33,34]. Drug release is also influenced based on indication, the route of administration and the API itself. Drug permeability is included as QTPP, aiming either to enhance passive diffusion or the carrier-mediated active transport mechanisms [35]. The described QTPPs are summarized in Table 1.

Table 1. Systematic collection of feasible QTPP elements for the development of polymeric micelle nanoDDSs.

QTPP Element	Details
indication	general API-based extension of general API-based
patient population	paediatrics or geriatrics general, API-based
administration route	conventional e.g., peroral alternative e.g., nasal
site of activity	based on indication based on API new, feasible sites
dosage strength	based on severity of disease based on indication, API and administration route
dosage form	colloidal solution colloidal gelling system freeze-dried powder for further reconstitution
viscosity	based on indication and administration route
osmolality	based on indication and administration route
pH	based on indication and administration route
mucoadhesive properties	based on indication and administration route
particle characteristics	particle size (Z-average) particle size distribution (polydispersity index, PDI) zeta potential encapsulation efficiency (EE%) drug loading (DL%)
safety	biocompatibility degradation products dosage form related
stability	aqueous solution freeze-dried powder dilution stability pH and/or temperature stability structural stability
solubility	solubility rate wettability and polarity redispersion time
drug release	rapid onset of action sustained release prolonged circulation time based on indication, administration route and API
drug permeability	passive diffusion enhancement carrier-mediated active transport enhancement

3.2. How to Choose the Proper QTPP Elements for the Research Project?

When QbD comes to the fore as a tool to use in research, the first step is to gather the QTPP elements; however, the question arises as to which ones are needed within the general elements or whether another one could be added to the QbD setup. Many questions must be answered in the beginning which will help the determination of QTPPs:

- With the formulation, do I change more than the physicochemical properties of the API?
- What would the final dosage form? What are the requirements for it?
- Is there something similar in the literature or on the market? What more can I add to the formulation?
- Who should be the recipients of my formulation? What are the criteria for that target population?
- Do I possess all the necessary tools in my experiments to validate my claims and to characterize the nanocarrier?
- What is the chosen dosage strength and what pharmacokinetic changes can be expected? How do these changes affect the target population and do I need to make adjustments?
- What can the polymers, surfactants and other excipients do? What are their main physicochemical and colloidal properties and how can I utilize them?
- What are the possible toxicological aspects of the formulation? Is the drug content or polymer concentration below a safe level?
- To what extent can I optimize the formulation and can I perform a scaling up?
- What are the drug product quality criteria (e.g., purity, sterility) to be used in clinical settings or to place them on market?
- What container closure system will be used and can the formulation adapt to that?
- What else can the formulation be used for besides my target?

The list of questions could go further based on the research project itself, but quality management tools such as an establishment of an Ishikawa diagram or mind map are encouraged to be utilized for selecting the QTPP elements [36].

3.3. Regulatory Reflections

The European Medicines Agency (EMA) published a joint MHLW/EMA reflection paper on the development of block copolymer micelle medicinal products, which contains aspects to take into consideration when applying QbD as well [21]. It is supplemented by the general ICH specifications, e.g., the guidelines of safety pharmacology studies for human pharmaceuticals (ICH S7A) [37] and the general development and manufacture of drug substances (ICH Q11) [38]. There are multiple factors that should be taken into account: first, the description and composition which are related to the later described CQA and CMA elements. Such factors are the content of the block copolymer and the active substance in the product, the composition and the polymer's material attributes, followed by the quality characterization of the product. Typical examples are the impurity profile, the micelle size, morphology, surface properties, drug loading and in vitro release/permeability profile, which can be generally measured to all polymeric micelle product. The joint paper also states that the stability of the block copolymer micelle products should be based on the ICH Q1A(R2) [39] guideline and for the ones containing biological or biotechnological entities, the ICH Q5C can be applied [40]. For example, if the stability is included in the QTPP profile of the product, it should be more specific depending on the manufacturer's goal—whether it should be physically and/or chemically stable—which is more important or, in other words, based on the material properties of the building agents which have the higher risk value. Non-clinical pharmacokinetics should include relevant measurements of the release and permeability profile of the product complemented by thorough active substance and micelle-forming polymer metabolite screening using biorelevant mediums (maybe organs and/or tissues). When applicable, safety pharmacology studies should be conducted in accordance with ICH M3(R2), ICH S7A and ICH S7B [37,41,42] with toxicological studies based on ICH S4, ICH S6(R1) and ICH S9 [43–45].

The ICH M3(R2) guidelines also define the starting dose for first-in-human studies. By keeping in mind this short summary and the knowledge of the specific guidelines, the CQA and CMA elements were collected in the next step.

3.4. Collection of CQAs for Polymeric Micelle Development

CQAs include those elements that define the quality of our main objectives, the physical, chemical or microbiological characteristics required to achieve the optimal formulation. During screening processes, two main things need to be determined or examined first: the nature of the polymeric micelle forming copolymer and the type of polymeric micelle. Copolymers can differ in the constitution of monomers and the sensitivity towards environmental changes. A distinction can be made between copolymers consisting of two block and those consisting of three blocks, the latter of which can be composed of two or three different monomers. Graft copolymers are considered to contain chain branches allowing a more diverse structure [46]. Innovative copolymers are already able to respond to stimuli by altering the tertiary or quaternary structure of the polymer. Such a stimulus can be, for example, pH, temperature, ionic strength or even binding to an immunological element [47]. The arrangement of conventional polymeric micelles is as follows: in a polar liquid medium, the hydrophilic side chain is solubilized to the outside world, while the hydrophobic moiety keeps the drug molecularly dispersed. The inverse of this can be also distinguished when talking about a reverse micelle. Mixed micelles are polymeric micelles in the construction of which several copolymers play a role. The polymer side chains can take various forms, depending on the material properties, such as a flower-like micelle, unimolecular star micelle or unimolecular dendritic micelle. In the hydrophobic core of a polymeric micelle, several compartments can be formed, mainly with oily substances, in which case, it is a multicompartiment micelle [46]. Morphology of the polymeric micelles are influenced by the dosage form (e.g., they are incorporated into a hydrogel or just a colloidal solution) and whether surface modifications have been formulated on the surface of the outer shell. These modifications all have the same aim: to improve or control the pharmacokinetic profile of the drug release from the carrier [48,49].

Among the CQAs, the factors describing the particle characteristics of the polymeric micelles are included. Such factors are: particle size, polydispersity index, encapsulation efficiency (EE%), drug loading (DL%) and zeta potential. These, combined with polarity and the definition of wetting parameters, are important elements of optimization. The average particle size of polymeric micelles is between 20 and 200 nm, which is influenced by the properties of the building copolymers and the API itself. A particle size distribution is claimed to be optimal if it is below 0.300. Both the EE% and the DL% are strongly related to the material properties, the extent of which is determined by the quantitative and qualitative features of the polymer. As the hydrophilic side chains are oriented towards the outer surface after encapsulation of the API, the values of the contact angles to water will decrease, while those to hydrophobic materials will increase. This leads to increased polarity, which is closely related to water solubility and thus also to dissolution parameters [50]. These factors are the ones that most often form part of the design of experiment (DoE) as to be optimized. Optimization can be performed by factorial experimental designs, e.g., Box–Behnken design, central composite design, Plackett–Burman design or the traditional 2^x DoE experiments. Nowadays, the creation of neural experimental design networks is also of key importance, as it is able to study the interactions between factors more broadly [51,52].

Further investigable CQAs include quantitative parameters related to the permeability of a carrier, for example flux, permeability coefficient (K_p) or to the drug release, e.g., whether a specific kinetic model can be fitted to the dissolution curve or not. Sterility and stability are included as CQAs if they are of high significance, but the same variables are taken into account as they were QTPPs. The possible CQAs of polymeric micelles are summarized in Table 2. Choosing the proper CQA elements for the desired product depends on the later collected material attributes as well and they should not be considered

equally potent and relevant to the development process; these differences should be highlighted and calculated later during an RA.

Table 2. Systematic collection of feasible CQA elements for the development of polymeric micelle nanoDDSs.

CQA Element	Details
type of copolymer	diblock copolymer (A–B type) triblock copolymer (A–B–A type) triblock copolymer (A–B–C type) graft copolymer stimuli-sensitive copolymer
type of polymeric micelle	conventional micelle reverse micelle mixed micelle sensitive micelle flower-like micelle multicompartment micelle unimolecular star micelle unimolecular dendritic micelle
surface modifications	none polyethylene glycole (PEG) conjugates (monoclonal) antibodies peptids, lipids, carbohydrates pH or temperature sensitive sidechain
morphology	spherical star-like crew-cut semi-bald
particle characteristics	particle size, PDI zeta potential wettability, polarity EE%, DL%
API content	based on patient, administration route or indication
permeability rate	based on aim, described with flux or K_p
dissolution rate	based on aim
drug release profile	kinetic or non-kinetic following
sterility	if needed
stability	same variables as in QTPPs

3.5. Collection of CPPs and CMAs for Polymeric Micelle Development

The precise definition of the CPP and CMA elements helps in the DoE process as these are the fundamental factors in getting from the raw material to the nanoDDS. In the case of polymeric micelles, the preparation can always start or end in a liquid medium, where four main factors are distinguished: the copolymer, the API, the solvent(s) and any excipients added. The general CMA factors are presented in Table 3.

Table 3. Systematic collection of feasible CMA elements for the development of polymeric micelle nanoDDSs.

General CMA Element	Details
polymer properties	molecular weight HLB value critical micellar concentration and temperature concentration solubility, logP blank particle size LD ₅₀ value
API	molecular weight solubility, logP melting point concentration LD ₅₀ value
solvent medium	pH, ionic strength volume temperature buffer or solution
excipients	pH control excess solubilizers cryoprotectant if needed

Several methods have been developed for the production of polymeric micelles. Direct dissolution method is commonly used when the micelle-forming copolymers have relatively high water solubility. The API and the copolymer are directly dissolved in an aqueous media associated with stirring, heating and/or sonication in order to form the drug-loaded polymeric micelles [53]. Thus, micelle formation happens by the dehydration of the core forming blocks. The dialysis method is for copolymers with low water solubility; therefore, organic solvents are used in this method. During the preparation, the API and the copolymer(s) are dissolved in a common organic solvent and they are subsequently dialyzed against water. This triggers the micelle formation besides washing away residual organic solvents from the formed polymeric micelle solution [54]. Oily substances can be used in the preparation, when the API is miscible or soluble in the oil phase. With constant mixing, polymeric micelles can form in the aqueous phase of the emulsion, but this method needs many after cleaning processes [55]. The freeze-drying method is associated with dimethylacetamide or tert-butanol as organic (co-)solvents because of their high vapor pressure offering rapid sublimation. After dissolving the API in the organic solvent-water mixture, a freeze-dried cake of polymeric micelles can be achieved which demonstrates adequate shelf-life with high water dispersibility [56]. The thin film method is a production method based on complete solvent evaporation, where the drug and polymer system dissolved in any solvent (mixture) is recovered in the form of a thin film. It is then followed by hydration in water (or water-based buffer) and depending on the properties of the polymer, the process can also be followed by ultrasonication, mixing or even filtration, just like in the production process for liposomes [8,9]. Possible CPP elements and specific CMAs associated with each production method are collected in Table 4.

Table 4. Systematic collection of feasible CPP elements for the different preparation methods of polymeric micelles.

Production Method	CPP/CMA Element
direct dissolution	API dissolution polymer dissolution mixing time rotation speed excipient addition post-preparation settings
dialysis method	flow rate dialysis tube diameter miscibility dialysis time contact volume post-cleaning
oil-in-water emulsion method	oil properties phase separation mixing time additives (e.g., other emulgents) temperature post-cleaning
freeze-drying method	cryoprotectant quality properties concentration of cryoprotectant solvent miscibility vapor pressure freezing temperature freezing time drying time drying pressure drying temperature reconstitution
thin film method/vacuum evaporation	temperature starting and ending pressure scale of decompression rotation speed duration film hydration time hydration media properties

3.6. Risk Assessment on Critical Quality Attributes

Based on the quality by design methodology, two risk assessment have to be performed: between QTPPs and CQAs, where the severity score of the CQAs is obtained, and between the CQAs and CPPs/CMAs, where the severity score of the latter can also be calculated. The severity scores of CQAs in declining order are presented on the Pareto diagram in Figure 2.

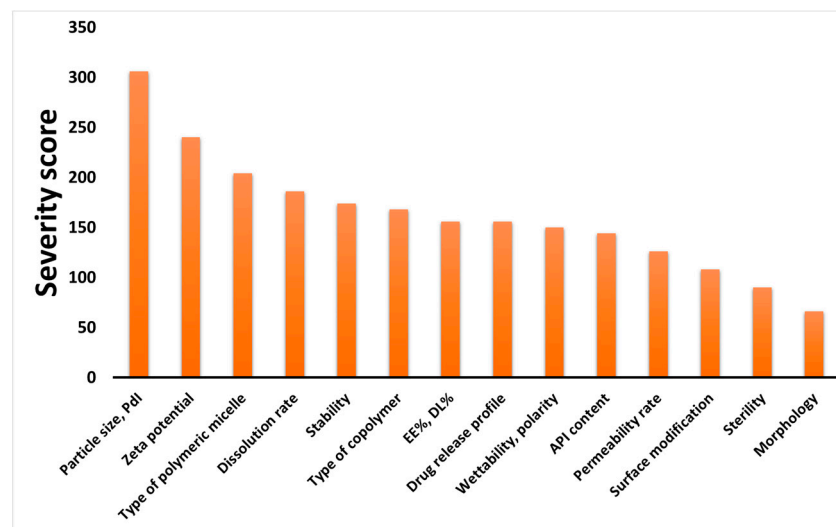


Figure 2. Pareto diagrams of the calculated severity scores of critical quality attributes (CQAs). Abbreviations: Pdl, polydispersity index; EE%, encapsulation efficiency; DL%, drug loading; API, active pharmaceutical ingredient.

Based on the calculated severity scores of the CQA elements, it can be seen that the particle characteristics are the most important to take into account in the formulation of polymeric micelles. These dependent factors pose a great challenge to achieve, but it comes with many advantages. By decreasing the particle size with uniform particle size distribution expressed as polydispersity index (Pdl), favorable solubility, wetting parameters, dissolution and permeability can be accomplished. Zeta potential is also of paramount importance, as the surface charge is directly connected to the physical stability in colloidal aqueous solution form.

3.7. Risk Assessment on Critical Process Parameters and Critical Material Attributes

The second step of the risk assessment was divided into two parts. Firstly, the factors included as CMAs of the preparation processes were taken into account and, then, the CPPs/CMAs were examined, broken down into each preparation process. The Pareto diagram of the calculated severity scores of CMAs are presented on Figure 3.

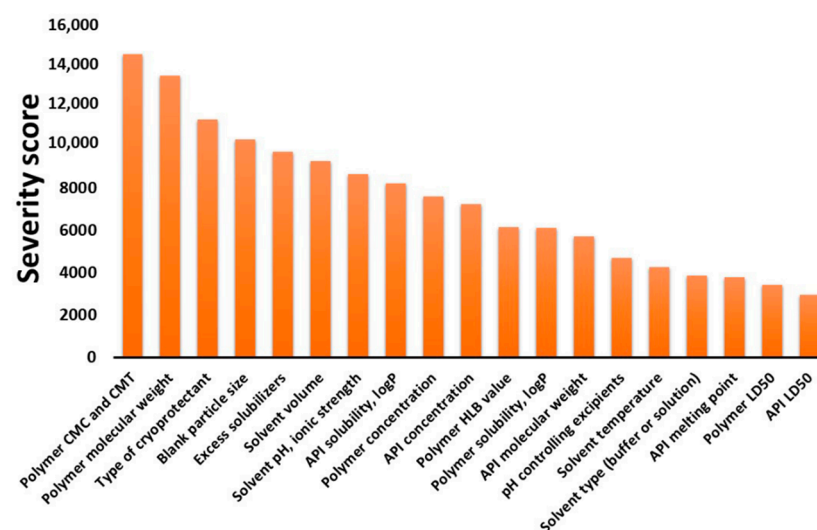


Figure 3. Pareto diagram of the calculated CMAs. Abbreviations: CMC, critical micelle concentration; CMT, critical micelle temperature; API, active pharmaceutical ingredient; HLB, hydrophilic-lipophilic balance; logP, partition coefficient; LD₅₀, median lethal dose.

The material properties of the polymer, the API, the solvents and other excipients were taken into account in the risk assessment. The factors also cover data from the basic physicochemical property to the safety elements. Safety numbers are presented with low severity scores, as dosage strength is highly controllable, making it able to present a polymeric micelle formulation with less chance of toxicity. The polymer, API and solvent properties cannot be ever excluded, as they are severely influence the formation of the nanoparticles. On Figure 4, Pareto diagrams of CPPs/CMAs for each preparation method are presented.

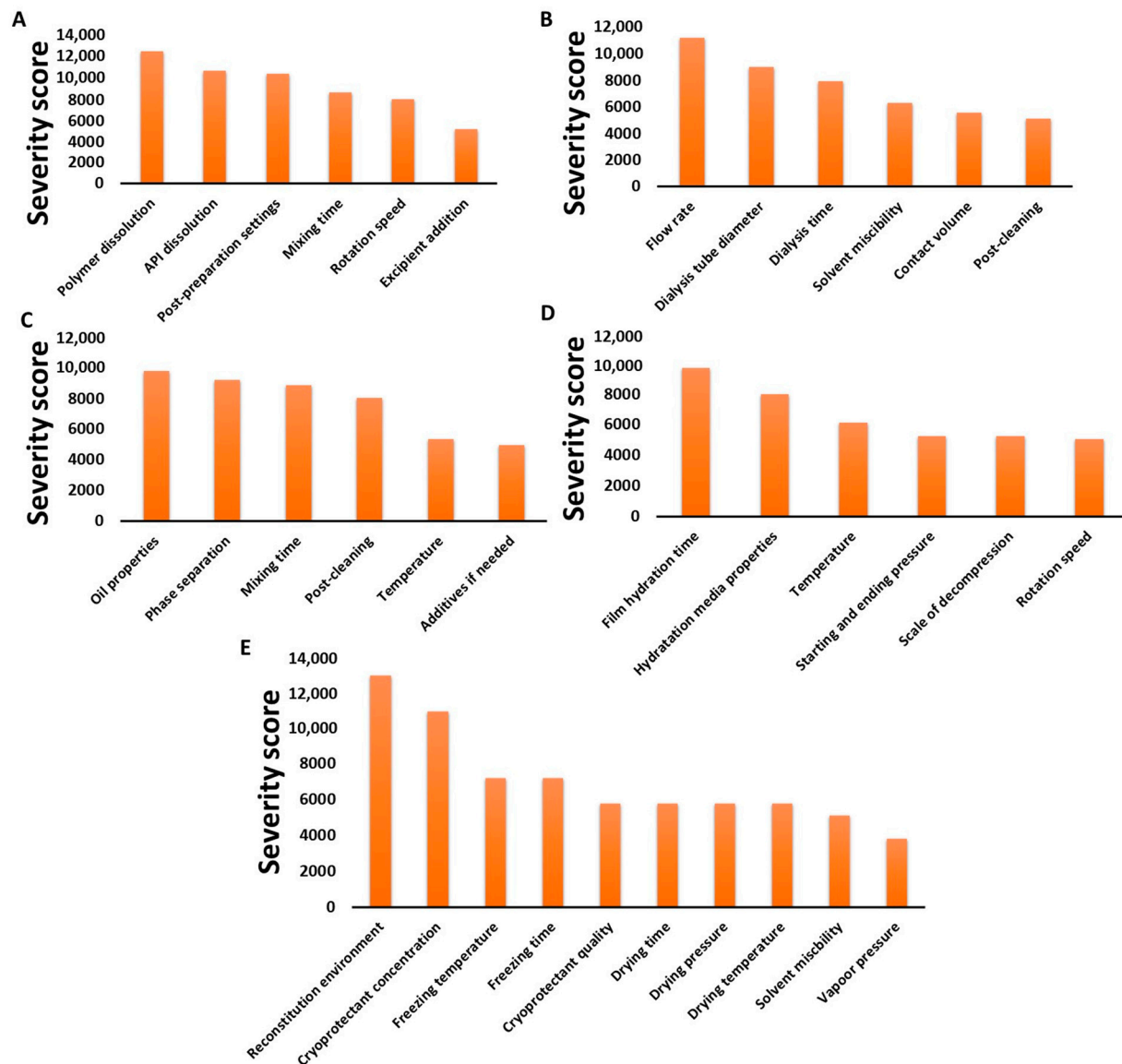


Figure 4. Pareto diagrams of the calculated CPP/CMAs: direct dissolution method (A), dialysis method (B), oil-in-water emulsion method (C), thin film hydration method (D) and freeze-drying method (E).

It can be seen that quite different factors also appear on the different charts in decreasing order of severity score. Although the production methods may be based on a similar principle, it is important to assess the risks associated with each sub-step as part of the manufacturing process. Furthermore, the risk factors that may arise mainly from human negligence, e.g., measurement error, incorrect data setting or risks due to manufacturer/measuring instrument failure, e.g., broken device faulty circuit, are not presented as they are constant among the possible risk factors in the manufacturing process.

3.8. Case Example for the Thought Process of Applying QbD-Based RA

In the rapidly evolving field of nanotechnology and the manufacturing of polymer-based nanocarriers, the assigned severity scores can vary based on many material and target quality-based factors. It can be claimed that there is an antipsychotic compound which has low water solubility and inefficient permeability can be experienced from the intestinal tract from previously formulated solid tablet formulations. Based on this sentence alone, many QTPP elements can be already determined: What is the marketed/clinically efficient dosage strength of the API? What other administration route can I exploit? What is the target population of this API? What is the major indication field of this substance? What physicochemical and pharmacokinetic attributes do I want to improve on? The next step is to make adjustments to this based on your goal: instead of the adult population, the target population should be children; therefore, my target dosage strength must be lowered accordingly to pharmacokinetic parameters. A novel article was found during the knowledge space development phase of my research where the suspension form of this API delivered by the nasal route showed higher brain concentrations, resulting in more advanced therapeutic effect in the major indication. Then, all process and material parameters should be taken into account, for example, in the research laboratory, we have a deep knowledge on freeze-drying production method for polymeric nanocarriers, so that should be the chosen formulation method and there are suitable micelle-forming copolymers which are able to decrease the particle size of APIs below 100 nm.

Gathering all this information, we can now determine the QTPP profile of the desired product, meaning we want to develop a API-loaded mixed polymeric micelle, which:

- has the micellar size less than a 100 nm in monodisperse distribution (QTPP: particle characteristics);
- is suitable for the treatment of psychotic episodes (QTPP: indication);
- can be applied for children (QTPP: target population);
- is administered intranasally (QTPP: administration route);
- in the form of a nasal spray (QTPP: dosage form);
- in half of the currently marketed drug strength (QTPP: dosage strength);
- allowing higher brain concentrations (QTPP: site of activity),
- with sustained drug release (QTPP: drug release profile);
- and enhanced permeability across the nasal mucosa (QTPP: permeability profile).

After the collection of QTPPs, the next step is to gather all the possible CQAs relevant to these targets: mixed polymer types, particle size and polydispersity index, pH, viscosity, mucoadhesivity, osmolality, dissolution rate, permeability rate, drug content uniformity, etc., and investigate the effect on the QTPPs in a 3-scale interdependence rating followed by the calculation of the severity scores using any QbD-modelling software. The same applies to the CMAs and CPPs: for example, each mixed micelle forming polymer concentration, solvent volume, freeze-drying temperatures, cryoprotectant concentration and reconstitution. After the calculation of the severity scores, the following results were observed:

- The highest CQA severity scores were for the particle size, permeability rate and dissolution rate (based on the material attributes of the to be used excipients, polymers and the desired target of the product);
- The highest CMA/ CPP severity scores were for the polymer ratios, the solvent volume and the cryoprotectant concentration (based on the establishment of knowledge about what does the equipment provided to us are able to perform and prior optimization processes for polymeric nanocarriers).

To continue next to set up a design of experiment, many aspects can be followed. One is to make one high-severity risk factor at a constant level or the other is to make it a dependent factor to our factorial design. We chose the cryoprotectant concentration to be fixed at 5 % *w/w* and, furthermore, we investigate the effect of the polymer ratios and the solvent volume on the independent factors: particle size, dissolution and permeability rate during a factorial design of our choosing.

3.9. Optimization Techniques of Polymeric Micelles via QbD-Based Design of Experiment (DoE)

One of the cornerstones of the QbD approach is that, at the end of the risk assessment, an extensive formulation optimization follows. This is most often done by setting up a factorial or neural experimental design, after which the design space is set up with proper statistical evaluation and then the formulation is characterized to validate it. If a quality defect is discovered during the life course of the formulation, then adjustments can be made. One good example of applying QbD as a part of the DoE set-up is the work of Khurana et al., where a 13-run central composite design was used to optimize resveratrol-loaded polymeric micelles [57]. Based on their risk assessment, the selected CQA elements with the highest risk severity were micellar incorporation efficiency (MIE), the particle size and the skin deposition potential. The effect of polymer ratio and the API content were investigated on these CQAs and a response analysis was carried out through polynomial equation. By plotting the surface plots, the optimized polymer to API ratio was found and satisfactory results were obtained: the observed MIE was 93.45% with a particle size of 142.67 nm and skin deposition of 51.63% which all meet the requirements of a polymer-based nanoDDS for topical drug delivery supplemented by advanced *in vivo* pharmacokinetics. Another great example of QbD-based DoE is the work of Lohan et al., where after the construction of an Ishikawa fish-bone diagram containing the factors influencing the galantamine-loaded mixed micelle formulation, a 7-factor 8-run Taguchi orthogonal array design was employed aiming to reveal the potential impact of various material attributes on product quality [58]. After the screening, they investigated the effect of DSPE-PEG 2000 and soy lecithin on the particle characteristics and drug release in a 13-run central composite design, as well as with 5 parallel measurements. A great tool to decrease the severity of the risk factors was applied by them: keeping the high-risk valued ethanol concentration at a fixed ratio, meaning that the optimized formulation should be matched with this factor. By the end of the optimization, the desirability functions were compared to the investigated parameters and a nanosized mixed micellar system was developed with a particle size of 175 nm, a zeta potential of -18 mV and a dissolution efficiency of 86%. In our previous work, the optimization of Meloxicam-loaded polymeric micelles via RA-based Box–Behnken factorial design was performed and a one-way ANOVA statistical analysis of the results was applied. The effect of the ethanol and sodium-hydroxide volume and the polymer concentration was investigated on particle size and particle size distribution with end results of 111.6 nm and a PDI of 0.114, allowing proper basis for nasal drug delivery [9]. In addition to these examples, many factorial/neural design studies are there in the literature for polymeric micelles; however, the lack of pre-optimization risk screening can be observed. That is why it is encouraging to use the demonstrated knowledge space development and risk assessment, along with statistical analysis of your choosing, so the micellar formulations can be matched to quality management as well.

4. Discussion

Through mandatory steps of quality by design, this article has collected and evaluated the factors that influence the successful development of a polymeric micelle based nanocarrier system. The QTPP elements, as proven, depend on the purpose; however, it is important to incorporate the mandatory elements of the ICH guidelines when setting up the pilot design. For polymeric micelles, as promising nanotherapeutics, this is not an easy task, as new indications and therapeutic possibilities may occur due to particle size reduction and modification of the administration route, leading to a different pharmacokinetic profile. The CQA, CPP and CMA elements were collected in their entirety to characterize a general formulation based on literature. These parameters are those that affect the quality of the product from the beginning of the manufacturing process to the patient's use.

During the course of our research, we first collected the QTPP, CQA, CMA and CPP factors that influence the quality of a polymeric micelle formulation. Amongst QTPPs, it can be seen that it can range from general application principles to the extent of physicochemical and pharmacokinetic factors. It is important to see that QTPP elements are those without

which risk assessment would not be possible. A separate risk assessment process is required for each polymeric micelle formulation, regardless of whether it contains an active substance or it concerns a development of a new polymeric carrier system able to form micelles. In the risk assessment with the CQA, CPP and CMA elements, we shed light on which posed the greatest risk for a general nanoformulation. Of course, a researcher has to decide for themselves which factors are relevant to the production process and product quality chosen, so we performed the analysis for several production methods common amongst developers. The risk assessment of R&D processes is of particular importance for nanocarriers. Greater emphasis should also be placed on the basic properties of polymers and the active substance, as well as on the steps in the manufacturing process. The optimization of the particle characteristics also depends, crucially, on the nature of the building polymer and the manufacturing process.

Although the main points presented on the tables and figures are just fragments of the evidence presented in many articles and development processes, the systemic collection of all the influencing factors as data is the novelty of this current work. To demonstrate that the CMAs and CPPs parallelly improve the transparency between these parameters and their relation between CQA elements, in Tables 1–4, the general collection of influencing factors can be seen, followed by an RA process as seen on Figures 2–4. The Pareto charts on Figures show the theoretical ranking of the severity of the influencing factors as part of an initial general RA.

This presented work can fit well into the research area of polymeric micelles as it is an extension of the previous knowledge acquired by prior results. QbD is also recommended by regulatory authorities and encourage researchers to build the process of nanocarriers into their development.

5. Conclusions

The novelty of the work was that polymeric micelles were systematically evaluated on the basis of knowledge and risk, as these nanotherapeutics require a special regulatory environment. The quality by design methodology offered a thoroughly quality-focused assurance system, which proved to be useful in the case of polymeric micelles. As an encouragement, it is recommended that all researchers use the previous literature and evaluate the significant factors under a risk assessment process, resulting in a more focused design of experiment. Later, knowledge of these factors provides an important basis for quality and process control and allows for an easier to manage, correctable manufacturing process.

Author Contributions: Conceptualization, B.S. and I.C.; methodology, B.S., G.K. and I.C.; software, B.S.; validation, G.K. and I.C.; formal analysis, G.K.; investigation, B.S., G.K. and I.C.; resources, I.C.; data curation, B.S., G.K. and I.C.; writing—original draft preparation, B.S. and G.K.; writing—review and editing, I.C.; visualization, B.S.; supervision, G.K. and I.C.; project administration, B.S., G.K. and I.C.; funding acquisition, G.K. and I.C. All authors have read and agreed to the published version of the manuscript.

Funding: The publication was funded by the University of Szeged Open Access Fund (FundRef, Grant No. 5232).

Institutional Review Board Statement: Not applicable.

Informed Consent Statement: Not applicable.

Data Availability Statement: The data presented in this study are available on request from the corresponding author.

Acknowledgments: This work was supported by EFOP 3.6.3-VEKOP-16-2017-00009, National Research, Development and Innovation Office, Hungary (GINOP-2.3.2-15-2016-00060) and Ministry of Human Capacities, Hungary grant, TKP-2020 projects.

Conflicts of Interest: The authors declare no conflict of interest.

References

1. Khanna, I. Drug discovery in pharmaceutical industry: Productivity challenges and trends. *Drug Discov. Today* **2012**, *17*, 1088–1102. [[CrossRef](#)] [[PubMed](#)]
2. Schweizer, L.; Dingermann, T. Introduction: Trends and Developments in the Pharmaceutical and Life Sciences Industry. In *Advances in Pharma Business Management and Research: Volume 1*; Schweizer, L., Dingermann, T., Russe, O.Q., Jansen, C., Eds.; Springer International Publishing: Cham, Switzerland, 2020; pp. 1–5, ISBN 978-3-030-35918-8.
3. Patil, A.S.; Pethe, A.M. Quality by design (QbD): A new concept for development of quality pharmaceuticals. *Int. J. Pharm. Qual. Assur.* **2013**, *4*, 13–19.
4. Yu, L.X.; Amidon, G.; Khan, M.A.; Hoag, S.W.; Polli, J.; Raju, G.K.; Woodcock, J. Understanding pharmaceutical quality by design. *AAPS J.* **2014**, *16*, 771–783. [[CrossRef](#)]
5. Li, J.; Qiao, Y.; Wu, Z. Nanosystem trends in drug delivery using quality-by-design concept. *J. Control. Release* **2017**, *256*, 9–18. [[CrossRef](#)] [[PubMed](#)]
6. Xu, X.; Khan, M.A.; Burgess, D.J. A quality by design (QbD) case study on liposomes containing hydrophilic API: I. Formulation, processing design and risk assessment. *Int. J. Pharm.* **2011**, *419*, 52–59. [[CrossRef](#)]
7. Rawal, M.; Singh, A.; Amiji, M.M. Quality-by-Design Concepts to Improve Nanotechnology-Based Drug Development. *Pharm. Res.* **2019**, *36*. [[CrossRef](#)] [[PubMed](#)]
8. Németh, Z.; Pallagi, E.; Dobó, D.G.; Csóka, I. A proposed methodology for a risk assessment-based liposome development process. *Pharmaceutics* **2020**, *12*, 1164. [[CrossRef](#)]
9. Sipos, B.; Szabó-Révész, P.; Csóka, I.; Pallagi, E.; Dobó, D.G.; Béltéky, P.; Kónya, Z.; Deák, Á.; Janovák, L.; Katona, G. Quality by design based formulation study of meloxicam-loaded polymeric micelles for intranasal administration. *Pharmaceutics* **2020**, *12*, 697. [[CrossRef](#)]
10. Katona, G.; Balogh, G.T.; Dargó, G.; Gáspár, R.; Márki, Á.; Ducza, E.; Sztojkov-Ivanov, A.; Tömösi, F.; Kecskeméti, G.; Janáky, T.; et al. Development of meloxicam-human serum albumin nanoparticles for nose-to-brain delivery via application of a quality by design approach. *Pharmaceutics* **2020**, *12*, 97. [[CrossRef](#)]
11. Warheit, D.B. How meaningful are the results of nanotoxicity studies in the absence of adequate material characterization? *Toxicol. Sci.* **2008**, *101*, 183–185. [[CrossRef](#)]
12. Fischer, H.C.; Chan, W.C. Nanotoxicity: The growing need for in vivo study. *Curr. Opin. Biotechnol.* **2007**, *18*, 565–571. [[CrossRef](#)] [[PubMed](#)]
13. Miyata, K.; Christie, R.J.; Kataoka, K. Polymeric micelles for nano-scale drug delivery. *React. Funct. Polym.* **2011**, *71*, 227–234. [[CrossRef](#)]
14. Lu, Y.; Park, K. Polymeric micelles and alternative nanonized delivery vehicles for poorly soluble drugs. *Int. J. Pharm.* **2013**, *453*, 198–214. [[CrossRef](#)] [[PubMed](#)]
15. Owen, S.C.; Chan, D.P.Y.; Shoichet, M.S. Polymeric micelle stability. *Nano Today* **2012**, *7*, 53–65. [[CrossRef](#)]
16. Hafner, A.; Lovrić, J.; Lakó, G.P.; Pepić, I. Nanotherapeutics in the EU: An overview on current state and future directions. *Int. J. Nanomed.* **2014**, *9*, 1005–1023. [[CrossRef](#)]
17. Csóka, I.; Pallagi, E.; Paál, T.L. Extension of quality-by-design concept to the early development phase of pharmaceutical R&D processes. *Drug Discov. Today* **2018**, *23*, 1340–1343. [[CrossRef](#)]
18. ICH. *Quality Risk Management Q9*; ICH Harmonised Tripartite Guideline; ICH: Geneva, Switzerland, 2005.
19. ICH. *ICH Q10 Pharmaceutical Quality Systems*; ICH: Geneva, Switzerland, 2008.
20. ICH. *Pharmaceutical Development Q8*; ICH Harmonised Tripartite Guideline; ICH: Geneva, Switzerland, 2009.
21. EMA. *Joint MHLW/EMA Reflection Paper on the Development of Block Copolymer Micelle Medicinal Products*; EMA: Amsterdam, The Netherlands, 2014.
22. Powell, T.; Sammut-bonnici, T. Capabilities and capability analysis; core competences; cost analysis; dynamic capabilities; efficiency; SWOT analysis; resource-based view. In *Wiley Encyclopedia of Management*; John Wiley & Sons, Ltd.: Chichester, UK, 2014; pp. 1–2.
23. Troiano, G.; Nolan, J.; Parsons, D.; Van Geen Hoven, C.; Zale, S. A Quality by Design Approach to Developing and Manufacturing Polymeric Nanoparticle Drug Products. *AAPS J.* **2016**, *18*, 1354–1365. [[CrossRef](#)]
24. Xiang, J.; Wu, B.; Zhou, Z.; Hu, S.; Piao, Y.; Zhou, Q.; Wang, G.; Tang, J.; Liu, X.; Shen, Y. Synthesis and evaluation of a paclitaxel-binding polymeric micelle for efficient breast cancer therapy. *Sci. China Life Sci.* **2018**, *61*, 436–447. [[CrossRef](#)]
25. Vlad, S.C.; Miller, D.R.; Kowall, N.W.; Felson, D.T. Protective effects of NSAIDs on the development of Alzheimer disease. *Neurology* **2008**, *70*, 1672–1677. [[CrossRef](#)]
26. Jin, H.K.; Kim, Y.H.; Rhie, S.J. Factors affecting medication adherence in elderly people. *Patient Prefer. Adherence* **2016**, *10*, 2117–2125. [[CrossRef](#)]
27. Mandal, A.; Bisht, R.; Rupenthal, I.D.; Mitra, A.K. Polymeric micelles for ocular drug delivery: From structural frameworks to recent preclinical studies. *J. Control. Release* **2017**, *248*, 96–116. [[CrossRef](#)]
28. Šmejkalová, D.; Muthný, T.; Nešporová, K.; Hermannová, M.; Achbergerová, E.; Huerta-Angeles, G.; Svoboda, M.; Čepa, M.; Machalová, V.; Luptáková, D.; et al. Hyaluronan polymeric micelles for topical drug delivery. *Carbohydr. Polym.* **2017**, *156*, 86–96. [[CrossRef](#)]
29. Kahraman, E.; Karagöz, A.; Dinçer, S.; Özsoy, Y. Polyethylenimine modified and non-modified polymeric micelles used for nasal administration of carvedilol. *J. Biomed. Nanotechnol.* **2015**, *11*, 890–899. [[CrossRef](#)] [[PubMed](#)]

30. Miura, Y.; Takenaka, T.; Toh, K.; Wu, S.; Nishihara, H.; Kano, M.R.; Ino, Y.; Nomoto, T.; Matsumoto, Y.; Koyama, H.; et al. Cyclic RGD-linked polymeric micelles for targeted delivery of platinum anticancer drugs to glioblastoma through the blood-brain tumor barrier. *ACS Nano* **2013**, *7*, 8583–8592. [CrossRef]
31. Sun, X.; Wang, G.; Zhang, H.; Hu, S.; Liu, X.; Tang, J.; Shen, Y. The Blood Clearance Kinetics and Pathway of Polymeric Micelles in Cancer Drug Delivery. *ACS Nano* **2018**, *12*, 6179–6192. [CrossRef]
32. Łukasiewicz, S.; Szczepanowicz, K.; Błasiak, E.; Dziedzicka-Wasylewska, M. Biocompatible Polymeric Nanoparticles as Promising Candidates for Drug Delivery. *Langmuir* **2015**, *31*, 6415–6425. [CrossRef]
33. Watanabe, M.; Kawano, K.; Yokoyama, M.; Opanasopit, P.; Okano, T.; Maitani, Y. Preparation of camptothecin-loaded polymeric micelles and evaluation of their incorporation and circulation stability. *Int. J. Pharm.* **2006**, *308*, 183–189. [CrossRef] [PubMed]
34. Yang, Z.; Zheng, S.; Harrison, W.J.; Harder, J.; Wen, X.; Gelovani, J.G.; Qiao, A.; Li, C. Long-circulating near-infrared fluorescence core-cross-linked polymeric micelles: Synthesis, characterization, and dual nuclear/optical imaging. *Biomacromolecules* **2007**, *8*, 3422–3428. [CrossRef]
35. Pepić, I.; Lovrić, J.; Filipović-Grčić, J. How do polymeric micelles cross epithelial barriers? *Eur. J. Pharm. Sci.* **2013**, *50*, 42–55. [CrossRef] [PubMed]
36. Ishikawa, K. *What Is Total Quality Control? The Japanese Way*; Prentice Hall: Hoboken, NJ, USA, 1985; pp. 247–249. Available online: <http://asq.org/learn-about-quality/cause-analysis-tools/overview/fishbone.html> (accessed on 2 May 2021).
37. ICH. *Safety Pharmacology Studies for Human Pharmaceuticals S7A*; ICH: Geneva, Switzerland, 2000.
38. ICH. *Development and Manufacture of Drug Substances (Chemical Entities and Biotechnological/Biological Entities) Q11*; ICH: Geneva, Switzerland, 2013.
39. ICH. *Stability Testing of New Drug Substances and Drug Products Q1A (R2)*; ICH: Geneva, Switzerland, 2003.
40. ICH. *Stability Testing of Biotechnological/Biological Products Q5C*; ICH: Geneva, Switzerland, 1996.
41. ICH. *Non-Clinical Safety Studies for the Conduct of Human Clinical Trials for Pharmaceuticals M3(R2)*; ICH: Geneva, Switzerland, 2013.
42. ICH. *Non-Clinical Evaluation of the Potential for Delayed Ventricular Repolarization (QT Interval Prolongation) by Human Pharmaceuticals S7B*; ICH: Geneva, Switzerland, 2005.
43. ICH. *Duration of Chronic Toxicity Testing in Animals (Rodent and Non-Rodent Toxicity Testing) S4*; ICH: Geneva, Switzerland, 1998.
44. ICH. *Preclinical Safety Evaluation of Biotechnology-Derived Pharmaceuticals S6(R1)*; ICH: Geneva, Switzerland, 2011.
45. ICH. *Nonclinical Evaluation for Anticancer Pharmaceuticals S9*; ICH: Geneva, Switzerland, 2008.
46. Simões, S.M.N.; Figueiras, A.R.; Veiga, F.; Concheiro, A.; Alvarez-Lorenzo, C. Polymeric micelles for oral drug administration enabling locoregional and systemic treatments. *Expert Opin. Drug Deliv.* **2015**, *12*, 297–318. [CrossRef]
47. Lee, E.S.; Na, K.; Bae, Y.M. Super pH-sensitive multifunctional polymeric micelle. *Nano Lett.* **2005**, *5*, 325–329. [CrossRef]
48. Mourya, V.K.; Inamdar, N.; Nawale, R.B.; Kulthe, S.S. Polymeric micelles: General considerations and their applications. *Indian J. Pharm. Educ. Res.* **2011**, *45*, 128–138.
49. Guo, M.; Jiang, M.; Zhang, G. Surface modification of polymeric vesicles via host-guest inclusion complexation. *Langmuir* **2008**, *24*, 10583–10586. [CrossRef] [PubMed]
50. Agrawal, R.D.; Tatode, A.A.; Rarokar, N.R.; Umekar, M.J. Polymeric micelle as a nanocarrier for delivery of therapeutic agents: A comprehensive review. *J. Drug Deliv. Ther.* **2020**, *10*, 191–195. [CrossRef]
51. Dejaegher, B.; Vander Heyden, Y. Experimental designs and their recent advances in set-up, data interpretation, and analytical applications. *J. Pharm. Biomed. Anal.* **2011**, *56*, 141–158. [CrossRef]
52. Rahmanian, B.; Pakizeh, M.; Mansoori, S.A.A.; Abedini, R. Application of experimental design approach and artificial neural network (ANN) for the determination of potential micellar-enhanced ultrafiltration process. *J. Hazard. Mater.* **2011**, *187*, 67–74. [CrossRef]
53. Croy, S.R.; Kwon, G.S. The effects of Pluronic block copolymers on the aggregation state of nystatin. *J. Control. Release* **2004**, *95*, 161–171. [CrossRef]
54. Pierri, E.; Avgoustakis, K. Poly(lactide)-poly(ethylene glycol) micelles as a carrier for griseofulvin. *J. Biomed. Mater. Res. Part A* **2005**, *75*, 639–647. [CrossRef] [PubMed]
55. He, J.; Zhou, Z.; Fan, Y.; Zhou, X.; Du, H. Sustained release of low molecular weight heparin from PLGA microspheres prepared by a solid-in-oil-in-water emulsion method. *J. Microencapsul.* **2011**, *28*, 763–770. [CrossRef]
56. Adams, M.; Kwon, G.S. Spectroscopic investigation of the aggregation state of amphotericin B during loading, freeze-drying, and reconstitution of polymeric micelles. *J. Pharm. Pharm. Sci.* **2004**, *7*, 1–6. [PubMed]
57. Khurana, B.; Arora, D.; Kumar Narang, R. QbD based exploration of resveratrol loaded polymeric micelles based carbomer gel for topical treatment of plaque psoriasis: In vitro, ex vivo and in vivo studies. *JDDTS* **2020**, *59*, 101901. [CrossRef]
58. Lohan, S.; Sharma, T.; Saina, S.; Swami, R.; Dhull, D.; Beg, S.; Raza, K.; Kumar, A.; Singh, B. QbD-steered development of mixed nanomicelles of galantamine: Demonstration of enhanced brain uptake, prolonged systemic retention and improved biopharmaceutical attributes. *Int. J. Pharm.* **2021**, *600*, 120482. [CrossRef] [PubMed]

III.



Sipos Bence*, Katona Gábor

Innovatív polimer alapú nanohordozók a központi idegrendszer betegségeinek kezelésére

A polimer micellák mint gyógyszerhordozó rendszerek alkotják a polimer alapú nanorészecskék specifikus csoportját. Nano-mérettartományuknak köszönhetően képesek a rossz vízoldékonysággal és/vagy permeabilitással jellemezhető hatóanyagok biohasznosulását növelni. Az önrendeződő struktúrák előnye, hogy felületaktív tulajdonságuk következtében már kis koncentrációban is képesek nagy mennyiségű hatóanyagot szolubilizálni. Ebből adódóan a polimer micellás készítmények kiválóan alkalmazhatók alternatív beviteli kapukon keresztül, így intranasalis úton történő terápia kiváltására. Jelen kézirat a polimer micellás hordozók nasalis gyógyszerbevitelre történő fejlesztésére fókuszál, amely segítségével direkt, a vér-agy gátat megkerülő hatóanyag-bevitelt lehet megvalósítani. A szaglóidegen keresztül axonális transzport kiaknázása számos központi idegrendszert érintő betegség hatékony terápiájának lehetőségét hordozza magában. Jelenleg ezen betegségek (neurodegeneratív betegségek, depresszió, szkizofrénia) kezelése általában magas hatóanyag dózisos bevitelét igényli, mely számos mellékhatás megjelenéséhez vezet az elégtelen agyi koncentrációk elérése mellett. A polimer alapú hordozók, így a polimer micellák pedig előnyös tulajdonságuknak köszönhetően képesek ezeket a problémákat kiküszöbölni.

Kulcsszavak: nanomedicina, polimer micella, nasalis bevitel, központi idegrendszer

BEVEZETÉS

A központi idegrendszert érintő betegségek hatékony terápiájának megvalósítása központi szerepet játszik napjaink kutatás-fejlesztési folyamataiban. A neurodegeneratív betegségek prevalenciája évről évre növekszik, amelynek oka elsősorban a múlt évszázadban bekövetkező hirtelen népességugrás. Ez a demográfiai változás a korfa idősebb korosztályok felé történő kiszélesedését eredményezte. Általánosságban elmondható, hogy a neurodegeneratív betegségek jelenlegi gyógyszeres terápiája a betegvárásokat csak részben képes kielégíteni. Ennek legfőbb oka a súlyos mellékhatásprofilal jellemezhető jelen terápiás megoldások, a dozírozásban fellépő hibák és a betegek

Innovative polymer-based nanocarriers for the treatment of central nervous system diseases

Polymeric micelles are among the nano drug delivery systems. Due to their nano size range, they are able to increase the poor water solubility and/or permeability of certain drugs. As self-assembling structures, they are able to solubilize large amounts of drug even at low concentrations, which solubilized formulations are suitable for administration through alternative delivery gates, such as the intranasal route. The aim of our research was to study the development of polymeric micellar carriers through the nasal pathway, the direct route, which bypasses the blood-brain-barrier. By utilizing the axonal transport, we can provide an effective therapeutic option for a number of diseases affecting the central nervous system. Treatment of neurodegenerative diseases, depression or schizophrenia usually requires high doses, leading to a number of side effects in addition to insufficient brain concentrations. Polymer-based carriers, such as polymeric micelles are able to overcome these problems due to their advantageous properties.

Keywords: nanomedicine, polymeric micelle, nasal delivery, central nervous system

életminőség-romlása a terápia során. Ezen tényezők együttesen olyan igényeket állítanak fel a gyógyszerkészítmények fejlesztése terén, amely a beteg-együttműködés (adherencia) növelése mellett csökkentett kockázattal és magasabb terápiás hatékonysággal képesek enyhíteni a betegség tüneteit [1]. A nanogyógyszerhordozó rendszerek mint innovatív termékek alternatív beviteli kapun keresztül (pl. orr) történő bejuttatása hatékony módja lehet ezen terápiás igények kielégítésének.

KIHÍVÁSOK A KÖZPONTI IDEGRENSZERI BETEGSÉGEK TERÁPIÁJÁBAN

A központi idegrendszer betegségeinek – jelenlegi –



Sipos Bence 2020-ban szerzett gyógyszerészdiplomát a Szegedi Tudományegyetemen. Jelenleg II. évfolyamos doktoranduszhallgató az SZTE Gyógyszer-technológiai és Gyógyszer-felügyeleti Intézet Nanotechnológiai Kutatócsoportjában. Kutatási területe nasalis bevitelű, polimer alapú hordozórendszerek fejlesztése a központi idegrendszerbe történő hatóanyag-bevitel és a biohasznosíthatóság fokozása céljából. Legfőbb elismerései: Szeged Megyei Jogú Város Ösztöndíja (2018/19 és 2019/20), Zsembery-pályadíj (2019), Nemzeti Felsőoktatási Ösztöndíj (2019/20), Új Nemzeti Kiválóság Program ösztöndíja (2019 és 2021) és Kedvessy György pályadíj (2020). Eddigi munkásságából 4 darab angol nyelvű, első szerzős, Q1 minősítésű, impakt faktoral rendelkező nemzetközi folyóiratban megjelent és 2 db társszerzős publikációja született (összesített IF: 35,07).

terápiájában alkalmazott gyógyszerek főként hagyományos beviteli kapukon keresztül, elsősorban szájon át (orálisan), vagy parenteralisan kerülnek alkalmazásra. A per os bevitelről köztudott, hogy maga után vonja a máj „first-pass” metabolizmusát. Ezenkívül a tápcsatorna teljes szakaszára jellemző változó pH-viszonyok jelentősen megnehezítik a programozott hatóanyag-leadást, valamint az emésztő enzimek lebontó hatása sem hagyható figyelmen kívül. A metabolikus folyamatok következtében a hatóanyag szerkezetében jelentős változások történhetnek, ezáltal markánsabb mellékhatások léphetnek fel, háttérbe szorítva a célterületen elérni kívánt hatás kifejtését. A metabolitok kialakulása sok esetben korlátozza a hatóanyag vér-agy gáton történő átjutásának lehetőségét is. A vér-agy gát mint természetes biológiai gát, képes a hatóanyagokat molekulatömegük és lipofilitásuk alapján kiszűrni, vagy csak csekély mértékben átengedni. Ez különösen igaz az antidepresszáns, antipszichotikus hatású hatóanyagokra. A neurodegeneratív betegségek (Alzheimer-, Parkinson-kór, sclerosis multiplex) terápiájában a kismolekulás hatóanyagokon kívül fehérje típusú anyagok is megtalálhatóak. A fehérjék orális bevitelére általánosságban elmondható, hogy fokozottan érzékenyek a gastrointestinalis rendszer lebontó folyamataira, amelyek a fehérje szerkezetének teljes megváltoztatása miatt ellehetetlenítik a központi idegrendszerbe történő eljutásukat. Nem mellékes, hogy a per os alkalmazás során a fehérjék vérbe történő felszívódása sem valósul meg megfelelő mértékben, amely elsősorban a nagy

méretük következtében ellehetetlenült passzív transzportfolyamatok le nem játszódásával magyarázható. Ezen okok miatt a fehérje típusú hatóanyagok terápia alkalmazására invazív (parentalis) beviteli módok alkalmazhatóak, elsősorban injekció vagy infúzió formájában, amely számos rizikótényezőt foglal magában a betegélmény negatív megélése mellett [2, 3].

A NASALIS GYÓGYSZERBEVITEL

Az utóbbi időben a gyógyszerkutatások középpontjába került az orrüregen keresztüli, azaz intranasalis gyógyszerbevitel kényelmes, ígéretes és megbízható beadási módja révén, különösen azoknál a hatóanyagoknál, amelyek orálisan elégtelenül szívódnak fel és váltják ki hatásukat, avagy invazív bevitelt igényelnek. Az orrüreg változatos anatómiai felépítése egyaránt lehetőséget ad helyi és szisztémás terápiás hatás kiváltására. Az orrüregben található a dús érhálózatral rendelkező, nagy felszínű orrnyálkahártya, amelynek több régiója az anatómiai különbségek mellett befolyásolja a hatóanyag felszívódását. Az orrüreg elülső, külvilággal közvetlenül érintkező nyálkahártya felszíne elsősorban a külső szennyeződések, mikroorganizmusok eltávolítására szolgál. Amennyiben az orrspray vagy orrcsepp adagolási egysége ezzel a régióval érintkezik, ez kiválóan biztosítja a helyi hatású hatóanyagok pl. dekongesztánsok, antibiotikumok felszívódását. A mélyebben fekvő, szaglós- és háromszögletű idegpályák által beidegzett orrnyálkahártya területén pedig a célzott hatóanyag-felszívódás érhető el az innovatív gyógyszerhordozók alkalmazásával. A nanohordozó rendszerek fizikai-kémiai karakterük révén (pl. lipofilitásuk, molekulatömegük, felületi töltöttségük és részecskeméretük) képesek ezen idegpályák mentén a becsomagolt hatóanyagot közvetlen az agyba juttatni. Ezenkívül maga a hatóanyag jellege, molekuláris szerkezete is befolyásolja a hordozó kiválasztását. Ennek tudatában a jövő nasalis gyógyszerformáinak piacra kerülésekor különös figyelmet kell szentelni a megfelelő orrspray-pumpafeltét kifejlesztésére is [4, 5].

Az orr mint alternatív beviteli kapu jelentős szerepet tölt be a vakcinák alkalmazása terén is, mivel az orrüreg közvetlen kapcsolatban áll az immunrendszerrel, így a nem invazív passzív immunizálás kiváltására alkalmas lehet. További előnye a nasalis bevitelnek, hogy javítja a beteg-együttműködést, valamint az egyszerű alkalmazás révén megkönnyíti az öngyógyoszerelést, ami fontos kritérium, hiszen a

I. táblázat A nasalis beviteli kapu fő előnyei és hátrányai

Előny	Hátrány
Nem invazív módszer	Ornyálkahártya érzékenysége, irritáció
Direkt út a központi idegrendszerbe	Kis egyszeri adagolási térfogat
Nem szükséges a sterilitás	Rövid tartózkodási idő
Könnyű (ön)alkalmazás	Gyors elimináció a mukociliáris clearance miatt
Gyors felszívódás és hatás	Patológias állapotok pl. rhinitis megváltoztathatja a felszívódási profilt
A máj degradatív enzimeinek megkerülése	
Kisebb a gyógyszer-túlادagolás veszélye	

neurodegeneratív betegségekben szenvedő betegek többségének ez nehézséget jelent. A gyermek- és időskorban fellépő nyelési nehézségek, illetve gyógyszer-beviteli képtelenségek pedig szükségessé teszik részben ezen alternatív beviteli út alkalmazását az orális gyógyszeres terápia kiváltásában [6, 7].

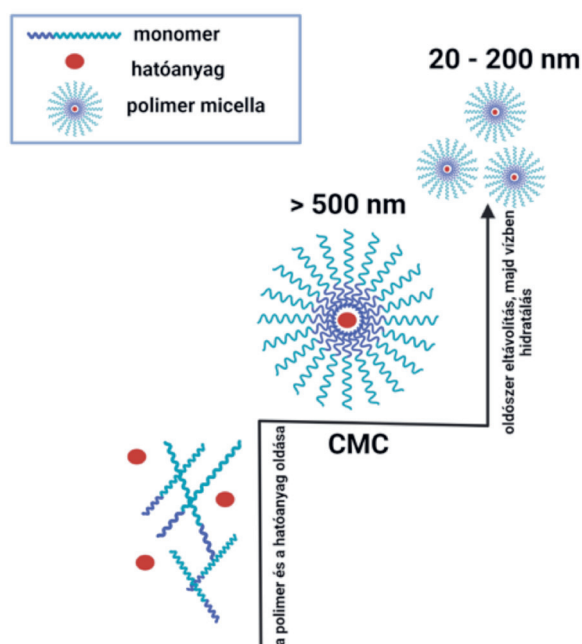
A beviteli kapu főbb előnyeit és hátrányait az **I. táblázat** mutatja be.

POLIMER MICELLÁK

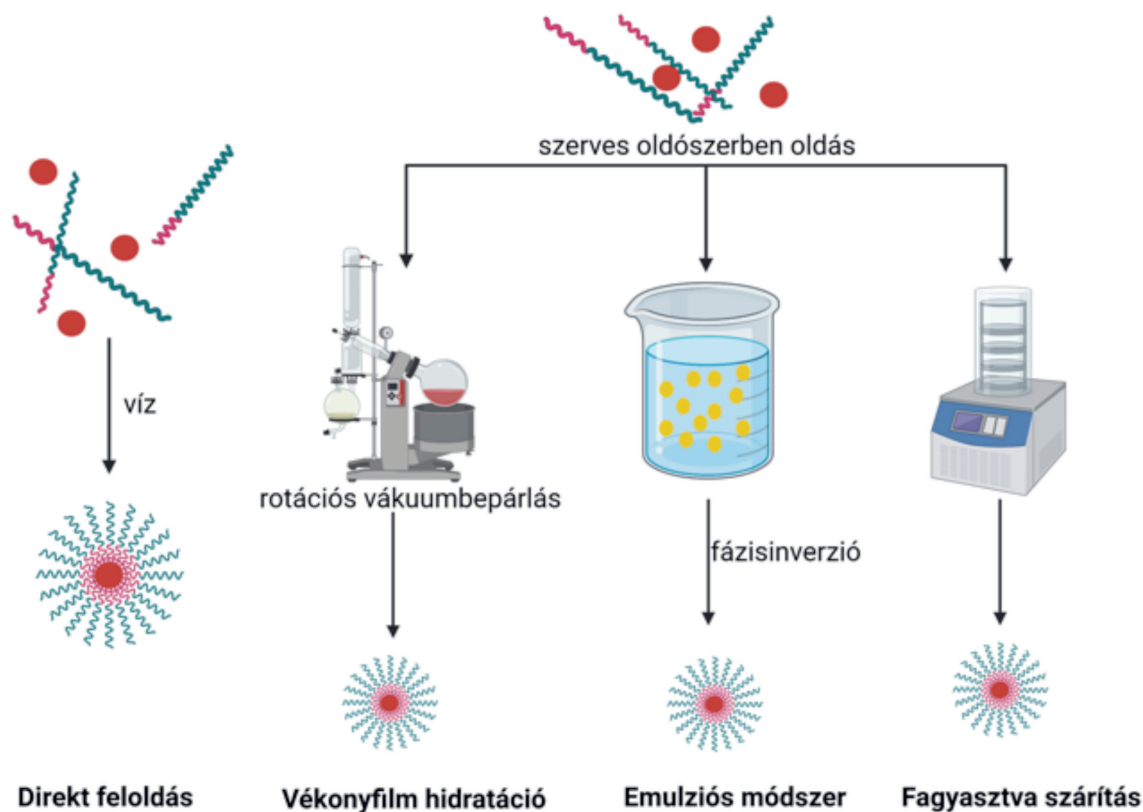
A polimer micellák a nano hatóanyag-hordozó rendszerek közé tartozó, önrendeződésre képes kolloidális részecskék. Felépítésükben az úgynevezett amfifil graft kopolimerek játszanak szerepet. Az amfifil tulajdonság, miszerint a molekula egyaránt tartalmaz hidrofil és hidrofób láncrészeket, megegyezik a klasszikus tenzidekre jellemző sajátsággal, azonban szerkezetüket összetettség jellemzi. A graft jelző alapján elmondható, hogy ezek a több polimerláncból (kopolimer jelleg) összekapcsolódott vegyületek nem csak lineárisan, hanem elágazó kapcsolódási rendszerrel is jellemezhetőek. Az eltérő elrendeződés, a láncok egymás utáni felépíthetősége befolyásolja magát a kopolimer oldékonysági és egyéb fizikai-kémiai tulajdonságait, valamint a szolubilizációs képességét is. Általánosságban véve gömbszerűek, a rendszerek szférikus alakkal rendelkeznek, azonban a láncelágazás változtatásával különböző formákat pl. csillag, féregnyúlvány is képesek vagyunk fejleszteni. Vizes közegben a hidrofil korona részlet felel a szolubilizálásért, míg a hidrofób mag a hatóanyagot molekulárisan diszperz eloszlásban, stabilan magába zárja [8, 9].

Mint önrendeződő rendszerek, fontos paraméterük a kritikus micellaképződési koncentráció (CMC), illetve hőmérséklet (CMT). A CMC alatt a polimerek részlegesen kapcsolódhatnak a hatóanyaghoz (annak anyagi sajátságaitól függően), viszont nem alkotnak kolloidális, micelláris rendszert. A CMC-t elérve azonban már kialakul a klasszikus micelláris

szerkezet. Amennyiben szerves oldószer is található a formulációs közegben, úgy a CMC-értéknél még nem jellemző a nano-mérettartomány optimális alsó határa, mivel a micellát alkotó polimer jelentős részben magába zárja az oldószert és kvázi egyensúlyban, nagy mennyiségben, stabilan magában tartja, ebből adódóan ezen a ponton a legnagyobb a polimer micellák mérete. Ahhoz, hogy termodinamikailag stabil legyen a micelláris szerkezet, ettől a felesleges oldószermennyiségtől megszabadul a rendszer. A CMC-értéket elérve a polimerláncok önrendeződésre törekednek a lehető legkisebb méret elérése, valamint a gömbforma kialakítása érdekében a polimerláncok a micella magján belül kapcsolatokat hoznak létre, amelyhez szignifikáns vonzóerők tartoznak. A vonzóerők folyamatos növekedése miatt nem képes a nagy térfogatú szerves oldószert megtartani a micella, kipréselődik a micella magjából, hátrahagyva a



1. ábra A polimer micellák spontán önrendeződésének sematikus ábrája a kritikus micellaképződési koncentráció (CMC-) érték fölött



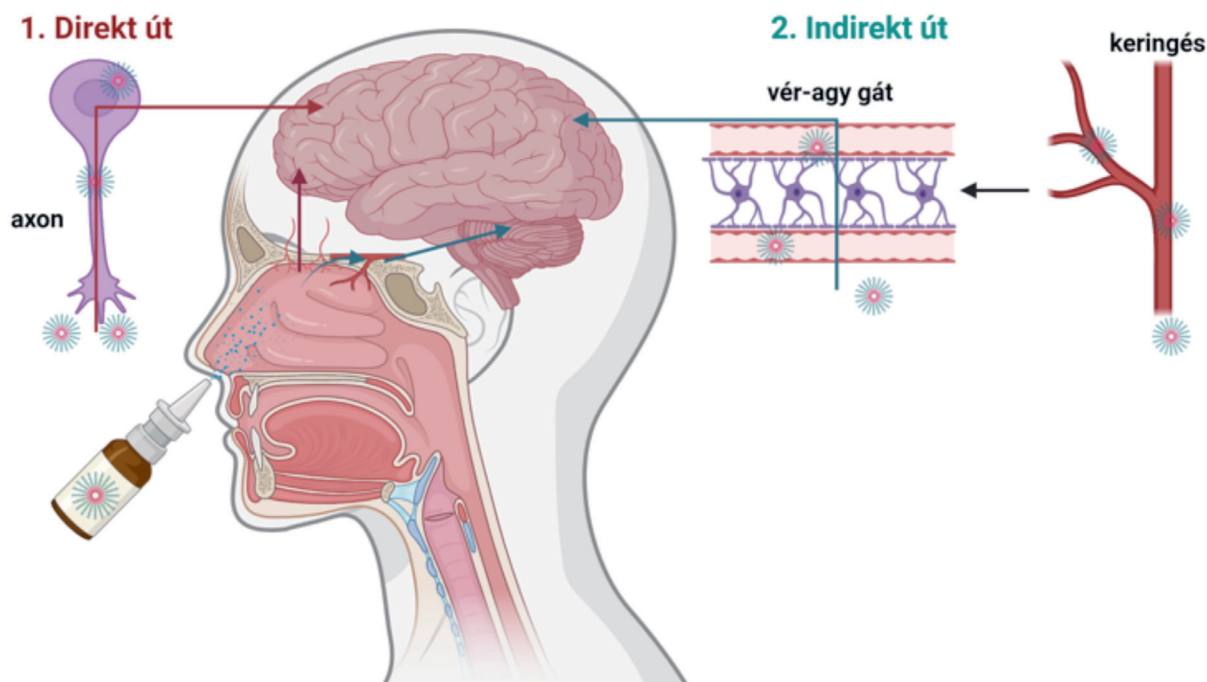
2. ábra A polimer micellák főbb előállítási módszereinek sematikus ábrája

hatóanyagot. Mivel a polimer micellákat általában magas lipofilitású hatóanyagok bezárására alkalmazzák, így a hatóanyag-polimer kapcsolat erősebb, mint a szerves oldószer-polimer esetében, emiatt a mag stabilan képes tartani a hatóanyagot. A polimer micellák kialakulásának további fontos feltétele a megfelelő oldószerrel (víz vagy adott pH-értékre beállított vizes puffer) történő hidratálás, az átlagosan 20–200 nm átmérőjű nanorészecskék elérése érdekében (1. ábra) [10].

A polimer micellák előállítási módjai

A polimer micellák előállítása eléggé változatos lehet, amelyet leginkább a hatóanyag és a felépítő polimerek oldékonysági viszonyai és hőstabilitása határoz meg. A polimerek és a hatóanyagok kiválasztása különös fontossággal bír, hiszen a polimerbe maximálisan betölthető hatóanyag mennyisége eltér különböző lipofilitású anyagok esetében. Amennyiben a hatóanyag relatívan jól oldódik vízben, úgy a direkt feloldás módszere is alkalmazható, azaz az elegy készítése után, megfelelő koncentrációban kialakul a micelláris szerkezet. Ehhez feltétel, hogy az átlagnál magasabb szolubilizációs kapacitással rendelkezzen a polimer.

Általánosabb eset, amikor szükség van segédoldószerekre (pl. etanol, terc-butil-alkohol, propilén-glikol). Ekkor filmréteg kialakítása is történhet rotációs vákuumbepárlás segítségével, ahol a kapott polimer-hatóanyag film vízzel történő hidratálása után alakulnak ki a micellák. A módszer fő előnye abban rejlik, hogy az elpárologtatott oldószer(elegy) összegyűjthető, így újra fel lehet használni, ami a zöld technológiák alapelve közé tartozik. Hátránya viszont, hogy nagymértékű léptéknövelhetőség nem valósítható meg ezzel a módszerrel. Alternatív megoldás, amikor a klasszikus szerves oldószerek helyett állandó kevertetés mellett egy olaj a vízben (O/V) emulziót képezünk, ahol a vizes fázisban alakulnak ki a hatóanyaggal töltött polimer micellák. Ezt követi az olaj és a be nem zárt hatóanyag elválasztása a rendszertől. A módszer előnye, hogy a hagyományos, emberi szervezetre toxikus jelleggel bíró szerves oldószerek kiválthatóak, azonban itt is nehézkes az ipari léptéknövelhetőség. Közvetlen fagyasztva szárítás esetén a hatóanyag és a polimer szerves és vizes oldószert egyaránt tartalmazó oldata kerül letöltésre. Ez egy közkeletelt módszer egyszerűsége és az adagolási egység egy lépésben történő kialakítása miatt. A szerves oldószerek nagy része azonban a klasszikus berendezések által



3. ábra A direkt („nose-to-brain”) és az indirekt („nose-to-blood”) útvonal a központi idegrendszerbe történő hatóanyag-eljutatás nasalis úton történő megvalósítása esetén

biztosított hőfokon nem fagy meg, így jelentősen leszűkül az oldószerek köre, amely így feldolgozható [11]. Az előállítási módszerek sematikus ábrája a 2. ábrán található.

A polimer micellák lehetőségek és kihívások

A polimer micellákat alkotó polimereket elsősorban ipari felhasználásra fejlesztették ki, kedvező termikus viselkedésük és könnyű feldolgozhatóságuk miatt olvadéktechnológiai alkalmazási céllal. Az olvadéktechnológia során olyan szilárd diszperziók kialakítása volt a cél ezen polimerek felhasználásával, amelyek vízben diszpergálva megnövekedett vízdékonysággal és kedvező permeációs hatékonysággal jellemezhetők. Azonban a kapott termékek a magas polimerkoncentráció miatt habzanak, mely felületaktív tulajdonságukra vezethető vissza, így a kutatás-fejlesztési trendek afelé mozdultak el, hogy minél kevesebb mennyiséget kelljen felhasználni belőlük. Később felfedezték, hogy kis mennyiségben alkalmazva, a hagyományos tenzidekhez képest alacsonyabb CMC mellett képesek a hatóanyagokat a micelláris magjukba bezárni. Azóta a kutatók rendkívül sokrétű polimereket alkottak, amelyek akár egyaránt vízdékonny és lipofil hatóanyagok szolubilizálására is képesek, avagy penetrációjukat fokozni. A nanomérettartomány és a hidrofil micelláris korona

jelenléte elősegíti a termodinamikai vízdékonyság növekedését, azaz folyékony, azon belül is oldat gyógyszerformák előállítása megvalósulhat. Így ezzel a LADMER biofarmáciai modell első lépését, azaz hatóanyag-felszabadulást (liberáció), megfelelően tudjuk programozni az ilyen micelláris rendszerek esetében, amely meggyorsítja a liberációt követő abszorpciót és disztribúciót [12, 13]. A beviteli kapukat tekintve alkalmazhatóságuk sokrétű, alternatív (intravaginalis, dermalis, nasalis, okuláris) és hagyományos hatóanyag-bevitelre (orális és parenteralis) egyaránt [14, 15].

A polimer micellák kedvező sajátságai azonban veszélyeket is rejtenek magukban, illetve a szervezet is idegen anyagként tekinthet a felépítő polimerekre, azok eltávolítását sürgetve. A polimer micella alkalmazásának alapfeltétele, hogy a szervezet vizeitében, a vérben tartsa meg a nano-mérettartományát, azaz a stabil szerkezetét. A vérben található albumin és egyéb fehérjék részben képesek magukhoz kötni a micellákat vagy a hatóanyagot magát, amely befolyásolja a farmakokinetikai viselkedését. A polimerláncok degradációját is okozhatja az albumin, a hatóanyag kiválhat a rendszerből és ezáltal nem tud célzottan a terápiás területre jutni nanohordozó formájában. A biológiai membránokra nézve nagy permeabilitással rendelkeznek ezek a hordozók, azonban magas dózisokban, nagy polimerkoncentrációban ez



veszélyes is lehet, hiszen megfelelő felületi módosítás nélkül olyan kompartmentekbe juthat el a hatóanyag, ahol nemkívánatos hatásokat fejtenek ki. Számos lehetőség rejlik ezek megoldásában.

A polimer micellák intranasalis útvonala

A polimer micellák egyik előnye, hogy segítségével a hatóanyag közvetlenül az idegi (axonális) pályákon keresztül a központi idegrendszerbe juttatható, ez azonban nem törvényszerű. A polimer molekulatömege, mérete, felületmódosítás megléte vagy hiánya egyaránt befolyásolja, hogy milyen útvonalon halad a hatóanyag-hordozó rendszer tovább a szervezetben. Az ornyálkahártyán keresztüli felszívódás többféle módon is megtörténhet, mely folyamat legfőbb helyszíne a szaglási (olfaktorius) és a légzési (respiratorikus) régió. Az orrüregbe érkező nanonizált hatóanyag egyrészt képes a sejtek között (paracelluláris útvonal), valamint a sejteken keresztül is (transzcelluláris útvonal) átjutni. Az így felszívódott hatóanyag általában a dús érhalózat miatt gyorsan a keringésbe kerül. Mivel a szaglórégió idegvégződésében gazdag, így az axonális útvonalon keresztül is az olfaktorius régióba jut a hatóanyag, mely a vér-agy gátat megkerülve nem metabolizált formában éri el az agyat (**3. ábra**) [16, 17].

Gyógyszer-technológiai fejlesztés során a polimer kiválasztása szorosan összefügg a biofarmáciai stabilitással, azaz a nanorészecske legyen képes megtartani a nano mérettartományát a keringésben fellépő higulás hatására, és szerkezete ne módosuljon. Ezek alapján megkülönböztetünk olyan polimereket, amelyek szignifikáns szolubilizáló és penetrációt fokozó hatással bírnak, de a keringésben gyorsan disszociálnak (pl. tokoferszolan), szemben olyanokkal, amelyek stabilizálni képesek a micelláris struktúrát. A bináris polimer micellák előnyei pont ebből fakadnak, melyben két kopolimer közösen alkot egy hatóanyaggal töltött micellát, ezáltal az egyedi hátrányokat képesek kiküszöbölni [18].

A két kopolimerrel történő bináris megvalósításon kívül azonban egyéb segédanyagok is szerepet játszhatnak a hatékony nasalis polimer micellák fejlesztésében. Ilyenek a mukoadhéziót, azaz az ornyálkahártyához történő tapadást elősegítő anyagok használata, pl. kitozán, hialuronsav, cellulózszármazékok. Ezek főleg az orrüregből történő kimosódás, eliminációs folyamatok (csilló aktivitás) ellen dolgoznak, hogy minél több idegi tudjon az orrban tartózkodni a

rendszer. A segédanyagok másik csoportját a felületmódosítás során alkalmazzuk, amikor a micellák vérkeringésben töltött idejét szeretnénk növelni zsírsavészterekkel, egyéb polimerekkel vagy ha ingerérzékeny (hőmérséklet, pH) struktúrát szeretnénk kialakítani. Az ingerérzékeny struktúrák képesek hőmérséklet, illetve pH hatására szerkezetet változtatni. Ilyen módon valósulhatnak meg például azon intelligens hordozók, amelyek a gyulladt, ezáltal magasabb hőmérséklettel jellemezhető területeken rendeződnek nano-mérettartományú polimer micellákká, ott kifejtve előnyös farmakokinetikai tulajdonságukat.

A polimer micellákkal elért eddigi eredmények

A kutatócsoportunk régóta foglalkozik nanoterápiás készítmények előállításával, és a „nose-to-brain” útvonalon keresztüli alkalmazás kutatásával. A polimer micellákkal történt kutatásink eddig a szteroid- és nemszteroid gyulladáscsökkentő vegyületek nasalis alkalmazhatóságát célozta a következő terápiás indikációval: (1) A nem szteroid gyulladáscsökkentők képesek az agyszöveti gyulladással, azaz a neuroinflammációval járó folyamatok enyhítésére akár krónikusan alkalmazva is; (2) akut, agyi traumák kezelésére is potenciális jelölt lehet a szteroid gyulladáscsökkentőkkel töltött polimer micella, mint például az agyödéma gyors elvezetésére használt dexametazon [19–21]. A polimer micellák esetében számos ígéretes formuláció került közlésre, azonban a nasalis úton történő hatóanyag központi idegrendszerére nem sok példát lehet találni a nemzetközi irodalomban. A következőkben pár példát mutatunk be az ilyen típusú készítményekre.

Nour és munkatársai klonazepám tartalmú polimer micellákat állítottak elő [22]. A klonazepám status epilepticusban történő felhasználása közismert, azonban a terápiás hatás sikeressége korlátozott a csekély vízdékonyság miatt, függetlenül attól, hogy az emésztőrendszerben jó permeációs képességgel rendelkezik. Farmakodinámiai és ^{99m}Tc radioizotópos térképezés vizsgálatok alapján bebizonyosodott, hogy az optimalizált formuláció sokkal nagyobb agyi hatóanyag biohasznosulási hatékonyságot és 99,3%-os „nose-to-brain” direkt transzport hányadost képes elérni, azaz a hatóanyag 99,3%-a preferálja ezt az útvonalat szemben az indirekt, véren keresztüli útvonallal. A munka eredményeképpen elmondható, hogy sikerült egy olyan epilepsziában használható polimer micelláris formulációt előállítani, amely megnyújtja

az epilepsziás állapotokban az újabb görcsállapot kialakulásának idejét és csökkenti esélyét.

Számos új hatóanyag gyógyszerkészítménnyé történő formulálása során a kezdeti kutatási fázisban is megfontolandó a közvetlen nanorendszerbe, így polimer micellába történő fejlesztése. Erre kiváló példa *Pokharkar* és munkatársai lurazidon hatóanyaggal töltött, bináris polimer micelláris alapú hidrogél formulációja [17]. Ez a neuroterapeutikum a bipoláris depresszió és a skizofrénia kezelésére alkalmas lehet, azonban a központi idegrendszerbe jutását akadályozza az alacsony vízdékonysága. A bináris polimer micella formuláció azonban *in vivo* állatkísérletben bebizonyosodva is növelte a hatóanyag agyi koncentrációját.

A rotigotin Parkinson-kór kezelésére szolgáló hatóanyag, amelyet *Wang* és munkatársai formuláltak egy olyan polimer micellába, amely termoszenzitív gélbe van ágyazva [23]. Ez a hőmérsékletre adott gél szerkezetben bekövetkező változás kiegészülve a nanonizálással megnövelte a rotigotin vízdékonyságát, agyi tartózkodási idejét és koncentrációját. Agyi szelektivitását tekintve a nagyagyban 170,5%-kal, a kisagyban 166,5%-kal és a *striatum*-ban 184,4%-kal nagyobb koncentrációban jelent meg, mint az intravenás beadást követően.

ÖSSZEFOGLALÁS

A fent említett példák és az ismertett mechanizmusok alapján elmondható, hogy a polimer micellák nasalis bevitelre szánt fejlesztése egy ígéretes megoldást nyújthat a központi idegrendszeri betegségek hatékony terápiájában. Az évről évre növekvő számú embert érintő pszichiátriai és neurodegeneratív betegségek pedig fenntartják az igényt arra, hogy gyors, programozott és célzott gyógyszerkészítmények kerüljenek alkalmazásra. Az innovatív polimer micelláris nanohordozók pedig többlettel rendelkeznek a korábbi készítményekhez képest, „value-added” formulációkként képesek lehetnek a terápiás hézagok kitöltésére és az életminőség fokozására.

KÖSZÖNETNYILVÁNÍTÁS

Szeretném köszönetemet kifejezni konzulenseimnek,

prof. dr. Csóka Ildikó intézetvezető egyetemi tanárnak és dr. Katona Gábor egyetemi adjunktusnak. A kéziratban szereplő ábrák megszerkesztése a <https://biorender.com> segítségével történt.

Irodalom

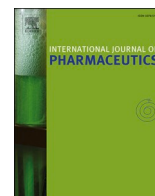
- Arlt S, Lindner, R et al. Adherence to medication in patients with dementia: Predictors and strategies for improvement. *Drugs Aging*. 2008;25:1033-1047. <https://doi.org/10.2165/0002512-200825120-00005> – 2. Agrawal M, Saraf S et al. Nose-to-brain drug delivery: An update on clinical challenges and progress towards approval of anti-Alzheimer drugs. *J Control Release*. 2018;281:139-177. <https://doi.org/10.1016/j.jconrel.2018.05.011> – 3. Heneka M.T, Carson M.J. et al. Neuroinflammation in Alzheimer's Disease. *Lancet Neurol*. 2015;14:388-405. [https://doi.org/10.1016/S1474-4422\(15\)70016-5](https://doi.org/10.1016/S1474-4422(15)70016-5) – 4. Merkus F.W, van den Berg M.P. Can nasal drug delivery bypass the blood-brain barrier? *Drugs R D*. 2007;8:133-144. <https://doi.org/10.2165/00126839-200708030-00001> – 5. Köping-Höggar M, Sánchez A et al. Nanoparticles as carriers for nasal vaccine delivery. *Expert Rev Vaccines*. 2005;4:185-196. <https://doi.org/10.1586/14760584.4.2.185> – 6. Shim S, Yoo H.S. The application of mucoadhesive chitosan nanoparticles in nasal drug delivery. *Marine Drugs*. 2020;18:605. <https://doi.org/10.3390/md18120605> – 7. Alagusundaram M, Chengaiah B et al. Nasal drug delivery system - an overview. *Int J Res Pharm Sci*. 2010;1:454-465. – 8. Agrawal R.D, Tatode A. A et al. Polymeric micelle as a nanocarrier for delivery of therapeutic agents: A comprehensive review. *Journal of Drug Delivery and Therapeutics*. 2020;10:191-195. <https://doi.org/10.22270/jddt.v10i1-s.3850> – 9. Yokoyama M. Polymeric micelles as a new drug carrier system and their required considerations for clinical trials. *Expert Opin Drug Deliv*. 2010;7(145-158). <https://doi.org/10.1517/17425240903436479> – 10. Ahmad Z, Shah A et al. Polymeric micelles as drug delivery vehicles. *RSC Adv*. 2014;4:17028-17038. <https://doi.org/10.1039/C3RA47370H> – 11. Croy S.R, Kwon G.S. Polymeric micelles for drug delivery. *Current Pharmaceutical Design*. 2006;12:4669-4684. <https://doi.org/10.2174/138161206779026245> – 12. Jain r, Nabar S et al. Formulation and evaluation of novel micellar nanocarrier for nasal delivery of sumatriptan. *Nanomedicine*. 2010;5:575-587. <https://doi.org/10.2217/nnm.10.28> – 13. Chaudhari S.P, Shinde P.U. Formulation and Characterization of Tranylcyproline loaded Polymeric Micellar In-Situ Nasal Gel for treatment of Depression. *Technology*. 2020;5. – 14. Quartier J, Lapteva M et al. Polymeric micelle formulations for the cutaneous delivery of sirolimus: A new approach for the treatment of facial angiofibromas in tuberous sclerosis complex. *Int J Pharm*. 2020;604:120736. <https://doi.org/10.1016/j.ijpharm.2021.120736> – 15. Durgun M. E, Güngör S et al. Micelles: Promising ocular drug carriers for anterior and posterior segment diseases. *Journal of Ocular Pharmacology and Therapeutics*. 2020;36:323-341. <https://doi.org/10.1089/jop.2019.0109> – 16. Ansari M.A, Chung I.M et al. Current nanoparticle approaches in nose to brain drug delivery and anticancer therapy - a review. *Current pharmaceutical design*. 2020;26:1128-1137. <https://doi.org/10.2174/1381612826666200116153912> – 17. Pokharkar V, Suryawanshi S et al. Exploring micellar-based polymeric systems for effective nose-to-brain drug delivery as potential neurotherapeutics. *Drug Dev Trans Res*. 2020;1019-1031. <https://doi.org/10.1007/s13346-019-00702-6> – 18. Sun C, Li W et al. Development of TPGS/F127/F68 mixed polymeric micelles: enhanced oral bioavailability and hepatoprotection of syringic acid against carbon tetrachloride-induced hepatotoxicity. 2020;137:111126. <https://doi.org/10.1016/j.fct.2020.111126> – 19. Sipos B, Szabó-Révész P et al. Quality by design based formulation study of meloxicam-loaded polymeric micelles for intranasal administration. *Pharmaceutics*. 2020;12:697. <https://doi.org/10.3390/pharmaceutics12080697> – 20. Sipos B, Katona G et al. A Systematic, Knowledge Space-Based Proposal on Quality by Design-Driven Polymeric Micelle Development. *Pharmaceutics*. 2021;13:702. <https://doi.org/10.3390/pharmaceutics13050702> – 21. Sipos B, Csóka I et al. Development of dexamethasone-loaded mixed polymeric micelles for nasal delivery. *Eur J Pharm Sci*. 2021;166:105960. <https://doi.org/10.1016/j.ejps.2021.105960> – 22. Nour S.A, Abdelmalak N.S et al. Intranasal brain-targeted clonazepam polymeric micelles for immediate control of status epilepticus: in vitro optimization, ex vivo determination of cytotoxicity, in vivo biodistribution and pharmacodynamics studies. *Drug delivery*. 2016;23:3681-3695. <https://doi.org/10.1080/10717544.2016.1223216> – 23. Wang F, Yang Z et al. Facile nose-to-brain delivery of rotigotine-loaded polymer micelles thermosensitive hydrogels: In vitro characterization and in vivo behavior study. *Int J Pharm*. 2020;577:119046. <https://doi.org/10.1016/j.ijpharm.2020.119046> –

Szegedi Tudományegyetem, Gyógyszerésztudományi Kar, Gyógyszertechnológiai és Gyógyszerfelügyeleti Intézet,

6720 Szeged, Eötvös utca 6.

*levelező szerző: sipos.bence@szte.hu

IV.



Soluplus® promotes efficient transport of meloxicam to the central nervous system via nasal administration

Bence Sipos^a, Zsolt Bella^b, Ilona Gróf^c, Szilvia Veszélka^c, Mária A. Deli^c, Kálmán F. Szűcs^d, Anita Sztojkov-Ivanov^e, Eszter Ducza^e, Róbert Gáspár^d, Gábor Kecskeméti^f, Tamás Janáky^f, Balázs Volk^g, Mária Budai-Szűcs^a, Rita Ambrus^a, Piroska Szabó-Révész^a, Ildikó Csóka^a, Gábor Katona^{a,*}

^a Institute of Pharmaceutical Technology and Regulatory Affairs, Faculty of Pharmacy, University of Szeged, Eötvös Str. 6, H-6720 Szeged, Hungary

^b Department of Oto-Rhino-Laryngology and Head-Neck Surgery, University of Szeged, Tisza Lajos Blvd. 111, H-6725 Szeged, Hungary

^c Institute of Biophysics, Biological Research Centre, Szeged, Temesvári Blvd. 62, H-6726 Szeged, Hungary

^d Department of Pharmacology and Pharmacotherapy, Albert Szent-Györgyi Medical School, Faculty of Medicine, University of Szeged, Hungary

^e Department of Pharmacodynamics and Biopharmacy, Faculty of Pharmacy, University of Szeged, Eötvös Str. 6, H-6720 Szeged, Hungary

^f Department of Medical Chemistry, Interdisciplinary Excellence Centre, University of Szeged, Dóm square 8, H-6720 Szeged, Hungary

^g Directorate of Drug Substance Development, Egis Pharmaceuticals Plc., Keresztúri Str. 30 – 38, H-1106 Budapest, Hungary

ARTICLE INFO

Keywords:

Nasal administration
Polymeric micelle
Meloxicam
Permeability enhancement
Brain

ABSTRACT

In our present series of experiments, we investigated the nasal applicability of the previously developed Soluplus® - meloxicam polymeric micelle formulation. Utilizing the nasal drug investigations, moderately high mucoadhesion was experienced in nasal conditions which alongside the appropriate physicochemical properties in liquid state, contributed to rapid drug absorption through human RPMI 2650 cell line. *Ex vivo* studies also confirmed that higher nasal mucosal permeation could be expected with the polymeric micelle nanoformulation compared to a regular MEL suspension. Also, the nanoformulation met the requirements to provide rapid drug permeation in less 1 h of our measurement. The non-toxic, non-cell barrier damaging formulation also proved to provide a successful passive transport across excised human nasal mucosa. Based on our *in vivo* investigations, it can be concluded that the polymeric micelle formulation provides higher meloxicam transport to the central nervous system followed by a slow and long-lasting elimination process compared to prior results where physical particle size reduction methods were applied. With these results, a promising solution and nanocarrier is proposed for the successful transport of non-steroidal anti-inflammatory drugs with acidic character to the brain.

1. Introduction

Administration of drugs to the central nervous system (CNS) is a challenging area in the medical field due to its many biological and pharmaceutical technological aspects. The need for efficient treatment of various CNS-related diseases is of paramount importance in today's research and development processes. The increasing prevalence of neurodegenerative diseases (such as Alzheimer's Disease, Parkinson's Disease etc.) holds the demand for novel and innovative products on the market which may help in their efficient therapy (Goldsmith et al., 2014; Saraiva et al., 2016). The problem also lies in the fact that potential drug candidates of these diseases cannot access the CNS in a sufficient concentration for clinical investigations. This challenge requires novel drug

delivery systems, which are suitable for efficient transport to the CNS, where a drug concentration sufficient for further investigations would be achieved (Wohlfart et al., 2012; Wong et al., 2019).

These neurodegenerative diseases are often associated with the inflammation of brain tissue, the so-called neuroinflammation (Sharma 2011; Shabab et al., 2017). The mechanism behind this condition is that the inflammatory cytokine balance is disrupted towards the emergence of the pro-inflammatory cytokines such as cyclooxygenase (COX). The treatment of COX enzyme-mediated neuroinflammation plays a pivotal role and holds a high demand in the field of unmet clinical needs (Choi et al., 2013; Heneka et al., 2015). Current potential drug candidates are hindered by their inability to bypass the blood-brain barrier (BBB) (Szabó-Révész, 2018). Epidemiological studies proved that long-term

* Corresponding author.

E-mail address: katona.gabor@szte.hu (G. Katona).

<https://doi.org/10.1016/j.ijpharm.2023.122594>

Received 20 October 2022; Received in revised form 15 December 2022; Accepted 5 January 2023

Available online 7 January 2023

0378-5173/© 2023 Elsevier B.V. All rights reserved.

use of non-steroidal anti-inflammatory agents (NSAIDs) decrease the risk of Alzheimer's Disease and prolongs its prognosis (McGeer and McGeer, 2007). *In vitro* and *in vivo* studies also proved that COX inhibition helps with the symptoms of neuroinflammation. Therefore, the possibility of introducing NSAIDs as COX enzyme inhibitors to the CNS represents a promising solution. The main protection mechanism is based on mitochondria depolarization and the inhibition of calcium uptake. This is possible due to the ionizable carboxylic groups of the NSAIDs, which have a similar effect to mild mitochondrial uncouplers (Calvo-Rodríguez et al., 2015; Sanz-Blasco et al., 2018).

Polymeric micelles are one of the novel nanocarriers. These nanomedicines can offer increased solubility, enhanced drug release and permeability through biological barriers. Polymeric micelles are made up by the so-called amphiphilic graft co-polymers, which just like classic micellar systems prepared by surfactants, tend to self-associate above the critical micellar concentration (CMC) and temperature, allowing a highly efficient drug encapsulation (Sipos et al., 2020; Ghezzi et al., 2021; Sipos et al., 2022). Generally, they can be described as non-toxic agents and they do not harm the cell membranes, less likely than in case of classic surfactant-like molecules (Zakharova et al., 2019; Katona et al., 2022). Their main advantage might lie in the fact that they can transport poorly water soluble active pharmaceutical ingredients (APIs) with low permeation tendency across biological barriers difficult to get through, such as the BBB (Sun et al., 2020). Based on the molecular weight of the co-polymer, the surface charge, the presence of surface modifying ligands and the desired route, various transport mechanisms can be experienced. Polymeric micelles with positively charged surface usually accumulate in the mucus layer followed by the passive diffusion of the drug. This mechanism is usually exploited when a local effect is desired with rapid onset of action. Polymeric micelles with negative charge or without charge on the micellar surface can be categorized as mucopenetrating micelles, where the biological mucus layer allows the micellar carriers to be absorbed via transcytosis or paracellular transport (Pepić et al., 2013). With proper characterization of the micellar system via the determination of zeta potential, as the value of the surface charge in liquid state, the therapeutic aspects can be taken into consideration prior to administration or even prior to drug selection. Moreover, micellar systems presenting polyethylene glycol (PEG) and other hydrophilic moieties at their surface are less prone to the scavenging process by the macrophages (Thotakura et al., 2021). This holds the information that PEG-based copolymers are more stable in circulation, allowing a higher residence time and protection against the biological environmental conditions, unlike co-polymers which are based for instance on polylactic acid (PLA) showing lower stability (Watanabe et al., 2006; Owen et al., 2012).

Besides choosing the proper drug and nanocarrier, the adequate administration route is just as important. By administering nanomedicines via the nasal route, a higher bioavailability can be achieved (Sabir et al., 2021). This is due to the fact that the nasal mucosa is highly vascularized with a large surface allowing a prominent drug transport across this barrier (Warnken et al., 2016; Sipos et al., 2021). After administration, the drug and the drug-loaded carrier system can take up on two pathways. The first is the nose-to-blood transport route, where the penetration occurs across the nasal mucosa followed by a rapid uptake to the blood vessels. Speaking of brain targeting, the absorbed substance can circulate through the body prior to drug and/or drug-loaded carrier absorption through the BBB (Khan et al., 2017). Polymeric micelles are among the best carrier systems for this role, as they show high circulation and dilution stability under these conditions (Owen et al., 2012). The other main advantage is the nose-to-brain pathway, which is made possible by the high innervation of olfactory nerves in the nasal mucosa (Pardeshi and Belgamwar, 2013). This allows a rapid solution to bypass the BBB where the intact carrier and/or drug can travel across the neural pathways directly to the brain (Khan et al., 2017; Li et al., 2017). The concrete mechanism has been not yet fully explored in case of polymeric micelles; however, the beneficial effects

can be experienced in case of enhanced brain targeting. Furthermore, studies have proven that Alzheimer's Disease most likely begins in the nerve network of the olfactory region where initial amyloid plaque formation can appear (Agrawal et al., 2018).

Previously, we developed a meloxicam (MEL)-loaded Soluplus® (SP) polymeric micelle system (SP-MEL) for nasal administration which has been structurally and *in vitro* tested for nasal administration (Sipos et al., 2020). SP was chosen as a biodegradable co-polymer which has a low toxicity potential ($LD_{50, oral} > 5,000$ mg/kg) besides the high solubilization capacity. The encapsulation was performed by utilizing SP which has a low CMC value in water besides its non-toxic behavior. The nanoparticles had an average particle size of 100.47 nm in monodisperse distribution with a polydispersity index (PDI) of 0.149 and high colloidal stability with a zeta potential of -26.7 mV preventing colloidal aggregation. Small and uniform particle size contributes to a uniform and rapid drug absorption profile across mucosal barriers, that is why it is important to keep the PDI as low as possible, most commonly below 0.300. The negative surface charge as explained above also contributes to carrier-intact paracellular or transcytosis-based take-up mechanisms. The physicochemical characteristics of the dissolved product meets the requirements of the nasal administration. Its hypotonic nature (240 mOsmol/l) can increase drug absorption alongside with the permeation enhancing effect of SP (Hong et al., 2019). The viscosity of the formulation (32.5 mPas) is also suitable to form an intranasal liquid formulation as it can be administered as a nasal drop or a spray. This low viscosity also contributes to a faster drug release as highly viscous formulation result in slower diffusion from the carrier matrix. The SP-MEL formulation provided a higher drug release in simulated nasal conditions as well as high drug absorption through artificial membranes.

Our goal with this present series of experiments is to justify that SP can efficiently promote the transport of MEL, a model drug with low water solubility and brain permeability to the CNS. Our hypothesis is that via nasal administration, higher concentrations of MEL can be achieved in the CNS. By the formulation of the nanocarrier, the administration of small molecular weight NSAIDs can be achieved. This would lead to gain an adequate concentration of the API in the central nervous system and it would open up the possibility to perform a better executed clinical trials later on to further describe the beneficial effects of NSAIDs in the treatment of neuroinflammation. To confirm our previous *in vitro* results, we performed nasal applicability studies starting from mucoadhesion and cell line studies, *ex vivo* penetration studies and we investigated the *in vivo* pharmacokinetics of this formulation.

2. Materials and methods

2.1. Materials

MEL (4-hydroxy-2-methyl-N-(5-methyl-2-thiazolyl)-2H-1,2-benzothiazine-3-carboxamid-1,1-dioxide) was applied as a model drug in our studies and acquired from EGIS Pharmaceuticals Plc. (Budapest, Hungary). Soluplus® (SP, polyvinyl caprolactam – polyvinyl acetate – polyethylene glycol graft co-polymer (PCL-PVAc-PEG)) as a micelle-forming agent was kindly gifted from BASF GmbH (Hannover, Germany). Simulated Nasal Electrolyte Solution (SNES) as a simulated nasal fluid was applied during some measurements which is composed of 8.77 g sodium chloride, 2.98 g potassium chloride, 0.59 g anhydrous calcium chloride in 1000 ml of deionized water at pH 5.6 (Castile et al., 2013). Chemicals for SNES as well as disodium phosphate, monopotassium phosphate for pH 7.4 phosphate-buffered saline (PBS) solution and all the other excipients for our measurements were acquired from Sigma-Aldrich Co. Ltd. (Budapest, Hungary) unless otherwise indicated.

2.2. Formulation of MEL-loaded polymeric micelles

For each investigation, formulations were prepared freshly, utilizing the thin-film hydration formulation method, which proved to be

successful previously after factorial design-based optimization (Sipos et al., 2020). Briefly, 15 mg of MEL was weighed into a beaker, it was dissolved with a few drops of 0.1 M sodium hydroxide solution (NaOH) and 10 ml of ethanol. 100 mg SP was added and the resulting solution was concentrated with a Büchi R-210 (Büchi, Flawil, Switzerland) rotary vacuum evaporator (50 °C with gradually decreasing pressure from 1000 to 100 bar with a rate of 50 bar/min, followed by 10 to 15 min of drying at 100 bar). After hydration of the polymeric film with purified water, the pH was adjusted between 5.6 and 7.4 and 5 % w/v D-trehalose dihydrate was dissolved with the formulation. Thereafter, 1 ml aliquots were freeze-dried at – 40 °C for 12 h under a 0.013 mbar pressure with additional 3 h secondary drying at 25 °C using a ScanVac CoolSafe 100–9 (LaboGene, ApS, Lyngø, Denmark) laboratory apparatus. After the freeze-drying process, samples were redispersed in a nominal MEL concentration of 2.5 mg/ml.

2.3. Dynamic light scattering measurements (DLS)

Prior to each investigation, the freshly prepared samples were evaluated via dynamic light scattering using a Malvern Zetasizer Nano ZS (Malvern Instruments, Worcestershire, UK) apparatus. The water dispersed freeze-dried cakes were measured at 25 °C in folded capillary cells with a set refractive index of 1.72. Each measurement was carried out in triplicate. The acceptance criteria were the following: average hydrodynamic diameter between 80 and 150 nm, with a PDI < 0.300 and a zeta potential below – 20 mV. If the formulation met these requirements, it was selected for further investigations demonstrated in this article.

2.4. Quantification of MEL concentration via HPLC

To determine the concentration of MEL during the experiments, high performance liquid chromatography (HPLC) was performed using an Agilent 1260 (Agilent Technologies, Santa Clara, CA, USA) device. The stationary phase was a Kinetex® C18 column (5 µm, 150 mm × 4.6 mm (Phenomenex, Torrance, CA, USA)). The injection volume was 10 µl. The temperature was set at 30 °C. As mobile phases, a 0.065 M KH₂PO₄ solution adjusted to pH 2.8 with phosphoric acid (A) and methanol (B) were used. A two-step gradient elution was used for the separation. The starting proportion of 50 % A eluent was reduced to 25 % in 14 min, and then raised again to 50 % in 20 min. The eluent flow rate was 1 ml/min and the detection of the chromatograms was carried out at 355 ± 4 nm using UV–vis diode array detector. Data were evaluated using a ChemStation B.04.03 software (Agilent Technologies, Santa Clara, CA, USA). The retention time of MEL was detected at 14.34 min. The determined limit of detection (LOD) and quantification (LOQ) were 16 ppm and 49 ppm, respectively (Sipos et al., 2020).

2.5. In vitro mucoadhesion study

To investigate the mucoadhesive properties of the SP-MEL

formulation via tensile test, a TA-XT Plus (Texture Analyser (Metron Ltd., Budapest) instrument equipped with a 5 kg load cell and a 1 cm-diameter cylinder probe was used (Horvát et al., 2015; Budai-Szűcs et al., 2018). The SP-MEL formulation and blank SP solution were placed in contact with a wetted filter paper. For wetting, 50 µl of an 8 % w/w mucin dispersion as simulated mucosal membrane was used, where the mucin dispersion was prepared with a pH 5.6 SNES. 5 parallel measurements were performed. 20 mg of the samples was attached to the probe and placed in contact with the mucin wetted filter paper. A 2500 mN preload was used for a duration of 3 min and the cylinder probe was moved upwards separating the sample from the substrate with a prefixed speed of 2.5 mm/min. The adhesive force as the maximum detachment force and the work of adhesion were measured. The work of adhesion was calculated as the area (AUC) under the force versus distance curve. The formulations were thermostated at 37 °C for 30 min before the measurement and the experiment was carried out at this temperature. As references, SP and the SP-MEL formulation were measured without the presence of mucin as negative controls, and as positive controls, 0.5 % w/v hyaluronic acid solution was applied due to its well-known mucoadhesive properties.

2.6. Cell cultures

Human nasal epithelial cells (RPMI 2650; ATCC cat. no. CCL 30) were grown in Dulbecco's Modified Eagle's Medium (DMEM, Gibco, Life Technologies, USA) supplemented with 10 % fetal bovine serum (FBS, Pan-Biotech GmbH, Germany) in a humidified 37 °C incubator in presence of 5 % carbon dioxide and 50 µg/ml gentamicin in order to prevent infection of the cells. The surfaces of the culture dishes were coated with 0.05 % rat tail collagen dissolved in sterile distilled water before cell seeding and the medium was changed every 2 days. When RPMI 2650 cells reached approximately 80–90 % confluency in the dish, they were trypsinized with 0.05 % trypsin and 0.02 % EDTA solution. One day before the experiment, retinoic acid (10 µM) and hydrocortisone (500 nM) were added to the cells to form a tighter barrier (Kürti et al., 2013). For the permeability measurements, epithelial cells were co-cultured with human vascular endothelial cells to create a more physiological barrier representing both the nasal epithelium and the submucosal vascular endothelium (Pedroso et al., 2011; Cecchelli et al., 2014). The human vascular endothelial cells were differentiated from CD34⁺ stem cells isolated from human umbilical cord blood as described earlier (Pedroso et al., 2011). Frozen batches of human vascular endothelial cells were received from the Laboratoire de la Barrière Hémato-Encéphalique, University of Artois, Lens, France. The endothelial cells were grown in endothelial culture medium (ECM-NG, ScienCell, USA) supplemented with 5 % FBS, 1 % endothelial growth supplement (ECGS, ScienCell, USA) and 0.5 % gentamicin on 0.2 % gelatine-coated culture dishes (10 cm diameter). For the permeability experiment, cells were used at passage 8.

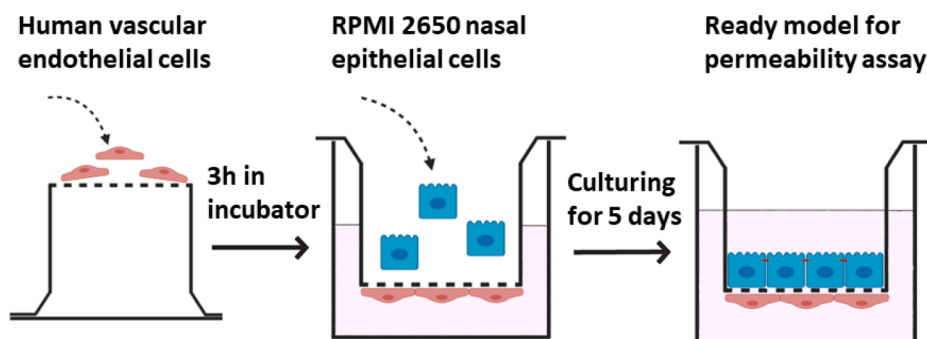


Fig. 1. The assembly of the human nasal epithelial cell and vascular endothelial cell co-culture model.

2.7. Cell viability assay

To follow cell damage and/or protection in living barrier forming cells and to quantify the viability of adherent cells, real-time cell electronic sensing technique was used. To register the impedance of cell layers, a RTCA-SP instrument (ACEA Biosciences, USA) was used. The registration took place every 10 min and the cell index was defined at each time point. The cell index was defined as $(R_n - R_b)/15$, where R_n is the cell-electrode impedance of the wall when it contains cells and R_b is the background impedance. E-plates with 96-well and built-in gold electrodes were coated in 0.2 % gelatine and placed for 20 min in the incubator. After the incubation, the gelatine was removed and 50 μ l of the culture medium was added to each well. The dispensed RPMI 2650 cell suspension had a density of 2×10^4 cells/well. When cells reached a steady growth phase, they were treated with SP-MEL and the building components. For the cell viability measurements $10 \times$, $30 \times$ and $100 \times$ dilutions from SP-MEL formulation as well as 2.5 mg/ml MEL suspension, 83.3 mg/ml D-trehalose dihydrate, 16.7 mg/ml SP solutions, corresponding to the concentration of components in SP-MEL formulation were prepared in cell culture medium.

2.8. Permeability study on the cell culture model

For the permeability experiments RPMI 2650 cells were cultured on inserts (Transwell, polycarbonate membrane, 3 μ m pore size, 1.12 cm², Corning Costar Co., MA, USA) placed in 12-well plates in the presence of endothelial cells for 5 days (Fig. 1). To prepare the co-culture model, endothelial cells were passaged (1×10^5 cells/cm²) to the bottom side of tissue culture inserts coated with low growth factor containing Matrigel (BD Biosciences, NJ, USA) then the cells were kept in an incubator for 3 h. After cell adhesion, cell culture inserts were placed in 12-well culture dishes containing 1.5 ml of endothelial culture medium, and RPMI 2650 nasal epithelial cells were pipetted (2×10^5 cells/cm²) onto the upper surface of the membrane, which were coated with rat tail collagen previously. The establishment of the co-culture model is illustrated in Fig. 1.

Transepithelial electrical resistance (TEER) was measured to check the barrier integrity by an EVOM voltohmmeter (World Precision Instruments, USA) combined with STX-2 electrodes, and was expressed relative to the surface area of the monolayers as $\Omega \times \text{cm}^2$. TEER of cell-free inserts was subtracted from the measured data. After the cell layer reached steady TEER values, the cells were treated. For the permeability experiments the inserts were transferred to 12-well plates containing 1.5 ml Ringer-HEPES buffer in the acceptor compartments. In the donor compartments 0.5 ml buffer was pipetted containing MEL or the SP-MEL polymeric micelle formulation. In static *in vitro* models the unstirred water layer above the barrier forming cells slows molecular diffusion and affects the P_{app} of compounds (Youdim et al. 2003). To reduce the formation of this aqueous layer and increase the reproducibility of results a moderate shaking procedure is suggested for permeability assays (Youdim et al. 2003). In our experiments the plates were kept on a horizontal shaker (120 rpm; PSU-2 T, Biosan, Riga, Latvia) during the assay which lasted for 60 min. Samples from both compartments were collected and the MEL concentration was measured by HPLC. To determine the tightness of the nasal epithelial co-culture model two passive permeability marker molecules were tested after the permeability experiment. In the donor compartments 0.5 ml buffer containing fluorescein isothiocyanate (FITC)-labeled dextran (FD10, 10 μ g/ml; Mw: 10 kDa) and Evans blue labeled albumin (167.5 μ g/ml Evans blue dye and 10 mg/ml bovine serum albumin; MW: 67.5 kDa) was added. The inserts were kept in 12-well plates on a horizontal shaker (120 rpm) for 30 min. The concentrations of the marker molecules in the samples from the compartments were determined by a fluorescence multiwell plate reader (Fluostar Optima, BMG Labtechnologies, Germany; FITC: excitation wavelength: 485 nm, emission wavelength: 520 nm; Evans-blue labeled albumin: excitation wavelength: 584 nm, emission

wavelength: 680 nm). The apparent permeability coefficients (P_{app}) were calculated as described previously (Bocsik et al., 2019). Briefly, cleared volume was calculated from the concentration difference of the tracer in the acceptor compartment ($\Delta[C]_A$) after 30 min and in donor compartments at 0 h ($[C]_D$), the volume of the acceptor compartment (V_A ; 1.5 ml) and the surface area available for permeability (A ; 1.1 cm²) using this equation:

$$P_{app} \left(\frac{\text{cm}}{\text{s}} \right) = \frac{\Delta[C]_A \times V_A}{A \times [C]_D \times \Delta t} \quad (1)$$

For the permeability measurement, 2.5 mg/ml MEL and $10 \times$ dilution of SP-MEL were prepared in Ringer-Hepes buffer and added to the donor compartments.

2.9. Immunohistochemistry

To evaluate morphological changes in RPMI 2650 cells caused by the MEL-loaded polymeric micelle formulation, immunostaining for junctional proteins zonula occludens protein-1 (ZO-1) and β -catenin was made. After the permeability experiments, cells on culture inserts were washed with phosphate buffer (PBS) and fixed with ice cold methanol-acetone (1:1) solution for 2 min then washed with PBS. The nonspecific binding sites were blocked with 3 % bovine serum albumin in PBS. Primary antibodies rabbit anti-ZO-1 (AB_138452, 1:400; Life Technologies, USA) and rabbit anti- β -catenin (AB_476831, 1:400) were applied as overnight treatment at 4 $^{\circ}$ C. Incubation with secondary antibodies anti-rabbit IgG Cy3 conjugated (AB_258792, 1:400) lasted for 1 h and Hoechst dye 33,342 was used to stain cell nuclei. After mounting the samples (Fluoromount-G; Southern Biotech, USA) staining was visualized by Leica TCS SP5 confocal laser scanning microscope (Leica Microsystems GmbH, Germany).

2.10. Ex vivo semiquantitative permeability study across nasal mucosa

Ex vivo permeability tests were performed on human nasal mucosa (mucoperiosteum). The pieces of the nasal mucosa for primary study were collected during daily clinical routine nasal and sinus surgeries (septoplasty) under general or local anesthesia. The patients were all female between 40 and 50 years. The surgical field was infiltrated with 1 % w/v Lidocain-Tonogen local injection and the mucosa was lifted from its base with a rasptorium or Cottle elevator. Transport from the operating room to the laboratory is performed in physiological saline solution. All experiments were performed freshly after the removal of the tissue. The experiments have been carried out under approval of University of Szeged's institutional ethics committee (ETT-TUKEB: IV/3880-1/2021/EKU). The nasal mucosa was excised with surgical scalpel into uniform square segments with a diameter of 6 mm to provide appropriate are of the semiquantitative study and it would fit into the membrane inserts for the later described quantitative study.

5 μ l of MEL suspension (2.5 mg/ml) and the SP-MEL formulation have been instilled on the epithelial surface of the nasal mucosa. After an incubation time of 1 h at 37 $^{\circ}$ C, the formulations were washed twice with physiological saline solution and the nasal mucosa was divided into 20 μ m thick cross-sections into the incision point (Leica CM1950 cryostat (Leica Biosystems GmbH, Wetzlar, Germany), then inverted to the cross-sectional side and placed on aluminum foil-coated glass slides. *Ex vivo* Raman chemical mapping was performed to describe the penetration pattern of the polymeric micelle formulation across the nasal mucosa using a ThermoFisher XRD Dispersive Raman instrument (ThermoFisher Scientific Inc., Waltham, MA, USA) equipped with a CCD camera and a diode laser operating at the wavelength of 780 nm. A 500 μ m \times 500 μ m surface was analyzed with a step size of 50 μ m. The exposure time was set at 4 s with an acquisition time of 4 s, for a total of 16 scans per spectrum in the spectral range of 3500 to 200 cm⁻¹. Cosmic-ray and fluorescence corrections have been performed. The

Raman spectra were normalized to eliminate the intensity deviation between the measured areas (Sipos et al., 2020).

2.11. Ex vivo quantitative permeability study across nasal mucosa

To investigate *ex vivo* the transmucosal passive diffusion, a modified Side-Bi-Side® type horizontal diffusion apparatus was applied. The setting was previously developed by our research team and is validated to investigate nasal powders and liquids as well. For further information, Gieszinger et al. reported the apparatus with proper description (Gieszinger et al., 2021). The diffusion of MEL suspension (2.5 mg/ml) and SP-MEL formulation was tested across the excised human nasal mucosa. The nasal mucosa was mounted between the donor and the acceptor compartments with a diffusion surface area of 0.785 cm² completely covering the membrane insert hole with a diameter of 5 mm. The donor was prepared by mixing 1.0 ml of the formulations with 8.0 ml of SNES while the acceptor phase contained 9.0 ml of pH 7.4 PBS to simulate nasal conditions. The temperature of the chambers was controlled at 35 ± 0.5 °C using a heating circulator (ThermoHaake C 10-P5, Sigma-Aldrich Co., Ltd., Budapest, Hungary). The compartments were continuously stirred at 100 rpm using magnetic stirrers. 100 µl aliquots from the acceptor phase were taken at predetermined time points and immediately replaced with fresh medium. The concentration of MEL was determined by HPLC. The flux (J (µg/cm²/h)) was calculated from the permeated drug quantity through the nasal mucosa (m_t), divided by the surface of the membrane insert (A) and the duration of the investigation (t) (Eq. (2)). The permeability coefficient (K_p (cm/h)) was determined by dividing the flux (J) with the drug concentration in the donor phase (C_d (µg/cm³)) (Sipos et al., 2021; Sipos et al., 2022).

$$J = \frac{m_t}{A \cdot t} \quad (2)$$

$$K_p = \frac{J}{C_d} \quad (3)$$

2.12. In vivo animal studies

All the experiments involving animal subjects were carried out with the approval of the National Scientific Ethical Committee on Animal Experimentation (permission number: IV/1247/2017). The animals were treated in accordance with the European Communities Council Directives (2010/63/EU) and the Hungarian Act for the Protection of Animals in Research (Article 32 of Act XXVIII). A 60-µg dose of MEL from the 2.5 mg/ml SP-MEL formulation was administered into the right nostril of 160 – 180 g male Sprague Dawley rats ($n = 24$) via a pipette. At predetermined time points (5, 15, 30, 60, 120 and 240 min), the blood of the rats (under isoflurane anesthesia) was collected into heparinized tubes via cardiac puncture. Then, the animals were sacrificed by decapitation and brain tissues were removed, rinsed in ice-cold PBS, weighed and stored at – 80 °C until assayed.

Plasma samples were centrifuged at 1500 × g for 10 min at 5 °C. To 100 µl of plasma sample, 10 µl of 0.1 % w/v aqueous formic acid and 330 µl acetonitrile containing 110 ng piroxicam (internal standard) were added and the mixture was spun for 60 s. The mixture was allowed to rest for 30 min at – 20 °C to support protein precipitation. The supernatant was obtained via the centrifugation of the mixture for 10 min at 10,000 × g at 4 °C. 20 µl of clear supernatant was diluted using 380 µl 0.1 % w/v aqueous formic acid and stirred for 30 s. 5 µl was injected into the LC-MS/MS system for analysis. The rat plasma calibration standards of MEL were prepared by moving the working standard solutions (in concentration range between 234 and 5000 ng/ml) into a pool of drug-free rat plasma. The sample preparation procedure described above was followed. The sample preparation procedure described above was followed.

Whole brain (1.6 to 2.0 g) of rats were homogenized in 1 % v/v

Table 1

Gradient applied for the analysis of MEL using LC-MS/MS analysis for the *in vivo* studies.

Time (min)	Eluent A (%)	Eluent B (%)	Flow rate (µl/min)
0	65	35	300
2	45	55	300
2.1	0	100	600
2.6	0	100	600
2.7	65	35	600
3.7	65	35	600
3.8	65	35	300
4.5	65	35	300

aqueous acetic acid (1 g tissue/4 ml) using an UCD-500 ultrasonic cell disrupter (Biobase Biodustry, Shandong, China) in an ice bath for 2 min, interrupted by cooling. To 200 µl of brain homogenate, 10 µl of 0.1 % w/v aqueous formic acid and 630 µl ice cold acetonitrile containing 1.6 ng piroxicam (internal standard) and 40 µl 0.1 M perchloric acid were added. The mixture was vortex-mixed for 60 s and allowed to rest for 30 min – 20 °C. After centrifugation for 10 min at 10,000 × g at 4 °C, 100 µl supernatant was diluted with 100 µl of 0.1 % w/v aqueous formic acid, vortexed and 20 µl was analyzed by LC-MS/MS. Rat brain calibration standards of MEL were prepared by moving the working standard solutions (in concentration range between 2.35 and 50 ng/mL) into a pool of drug-free rat brain homogenate. The sample preparation procedure described above was followed.

2.13. LC-MS/MS analysis of in vivo studies

The quantitative analysis of MEL was performed by using a Waters Acquity I-Class UPLCTM system (Waters, Manchester, UK), connected to a Q Exactive™ Plus Orbitrap mass spectrometer (Thermo Fisher Scientific, San Jose, CA, USA) equipped with a heated ESI ion source (HESI). Gradient chromatographic separation was performed at room temperature on a Acquity BEH C18 column (50 mm × 2.1 mm, particle size 1.7 µm) protected by a C18 guard column (2 × 2 mm, Phenomenex, Torrance, CA, USA) by using 0.1 % aqueous formic acid as Solvent A and acetonitrile with 0.1 % formic acid as Solvent B. The gradient applied for the analysis can be seen in Table 1.

The mass spectrometer was used in a positive mode with the following parameters of the HESI source: spray voltage at 3.5 kV, capillary temperature at 256 °C, aux gas heater temperature at 406 °C, sheath gas flow rate at 47.5 l/h, aux gas flow rate at 11.25 l/h, sweep gas flow rate at 2.25 l/h, and S-lens radio frequency (RF) level at 50.0 (source auto-defaults). Parallel-reaction-monitoring (PRM) mode was used for quantifying by monitoring the following transitions: m/z 352 → 115 for MEL and m/z 332 → 95 for piroxicam. Due to the low concentrations of MEL in the biological samples, piroxicam was applied in order to achieve the analysis via standard addition and the transition degree matches with MEL as they are similar in structure. The normalized collision energies (NCEs) for specific quantification were optimized to maximize the sensitivity. The NCEs were 24 for MEL and 29 for piroxicam. A valve placed after the analytical column was programmed to switch the flow onto MS only when analytes of interest elute from the column (1.15–2.15 min) to prevent excessive contamination of the ion source and ion optics. Washing procedures of the autosampler before and after injecting samples were programmed in order to avoid the carry-over of analytes. Data acquisition and processing were carried out using Xcalibur and Quan Browser (version 4.5.474.0) software (Thermo Fisher Scientific, San Jose, CA, USA).

2.14. Pharmacokinetic studies

Pharmacokinetic parameters were analyzed via PK Solver 2.0 Software through non-compartmental analysis of the measured brain and plasma data. The area under the curve (AUC) of the time (min) –

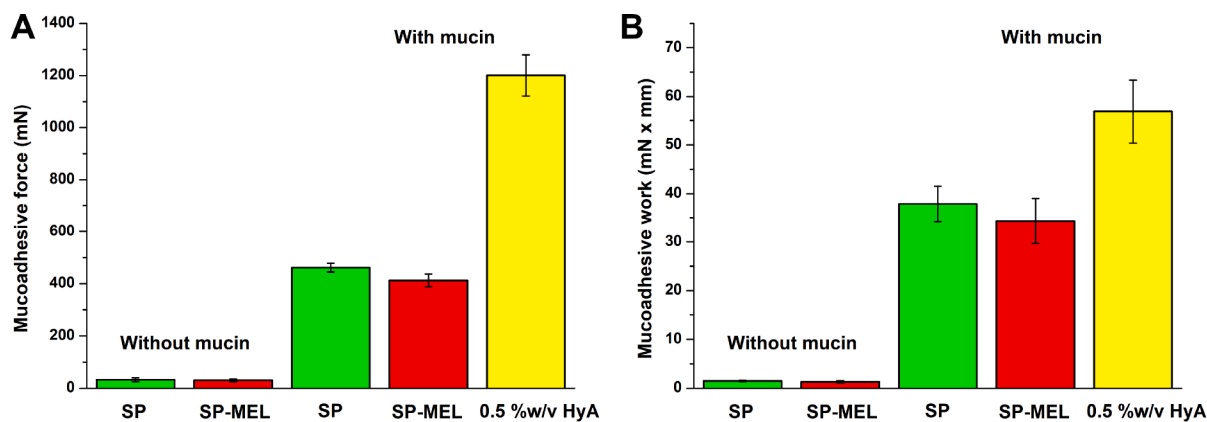


Fig. 2. Mucoadhesive force (A) and mucoadhesive work (B) measured during the tensile test. The column diagram represents the average of 5 measurements with standard deviation. Statistical analysis: n.s. (not significant), $p > 0.05$. As positive control 0.5 % w/v hyaluronic acid (HyA) solution was applied and as negative controls, mucinless experiments were carried out.

concentration curves of each animal were fitted with a linear trapezoidal method (Alshweiat et al., 2020). All reported data are means \pm SD.

3. Results and discussion

3.1. *In vitro* mucoadhesion study

Based on the previous results mentioned earlier regarding the SP-MEL formulation, adequate nasal administration can be achieved due to its physicochemical properties. The adhesion to the nasal mucosa, expressed as mucoadhesion, plays a pivotal role in the successful and efficient absorption of nanocarriers through the nasal route by increasing the residence time of intranasal administered formulations inhibiting the rapid elimination through mucociliary clearance. Mucoadhesive properties of polymeric micelle forming polymers can be characterized with good features. The surface residence time provided by the polymer depends on its ability to form physical and/or chemical secondary bonds (e.g., hydrogen bonds) between the outer shell and the nasal mucosa. SP itself in aqueous solution forms polymeric micelles where the shell's surface is covered by hydroxyl groups originated from the PEG 6000 chain. This allows bond formation, therefore increased residence time (Ascentiis et al., 1995; Shojaei and Li, 1997). To test whether the adhesive force needed to separate the formulation from the simulated nasal membrane and the adhesive work referring to the whole mucoadhesion process are influenced by MEL loading, tensile test was applied (Sipos et al., 2021). Based on the results in Fig. 2., no significant ($p > 0.05$, not significant) decrease can be experienced after drug loading. A slight decrease can be justified by the orientation of polymeric chains towards the hydrophilic molecule parts of MEL; however, a moderately high force and work can be claimed about the formulation itself. Another advantage of this result is that via this moderate mucoadhesion, rapid drug release is expected and tested *in vitro* before (Sipos et al., 2020), therefore not hindering the quick transport of the nanocarriers via either nose-to-blood or nose-to-brain transport. It is also clearly indicated that strong mucoadhesion cannot be claimed about the formulations compared to a commonly applied mucoadhesive agent in a typical concentration, which is a 0.5 % w/v hyaluronic acid solution. Without mucin, negligible adhesion properties could be experienced which also indicates that the main forces occur between the formulation and the mucin itself. Thus, as the value of mucoadhesive force and work regarding the formulation and the co-polymer SP solution lies in between these values, a moderately high mucoadhesion can characterize the product.

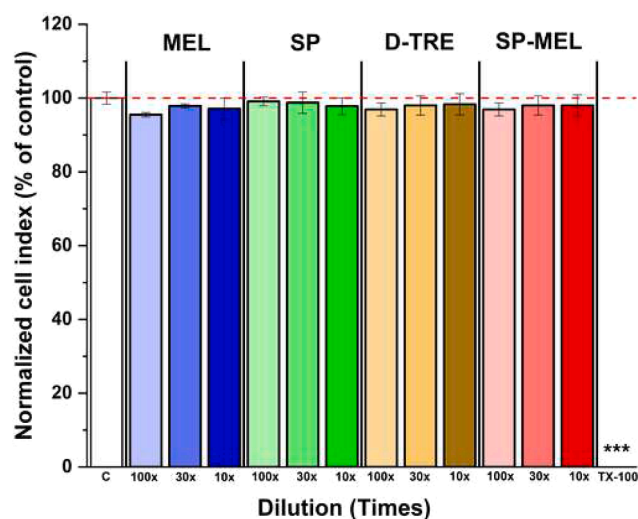


Fig. 3. Cell viability of RPMI 2650 nasal epithelial cells after 1-hour treatment with meloxicam, the nanoformulations or their components measured by impedance. The values presented as a percentage of the control group. Values are presented as means \pm SD, $n = 6-12$. Statistical analysis: ANOVA followed by Dunnett's test. *** $p < 0.01$, compared to the control group. TX-100, Triton X-100 detergent.

3.2. Cell viability assay

The potential toxicity of polymeric nanoparticles is the main problem concerning their use in medicine, however due to their specificity and efficacy, their utilization as advanced drug delivery systems in targeted drug delivery shows a growing demand (Patel et al., 2021). Therefore, to dispel the toxicity concerns in terms of the developed formulation, cell viability assay was conducted. Impedance measurement, as a sensitive method to detect alternation in cellular viability, did not show cell damage after the 1-hour treatment of the tested SP-MEL formulation or its own components (Fig. 3). Different dilution series was investigated for each component representing the dilution process in the nasal cavity. The measured and calculated normalized cell index percentages remained in the adequate ratio compared to the control group. As a reference compound to cause cell death, Triton X-100 detergent was applied which decreased cell impedance to baseline (Fig. 3). No significant difference ($p > 0.05$) in the normalized cell index was obtained in case of neither MEL, SP, D-TRE nor SP-MEL in comparison to control group. These results contribute to the fact that SP-MEL can be safely administered through the nasal cavity as previous studies

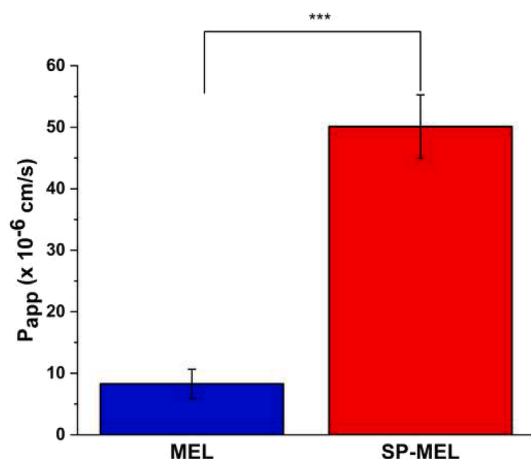


Fig. 4. Apparent permeability of MEL (2.5 mg/ml in all samples) and MEL in SP-MEL nanoformulation across a co-culture model of human RPMI 2650 nasal epithelial cells and vascular endothelial cells (1-hour assay). Values are presented as means \pm SD, $n = 3$. *** $p < 0.001$ significantly different from MEL control.

has also proved and also it reflects to the non-toxic behavior of SP as well on RPMI 2650 cell line. Similar results were obtained by Alopaeus et al. according to which even a 10 % w/w SP solution did not show cytotoxic effect on HT29-MTX cell lines (Alopaeus et al., 2019). Moreover, it has been revealed SP was biocompatible towards mucus-producing HT29-MTX cells, indicating no inhibition in mucin secretion, therefore, change in mucoadhesive properties.

3.3. MEL permeability across the culture model of the nasal mucosa barrier

The permeability of MEL was tested on the co-culture model composed of nasal epithelial and vascular endothelial cells. After 1-hour treatment, the SP-MEL formulation showed a 5-fold increase of MEL across this co-culture model (Fig. 4). The significantly higher (***, $p < 0.001$) apparent permeability values can be due to the fact of the permeation enhancer effect of SP across biological barriers along with the nano particle size.

Our results about the permeability enhancement of SP across RPMI 2650 cell line is corroborated by the work of Pozzoli et al. where they found 2.5 times higher permeability of budesonide with SP as an excipient (Pozzoli et al., 2017). The higher degree of permeation in our case contributes to the fact that different dosage forms also affect the permeability. Whilst Pozzoli et al. formulated a freeze-dried nasal powder, our polymeric micelle formulation can utilize the benefits of a

liquid state nasal formulation, whereas the API is in dissolved form allowing quicker and more efficient transport across the cells. Similarly other nanocarriers, such as human serum albumin nanoparticles were investigated on human RPMI 2650 cell line (Katona et al., 2020).

We found good TEER and low permeability values for paracellular markers indicating a good barrier property of the nasal mucosa co-culture model (Fig. 5A) The TEER values remained at the level of the control group after 1-hour treatment with the SP-MEL formulation indicating that it does not damage the barrier function. MEL increased TEER and all three treatments decreased P_{app} values for the two hydrophilic paracellular marker molecules, dextran and albumin (Fig. 5B). As previous studies also proved with other nanocarriers, this result suggests that MEL may have a beneficial effect on the nasal barrier either by itself or in separate formulations.

3.4. Immunohistochemistry

The change in the staining pattern of the junctional linker proteins ZO-1 and β -catenin was investigated on human RPMI 2650 nasal epithelial cells in the co-culture model to detect whether the SP-MEL formulation affects natural membrane integrity. The cells were typical cobblestone shaped with visible junctional proteins in a belt-like manner bordering the cells. No change in the staining pattern can be observed after the 1-hour treatment of the model with MEL and SP-MEL formulation compared to the control group which received only medium (Fig. 6). This microscopic imaging also contributes to the safe and non-toxic administration of polymeric micelle formulation. The results also exclude that classic surfactant-like permeation enhancement are achieved via SP as classic surfactants usually damage the barrier model unlike in our case.

3.5. Ex vivo permeability measurements across nasal mucosa

Ex vivo permeability measurements across the nasal mucosa was carried out in order to investigate the permeation enhancement of MEL via SP compared to the reference MEL suspension. Semiquantitative investigation was performed via Raman spectroscopy after instillation upon the mucosal surface. The characteristic absorption peaks of MEL (at 1305 cm^{-1} (ν_{OH}), 1267 cm^{-1} ($\nu_{\text{C-N-C}}$) and 1164 cm^{-1} ($\nu_{\text{C-S}}$) were fitted on the surface map acquired via Raman chemical mapping (Fig. 7).

Based on Fig. 7, a deeper tissue penetration can be achieved via administering the SP-containing MEL formulation. SP can penetrate into deeper tissue regions compared to a regular, excipient-free formulation. This penetration is not cell damaging as the nasal cytotoxicity and immunohistochemistry investigations proved. This mechanism however is still similar to classic surfactant-based permeation enhancement (e.g.,

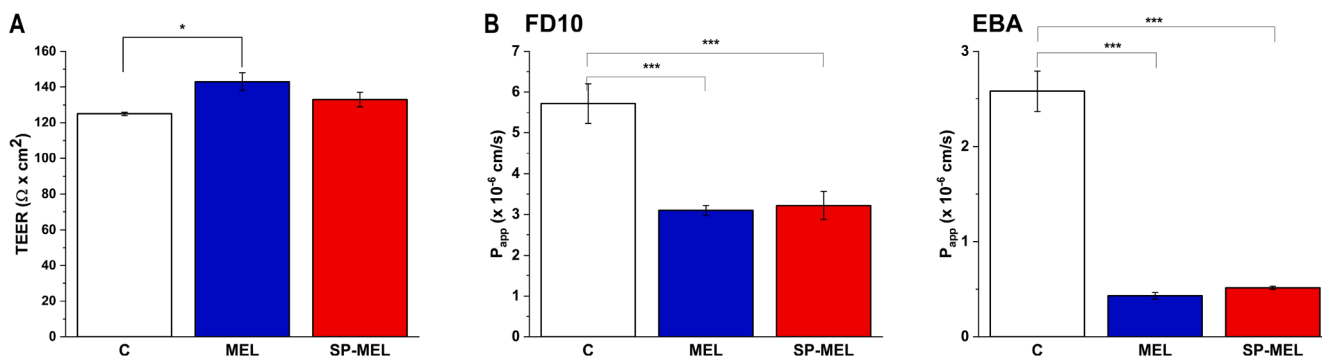


Fig. 5. (A). Transepithelial electrical resistance (TEER) of the co-culture model after 1-hour treatment with MEL and SP-MEL (B) Values for paracellular permeability markers fluorescein isothiocyanate-labelled dextran (FD10) and Evans blue labelled albumin (EBA) after 1-hour treatment with MEL and SP-MEL. Values are presented as means \pm SD, $n = 3$. C: control. * $p < 0.05$; *** $p < 0.001$ significantly different from control. (For interpretation of the references to colour in this figure legend, the reader is referred to the web version of this article.)

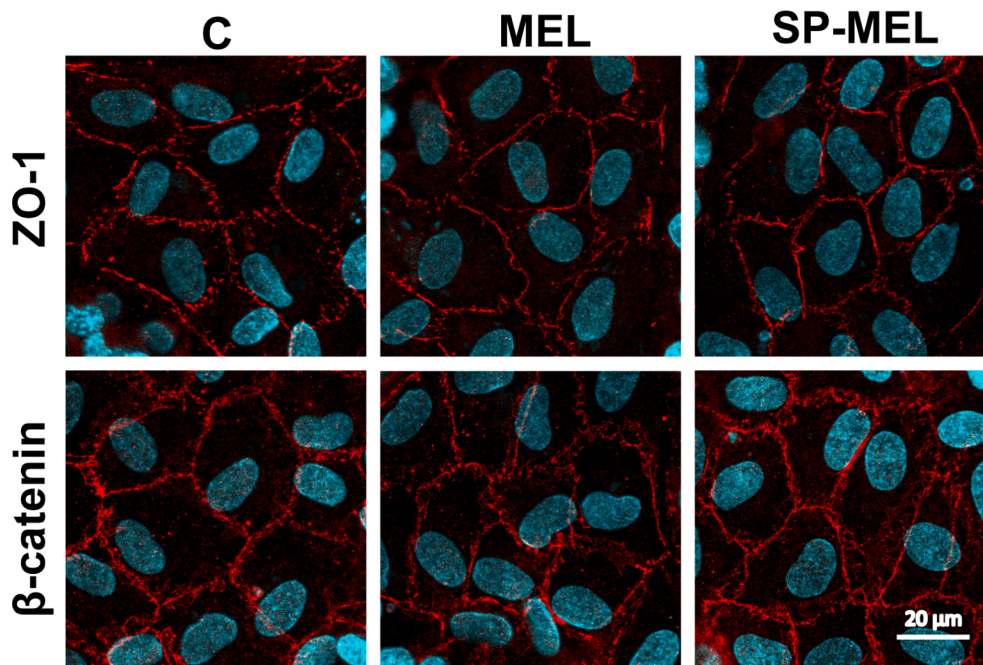


Fig. 6. Immunostaining for junctional linker proteins ZO-1 and β -catenin on human RPMI 2650 nasal epithelial cell layers following a 1-hour treatment with MEL and SP-MEL. The control group (C) received only medium. Red: junctional proteins; blue: cell nuclei. Scale bar: 20 μm . (For interpretation of the references to colour in this figure legend, the reader is referred to the web version of this article.)

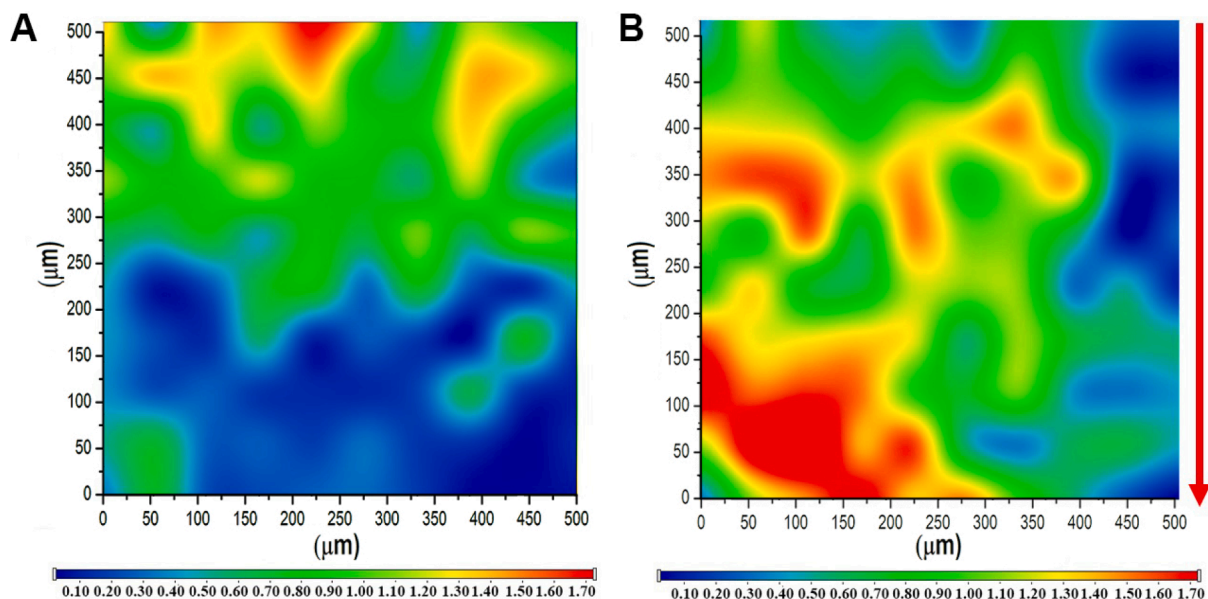


Fig. 7. *Ex vivo* semiquantitative permeability measurement of MEL (A) and SP-MEL (B) across human nasal mucosa. The red arrow indicates the direction of transport across the incised tissue region. The Raman spectra were normalized. (For interpretation of the references to colour in this figure legend, the reader is referred to the web version of this article.)

in the case of Tween 20), where the main leading force is that the API would transfer to the highly vascularized tissue regions.

The investigation was performed in a modified Side-by-Side® type horizontal diffusion cell apparatus, where the cut tissue was mounted between the donor and acceptor compartments. The flux and permeability were evaluated after the quantification of aliquots in the acceptor compartment at predetermined time periods (Fig. 8).

The higher cumulative permeability values refer to the amount of permeated MEL across the tissue. The solubility enhancement induced increased permeability is caused by the SP micelle-forming polymer. As

the *in vitro* drug release study showed in our previous study, a burst-like drug release can be experienced which corroborates that no lag time is needed to achieve the increased concentrations. The calculated flux is 410.54 $\mu\text{g}/\text{cm}^2$ at the final time point and the permeability coefficient is 0.493 cm/h which values are significantly higher than in case of MEL suspension: 77.491 $\mu\text{g}/\text{cm}^2$ and 0.068 cm/h (** $p < 0.01$ in both cases).

3.6. *In vivo* animal studies

To determine the promotion tendency of SP regarding MEL

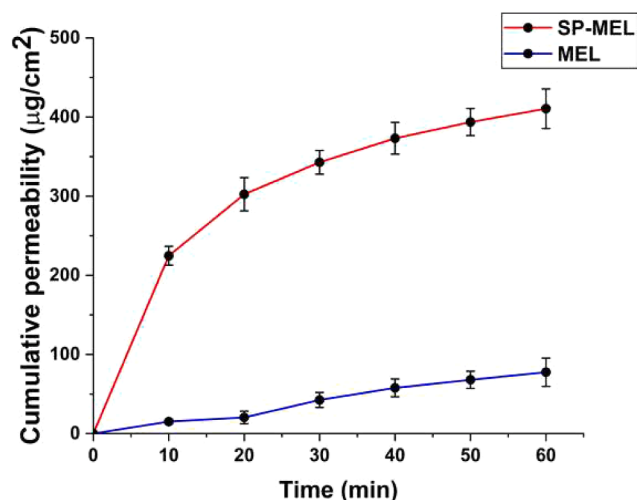


Fig. 8. *Ex vivo* quantitative permeability study performed in a modified Side-by-Side® type horizontal diffusion cell. The cumulative permeability values depicted at predetermined sampling time points in case of SP-MEL polymeric micelle formulation and the reference MEL suspension. All measurements were carried out in triplicate and data are presented as means \pm SD ($n = 3$).

administration to the central nervous system, *in vivo* measurements were performed. The experiment lasted 4 h, where at predetermined time points aliquots were withdrawn from the plasma and in the brain after the under-anaesthesia sacrifice of animals (Fig. 9).

Our results can be compared by our research group's intranasal *in vivo* measurements, where physical particle size reduction techniques were applied on MEL (Bartos et al., 2018). Spray-drying was applied as reduction method, and the achieved MEL concentration in the brain was <1 nM. Compared to our results, approx. 35 to 40-times higher concentrations were achieved. The higher AUC values (approx. 35 nmol/ml \times min in case of spray dried formulations vs approx. 5000 nmol/ml \times min in case of SP-MEL formulation) also contributes to the fact that higher effective MEL transport was achieved to the central nervous system (Table 2). This shows the superiority of encapsulation into nanocarriers, as not only the decreased size resulted increased surface area is of paramount importance, but the need for permeability enhancers is there. Based on these and the *ex vivo* permeation results, SP formed micelles can penetrate into the deeper nasal regions where the uptake via the richly vascularized nasal mucosa region. As the olfactory nerves are innervated around this region, high chance of direct nose-to-

brain transport can also be assumed. The brain curves have a maximum at 5 min which support this theorem, and the other maximum can be found at 60 min which can be identified as the typical nose-to-blood mediated brain transport time. The curves are not drastically decreasing after 2 h, leaving the opportunity that a long-lasting and constant permeation to the CNS can occur. The supporting pharmacokinetic parameters can be found in Table 2.

Based on the pharmacokinetic investigations and calculations, the following can be stated. The AUC values regarding the brain concentration of MEL after intranasal administration of SP-MEL are significantly higher compared to the previously measured particle size-reduced MEL formulation. The clearance of SP-MEL and the high value of the MRT value indicates that a slow elimination process could be experienced in case of the nanocarrier. Besides the initial burst, based on these parameters a long-lasting effect can also be observed due to the previously mentioned fact that polymeric micelles could provide a higher circulation stability. Since the plasma concentration after IN administration followed the natural elimination curve with the high presence of MEL in the brain, the nose-to-brain pathway is more likely in the early stages after administration, however the long elimination can contribute to later penetration across the BBB as well. This is supported by the results of *in vitro* cell line and *ex vivo* nasal mucosa permeation studies where intensive, rapid, burst-like permeation could be found which is a potential sign that the immensely innervated nasal mucosa also takes up the active substance towards the neural pathway. Since the polymeric micelle formulation had a negative zeta potential value, carrier-intact paracellular or transcytosis-type permeation could also be a possibility in our case.

Table 2

Calculated pharmacokinetic parameters regarding the intranasally administered SP-MEL formulation. All data are presents as means \pm SD ($n = 4$). Abbreviations: K_e – elimination rate constant; $t_{1/2}$ – half-time; AUC_{0-t} – area under curve value between 0 and the measurement time (t); $AUC_{0-\infty}$ –area under curve value between 0 and infinity; Cl – Clearance; MRT – mean residence time.

Pharmacokinetic parameter	Plasma	Brain
K_e (min^{-1})	$0.00091 \pm 2.2 \cdot 10^{-4}$	$0.00132 \pm 3.6 \cdot 10^{-5}$
$t_{1/2}$ (h)	804.143 ± 22.362	525.174 ± 14.378
AUC_{0-t} ($\mu\text{mol}/\text{ml} \times \text{min}$)	811.228 ± 12.281	5.263 ± 0.051
$AUC_{0-\infty}$ ($\mu\text{mol}/\text{ml} \times \text{min}$)	5115.035 ± 124.78	22.991 ± 0.674
Cl ($\mu\text{g}/\text{kg}/(\text{nmol}/\text{ml})/\text{min}$)	$7.6 \cdot 10^{-5} \pm 1.6 \cdot 10^{-5}$	$0.0163 \pm 4.8 \cdot 10^{-4}$
MRT (min)	1197.25 ± 315.44	796.337 ± 23.17

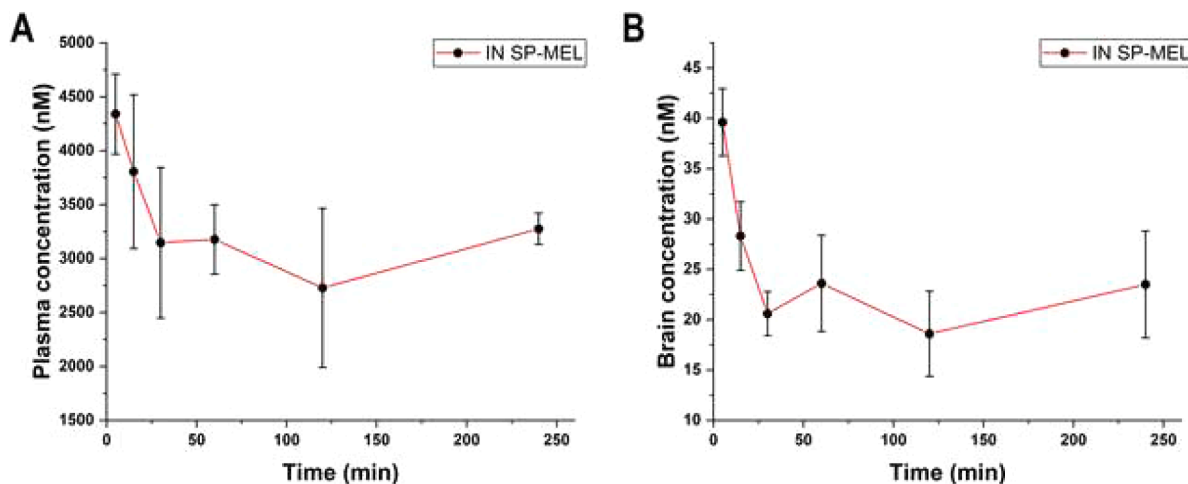


Fig. 9. *In vivo* plasma (A) and brain (B) concentration of MEL after the intranasal (IN) treatment with the SP-MEL polymeric micelle nanoformulation. Results are expressed as average \pm SD ($n = 4$).

4. Conclusion

In conclusion, we successfully proved our hypothesis by the detailed *in vitro* to *in vivo* nasal applicability studies. Based on our previous experience and results, the *in vitro* characterization offered a promising solution for the SP-MEL formulation to be further investigated. Alongside the proper physicochemical parameters, the general mucoadhesive tendency of SP is not significantly lowered after the loading of MEL in the system. It is not high enough to offer the same residence time as a gelling system, however it contributes to a proper adhesion to the nasal mucosa where, based on our cell line studies, a rapid and highly efficient MEL transport can be achieved. This enhanced permeation takes place without the damaging properties of commonly applied surfactant molecules and SP proved to be safe to administer. *Ex vivo* studies also confirmed the high tissue permeation followed by the *in vivo* pharmacokinetic characterization of our formulation. High brain concentrations were achieved with the SP-MEL formulation compared to prior results achieved via physical particle size reduction techniques. Our results offer the utilization of this nanocarrier system as a tool to efficiently transport non-steroidal anti-inflammatory agents as possible remedies to inflammation-based and/or inflammation-associated neural diseases.

CRedit authorship contribution statement

Bence Sipos: Conceptualization, Methodology, Software, Formal analysis, Investigation, Data curation, Writing – original draft, Visualization, Project administration. **Zsolt Bella:** Investigation, Resources, Writing – review & editing. **Ilona Gróf:** Investigation, Data curation, Software, Writing – original draft. **Szilvia Veszelka:** Investigation, Data curation, Writing – original draft. **Mária A. Deli:** Data curation, Resources, Formal analysis, Writing – review & editing. **Kálmán F. Szűcs:** Investigation, Data curation, Writing – review & editing. **Anita Sztjokov-Ivanov:** Investigation, Data curation, Software, Writing – review & editing. **Eszter Ducza:** Investigation, Data curation, Writing – review & editing. **Róbert Gáspár:** Investigation, Resources, Formal analysis, Writing – review & editing. **Gábor Kecskeméti:** Investigation, Data curation, Writing – review & editing. **Tamás Janáky:** Investigation, Resources, Formal analysis, Writing – review & editing. **Balázs Volk:** Resources, Formal analysis, Writing – review & editing. **Mária Budai-Szűcs:** Software, Investigation, Writing – original draft. **Rita Ambrus:** Conceptualization, Validation, Resources, Writing – review & editing, Project administration. **Piroska Szabó-Révész:** Validation, Resources, Writing – review & editing. **Ildikó Csóka:** Conceptualization, Methodology, Validation, Formal analysis, Resources, Writing – review & editing, Supervision, Project administration, Funding acquisition. **Gábor Katona:** Conceptualization, Methodology, Validation, Formal analysis, Resources, Writing – review & editing, Supervision, Project administration.

Declaration of Competing Interest

The authors declare that they have no known competing financial interests or personal relationships that could have appeared to influence the work reported in this paper.

Data availability

Data will be made available on request.

Acknowledgements

This work was supported by Project no. TKP2021-EGA-32 implemented with the support provided by the Ministry of Innovation and Technology of Hungary from the National Research, Development and Innovation Fund, financed under the TKP2021-EGA funding scheme. S. V. was supported by the Premium Postdoctoral Research Program

(Premium-2019-469) of the Hungarian Academy of Sciences and the OTKA Young Researcher Excellence Program (OTKA-FK 143233) by National Research, Development and Innovation Office of Hungary.

References

- Agrawal, M., Saraf, S., Saraf, S., Antimisiaris, S.G., Chougule, M.B., Shoyele, S.A., Alexander, A., 2018. Nose-to-brain drug delivery: an update on clinical challenges and progress towards approval of anti-Alzheimer drugs. *J. Control. Release* 281, 139–177. <https://doi.org/10.1016/j.jconrel.2018.05.011>.
- Alopaes, J.F., Hagesaether, E., Tho, I., 2019. Micellisation mechanism and behaviour of soluplus®-furosemide micelles: preformulation studies of an oral nanocarrier-based system. *Pharmaceutics* 12, 1–23. <https://doi.org/10.3390/ph12010015>.
- Alshweiat, A., Ii, I., Csóka, F., Tömösi, T., Janáky, A., Kovács, R., Gáspár, A., Sztjokov-Ivanov, E., Ducza, Á., Márki, P., Szabó-Révész, R.A., 2020. Nasal delivery of nanosuspension-based mucoadhesive formulation with improved bioavailability of loratadine: Preparation, characterization, and *in vivo* evaluation. *Int. J. Pharm.* 579, 119166. <https://doi.org/10.1016/j.ijpharm.2020.119166>.
- Bartos, C., Ambrus, R., Kovács, A., Gáspár, R., Sztjokov-Ivanov, A., Márki, Á., Janáky, T., Tömösi, F., Kecskeméti, G., Szabó-Révész, P., 2018. Investigation of absorption routes of meloxicam and its salt form from intranasal delivery systems. *Molecules* 23, 1–13. <https://doi.org/10.3390/molecules23040784>.
- Bocsik, A., Gróf, I., Kiss, L., Ötvös, F., Zsifros, O., Daruka, L., Fülöp, L., Vastag, M., Kittel, Á., Imre, N., Martinek, T.A., Pál, C., Szabó-Révész, P., Deli, M.A., 2019. Dual action of the PN159/KLAL/MAP peptide: Increase of drug penetration across caco-2 intestinal barrier model by modulation of tight junctions and plasma membrane permeability. *Pharmaceutics* 11. <https://doi.org/10.3390/pharmaceutics11020073>.
- Budai-Szűcs, M., Kiss, E.L., Szilágyi, B.Á., Szilágyi, A., Gyarmati, B., Berkó, S., Kovács, A., Horvát, G., Aigner, Z., Soós, J., Csányi, E., 2018. Mucoadhesive cyclodextrin-modified thiolated poly(aspartic acid) as a potential ophthalmic drug delivery system. *Polymers (Basel)* 10. <https://doi.org/10.3390/polym10020199>.
- Calvo-Rodríguez, M., Núñez, L., Villalobos, C., 2015. Non-steroidal anti-inflammatory drugs (NSAIDs) and neuroprotection in the elderly: a view from the mitochondria. *Neural Regen. Res.* 10, 1371–1372. <https://doi.org/10.4103/1673-5374.165219>.
- Castile, J., Cheng, Y.H., Simmons, B., Perelman, M., Smith, A., Watts, P., 2013. Development of *in vitro* models to demonstrate the ability of PecSys®, an *in situ* nasal gelling technology, to reduce nasal run-off and drip. *Drug Dev. Ind. Pharm.* 39, 816–824. <https://doi.org/10.3109/03639045.2012.707210>.
- Cecchelli, R., Aday, S., Sevin, E., Almeida, C., Culot, M., Dehouck, L., Coisne, C., Engelhardt, B., Dehouck, M.P., Ferreira, L., 2014. A stable and reproducible human blood-brain barrier model derived from hematopoietic stem cells. *PLoS One* 9. <https://doi.org/10.1371/journal.pone.0099733>.
- Choi, S.H., Aid, S., Caracciolo, L., Sakura Minami, S., Niikura, T., Matsuoka, Y., Turner, R.S., Mattson, M.P., Bosetti, F., 2013. Cyclooxygenase-1 inhibition reduces amyloid pathology and improves memory deficits in a mouse model of Alzheimer's disease. *J. Neurochem.* 124, 59–68. <https://doi.org/10.1111/jnc.12059>.
- De Ascentiis, A., deGrazia, J.L., Bowman, C.N., Colombo, P., Peppas, N.A., 1995. Mucoadhesion of poly(2-hydroxyethyl methacrylate) is improved when linear poly(ethylene oxide) chains are added to the polymer network. *J. Control. Release* 33, 197–201. [https://doi.org/10.1016/0168-3659\(94\)00087-B](https://doi.org/10.1016/0168-3659(94)00087-B).
- Ghezzi, M., Pescina, S., Padula, C., Santi, P., Del Favero, E., Cantù, L., Nicoli, S., 2021. Polymeric micelles in drug delivery: an insight of the techniques for their characterization and assessment in biorelevant conditions. *J. Control. Release* 332, 312–336. <https://doi.org/10.1016/j.jconrel.2021.02.031>.
- Gieszinger, P., Kiss, T., Szabó-Révész, P., Ambrus, R., 2021. The development of an *in vitro* horizontal diffusion cell to investigate nasal powder penetration *in line*. *Pharmaceutics* 13 (6), 809. <https://doi.org/10.3390/pharmaceutics13060809>.
- Goldsmith, M., Abramovitz, L., Peer, D., 2014. Precision nanomedicine in neurodegenerative diseases. *ACS Nano* 8, 1958–1965. <https://doi.org/10.1021/nn501292z>.
- Heneka, M.T., Carson, M.J., El Khoury, J., Landreth, G.E., Brosseron, F., Feinstein, D.L., Jacobs, A.H., Wyss-Coray, T., Vitorica, J., Ransohoff, R.M., Herrup, K., Frautschy, S. A., Finsen, B., Brown, G.C., Verkhratsky, A., Yamanaka, K., Koistinaho, J., Latz, E., Halle, A., Petzold, G.C., Town, T., Morgan, D., Shinohara, M.L., Perry, V.H., Holmes, C., Bazan, N.G., Brooks, D.J., Hunot, S., Joseph, B., Deigendesch, N., Garaschuk, O., Boddeke, E., Dinarello, C.A., Breitner, J.C., Cole, G.M., Golenbock, D. T., Kummer, M.P., 2015. Neuroinflammation in Alzheimer's disease. *Lancet Neurol.* 14, 388–405. [https://doi.org/10.1016/S1474-4422\(15\)70016-5](https://doi.org/10.1016/S1474-4422(15)70016-5).
- Hong, S.S., Oh, K.T., Choi, H.G., Lim, S.J., 2019. Liposomal formulations for nose-to-brain delivery: recent advances and future perspectives. *Pharmaceutics* 11, 1–18. <https://doi.org/10.3390/pharmaceutics11100540>.
- Horvát, G., Gyarmati, B., Berkó, S., Szabó-Révész, P., Szilágyi, B.Á., Szilágyi, A., Soós, J., Sandri, G., Bonferoni, M.C., Rossi, S., Ferrari, F., Caramella, C., Csányi, E., Budai-Szűcs, M., 2015. Thiolated poly(aspartic acid) as potential *in situ* gelling, ocular mucoadhesive drug delivery system. *Eur. J. Pharm. Sci.* 67, 1–11. <https://doi.org/10.1016/j.ejps.2014.10.013>.
- Katona, G., Balogh, G.T., Dargó, G., Gáspár, R., Márki, Á., Ducza, E., Sztjokov-Ivanov, A., Tömösi, F., Kecskeméti, G., Janáky, T., Kiss, T., Ambrus, R., Pallagi, E., Szabó-Révész, P., Csóka, I., 2020. Development of meloxicam-human serum albumin nanoparticles for nose-to-brain delivery via application of a quality by design approach. *Pharmaceutics* 12. <https://doi.org/10.3390/pharmaceutics12020097>.
- Katona, G., Sipos, B., Ambrus, R., Csóka, I., Szabó-Révész, P., 2022. Characterizing the drug-release enhancement effect of surfactants on megestrol-acetate-loaded granules. *Pharmaceutics* 15. <https://doi.org/10.3390/ph15020113>.

- Khan, A.R., Liu, M., Khan, M.W., Zhai, G., 2017. Progress in brain targeting drug delivery system by nasal route. *J. Control. Release.* 268, 364–389. <https://doi.org/10.1016/j.jconrel.2017.09.001>.
- Kürti, L., Veszelka, S., Bocsik, A., Ózsvári, B., Puskás, L.G., Kittel, Á., Szabó-Révész, P., Deli, M.A., 2013. Retinoic acid and hydrocortisone strengthen the barrier function of human RPMI 2650 cells, a model for nasal epithelial permeability. *Cytotechnology* 65, 395–406. <https://doi.org/10.1007/s10616-012-9493-7>.
- Li, Y., Li, M., Gong, T., Zhang, Z., Sun, X., 2017. Antigen-loaded polymeric hybrid micelles elicit strong mucosal and systemic immune responses after intranasal administration. *J. Control. Release.* 262, 151–158. <https://doi.org/10.1016/j.jconrel.2017.07.034>.
- McGeer, P.L., McGeer, E.G., 2007. NSAIDs and Alzheimer disease: epidemiological, animal model and clinical studies. *Neurobiol. Aging.* 28, 639–647. <https://doi.org/10.1016/j.neurobiolaging.2006.03.013>.
- Owen, S.C., Chan, D.P.Y., Shoichet, M.S., 2012. Polymeric micelle stability. *Nano Today* 7, 53–65. <https://doi.org/10.1016/j.nantod.2012.01.002>.
- Pardeshi, C.V., Belgamwar, V.S., 2013. Direct nose to brain drug delivery via integrated nerve pathways bypassing the blood-brain barrier: an excellent platform for brain targeting. *Expert Opin. Drug Deliv.* 10, 957–972. <https://doi.org/10.1517/17425247.2013.790887>.
- Patel, P., Vyas, N., Raval, M., 2021. Safety and toxicity issues of polymeric nanoparticles: a serious concern. *Nanotechnol. Med. Toxicity and Safety* 156–173.
- Pedroso, D.C.S., Tellechea, A., Moura, L., Fidalgo-Carvalho, I., Duarte, J., Carvalho, E., Ferreira, L., 2011. Improved survival, vascular differentiation and wound healing potential of stem cells co-cultured with endothelial cells. *PLoS One.* 6, 1–12. <https://doi.org/10.1371/journal.pone.0016114>.
- Pepić, I., Lovrić, J., Filipović-Grčić, J., 2013. How do polymeric micelles cross epithelial barriers? *Eur. J. Pharm. Sci.* 50, 42–55. <https://doi.org/10.1016/j.ejps.2013.04.012>.
- Pozzoli, M., Traini, D., Young, P.M., Sukkar, M.B., Sonvico, F., 2017. Development of a Soluplus budesonide freeze-dried powder for nasal drug delivery. *Drug Dev. Ind. Pharm.* 43, 1510–1518. <https://doi.org/10.1080/03639045.2017.1321659>.
- Sabir, F., Katona, G., Ismail, R., Sipos, B., Ambrus, R., Csóka, I., 2021. Development and characterization of N-propyl gallate encapsulated solid lipid nanoparticles-loaded hydrogel for intranasal delivery. *Pharmaceuticals* 14. <https://doi.org/10.3390/PH14070696>.
- Sanz-Blasco, S., Calvo-Rodríguez, M., Caballero, E., Garcia-Durillo, M., Nunez, L., Villalobos, C., 2018. Is it all said for NSAIDs in Alzheimer's disease? Role of mitochondrial calcium uptake. *Current Alzheimer Research* 15 (6), 504–510.
- Saraiva, C., Praça, C., Ferreira, R., Santos, T., Ferreira, L., Bernardino, L., 2016. Nanoparticle-mediated brain drug delivery: overcoming blood-brain barrier to treat neurodegenerative diseases. *J. Control. Release.* 235, 34–47. <https://doi.org/10.1016/j.jconrel.2016.05.044>.
- Shabab, T., Khanabdali, R., Moghadamtousi, S.Z., Kadir, H.A., Mohan, G., 2017. Neuroinflammation pathways: a general review. *Int. J. Neurosci.* 127, 624–633. <https://doi.org/10.1080/00207454.2016.1212854>.
- Sharma, V., 2011. Neuroinflammation in Alzheimer's disease and involvement of interleukin-1: a mechanistic view. *Int. J. Pharm. Sci. Drug Res.* 3, 287–291.
- Shojaei, A.H., Li, X., 1997. Mechanisms of buccal mucoadhesion of novel copolymers of acrylic acid and polyethylene glycol monomethylether monomethacrylate. *J. Control. Release.* 47, 151–161. [https://doi.org/10.1016/S0168-3659\(96\)01626-4](https://doi.org/10.1016/S0168-3659(96)01626-4).
- Sipos, B., Szabó-Révész, P., Csóka, I., Pallagi, E., Dobó, D.G., Béltéky, P., Kónya, Z., Deák, Á., Janovák, L., Katona, G., 2020. Quality by design based formulation study of meloxicam-loaded polymeric micelles for intranasal administration. *Pharmaceutics* 12, 1–29. <https://doi.org/10.3390/pharmaceutics12080697>.
- Sipos, B., Csóka, I., Budai-Szűcs, M., Kozma, G., Berkesi, D., Kónya, Z., Balogh, G.T., Katona, G., 2021. Development of dexamethasone-loaded mixed polymeric micelles for nasal delivery. *Eur. J. Pharm. Sci.* 166 <https://doi.org/10.1016/j.ejps.2021.105960>.
- Sipos, B., Csóka, I., Ambrus, R., Schelz, Z., Zupkó, I., Balogh, G.T., Katona, G., 2022. Spray-dried indomethacin-loaded polymeric micelles for the improvement of intestinal drug release and permeability. *Eur. J. Pharm. Sci.* 174 <https://doi.org/10.1016/j.ejps.2022.106200>.
- Sun, P., Xiao, Y., Di, Q., Ma, W., Ma, X., Wang, Q., Chen, W., 2020. Transferrin receptor-targeted peg-pla polymeric micelles for chemotherapy against glioblastoma multiforme. *Int. J. Nanomedicine.* 15, 6673–6688. <https://doi.org/10.2147/IJN.S257459>.
- Szabó-Révész, P., 2018. Modifying the physicochemical properties of NSAIDs for nasal and pulmonary administration. *Drug Discov. Today Technol.* 27, 87–93. <https://doi.org/10.1016/j.ddtec.2018.03.002>.
- Thotakura, N., Parashar, P., Raza, K., 2021. Assessing the pharmacokinetics and toxicology of polymeric micelle conjugated therapeutics. *Expert Opin. Drug Metab. Toxicol.* 17, 323–332. <https://doi.org/10.1080/17425255.2021.1862085>.
- Warnken, Z.N., Smyth, H.D.C., Watts, A.B., Weitman, S., Kuhn, J.G., Williams, R.O., 2016. Formulation and device design to increase nose to brain drug delivery. *J. Drug Deliv. Sci. Technol.* 35, 213–222. <https://doi.org/10.1016/j.jddst.2016.05.003>.
- Watanabe, M., Kawano, K., Yokoyama, M., Opanasopit, P., Okano, T., Maitani, Y., 2006. Preparation of camptothecin-loaded polymeric micelles and evaluation of their incorporation and circulation stability. *Int. J. Pharm.* 308, 183–189. <https://doi.org/10.1016/j.ijpharm.2005.10.030>.
- Wohlfart, S., Gelperina, S., Kreuter, J., 2012. Transport of drugs across the blood-brain barrier by nanoparticles. *J. Control. Release.* 161, 264–273. <https://doi.org/10.1016/j.jconrel.2011.08.017>.
- Wong, K.H., Riaz, M.K., Xie, Y., Zhang, X., Liu, Q., Chen, H., Bian, Z., Chen, X., Lu, A., Yang, Z., 2019. Review of current strategies for delivering Alzheimer's disease drugs across the blood-brain barrier. *Int. J. Mol. Sci.* 20 <https://doi.org/10.3390/ijms20020381>.
- Youdim, K.A., Avdeef, A., Abbott, N.J., 2003. In vitro trans-monolayer permeability calculations: often forgotten assumptions. *Drug Discov Today* 8 (21), 997–1003. [https://doi.org/10.1016/s1359-6446\(03\)02873-3](https://doi.org/10.1016/s1359-6446(03)02873-3).
- Zakharova, L.Y., Pashirova, T.N., Doktorovova, S., Fernandes, A.R., Sanchez-Lopez, E., Silva, A.M., Souto, S.B., Souto, E.B., 2019. Cationic surfactants: Self-assembly, structure-activity correlation and their biological applications. *Int J Mol Sci.* 20 (22), 5534 <https://doi.org/10.3390/ijms20225534>.